CRANFIELD UNIVERSITY

IOANNIS ALISSANDRATOS

Novel Bioprocessing Technologies for the Cultivation of Microalgae

School of Aerospace, Transport and Manufacturing
PhD in Manufacturing

SUBMITTED IN PARTIAL FULLFILMENT OF THE
REQUIREMENTS FOR THE DEGREE OF DOCTOR OF
PHILOSOPHY
Academic Year: 2018 - 2019

Supervisor: Professor Charalampos Makatsoris
Associate Supervisor: Professor Mark Jolly
July 2019

CRANFIELD UNIVERSITY

Aerospace, Transport and Manufacturing
PhD in Manufacturing

PhD in Manufacturing

Academic Year 2018 - 2019

Ioannis Alissandratos

Novel Bioprocessing Technologies for the Cultivation of Microalgae

Supervisor: Professor Charalampos Makatsoris
Associate Supervisor: Professor Mark Jolly
07/19

This thesis is submitted in partial fulfilment of the requirements for
the degree of PhD
*(NB. This section can be removed if the award of the degree is
based solely on examination of the thesis)*

ABSTRACT

Microalgae are single cell photosynthetic organisms which have the potential to be game changers in industrial biotechnology. In spite of their many reported benefits, their technological advancement and industrial adoption rate has fallen behind expectation. As reported by numerous influential publications in the past decade, this can be traced to a lack of communication between engineering and science, leading to the development of technology (photobioreactors) which systematically underestimate algal growth parameters at scale; suggesting that that there is a need for considerable redesign of the photobioreactor technology. Therefore, in this work the development of a novel photobioreactor based on continuous flow technologies is introduced. Using the work carried out by the Makatsoris Group in the field of oscillatory baffled flow reactors as a foundation, the development of an enabling platform in the shape of a continuous oscillatory baffled flow photobioreactor ensued. This platform aimed to facilitate scalability, increase cost effectiveness and intensify the cultivation of microalgae; carried out via the implementation continuous plug flow mixing and novel light utilisation techniques. This resulted in a technology which in combination with a novel cost-effective nutrient mix tailored to *C.Vulgaris*, the model strain, achieved three key results. First accelerated the growth rate of microalgae. Second, it reduced the cost of media from 0.04 £/l to 0.0046 £/l. Third it systematically produced high biomass yields in the range of 1.65 and 2.8 g/l in 8-10 days, at a price per unit biomass of approximately 2.1£/kg; for both laboratory (<100ml) and pilot scale (>10L). The success of this work led to the creation of a spinout commercial entity called Centillion Technology Ltd, which operates the technology at ramped up volumes, at the Cranfield University pilot plant.

Keywords:

Microalgae, Photobioreactor, Continuous Flow, Industrial Biotechnology, Continuous reactor development, Systems integration, Chlorella Vulgaris.

To my grandmother, Hellen Mary Ewart

ACKNOWLEDGEMENTS

TABLE OF CONTENTS

LIST OF FIGURES

LIST OF TABLES

LIST OF EQUATIONS

LIST OF ABBREVIATIONS

IT	Information Technology
OBR	Oscillatory Baffled Flow Reactor
PBR	Photo Bio Reactor
PFR	Plug or Piston Flow Reactor
CSTR	Continuous flow stirred tank reactor
CDO	Conceptual Design Methodology
PE	Photosynthetic Efficiency
PFD	Photon Flux Density
PI	Photosynthetic Irradiance
PSU	Photosynthetic Unit
IR	Infrared
PAR	Photosynthetic Active Radiation
DO	Dissolved Oxygen
OD	Optical Density
L/D	Light and Dark
LED	Light emitting diode
Re	Reynolds number
St	Strouhal number
Re_o	Oscillatory Reynolds number
RTD	Residence Time Distribution
CO_2	Carbon Dioxide
O_2	Oxygen
CM	*Centillion Media*
CV	*Chlorella Vulgaris*
DoE	Design of Experiments
EDX	Energy Dispersive X-ray Spectroscopy
TIS	Tank In Series
NTU	Nephelometric Turbidity Units

1 Introduction

Microalgae are photosynthetic microorganisms which convert sunlight and carbon dioxide into algal biomass. Algae, either multicellular (macroalgae) or unicellular (microalgae) are considered as the earliest forms of life (Falkowski *et al.*, 2004). With over 3 billion years of evolution, microalgae taxonomy measures upwards of 50.000 species, with only 60% of those actively being researched (Sathasivam et al., 2017). Microalgae have been in a focal point of research for more than half a century (Richmond, 2000; Chisti, 2007). This is due to their unique ability to generate large quantities of valuable compounds, such as lipids, carbohydrates, vitamins and proteins; which can be used in a range of industries such as the pharmaceutical, nutraceutical, chemical, and petroleum (Muller-Feuga, 2013; Hanifzadeh *et al.*, 2018; Khan, Shin and Kim, 2018).

In order to utilise these compounds, a series of critical steps in the processing of algae must take place (Halim, Danquah and Webley, 2012). First, the controlled cultivation of a single algal species, in an aqueous habitat, under the irradiance of solar or artificial lighting. This can occur outdoors, in open systems, or indoors, in closed systems called photobioreactors. Second the efficient separation of the biomass, extraction of desired compound (e.g. lipid, protein) and conversion or purification of the compound into the various end uses (e.g. biodiesel, food supplement).

In addition to the value from the fundamental biological functions of the cell itself, the bioprocessing of microalgae also makes a strong environmental case. First and foremost, as photosynthetic organisms' algae capture CO_2, converting it to O_2 as they grow. Moreover they occupy non-arable lands, can grow in waste water with high contents of contaminants such as nitrogen and phosphorus (Ledda *et al.*, 2013a). Finally microalgae are capable of producing a number of compounds from a single bioprocess line, resembling a modern biorefinery (Caporgno and Mathys, 2018).

Microalgae are considered 'miracle plants' (Yusof *et al.*, 2011). They are considered an important agricultural commodity for the 21st century (Richmond,

2000), as they are a more sustainable protein source than the conventional pork or beef and it's been projected to overtake these sources by 2050 (Caporgno and Mathys, 2018). Finally, algae have been thought of as the only potential plant life capable of supplying the total current transportation fuel requirements of the US, at a fraction of the arable land which would be required for conventional energy crops. Therefore, algae is capable of an crucial counterargument for the food vs fuel debate (Chisti, 2007, 2008; Torzillo and Seibert, 2013) .

In spite of the attention and focus microalgal biotechnology has received, its development has not followed the same trajectory. Current figures of total production of microalgae biomass range from 5,000 to 15,000 MT/year (Sathasivam et al., 2017). Where 90% of this production occurs in open ponds (artificial water reservoirs where algae freely float on the surface). which are extremely inefficient (Płaczek, Patyna and Witczak, 2017) and act as a major regulatory barrier in the production of compounds for the nutraceutical and pharmaceutical industry (Khan, Shin and Kim, 2018). Furthermore, microalgae derived biodiesel is to this date not cost effective, costing 10 times more than that of crude oil in the international market; placing algal biodiesel nearly a decade away from being an economically viable (Khan, Shin and Kim, 2018). Which considering the target of 36b gallons/annum by 2022 described by the US renewable fuels standard (RFS) (Qari, Rehan and Nizami, 2017), still ranked microalgae well below other sources renewable fuels; e.g. bioethanol which production is already at 22-35b gallons/year, and projected to surpass 100b gallons/year in the same time span (Bharathiraja et al., 2014; Khan, Shin and Kim, 2018).

In view of this, the natural question that arises is why? What are the key reasons, which despite their potential, microalgae biotechnology has failed to take off? The answer seems to be already given in the turn of the 21st century by Richmond (2000) and reiterated later by Mandenius (2016).

Richmond (2000), who is considered one of the seminal authors in algal biotechnology, states that the microalgae doctrine inspired by Burlew (1953), according to whom microalgae will replace all traditional agriculture, was

evidently not realisable in the 20th Century (Burlew, 1953; Richmond, 2000). In Richmond's (2000) opinion the main causes for algal biotechnology's slow progress can be condensed to three points. First of all, he highlighted the lack of communication between biology and technology, specifically in the context of light and its implementation. Then, he argued about the colossal design errors in industrial scale photobioreactors, which stem from the fallacy that each growth factor is independent of others. Finally, he suggested the lack of cost effectiveness of microalgae cultivation, which covers both technical (capital and operational costs of bioprocessing installations) as well as biological aspects (cellular productivities and yields).

In a later publication, Mandenius (2016) adopting a more technical position, suggests that the main challenge modern algal biotechnology faces is transferring the complex understanding of biology from the focus of natural sciences into the engineering domain. He emphasizes that there is a prevailing mindset that is biased towards product optimisation dictated by natural sciences rather than process development driven by engineering. This has resulted in very slow and incremental progress in photobioreactor (PBR) and bioprocess design with no significant advances.

The point Richmond (2000) and Mandenius (2016) made is supported by evidence provided by Chisti (2016), Placzek, Patyna and Witczak (2017) amongst others. Specifically, as per Chisti (2016) from the 1960's open pond cultivation has been used in mass production of microalgae biomass, although it has demonstrated high inefficiencies such as, low biomass productivities, large water volume requirements and high operational costs (Chisti, 2016). Corelating to that, in the exhaustive state of the art reviews of cultivation techniques carried out by Placzek Patyna and Witczak (2017) and Kumar et al. (2011); where both suggest that no major technological advancement has been made in the field of algal cultivation in the past two decades. Both authors provide evidence that little progress has been made in discovering novel cultivation techniques; but rather more effort has been given in the incremental optimisation of the current photobioreactors (Tubular, Vertical, Flat panel).

Huang et al., (2015), and Reis and Da Silva (2016), summarised that the design of photobioreactors is still taking place semi-empirically. Thus many important environmental factors, which critically influence the microalgae (i.e. light, mixing, mass transfer, pH, temperature), are systematically underestimated. They therefore, become limiting barriers towards any practical scale-up of the algal mass cultivation (Chisti, 2016; Huang et al., 2015; Kumar et al., 2011; Płaczek, Patyna and Witczak, 2017; Reis and Da Silva, 2016).

Evidence supporting the above is given by Bajpai, Prokop and Zappi (2014), suggesting that there is a very strong link between algal growth parameters and PBR design features. Specifically, the evidence provided by the authors show that the geometric features of the PBR (Length, Height, Width, Diameter) affect light penetration and mixing uniformity whereas it's shape (Tubular, Plate) and orientation (horizontal, Vertical) affects mass transfer (Bajpai, Prokop and Zappi, 2014). In addition, the authors suggest that, there are practical limitation to the methods of mixing as well. Since light supply and PBR architecture are fixed, effective agitation induces mobilisation in the algae, dictating the cyclic pattern of the culture between light and dark cycles, effective nutrient absorption from the substrate and enables gas transfer between the cell and the environment (Bajpai, Prokop and Zappi, 2014). Complementary, Kumar (2011) argues that the effect of proper mixing incurs an increase of up to 40% in productivities. Currently, devices for agitation, which are implemented in PBRs, are the injection of air and mixing with paddlewheels stirring with impellers or pumping through a network of tubes all of which pose very difficult scaling issues (Nauman, 2002; Camacho *et al.*, 2011; Soman and Shastri, 2015)

Based on the information presented here, the suggestion given by Mandenius (2016) that engineering, and science are disassociated is clearly evident. The lack of scalable and optimised technologies for the cultivation of algae, coupled with the limitations of current mixing technologies, which one would consider archaic, uncover the need for transformation focussing on the development of cost effective and scalable photobioreactors.

1.1 From ponds and batch to flow and continuous cultivation.

Algae are dynamic systems, which the continuous and natural sinusoidal motion of the waves, and constant replenishment of the substrate (sea, lake) create wakes, that mobilise the culture, enabling mass transfer and photosynthesis. Therefore, to emulate nature an environment must be created where microalgae are always in non-equilibrium conditions.

Regardless of the PRB (e.g. pond, raceway, column, tube, plate) and mixing technology (static, mixed, stirred, aerated, pumped) in place, cultivation can occur in three modes, batch, semicontinuous (fed-batch) and continuous modes. In batch cultivation, the inoculum and substrate (growth media) are loaded into the PBR at the start of the cultivation period and then removed at the end. In fed-batch systems additional substrate (nutrients) are fed into the system during the cultivation, where both the products and nutrients are removed in the end. Finally in continuous there is a constant stream of nutrients fed into the system, at the same time as the effluent of the system containing cells, products and residuals are removed continuously; this is contrary to perfusion mode, where the substrate continuously enters and exits the system but the cells are retained. (Matos, Coeli, *et al.*, 2014; Larroche *et al.*, 2016). There are significant advantages in continuous compared to batch. Such as reduced downtime during cultivation cycles, effective controllability of process conditions and most importantly reduction of risk, since the biotic parameters can be monitored closely (Doran, 2013).

In order for a microalgal cell to grow it requires light, carbon and a combination of nutrients in an aqueous environment. These nutrients make up the substrate in which the microalgal cultivate. The correlation between growth and elemental make up of a substrate has been the topic of much deliberation (Doran, 2013), and as suggested by Mandalam and Palsson (1998) in order to maximise growth of the microalgal cell which leads to increased productivities focus must be given to the quantity and selection of each element. (Mandalam and Palsson, 1998)

Microalgal cells grown in batch conditions undergo multiple phases (Figure 1-1).The onset and duration of these phases is highly correlated, amongst others, with the quantity of nutrients that remain in the substrate. The cultivation starts

from the lag phase (1), where the microorganism is acclimatising to the new environmental conditions, the accelerated growth phase (2) occurs where cells transition towards achieving maximum growth rates , the linear (exponential) growth stage (3) where, the rate of growth reaches its maximum, the decline phase (4) where the growth rate declines due to the substrate reaching limiting nutrient levels and finally the stationary phase (5) where growth is absent, and eventually the death phase in (6) where cells inevitably die due to the culture reaching conditions inhibitory to growth, Which is typically due to nutrient depletion from the substrate (Doran, 2013). It is evident that the quantity of nutrients plays a significant part in the growth cycle of the cell, and in order to maintain a thriving culture there must be a strategy employed where these nutrients are supplied.
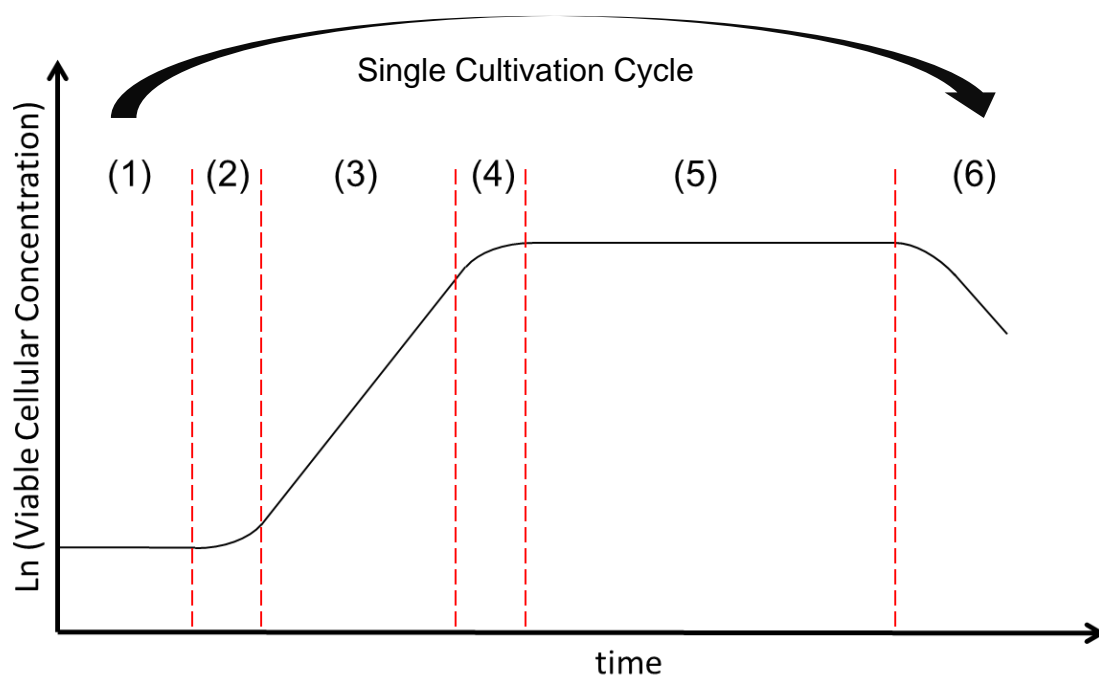
Figure 1-1 Growth stages indicated on the cellular concentration profile against time in batch cultivation mode.

Transitioning from batch, in semi-continuous and continuous cultivation, the input of material to replenish the substrate creates a different profile than that of batch. As shown in Figure 1-2, the batch (c), fed batch (b) and continuous (a) cellular concentration profiles during cultivation are compared. For the batch, as has been

described, the cultivation method results in periods where the whole system is static or even declining, on the contrary in the semi-continuous (b) and continuous (a) modes, these periods are not present. They are overcome by either the periodic injection of material (substrate) into the culture (i.e. sub-culture), where the concentration drops, or the continuous, and balanced input and output of material from the system resulting in a constant concentration profile. In both these cases the cultivation is always kept in a dynamic state. This translates to reduced wasteful periods, reactor downtime, and heavily reduced threat to the cell's viability, resulting in increased yields and productivities.
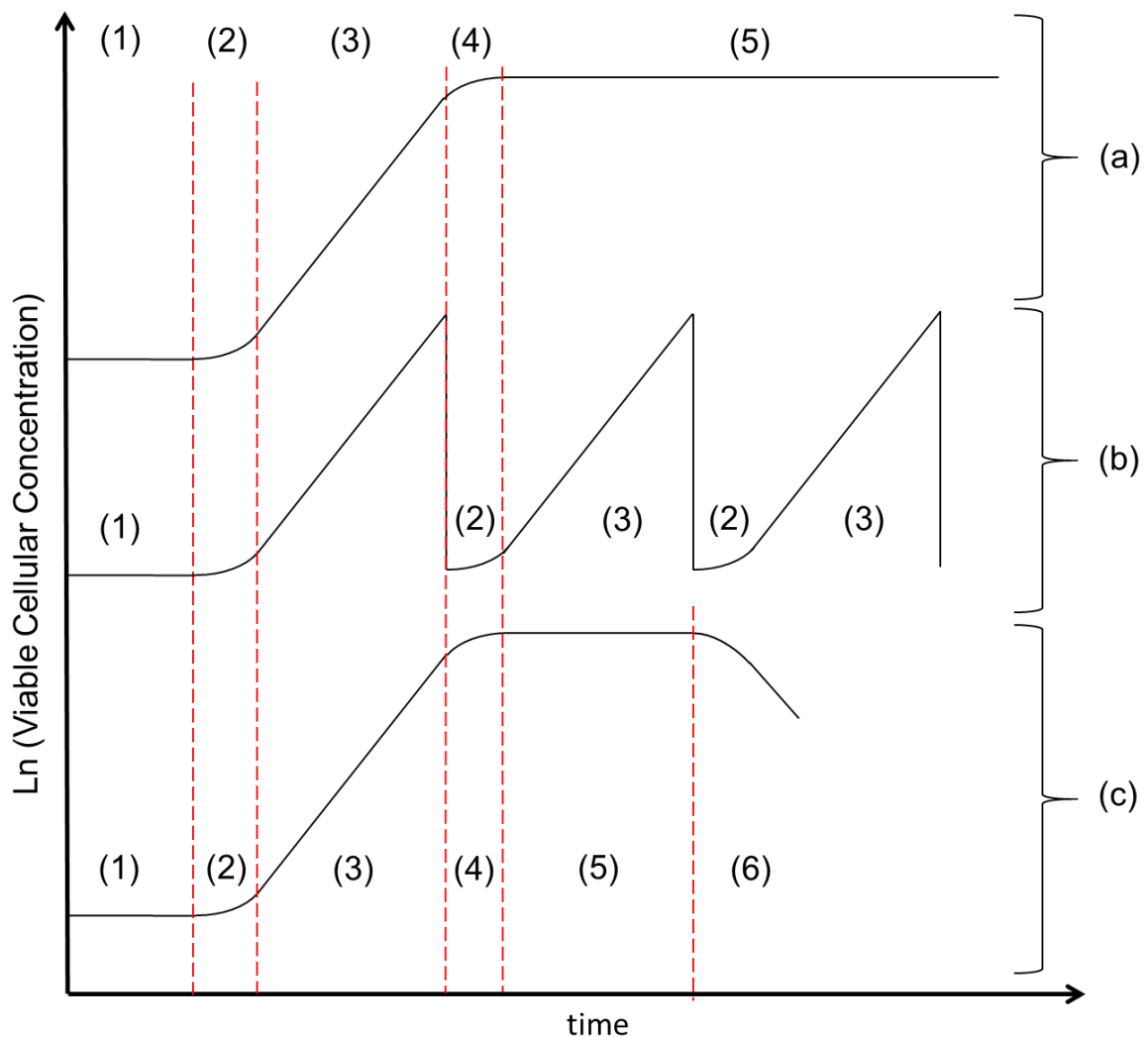
Figure 1-2 Batch (c), semi-continuous (b) and continuous (a) cultivation methodologies. Cellular concentration profile against time.

Although there is no single rule or criteria matching process to technology, or vice versa, it is evident that some technologies take advantage of the benefits offered by the different bioprocessing modes, thus bioprocess and PBR work synergistically to create an optimised system. For example, operation of column reactors is predominantly batch, however can also be carried out in semi-continuous and continuous, as reported by Khoo, Lam and Lee (2016) and Matos et al., (2014), whose experiments supported that semi-continuous and continuous operations enhance growth are both viable and more effective alternative to batch operation (Matos, Coeli, *et al.*, 2014; Khoo, Lam and Lee, 2016). This is similar with what is occurring in adjacent sectors in industrial biotech where, as stated by Doran (2013), currently most of the microorganism bioprocessing occurs in vessels such as stirred tank reactors (STRs).

As the name suggest STRs are essentially large cylindrical vessels of a fixed volume, with an impeller used for mixing, and are predominantly operated in batch. Similarly with column reactors, they can also operate in semi continuous (fed-batch) or continuous regimes, aptly named continuous stirred tank reactor (CSTR) (Nauman, 2002; Doran, 2013). In industrial biotechnology such vessels are at the forefront of technical and scientific focus. This is counterintuitive according to Plumb (2005) and McGlone (2015) since they suffer from significant drawbacks, regardless of their operating mode (batch or continuous). Specifically, they lack the parametrisation required for complex processes, they have poorly understood kinetics, they are notoriously difficult to scale up and suffer from limiting mixing efficiency which often lead to suboptimal yields and poor reproducibility, especially in continuous mode.

On the other hand, in the same field, a technological breakthrough which has the potential to advance continuous processing are flow reactor technologies. Flow technologies are an end to end infrastructure which enable continuous manufacturing to occur. In combination with flow technologies continuous manufacturing reports very attractive benefits. As stated by McGlone et al., (2015), continuous manufacturing in flow technologies, offer efficient use of raw materials, increased controllability improved yields, process reliability,

reproducibility, and most importantly are scalable (Abbott *et al.*, 2012; McGlone *et al.*, 2015).

A critical component enabling this transformative technology is the flow reactor, one example of this is the plug flow reactor (Abbott *et al.*, 2012). Plug flow reactors, as explained by Doran (2013) are an alternative to mixed operation (CSTRs and STRs), in which mixing occurs as the processed liquid passes through the reactor length in a discrete 'plug'. Since the processing fluid propagates through the reactor at a constant speed all parts of it experiencing the same residence time. (Doran, 2013).

In algal bioprocessing, continuous operation of plug flow reactors has not yet been reported, however flow systems exist. Systems such as the tubular PBR and raceway ponds, are very commonly used, but as has been already highlighted and reiterated by Gupta and Choi (2015) the severely inhibited, uncontrollable, inefficient and costly mixing, coupled with a lack of scalability, do not provide a suitable platform for continuous flow to take hold (Gupta and Choi, 2015).

One reactor with the potential to change that is the oscillatory baffled flow reactor (OBR). The OBR is a type of plug flow reactors, which as its name suggest induces an oscillatory motion across a series of constrictions (baffles), as the liquid flows downstream. This complex motion enables highly controllable, and effective continuous manufacturing which according to Abbott et al., (2012) has the potential to be a major gamechanger in bioprocessing.

Specifically, in algal biotechnology, which in large scale is predominantly batch driven, the implementation of scalable continuous flow technologies, such as OBRs, would enable a pathway in which,

- Scaling would facilitate expediting the transfer of knowledge and technology from lab to pilot scale,
- Mixing would be re-examined, and transformed from pumping and gas agitation, to an oscillatory flow where mass transfer is increased at very low shear rates and a much lower power requirement.

In summary the main challenges which modern algal biotechnology face, is the lack of a suitable technology which is scalable and optimised to operate effective and controllable flow regimes. Therefore, in employing a strategy to address these issues, the development of a novel photobioreactor based on the OBR technology, would inherently benefit a given process since scalability and mixing efficiency will be implemented by design. The combination of novel technology and an effective cultivation strategy, with consideration to substrate (growth media make-up) would lead to a cost effective and optimised system for the cultivation of microalgae.

1.2 Aim and objectives

The aim of thesis is to develop an enabling platform for algal biotechnology to become commercially significant and industrially attractive. The platform will aim to facilitate scalability, increase cost effectiveness and intensify the cultivation of microalgae, via the implementation of continuous flow technologies (plug flow) into a new PBR, resulting in the delivery of a novel technology, which design is driven by a strategy combining scientific research and technical development.

The objectives are to:

1. Reduce the cost of the cultivation by means of optimising the substrate media formulation.
2. Design a novel PBR technology, based on the critical design considerations and current drawbacks identified by current state of the art.
3. Scale up the PRB design from laboratory to pilot plant and test the performance of the scaleup.

1.3 Research Context

The Makatsoris Group has been active in the field of continuous manufacturing using flow reactor technology for the past decade. The group has successfully developed and modular chemical flow reactor system (Makatsoris, US 2015/0010445 A1), and a framework which transfers batch chemistries to multiscale flow systems. The reactor has demonstrated its ability to host crystallisation, extraction and conversion reactions, with potential in

pharmaceutical, chemical and bioprocessing industries. Most notable examples being the synthesis of meta stable materials (Frandrin, 2019), the synthesis of gold nanoparticles in the range of 5-15nm, synthesis of quantum dots and the extraction and conversion of lipids to algal based biofuels (Alissandratos, 2014), All carried out in continuous flow conditions using both microscale and mesoscale systems (Alissandratos, 2014a; Flandrin, 2019)

The Group's interest in algal bioprocessing was driven by successful experimentation in downstream bioprocessing coupled with the recognised gap in technological advancement (Alissandratos, 2014). The concept was to transfer the technical and scientific knowledge as well as engineering experience, into algal biotechnology, which would endeavour to potentially develop a flexible system, processing a variety of photoautotrophic and mixotrophic strains, from cultivation to in situ downstream extraction and conversion.

This concept attracted investors which lead to the formation of a technology start up called Centillion Technology Ltd. (Reg No: 11059163). This company became the commercialisation route for the intellectual property generated by the continuous flow laboratories and financially supported 30% of the algae project, specifically the financing and support of a bioprocessing pilot plant on the Cranfield University campus.

2 Literature Review

2.1 Microalgae Bioprocessing

The transformation of algae from cell to products enabled by a suitable process. Algal bioprocesses typically comprise of three major steps: cultivation, harvesting and conversion. Cultivation is where algae grows, and duplicates given a suitable environment. Harvesting is the operation where the biomass is separated from the water; and finally, conversion is where the biomass is processed and transformed into a target product, (e.g. oils, fuels, nutraceuticals)
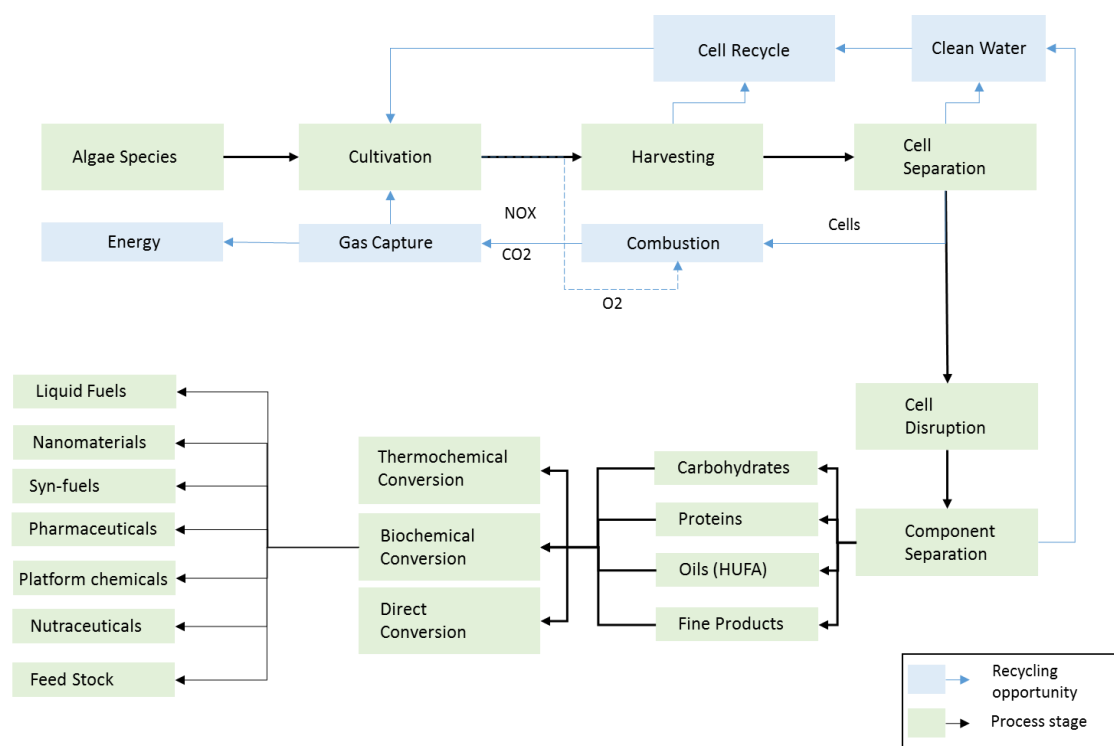
Figure 2-1 Typical Bioprocessing routes for microalgae, potential recycling/recovery pathways indicated.

A biological organism, microalgae require an environment which offers favourable conditions for it to thrive. For this to be achieved a precise set of parameters need to be met on a consistent basis. Considering the diverse taxonomic grouping of algae, it is expected that, desired growth conditions will vary, from strain to strain, however as a minimum all microalgae require; a nutrient rich environment, a constant supply of carbon, and an energy input.

Cultivation is a single step in the whole bioprocessing line and is critical to the success of all downstream processes. This fact is prominent considering the bias attributed to it, in comparison with the rest of the downstream bioprocessing line. Research emphasis throughout the years has been given to all aspects of cultivation; such as the growth media formulation, (Millington, Goulding and Adams, 1988; Lv et al., 2010) which is driven by tuning the elemental balancing of the nutrients in the growth media to the algal strain requirements (Danquah and Harun, 2010; Rasdi and Qin, 2015; Seyhaneyildiz Can, Koru and Cirik, 2017),

Cultivation of algae is a broad topic, which evidently attracts the interest of biologists and engineers alike. Microalgae can either grow *in vivo*, taking advantage their naturally evolved intrinsic ability to grow and thrive as part of their respective eco-habitat, without any human intervention, or *in vitro*, where they are taken from their natural habitat and introduced into a varying scale laboratory environment thereby controlling their growth factors for maximum culture grow and cell multiplication. Although the line between the two approaches isn't as clear cut as in other applications there is a third midway point when it comes to growing algae, that is by human intervention in their respective habitat, the raceway or algae ponds.

Algae ponds are a system of open lakes or ponds which process parameters are minimally controlled. The advantage of such a system is primarily due to the fact that the environmental parameters and variables are matched with a specific algal strain. Such environmental parameters are water salinity; marine algae species such as *Spirulina plantesis* thrive in waters with high sodium bicarbonate concentrations whereas *Chlorella vulgaris* cannot survive unless water has a low salt content, i.e. fresh water algae (Singh R.N., et al. 2012).

Raceway ponds are a very low-cost option for algae cultivation in terms of maintenance and production cost, due to their extreme operational simplicity and primary reliance on existing environmental conditions (Singh R.N., et al. 2012). The pond or lake is typically artificially modified by having a section dug up and creating a shallow track, typically an oval channel from concrete or PVC piping. Algae are circulated around the 'raceway' track with the use of a pump or a

paddlewheel, providing agitation and mixing, promoting nutrient absorption while expelling unwanted oxygen, thus achieving a thriving growing culture. This method is very simple in its operation, and facilitates easy monitoring and sub culturing. This method essentially is a more monitored and controlled natural environment exploiting the environmental nutrients and parameters such as heat, water pH, solar irradiance and carbon dioxide provided by the environment and simply monitoring and controlling them as necessary. Algae 'raceway' ponds can be artificially constructed in most sized ponds. The largest commercial algae production facility using this method covers an area of 750 hectares (Borowitzka M.A., 2005), but as the size of the facility increases so are the disadvantages and difficulties of maintaining such a system. The size of a system is directly linked to the probability of foreign contaminants penetrating and inhibiting the growth of a system, foreign contaminants terminating the system or any losses due to marine and freshwater life feeding off the algae. The intermittency of solar irradiance and temperature fluctuation threaten both small and large open pond systems as well as the seasonality of some tropical microalgal species, due to longer hot and sunny weather periods which are more predictable and have a higher output than European and North American species; making the output of any facility unpredictable.

On a bioprocess level a major disadvantage of such a system is its low yield. Although open pond/lake systems are far less costly to construct and maintain considering their alternative (*in vitro*: PBR), the average yield of an open pond system is 20-22 $g/m^2/d$ of which the lipid content is 24-40% of the dry weight (Borowitzka M.A., and Moheimani N.R., 2010). The current global demand for algal biomass is 15,000 tonne (15M Kg/y), currently 90% of it is being carried out by pond systems. (Płaczek, Patyna and Witczak, 2017).The current global fossil fuel requirement in 2010 was 84.3 106 bbl /day (bbl = barrel=158.984L); meaning that trying to achieve a 0.5% (est. 100,000 bbl lipids) of the demand with open pond algal cultures would require a land area of approximately 21 km^2 in which 7-14 km^2 would be required to be a working pond system. If algal based biofuels were to meet the global demand it would require a total land area of 1,922,334

km^2 approximately 0.11% of the earth's prime 'green' land (Borowitzka M.A., and Moheimani N.R., 2010).

Furthermore, optimisation of raceway ponds is an unlikely scenario, since any further increase in productivities of an open pond algae systems exceeding the average 20-24g/m^2/d ($Px_{max} = 30$g/m^2/d) stresses the algal culture, thus requiring a sharp increase in maintenance costs. This is due to the need for more control of: nutrients, solar radiation leading to photosynthetic efficiency and an effective barrier between marine life and the algae itself.

Bioreactors are enclosed vessels which replicate ideal environmental conditions required for a specific microorganism to thrive. Photobioreactors (PBRs) are illuminated bioreactors specifically suited to photosynthetic microorganisms. In vitro cultivation of algae predominantly requires a laboratory setting, and a photobioreactor of such a scale depending on the desired output. The larger the scale the larger the yield, the cost of production and maintenance, are inherently much higher than the cost of comparable open pond system.

With cost as their only major disadvantage PBRs can create the optimum environment for any algae species, ensuring its survival and accelerated growth. PBRs are capable of minimizing contamination and predation risk, by being held in an isolated clean and contaminant and free environment. They are capable or accurate dosing of nutrients, CO_2 and water, required for growth and sub culturing. Complicated and high intensity mixing of all nutrients as well as extraction of unwanted gas O_2. And finally, the ability of controlling light intensity. This all leads to a healthier culture, enabling higher cell concentrations, denser cultures, thus higher consistent yields. (Singh R.N., et al. 2012). Photobioreactors much like algae widely vary in design and function. Each designed and modified to ensure its suitability with a specific algal subspecies. On the other hand drawbacks such as fouling of the PBR's inner tubing, inadequate flow design forcing the cells to rupture under high stress and impacts due to high flow rates and the near impossible task to reduce any non-illuminated spots of the bioreactor have forced experts to constantly revise and redesign PBR's in order to minimise limitation and ensure a highly productive and efficient system.

2.1 Photobioreactors: Current state of the Engineering

There are many types of PBR's in industry, many being adaptations of others, the main categories of PBR are the vertical (bubble) column, the flat panel, the tubular and other iterations such as the bag and stirred tank photobioreactor). (Singh R.N., et al. 2013).

2.1.1 Vertical (Bubble) Column

As the name suggests bubble columns are cylinder shaped vessels in which the algae culture is mobilised by the injection of air. Bubble columns are usually found with an internal diameter of >200mm with a ratio of height to diameter in the range of 4-8 so that the surface area to volume ratio is driven to optimum levels (Płaczek, Patyna and Witczak, 2017). A typical installation of a vertical column PBR would be a tall cylinder with 400mm internal diameter and 4m height, made from a transparent material to enable light transmission. Agitation and mixing in the PBR is achieved by a gas inlet at the bottom of the reactor which also feeds the culture with Air + CO_2 or pure CO_2. Bubble column reactors come in three different configurations: a simple vertical bubble column, a vertical bubble column with divided plate placed internally, or separate non-agitation column placed adjacent which purpose is to separate the flow to a riser and down-comer region forming a loop (Płaczek, Patyna and Witczak, 2017).

2.1.1.1 Light

In outdoor applications light is provided by solar radiation, which it is not a major consideration. However, when placed indoors the requirement for large light installations would potentially be cost prohibitive. Bubble column PBRs are typically light harvesting units therefore the photosynthetic efficiency depends on the agitation provided, which drives cells from the photic (near the surface) to the dark (near the middle) zones and vice versa. Bubble columns typically operate at high efficiencies due to their ability in creating circular patterns in the flow of liquid between the inner and outer regions (Kumar *et al.*, 2011).

2.1.1.2 Mixing

Mixing is achieved by the input of air at the bottom of the vessel, therefore the use of mechanical parts such as stirrers, impellers are not required. This has a positive effect since it reduces potential shear stresses that could potentially cause cell degradation (Kumar et al., (2011). Mixing intensity is proportional to the scale of the reactor, however in scaled up variants distribution of the bubbles becomes a challenge. At extreme diameters, localised generation of bubbles causes ineffective mixing and biomass sedimentation, which combined with large column heights, coalescence of the bubbles reduces the mixing intensity even more. One solution for larger scales is to use a series of perforated plates, placed equidistantly along the height of the reactor, which force the redistribution of the coalesced bubbles (Kumar *et al.*, 2011; Płaczek, Patyna and Witczak, 2017).

2.1.1.3 Mass transfer

Vertical bubble columns are characterised by their high volumetric CO_2 transfer rates, which enable efficient and simultaneous CO_2 utilisation and optimal O_2 removal. However at large scales, high superficial gas velocities are required in order to achieve uniform gas distribution along the height of the column, which would inevitably incur some cell damage in the lower regions of the column (Wang, Lan and Horsman, 2012).

In the airlift reactors, where the algae is elevated upwards by the bubbling in the riser section, efficiency is linked with the gas holdup time of the algae, the degassed algal cells then moves down in the annular space in laminar fashion until it enters the bubbled region and begins the upward path again. The residence time in the phases, heat transfer, mixing, turbulence and mass transfer are driven by the gas inlet flowrate and bubble size.

2.1.1.4 Process parameters

These types of reactors are relatively easy to scale. Scaling up the reactor would entail a disproportionate increase in height compared to the diameter, which would result in a small increase in additional spatial requirements. However, any further increase in diameter would reduce the light exposition, thus limiting the

penetration depth of light from the outer area towards the centre. Material costs in scaling up are relatively low since the design and construction are cheap. On the other hand, the costs of mixing could be inhibitory since the cost of gas would limit the profitability of the installation. For this reason this design is often used in CO_2 mitigation or sequestration applications, which position it adjacent to a supply of flue gases and sources of urban pollution. An additional challenge in scale up according to Barbosa et al. (2003) as cited by Kumar et al., (2011), is the design of suitable gas delivery systems enabling the control of L/D cycles and mass transfer in airlift reactors. Considering this bubble columns are limited to a selection of algal strains they can host, therefore limiting the applicability of these PBRs. Placzek et al. (2017), identified that airlift reactors are not suitable for algae with low specific weight due to them being susceptible to flotation effects. The specific weight of algae is inversely proportional to the volume of lipids, therefore bubble column PBRs are not suitable bioprocesses where the product is oils, therefore limiting the applicability even more (Kumar *et al.*, 2011; Płaczek, Patyna and Witczak, 2017). Furthermore, temperature control of these reactors is often a difficulty with larger scales, since large scale airlift PBRs are only used for outdoor cultivation, which reduces the ability to control temperature and light. For low density cultures this poses an even higher risk since photoinhibition during times which the solar intensity is high. Thermostats have been known to being used however the cost is considerable and proportional to the scale. (Płaczek, Patyna and Witczak, 2017).

2.1.2 Tubular Horizontal & Vertical

Tubular horizontal and vertical are most popular configurations of reactor (Wang, Lan and Horsman, 2012). Tubular photobioreactors comprise of a series of parallel tube sections which are joined together forming a loop. These parallel tube arrays can either be placed vertical with each tube placed above or below the previous, or horizontal with each tube placed to the left or right of the previous. Tubular photobioreactors are suitable for continuous cultivation processes. These are considerably large installations, with tube lengths reaching several

meters, making them suitable for outdoor cultivation (Płaczek, Patyna and Witczak, 2017). As with the bubble column, the design of these reactors is restricted by both, biotic and abiotic parameters. The tubular diameter of the light harvesting unit is typically found to by between 10-60mm and an optical path length of several hundred metres. Smaller diameters in the range of 10mm are used in applications of high cellular densities, however as cited by Placzek et al., (2017), the upper limit is 0.1m (Huang *et al.*, 2017a; Płaczek, Patyna and Witczak, 2017). Furthermore, as mentioned by Chisti (2008), an additional design consideration is the length of the tubular sections of the reactor which is limited by the dissolved oxygen concentration to be removed from the system. As a rule of thumb, the length of the tubular sections should not exceed 80m of tube lengths.
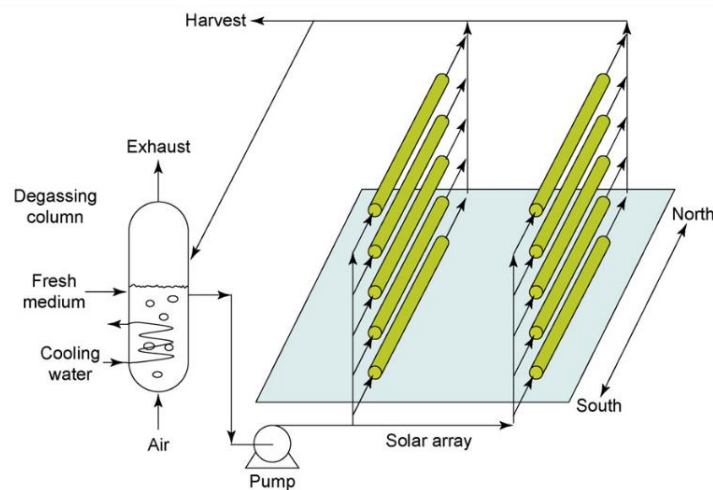
Figure 2-2: Tubular Horizontal PBR system arrangement, with the light harvesting unit-oriented North/South so that maximum light harvesting is conducted (Chisti 2008).

There are three variants of these reactors, for which design is stemmed by parametric optimisation based on the strain and application. The first is as described and is considered the "original" design where the tubes are arranged in a vertical or horizontal manner. The second is achieved by arranging parallel tubes at 5-7° from the horizontal plane, this enables gas exchange to occur in the light harvesting unit; since the gas naturally bubbles up towards a collector vessel which is connected to all the tubes at the highest point of the system. In addition

to being a more effective light collector, It is also a more effective light harvester since the inclination angle allows for less shaded areas (Huang *et al.*, 2017a; Płaczek, Patyna and Witczak, 2017). The size of these units is reported to be 43mm diameter and 6.4m in length per tube, where the largest experimental unit in operation was at 4000L consisting of 8 parallel units and 44 metres, which reported productivity when cultivating *Nannochloropsis* was 0.7g/l/d. As cited by (Kumar *et al.*, 2011), Tredici and Zittelli (1998) designed a similar system with 34mm diameter tubing at a 5° to the horizontal plane with implemented temperature control achieving higher productivities than a flat plate reactor at 1.26 g/l/d using a *spirulina* sub-strain called *Anthrospira*. The third variant is the helical tubular reactor. As the name suggests this reactor is characterised by flexible tubing which is spirally wound around a truncated pyramid or cone mounting structure. The internal diameter of the reactor is 24 to 50mm and similar to the conventional vertical and horizontal configuration the length is limited by the O_2 generation in the system, however since the helical PBRs arrangement allows for the gas to rise through the coil upwards it allows for easier gas expulsion. As cited by Kumar et al., (2011), Tredici and Zittelli (1998), designed a coil type PBR with 30mm diameter at a coil inclination of 2° achieving 0.9 g/l/d. Since this is one of the few comparative study between the two variants it was found that the photosynthetic efficiency between the inclined horizontal and the helical was superior on the inclined variant than the coiled, with 23% versus 6.84% (Kumar *et al.*, 2011).

2.1.2.1 Light

Tubular PBRs are typically used for outdoor applications, due to their long length and flexibility they can be arranged and positioned as to maximise the capture of solar radiation throughout the day. Like in bubble column reactors, there is a size limitation in the internal diameter of the tube section, which are typically designed in the range of 10-60mm with upper limit being 100mm,Thus avoiding restriction of light penetration into the deeper levels of the algae culture (Płaczek, Patyna and Witczak, 2017). Having said that, these PBRs are usually placed outdoors where the solar intensity averages are lower than artificial lighting (Fluorescent, LED). Which depending on the configuration the penetration depth is

41

considerably higher, albeit at a higher cost. Light and Dark (L/D) cycles are achieved through the turbulent flow regime which enables suspended cells to circulate between the centre (light diminished region) and the outer regions (light surplus) of the tubing. Due to the characteristics of the turbulent flow regime, optimisation of the L/D cycle is not effective in these reactors. This occurs predominantly due to the uncontrollable nature of turbulent flow regimes, in addition to the lack of control in the residence time of the algae in any holding or buffer tanks in place.

2.1.2.2 Mixing

The tubular pipe section of the reactor is used to harvest the light, the flow through the tubes is achieved by using a mechanical pump (centrifugal, membrane, peristaltic), the flow regime although turbulent, its purpose is not mixing, but rather to ensure that algal suspensions do not sediment or attach to the inner surfaces of the tubes. The primary mixing and mass transfer occurs in a separate vessel which the flow is circulated from (Płaczek, Patyna and Witczak, 2017).

2.1.2.3 Mass transfer

Solid-liquid, liquid-gas mass transfer in tubular systems occurs in vessels placed inline with the flow. These vessels like the bubble columns, are where the gas and nutrients are inserted into the system and mixed, the gas transfer of CO_2 and removal of O_2 from the system occurs there, as well as the input of nutrient material into the system (Placzek, Patyna and Witczak, 2017).

2.1.2.4 Process parameters

Like the vertical column this type of reactor is relatively easy to build, with cheap material costs, and excellent biomass productivity, however profitability however does incur penalties due to the large spatial requirements of this PBR.

One of the main drawbacks of this type of reactor is the energy consumption. In outdoor applications the light energy is provided by solar energy which is abundant and free, however it does limit applicability and temperature control in addition to requiring vast areas of land. In this scenario the main parameter that drives energy consumption is the use of mechanical pumping. The consumption

is reported to be approximately 2000 W/m^3 (compared with 50 W/m^3 for flat plate reactors), The high energy is required in order to propagated the liquid through the tubing network as average linear velocities of 20-50 m/s, this figure is according to Kumar et al., (2011) (Kumar *et al.*, 2011), whereas other authors report an order to 10 less at 0.20 -0.50 m/s. (Płaczek, Patyna and Witczak, 2017)(Huang *et al.*, 2017a)

Temperature control of the reactor is also a cost consideration. Due to the large surface are they cover conventional heating/cooling methodologies are not applicable. Solutions that has been reported in literature involve, the physical shading of the tubes to reduce the solar intensity thus cooling the PBR tubes, or submersion of the reactor in water. Both of which have demonstrated potential however the cost majorly outweighs the benefit. (Wang, Lan and Horsman, 2012).

Scalability of tubular reactors is easy with the addition of extra members or arrays of light harvesting tubes, however as reported by various authors there are both biotic and process limitations in scaling up. The obvious and predominant limitation in scale up is the size of the internal diameter of the reactor, which is required to be large enough to create light and dark regions in the cross-section of the tubing, however exceeding sizes in the range of 100mm created unproportioned dark to light regions. Length is also consideration, predominantly due to the O$_2$ accumulation in the system the length of the straight pipe is limited to 80m as reported by Chisti (2008), however scale up by addition of extra parallel tubes will incur higher pumping costs, due to the pressure loss of the extra U-bends. Inclined and helical configurations do solve the gas exchange issue when a gas collection vessel are positioned at the top of the PBR, where bubbles naturally tend to accumulate, however scaling up by addition of extra tube length does increase energy loss through the complex tubing network. (Kumar *et al.*, 2011)

In terms of applicability this type of reactor has a very important constraint, which limits its use with certain types of algal stress which are susceptible to high stresses induced by centrifugal pumps (Kumar *et al.*, 2011; Wang, Lan and Horsman, 2012; Huang *et al.*, 2017a)

2.1.3 Flat Panel

Flat panel PBRs were first described by Burlew in 1953. Since then there have been many iterations of the original design. These types of PBR often come in the shape of a rectangular plate which dimensions dictate the surface to volume ratio, the illuminated area, and the optical light path (Wang, Lan and Horsman, 2012).

2.1.3.1 Light

The key benefit of is the large illuminated area which offers high photosynthetic efficiencies (Płaczek, Patyna and Witczak, 2017). On the same note the key dimensional parameter is the thickness of the plate, dictated by the light implementation (dual or single sided) the thickness faces similar constraints with light penetration as the other reactor types. It is generally reported that a smaller width offers a shorter light path therefore the higher the optical density of the reactor. The thickness rangers from a few millimetres up to 70mm, from which the length of the reactor is derived in order to keep the volume to surface area high. The generally accepted ratio is approximately 400 m^2/m^3 (Płaczek, Patyna and Witczak, 2017). In order to be industrially relevant these reactors are mostly found outdoors; where solar light is utilised. Therefore, their arrangement configuration is such as to maximise light utilisation. They are often placed vertically and stacked at a set distance between them.

2.1.3.2 Mixing

Agitation is achieved by either gas injection or mechanical pumping. In the case of the former, similar to the bubble column, gas is injected at the bottom of the reactor (predominantly along the shorter length). In this occasion the gas inlet will demand more focused design compared to the bubble column. An accepted value of gas flowrate is 1L of air per 1litre of culture volume per minute (Płaczek, Patyna and Witczak, 2017). The latter method of agitation is pumping or pump-flow, this method depends on an adequate flow regime coupled with suitable reactor arrangement/configuration that will enable a loop.

2.1.3.3 Mass transfer

Since there are two methods of agitation the mass transfer predominantly depends on the applied. If gas sparging is used, the mass transfer, given the sparger design is optimal, is like the CO_2/O_2 exchange observed in bubble columns. The conventional pumping using a pump, would involve high energy input to create to turbulent regimes that are required for optimum mass transfer, however this would majorly influence the culture viability due to increase shear stresses. (Kumar et al., 2011)

2.1.3.4 Process parameters

Considering the materials of construction flat plate PBRs are cheap to construct, however due to their size and shape the cost of support structure and connective elements are a substantial cost. Scaling up the reactor is limited to the ratio of surface area to volume, secondary considerations are the use of agitation incur a large cost, both if a free supply of gas is unavailable, and pumping costs which are similar to the tubular reactors. Scaling out the reactor is an easier option, it involves the implementation of additional plates, places either in parallel or in series with the rest of the array, this is limited by the land usage as well as the connective and support element cost.

Temperature control is a problem with this reactor since the large surface area absorbs heat easily, shading has proven to help, however with shading comes diminished light intensity, therefore reducing the growth rates.

2.1.4 Other PBR designs

The above PBR designs are the most commons reactor types. Their original shape and further redesigned variants are a suitable example demonstrating how small changes in a PBR design, can change biotic, abiotic behaviour of the algae which in turn optimise the growth by altering process parameters. There are however recent and novel developments in PBR design which approach the issue from a new standpoint.

An example of a new cultivation system is the pyramid reactor. The design approach of this type of reactor is to build a system that is automated and computerised (Płaczek, Patyna and Witczak, 2017). Mixing occurs via agitation of the algae suspension by bubbling, like an airlift system. The main novelty is the shape of the reactor with a large base and inclined walls which offer maximum light utilisation when placed outdoors, at a small spatial footprint. Long term usability and applicability of these reactors does not yet exists since it is still in the experimental pilot stage, however published values have been reported of 1.45 g/l/d for *Spirulina* (Płaczek, Patyna and Witczak, 2017)

Another attractive option in PBR design is the use of plastic bags. Particularly attractive due to their low cost, ease of manufacturing, maintainable and provide excellent sterility, plastics bags can be moulded to any shape of size required. Typically made from polyethylene, they can be designed to hold up to 2000l. Although a very effective cost reducing method, they are still in limited use today. The disadvantage of using such a system is their fragility, this in turn limits the mixing intensity thus reduces the mass transfer of CO_2 in the culture. A reported phenomenon is culture crashing which is particularly evident in larger scales (Kumar *et al.*, 2011)

Hybrid reactors and not particularly new systems, on the other hand they are systems which combine and exploit the benefits and advantages of two or more PBRs into one system. For example, the light harvesting capability of the horizontal tubular reactor can be combined with the mass and gas transfer and O_2 advantages of an airlift photobioreactor. On a similar note, a bubble column has been extensively used as a feeder to tubular, helical, or any other arrangement of a flow type reactor. The reason for this preference is the ability of effective mass transfer where initial mixing of the nutrients can occur, as well as a suitable position were measuring ports can be implemented (Kumar *et al.*, 2011). Reported applications of these type of reactors are an integrated airlift and external tubular loop of 200l volume, placed in a pond of water offering temperature control.

2.2 PBR Design: Design Considerations & Challenges

The most important design considerations in developing a photobioreactor (PBR) are, adequate light exposure, effective low cost mixing, CO_2 delivery, nutrient supply, pH and temperature control. (Soman and Shastri, 2015). In literature there are numerous variations of photobioreactors (Huang et al., 2017; Kumar et al., 2011; Wang, Lan and Horsman, 2012). The number of PBR variants found in academic studies and diversity between examples of the same type, are all in effort to optimise the biological processes that contribute to the successful cultivation of algae; whilst at the same time reducing the cost of construction, operation and maintenance.

2.2.1 Light

Light is a key growth parameter for algae. *In vivo* photosynthesis is achieved by the natural succession of day and night, the duration of each phase varies for algae accustomed to different geographical locations. *In vitro* this is provided via the manipulation of artificial light sources such as LEDs. When designing a scalable photobioreactor (PBR) the effective implementation of a light regime becomes a very complicated task. Algae in PBRs are exposed to complicated light environments. Light and light-deplete (dark) phase characteristics are governed by a combination of PBR design and process parameters; namely light fraction, cycle time, light path length, cell concentrations (culture density), mixing regime (laminar, turbulent) and light intensity (Qiang, Richmond and Zarmi, 1998; Richmond and Zou, 1999; Barbosa *et al.*, 2002; Simionato *et al.*, 2013)

Light engineering concerns its implementation into a PBR, is a topic that has been studied throughout the years, most notably by Little (1964) and Buriew (1953) providing evidence that intermittent light and dark periods in the range of seconds significantly increase overall photosynthetic efficiency in comparison with flashing light in the range of 10ms. On a similar note Richmond et al. (1980) stated that light and dark cycles ranging from seconds to minutes have stimulatory effects on the productivity output of microalgal cultures

Moreover associating light cycles with reactor design, namely airlift and tubular PBRs as well as flat panel type PBRs, Janssen et al. (1999) found that with the algae strain *C.Reinhardtii* the influence of medium duration light/dark cycles was not evidently clear, following this study Barbosa and Janssen (2001) concluded that for *Dunialiella tertiolecta* under equal light fractions of 0.5, cycle time reduction from 55 to 10s developed higher biomass yield, whereas at higher light fraction of 0.869 longer cycle times were preferable for higher growth yields. On the down side light degradation from the column surface influences the frequency and light cycle the cell endures and should be taken into account upon PBR design, indicating the strong association of light regime with mixing. (Burlew, 1953; Bosca, Dauta and Marvalin, 1991; Barbosa *et al.*, 2002)

In an earlier study Grobbelaar (1991) compared mixing and light cycle effect on algae cultures referring to light intermittence being associated with two basic parameters, the photoperiod and the frequency of the cycle. The study concludes that by comparing the medium frequency light cycles with the laminar cyclic rhythm that waves cause in the surface of water in lakes and short light/dark cycles as a prevalence in turbid waters (rivers and streams). In the same study Grobbelaar (1991) investigating the influence of light and dark cycles on *Chlorella Scendesmus spp.* Using a custom designed PBR, with a venetian blind device attached to tungsten (W) light, and altering frequency from 2-260 sec. He noted that higher photosynthetic efficiencies were evident under fluctuating light compared to steady light, furthermore he reported that an increase in agitation via stirring, increased growth rates leading to a correlation between turbulent culture conditions and light cycles. Which combined effect increased photosynthetic efficiencies by exchanging metabolites through a decreased boundary layer between cell and environment thus utilizing more light energy (Grobbelaar, 1991).

In a much later study Hu, Zarmi and Richmond (1998) whilst studying the combined effects of light path with highly turbulent flow in a flat plate reactor with high culture densities of *Spirulina Plantesis* found that as the light path was minimised from 200mm to 7.5mm the volume output (mg/l) grew by a 50-fold

increase. Comparing his findings with an open raceway the output rate was 100 times higher. This provides evidence of the practical advantages of short light paths for ultrahigh densities. Upon further analysis the authors clarify that the actual light regime is difficult to analyse and goes beyond the simplistic manipulation of the light source but rather the turbulence inducing motion between the cell in the culture forces the cells to move from the photic zones to the dark in an erratic manner (Hu et al., 1998), exposing the cells to a wide range of light/dark mini-cycles some of which are close to optimal; assuming a long processing period all cells will undergo equal distribution of light/dark cycles. His analysis showed that as the cell density increases in the there is a clear need for a higher Reynolds number dominating the flow regime to ensure that the frequency of L/D cycles increases equally to ensure high photosynthetic efficiency. Following this trend Richmond, and Ning Zhou (1999) found whilst studying *Spirulina* and *Nannochloropsis* that the smaller the light path (13mm,26mm) the higher the growth rate and the volume output rate, since it increases the frequency of cells moving from the dark to photic zones, essentially increasing the frequency of light/dark cycles. However, the case with areal productivity is not clear as evidence from his experiments conclude that in the case of *Spirulina pl.* it was inversely related to the light path length whereas in *Nannochloropsis sp.* The areal output rate increased with increasing light path.

It is evident that the light cycle period and frequency whether from physical manipulation of a light source (flashing or other forms) or via the combination of light source manipulation, optical path length and highly turbulent flow regimes in ultra-high-density cultures, the light cycle does influence the photosynthetic efficiency and in turn increases algae productivity. It is also evident that different algae strains require different manipulation of the light cycle and flow regime to provide the optimal L/D cycle to the cell for maximal growth. Although results are slightly contradictory in literature and comparison between experimental reports is done so with caution, there seems to be a preference in medium light cycles, and high turbulences in combination with short optical light paths as pointed out in Richmond (2004). (Richmond, 2004). Additional information on light parameters and their effect can be found in Appendix A.1.

2.2.2 Mixing

Mixing is a key for successful algal cultivation (Huang *et al.*, 2017a). The mixing regime in a photobioreactor does not solely dictate the light exposure that algae are subjected to, but also plays a critical role in reducing and regulating pH, increasing heat transfer and reducing temperature gradient, increasing nutrient uptake, preventing cell sedimentation, clumping and cell attachment to the walls of a PBR. (Wang, Lan and Horsman, 2012; Huang *et al.*, 2017a).

Mixing is achieved by aeration, pumping or stirring by mechanical means such as agitators, stirrers, impellers to mobilise the culture, or a combination of the aforementioned (Wang, Lan and Horsman, 2012). The employed method of agitation dictates the PBR design and vice versa, which is often the biggest distinction between PBRs, in shape and in operation.

Another distinction when characterising mixing, concerns the bioprocess itself. Specifically, whether the process is carried out in batch (static), semi-batch or in flow conditions. Concerning the former, batch PBRs typically rely of aeration and mechanical systems to mobilise the culture, whereas the latter relies on the addition of a network of tubing which architecture combined with the flow characteristics create a distinct flow profile. Hydrodynamics play an important role in the performance of a PBR (Soman and Shastri, 2015). They dictate gas retention/rejection times and enable solid liquid mass transfer of the nutrients to the cells. Hydrodynamics also dictate the diffusion of gas (CO_2) into the culture and O_2 expulsion of from the system.

Mixing is the primary means of mobilisation of algae cells suspended in the culture, thus it dictates the L/D cycles and light intensity distribution of algal cultures. Since this parameter is very interlinked with light, it is hard to isolate the effects of mixing in a culture; as expected there are few publications that have reported on this. As reported by Huang et al., (2017) when developing a novel airlift PBR, the addition of radial mixing to a mixed bubble column enhanced the growth rate by 1.7 times (Huang et al., 2017) In addition to that when doubling the mixing intensity for a culture of *Chlorela sorokiniana* growing in a short path length PBR little effect was noticed. On the other hand, as cited by Kunkapur and

Eldridge (2010), when non-limiting environmental conditions are met, the level of mixing is the primary determinant of algae growth rates. However caution is warranted with mixing as it is the primary cause of cell death from shear stresses in a PBR (Huang et al., 2017; Kumar et al., 2011; Kunjapur and Eldridge, 2010; Wang, Lan and Horsman, 2012).

2.2.3 Mass Transfer - CO_2/O_2 Balance

Microalgae are aerobic organisms, therefore their cultivation at a cellular level involves the following competing processes, photosynthesis, photorespiration and dark respiration (Huang et al., 2017). The predominant process being photosynthesis, converts CO_2 to energy whilst expelling O_2 as a biproduct. Algal CO_2 concentration tolerance varies between strains; based on Lam Lee and Mohamed (2012), the algae tolerance for CO_2 varies between 5-20%, with C.vulgaris ranging from 1-2% for conventional PBRs and 10% when fermenters are employed as bioreactors (Lam, Lee and Mohamed, 2012). Kumar et al., (2011) reports the identical figures and supplements that 2% and 0.25vvm flowrate is the optimum for *C. vulgaris,* utilising approximately 1.7-1.8 gCO_2/g biomass. Which at concentrations above 10% (v/v) CO_2, the specific growth rate gain becomes insignificant. It is noteworthy to mention that *B.braunii* a totally different species reports the same tolerance as *C.vulgaris* at 10%. (Lam, Lee and Mohamed, 2012). Finally for most algae species the maximum photosynthetic efficiency is achieved at 1-5% by volume (Huang et al., 2017).

If CO_2 levels exceed the tolerances, it creates additional environmental stresses which reduce the carbon sequestration capacity of algae. Furthermore since CO_2 is a known pH regulator, any increase in CO_2 drives the pH towards the acidic range (Kumar *et al.*, 2011). In PBRs CO_2 is delivered at strategic locations which enhance and promote uniform agitation in the system. The gas inlet velocity as well as the bubble size are directly linked with the algal capability to utilise carbon (Lam, Lee and Mohamed, 2012). The characterisation of mass transfer is given by the volumetric mass transfer coefficient (K_La) which is proportional to the CO_2 demand of microalgal cells, and inversely proportional to the concentration of CO_2 in the inlet stream, regardless of photobioreactor type (Kumar *et al.*, 2011). From

this observation two points are deduced. First, as is suggested K_La dictates the inlet flow rate and the inlet concentration of CO_2, meaning that in low CO_2 concentrations the inlet bubble speed will be high, which would cause excessive shear stresses in the system causing a decrease is growth rates. Secondly it is argued that CO_2 supply will have inhibitory effects to the growth if the supply is too low, so as to match the algal species demands (Huang et al., 2017).

Another key consideration in PBR design is the concentration of dissolved oxygen (DO) in the system. As previously mentioned, O_2 is the product of photosynthesis, however when DO concentrations are at high levels in the system, the Calvin cycle turns towards consuming O_2 to produce CO_2 in a phenomenon called photorespiration (Huang et al., 2017). Therefore excessive levels of DO will inevitably lead to severe culture degradation, not only due to the suppression of the photosynthetic process, but also to cellular toxicity in the algae which leads to cell death. This phenomenon is predominant in PBRs which are closed system and the environment is isolated. Thus effective means of gas exchange with the environment must be designed into the system; such as a degassers (Huang et al., 2017; Kumar et al., 2011). A degasser port or nipple is an effective means to regulate the DO concentration for PBRs. This is an easy task for PBR's with a favourable shape (tank, conical, vertical tubular, bubble column). On the other hand, the issue becomes complex in PBRs comprising of long light harvesting units such as the helical or tubular horizontal. In such circumstances the accumulation of O_2 can be regulated by multiple degassing units along the network of tubing between the system's inlet and outlet. This measure coupled with a suitable flow regime will enable a higher degree of mass transfer to occur and will propel the DO towards exiting the system.   (Huang et al., 2017). Therefore, in PBR design, the consideration and design of effective mixing mechanism which increases mass transfer, coupled with the implementation of degassing units at strategic locations, and the controlled injection of CO_2 will drive the balance of CO_2/O_2 to a desirable ratio; preventing damage to algal cells (Huang et al., 2017; Kunjapur and Eldridge, 2010; Wang, Lan and Horsman, 2012). Additional information on carbon and nutrients can be found in Appendix A.1.

2.2.4 Temperature

Temperature is a very important factor in the process of cultivating algae, since it influences the metabolic rate of the cell. Considering how important the factor is, there is a unproportionable number of studies being conducted on temperature control. At small scales temperature control is not a challenge, however as operational volumes increase the complexity of maintaining a constant temperature throughout cultivation increases also.

Algae cultivation in a PBR can occur either indoors or outdoors. In the case of the former temperature control can be achieved by introducing thermostatically controlled heaters, or localised industrial heaters, setting the temperature to the desired range for the specific algal strain.

In the event of outdoor cultivation, heating and cooling must be implemented in the reactor design as the environmental ambient temperature fluctuates between the phases of solar intensity (day and night). One key consideration in temperature control is the shape of the reactor, since it can play a predominant role in heat dissipation, and maintenance. For instance, the most difficult reactor type to control the temperate are flat plate reactors, where the large surface absorb most of the heat, whereas at night the opposite effect takes place cooling the reactor to below optimal levels. In a review by Bajpai, Rakesh and Prokop (2014) the most common approaches to temperature control that are currently in place in various applications are listed and summarised by Bajpau, Rakesh and Prokop (2014) (Bajpai, Rakesh Prokop, 2014). Manually shading reactor tubes or flat plate surfaces with dark coloured sheets, is one approach tested by Torzillio (1997) which showed to be an expensive option in scaled systems. It was also reported that in higher temperatures up to 80% of the reactor area has to be covered in order to have an effect. Another approach is spraying the reactor with coolant. Tested by the same author Torzillio (1997) this approach was applied to keep the water evaporation in systems running between in 33-35°C to 1-2 l/d, however the author does not mention the scale of the reactor in order to gauge whether the water lost is insignificant or not. As expected, the cost of the water or coolant will be a significant factor affecting the profitability, however this

53

can be mitigated with a coolant or water recovery system. In tubular systems where the temperature difference can be as high at 10-15°C in the tubes, the cooling can be achieved by aluminium or stainless-steel water jackets. Barbosa et al. (2003) applied this method at the bottom of the reactor so that it does not interfere with the illumination with positive effects (Bajpai, Rakesh Prokop, 2014). Other methodologies such as submersion of cooling/heating coils in the culture medium can be employed, or for example submersion of the reactor tubes in a cooling medium, or pond (in large scale applications) has been trialled and tested with varying results, specific to applications.

2.2.5 pH

Microalgal growth occurs between a pH of 7 and 9, where the optimum pH range depends on the species, with some strains capable of tolerating adverse pH conditions (Wang, Lan and Horsman, 2012). Most growth media pH ranges from 6.5-7, and it raises steadily in a culture as CO_2 is consumed. Although pH is a parameter which is regulated by the biotic functions of the cell, it's control can be engineered into a system. As has been mentioned, pH can be regulated by the input of CO_2, or by a buffer addition in nutrients. One the other hand depending on scale the pH can vary substantially from one location to the next, leading to complications in its control. Either way, pH is a parameter so influential to the viability of cultures that it requires close monitoring and constant regulation.

2.2.6 Nutrient Delivery

In addition to the photosynthesis reactants, algae require a supply of macro and micronutrients. nitrogen (N) and phosphorus (P) are the two most important macronutrients controlling the growth and formation of lipids in the cell (Kunjapur and Eldridge, 2010). In addition to these other essential nutrients are, carbon (C), hydrogen (H), sulphur (S), calcium (Ca), magnesium (Mg), sodium (Na), potassium (K) and chlorine (Cl). Micronutrients (salts) are also required but in much smaller quantities, which are iron (Fe), boron (B), manganese (Mn), copper (Cu), molybdenum (Mo), vanadium (V), cobalt (Co), nickel (Ni), silicon (Si) and selenium (Se). (Kunjapur and Eldridge, 2010). There are several growth media recipes that are published, the most popular being the BG-11, Bold Basal Media,

Diatom Media, J. Media (Jaworski) and the Bristol media. These are created with elements in excess in order to extend their suitability for a large number of strains. The nutrient mix which comprises the growth media is one of the few parameters that is directly driven by the elemental composition of the algal species; therefore it is often the case that media is customised to the specific strain via methodologies such as elemental and biomass capacity analysis (Danquah and Harun, 2010; Azma *et al.*, 2011; Hadj-Romdhane *et al.*, 2012; Rudnicki *et al.*, 2017). Nutrients are supplied as salts, this coupled with the number of nutrients microalgae need, makes the engineering of a delivery system a complex task. In vivo applications the media is supplied in the form of salts, which are weighed and tipped into the raceway pond, directly behind the paddlewheel. In laboratory scale PBR systems media made up using concentrated solutions of each nutrient and supplied by pipetting the contents into the culture. In large outdoor tubular type PBRs nutrients are injected in the buffer tanks. Whichever the case the controlled, monitored and cost-effective delivery of nutrients must be implemented into the system.

2.2.7 Decontamination, Sterility and Cleaning

Microalgae can grow either in photoautotrophic, heterotrophic or mixotrophic mode (Wang, Lan and Horsman, 2012). The main differences between these modes is the presence and/or balance of inorganic and organic carbon. For heterotrophic cultures sterility is not usually an issue due to the lack of organic carbon compounds, which invasive microbial contaminants feed on. However lack of decontamination and sterilisation procedures (methodologies and protocols) will endanger an algal culture, in a PBR, due to the emergence and uncontrollable growth of exotic predatorial species which feed on the algae (Wang, Lan and Horsman, 2012).

Decontaminations and sterility in PBRs are two factors that need consideration during the design process of the vessel, in combination with the design of operational procedures. Leading to a PBR designed with the ability to be sterilised and decontaminated when necessary.

Cleaning and maintenance scheduling are design considerations and should be considered early on the design process. Cleaning is of critical importance in a PBR; during the design process the selection of materials (PTFE, St Steel, Acrylic, Polycarbonate), machining processes (extrusion, machining, casting), reactor configuration (tubing architecture, reactor shape) and the implementation of probes (process analytical techniques, online measurements, degassing units) must be thoroughly considered so to avoid and/or enable the following (Reis and Da Silva, 2016):

1. Prevention of wall growth and biofilm formation on the internal surfaces of the reactor.

2. Prevention of volume dead spots and minimisation of excessive u-bends and which will cause fouling and potentially enable the growth of contaminants and invasive species.

3. Enable the convenient cleaning and decontamination maintenance routines as processes to maintain the high light transmission and extend the lifetime of the PBR.

4. Consider the mounting of the probes with the use of ascetic connective elements to reduce the chance of contamination.

5. Implement automated clearing regimes to keep the efficiency of the light harvesting units high.

The ease of decontamination and sterilisation of a PBR depends primarily on the scale and shape of the reactor. Smaller sized units can be sterilised by means of autoclave or gamma radiation, whereas larger units are limited to industrial steam cleaning and or flushing with a sterilisation agent or chemical, such as hydrogen peroxide, isopropyl-alcohol solution or ethylene oxide (Mandenius, 2016 p.267). In terms of the former the parameters that characterise sterilisation is time, however for larger scale PBRs the effectiveness of sterilisation also depends on the mixing intensity; which must enable high turbulence so that all internal areas of the reactor encounter the chemical.

2.2.8 Critical Culture Density

Microalgae cultures *in vivo* are at a density of approximately 10^3 cells/ml, with a intercellular distance of approximately 1000μm, *in vitro* microalgae culture densities can reach as a high as 10^9 cells/ml. Dense cultures have detrimental effects on the transmission of light, the effectiveness of mixing and the mass transfer and consumption of dCO_2. Monitoring of the culture density either by probe at critical locations or by empirical modelling is critical to keep the culture density at viable operational levels. (Wang, Lan and Horsman, 2012).

2.2.9 Scale up

For algae bioprocessing to have significant business impact, it must be produced at large scales. Academic research on algae bioprocessing, and most notably yield and productivity figures are all based on experiments at laboratory scale. These figures are often used to project productivities and yields at large scale leading to erroneous assumptions, which then lead to failures (Reis and Da Silva, 2016).

Scaling a PBR and its hosted bioprocess is a complex task, in which the relationship between variables is not fully understood. The biggest considerations in scaling PBRs is the light (intensity and modulation), temperature, mixing, nutrient provision, contamination, biomass film formation, and oxygen build up. As indicated in previous chapters each one if these challenges in scaling is depended on the reactor type. A very informative review on the challenges is given by (Reis and Da Silva, 2016) and (Jianye *et al.*, 2015).

Industrial instances of scaling studies are few and far between, however notable outcomes from these studies indicate three main points. Firstly, the scaling of a 20L reactor to a 200L vessel, for the cultivation of a freshwater algal species, revealed that the overall costs per biomass to be seven times lower than the cost in the smaller vessel. Secondly increasing scale by a factor of 100 can potential result to a reduction of biomass productivities by a factor of 10, as was demonstrated when a $1000m^2$ production area was scaled to $100,000m^2$ which resulted in an algal productivity of 3 $g/m^2/d$ relative to 20-30 $g/m^2/d$ in the lower

case. And lastly scaling up the PBR and algal cultivation must include the downstream processing of algae, as the harvesting and dewatering of algae pose major challenges (Reis and Da Silva, 2016).

In order to effectively manage scaling one must address two interlinked issues: the biological physiology of the organism and secondly to understand the flow dynamics of the reactor itself (Jianye *et al.*, 2015). Unlike chemical processes, in bioprocessing the reactors process organisms that are alive and responsive to change, therefore complete understanding and control of the flow characteristics and its influence on the organism's metabolism is a crucial prerequisite. For this task tools such as computational fluid simulation and theoretical modelling (Monod-type) of the bioreaction kinetics can be employed to uncover potential bottlenecks in scaling up (Jianye *et al.*, 2015). Despite the critical importance of scaling, there are no universal laws or governing strategies, rather it is down to each individual scientist or engineering to follow an applicable rationale to scaling.

2.2.10 Defining the problem – Identifying the challenge.

In PBR design it is evident that biotic, abiotic and process parameters are heavily interlinked. For instance, the dimensional characteristics of the reactor (shape, length, width and overall size) predominantly dictate light utilisation, as well as ensuring suitable and cost-effective mixing.

Mixing can be deployed either via bubbling (gas injection) and mechanical pumping. Two rudimentary methods which selection depends on the orientation and configuration of the PBR. Moreover, effective mixing ensures heat and mass transfer is achieved uniformly throughout the system, algal cells are kept suspended in the reactor, fouling and wall growth are kept in check, and that O_2 is efficiently ejected from the system. Finally mixing has demonstrated to play a crucial role in dictating the light regime which algal cells are subjected to. Given the appropriate design considerations (thin walled, small cross-section of the tube and/or plate) mixing dictates the frequency that algal cells are exposed to light, which in turn regulates the overall photosynthetic efficiency of the culture.

It is evident that modern PBRs although numerous in designs and varying in specification, are currently designed to improve light utilisation and multiphase mixing. Although effective mixing has benefits, excessing mixing hinder growth by increased shear forces that damage the cellular wall. As one can expect it is impossible for one reactor system to consider all these factors therefore each reactor configuration and subsequent iteration attempts to create an environment where all parameters are operating within the limits of synergy. Focusing on microalgae processing when it comes to PBR an important research goal is being able to produce:

- Cost-effective design that is characterized by a high area to volume ratio, whilst illuminated from all surfaces (Richmond, 2004).
- Keeping a small enough flow path to avoid mutual shading or light degradation (Barbosa et al. 2002).
- Able to sustain continuous mono-algal cultures, without biofouling and wall growth checked and controlled (Richmond, 2004).
- Being able to not only incorporate fluctuating light regimes but also a range of turbulences, readily available and maintained (Grobbelaar. 1991).

Moreover, issues such as scalability play a very important role in the profitability and social, environmental and sustainability of the reactor system (Reis and Da Silva, 2016). Therefore, a robust scaling strategy must be considered in any novel PBR design presented. For this all to be achieved, there must be a fundamental re-design of the photobioreactor, not only in terms of shape (i.e light utilisation, volume, scale-up etc), but also in terms of parametrisation (controllable mixing), process monitoring and downstream bioprocess integration (telescoping).

2.3 Plug Flow Reactors

In industrial biotech chemical reactor and process design, concerns two kinds of reactors the stirred tank reactor (STR) and the plug flow reactor (PFR). Although all four have interesting theoretical applications the most commonly used models for batch are the batch reactor, and for flow are the PFR and the CSTR (Nauman, 2002)

Batch reactors are large systems with industrial examples is the range of 100,000 litres capacity which reactants are charged into the system and mixed via mechanical means (impeller or pumping) for a fixed period. Temperature control (heating and cooling jackets, submersed coils, or heat exchanger connected to a coiled loop) is a necessary measure in batch reactors since exothermic and endothermic reactions cause significant temperature variations and gradients in the vessel.

CSTRs on the other hand, are identical to STRs, with only difference that they have a continuous input and output stream (i.e. flow of material in and out). It operates with the assumption that the heat and agitation is uniform in the vessel, and any material entering the system is rapidly dispersed and heated/cooled so that it instantly assumes uniform concentration and density. The internal volume of the reactor is assumed constantly to be at steady state and the concentration of components/reactants are the same as the product outflow stream (Jordan, 1996; Nauman, 2002).

PFRs are visualised as long tubes, where material is fed in one side and the outflow of product is on the opposite. As the components of a reactor enter the system on one side, they assume to form a plug; this plug remains intact and reacts as it flows down the tube. The composition of the plug changes with time and position down the tube, with the same assumptions made for a batch reactor (Nauman, 2002). Ideal piston flow reactors are characterised as a series of continuously flowing ideal tanks with $V_{plug} = V_{tank}$, which in small volume production the material handling, economics and process related factors do not influence selection, and flow does not offer any additional benefit to batch. On the other hand, for larger volumes and productivities, the continuous output of product in flow versus the cyclic production of batch is a more attractive option for economies of scale.

In the event where flow is more suitable to batch, there is a distinction to be made in flow operation as well, between CSTRs and PFRs which is essentially between tank and tube. It has been reported that, all things being equal, the reaction rate in PFR is far superior that at any point in the CSTR. Which leads to the

generalisation that conversion efficiency and selectivity in PFRs are much higher than in CSTRs (Nauman, 2002).

Unlike laminar and turbulent flows, where the velocity component differs along the cross-sectional area of the tube; plug flow is characterised by no velocity gradient and thus complete mixing in the radial direction of the tube. Therefore all fluid elements along the vessel will axially travel at the same speed therefore have equal residence time (Ni, 2006).
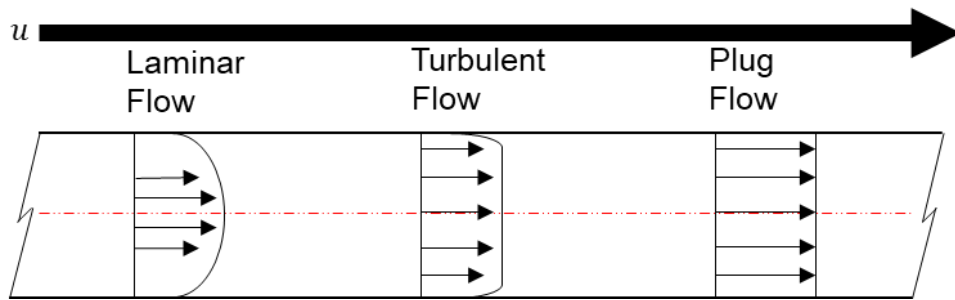
Figure 2-3 Laminar, Turbulent and Plug flow velocity profiles reconfigured based on Ni (2006).

The fluid dynamics that are attributed to OBRs are governed by a series of dynamic equations and certain dimensional ratios that must be adhered to in order to have the desired fluid behaviour (Phan and Harvey 2011).

Specifically, for the dimensional ratios, parameters such as baffle spacing (L), tube diameter (D), tube and orifice diameter (D and d respectively) and baffle thickness are all interlinked parameters that allow the desired fluid kinematic profile to be achieved. According to Phan and Harvey (2011) typical dimensional ratios that are found in any OBR are the orifice diameter (d) to be 0.15 to 0.6 (D), also known as the constriction ratio, and the baffle spacing length (L) to tube diameter (D) ratio to be in the range of 1.5-2.0.

$$\frac{D}{d} = 0.15 - 0.6 \qquad\qquad \textbf{(2-1)}$$

$$\frac{L}{D} = 1.5 - 2.0 \qquad\qquad \textbf{(2-2)}$$

In addition to the above the, dimensionless quantities are the Reynolds net flow number (Re) the Oscillatory Reynolds Number (Re_o) the Strouhal number (St), and the velocity ratio (ψ).

$$Re = \frac{\rho v D}{\mu} \qquad \text{(2-3)}$$

$$Re_o = \frac{\rho 2\pi f x_o D}{\mu} \qquad \text{(2-4)}$$

$$St = \frac{D}{4\pi x_o} \qquad \text{(2-5)}$$

$$\psi = \frac{Re_o}{Re} \qquad \text{(2-6)}$$

Where ρ is the fluid density (kg/m^3), v is the axial velocity (m/s), D is the diameter of the tube/passage, μ is the dynamic viscosity (Pas), f frequency of oscillations (Hz), and x_o the centre to peak amplitude of oscillation (m).

The above non-dimensional dynamic groups do not include any geometrical parameters other than the diameter, however they have a dominating role in characterising the fluid flow regime in terms of dynamic vortex creation and dispersion rate. (Stonestreet and Van Der Veeken, 1999).

2.3.1 Oscillatory Baffled Flow Reactor

One example of a plug flow reactor is the oscillatory baffled flow reactor (OBR). Conventional STRs, and continuously STRs and tubular reactors base their mixing efficacy on inducing eddies in the fluid by mechanical means (stirrers, impellers etc) , long fluid paths and high volumetric flowrates (Nauman, 2002; Doran, 2013). On the other hand, OBRs achieve mixing by superimposing an oscillatory motion on a unidirectional net flow. This combinatory flow regime, in the presence of equidistantly placed constrictions (baffles), create a flow regime called plug flow (Levenspiel, 1998). OBRs are characterised by a distinct

geometrical parameter system which enforce a fluid dynamic regime. Periodic flow constrictions are achieved with the use of strategically placed baffles. The geometry of both flow path (Diameter [D], and Length [L]) and baffle (diameter [d], length [l]) are related according to certain governing geometric ratios.

The induced oscillatory motion occurs in two phases, the upstroke and downstroke. As a fluid particle accelerates past a baffle during the upstroke, a sudden reverse in direction (downstroke) causes dynamic separation between two particle packages of fluid causing a toroidal vortex (eddy) downstream of the baffle. Similarly transitioning from downstroke to upstroke the same phenomenon occurs forming an eddy upstream of the baffle. This oscillatory motion occurs between each baffle enabling significantly more mixing in the radial direction, and minimal to none in the axial.

2.3.1.1 Characterising the flow

Oscillatory baffle flow reactors operate two flow profiles, an oscillatory and an axial net flow (Stonestreet and Van Der Veeken, 1999). The net flow is characterised by the $Re,$ which depends primarily on the fluid's superficial fluid velocity. Depending on the magnitude of Re flow is either laminar ($Re < 2100$) or turbulent ($Re > 2100$). On the other hand, the Re_o number is characterised by the oscillation frequency (f) and the centre to peak amplitude of oscillations (x_o) which replace the velocity parameter (v).

Depending on the values of f and x_o the magnitude of is either considered soft ($50 < Re_o < 250$), transitional turbulent ($Re_o > 250$) and fully turbulent ($Re_o > 2000$). The key difference between the soft and turbulent mixing, is in soft-mixing regime a two dimensional, axi-symmetric profile with low intensity mixing and dispersal is evident. Whereas for $Re_o > 250$ a three dimensional non axi-symmetric mixing regime starts to manifest (Stonestreet and Van Der Veeken, 1999).Since the oscillatory flow is complex the Re and Re_o alone cannot fully characterised it. To do so a metric of their relationship is required to define which of the two flows are dominant. The velocity ratio between the oscillatory and net flow velocity does just that.

It is widely regarded that a velocity ratio should be greater than one, meaning that oscillatory velocity is greater than the net. Which would indicate that vortex cycles are realised, and the flow is fully reversing. (Ni, Jian, & Fitch, 2003; Stonestreet & Van Der Veeken, 1999). The final parameter in characterising the flow is the Strouhal number (St), which is modified by Stonestreet and Van der Veeken (1999) to work with baffled tubes. Which is effectively the tube diameter to oscillatory amplitude ratio.

Although the above non-dimensional dynamic groups do not include any geometrical parameters, other than the diameter, they have a dominating role in characterising the fluid flow regime and specifically in terms of dynamic vortex creation and dispersion rate. (Stonestreet and Van Der Veeken, 1999).

The main advantage of OBR's is that mixing is independent to the net flow. In oscillatory motion, mixing is highly controllable by adjusting the oscillatory conditions, such as frequency and amplitude. This infers that mixing is still possible with no net flow present in the vessel. Albeit, this is not optimal since it acts as an STR rather than a continuous reactor. In order achieve an effective plug flow regime an appropriate net flow must be matched with a oscillatory motion which enable a sufficiently high velocity ratio (Levenspiel, 1998; Phan, Harvey and Lavender, 2011).

2.3.1.2 Scaling the OBR

Scalability is considered one of the greatest advantages of using oscillatory baffled flow reactors. By keeping the dimensionless parameters constant (Re_o Re_n St_r), it is possible to achieve similar mixing conditions and velocity profiles in any given baffle geometry (Abbott *et al.*, 2012).

Like the behaviour of the velocity profile under oscillatory flow, scalability and its influence on mixing has been heavily researched. Be that as it may, understanding of the full effect of scale-up on performance of OBRs is still lacking, and application of scale up routines is still troublesome. Jian and Ni (2005), attribute this to the complexity of the scale-up procedure of a vessel, stating that

the three-dimensional nature of the vessel, in addition to the complex relationships between geometrical parameters and operational variables. Furthermore, the same author also highlights the fact that there is ongoing academic disagreement on the appropriate scale up criteria. For example geometric relevance, power density, mass transfer coefficient, flow structure, absorption rate, axial velocity component, have been used as scale up criteria in CSTRs (Jian and Ni, 2005). Similarly the same complexities exist in industrial biotech with scale up criteria that have been considered, the reactor geometry, volumetric oxygen transfer, shear stress, gas velocity, mixing time, impeller dimensions and Reynolds number, momentum factor, and power input and volumetric gas flow rate per unit volume of liquid.(Ju and Chase, 1992)

In the case of OBR scale up, three important factors have been identified. First of all, it has been reported that scaling up from 50 – 100mm diameter for a constant power density the mass transfer coefficient increased. Secondly in scaling OBRs up from 5 to 38mm diameter, it was found that power dissipation (W/kg) was reduced for larger scales, whilst maintaining identical particle size distributions. And lastly in numerical simulations it was found that scale up behaviour in OBRs from 50-100-200mm can be taken as linear. Since scaleup is achieved simply by diametric scaling and by maintaining the average superficial net velocity and velocity ratio equal, since these parameters are independent of the scale up factor (Jian and Ni, 2005).

2.3.1.3 Bioprocessing in the OBR

In bioprocessing the mechanic and kinematic effectiveness of reactors is measured by the ability achieve a high level of mixing. Up to now conventional reactors have approached increasing the efficacy of a given reactor by increasing the fluid pass length and optimising the flow type. However, by doing that they are either exponentially increasing capital or operating expenditure. OBR technologies' key advantage is that it achieves mixing through creating a plug type flow profile. In addition to that the key advantages of OBR technology against conventional STR reactors are the following, as set out by Abbott et al., (2012).

- <u>Size:</u> Conventional reactors rely on long fluid paths to ensure adequate residence time and mixing, their size makes them impractical as well as hard to maintain, OBR's can mix much more efficiently requiring small set-up area and are even less energy intensive.

- <u>Uniform Mixing</u>: Strong vortices occurring in OBR's allow equal radial transfer of particles across the whole tube length as well as spreading and utilising the whole volume of the reactor.

- <u>Low shear stresses</u>: This advantage allows OBR's to be able to process living organisms allowing for efficient mixing whereas conventional reactors require intense redesign to ensure the survival of fragile organisms.

- <u>Increased mass transfer</u>: Very important when mixing gases with liquids OBRs minimise gas transfer holdup as found in most conventional reactors with efficient dispersal enhancing mass transfer.

The evident superiority OBR's have against their conventional counterparts have allowed this relatively new technology to penetrate industries from biological handling processes to pharmaceuticals to bio-fuels with a high success rate. The OBR's ability to process living cellular organisms as well as rare chemicals effectively by increasing yield whilst, minimising fouling and wasted chemical use through efficient mass transfer have placed OBR's in the forefront of scientific inquiry and interest (Abbott *et al.*, 2012).

The OBR technology has many intrinsic advantages that could potentially enhance the productivity and increase both efficiency and robustness of a bioprocess. Increased mass transfer, ability to handle multiphase inputs, adjustable and controllable mixing through a large range of mixing intensities, the ability to handle long residence times in a small spatial footprint, the capability of implementing online monitoring tools and in situ characterisation and most importantly the linear scale up capabilities; make the OBR very suitable to handling bioprocesses.

Bioprocessing in the OBR is a complex and challenging task. As previously mentioned, industrial biotech is generally risk averse and technologically conservative. Therefore, it has yet to develop robust infrastructure and strategies in adopting novel reactor technologies. At the time of writing there is no industrial example of an OBR being used in bioprocessing and thus has not yet been proven in large scale applications.

2.3.2 The Centillion Oscillatory Baffled Flow reactor

The conventional design of the OBR is similar to what is portrayed in Figure 2-4. These reactor systems primarily consist of a series of, parallel long glass tubes, with a set of constrictions placed internally, formed by a train of metallic equidistant orifice plates, held in place by two rods running the length of the reactor tube similar to Figure A-2 in the appendix section.

Figure 2-4 Oscillatory Baffled flow reactor (University di Porto, 2019)

This design enables the system to handle a range of hazardous chemicals, at high temperatures, however, becomes limiting when considering space, modularity and flexibility.

Although modularity and cost-effective spatial requirements are claimed for all commercial and academic OBR variants, the Centillion technology OBR (C-OBR) features design solutions which enable modularity down to a single baffled orifice. The C-OBR is a continuous oscillatory baffled flow reactor designed to effortlessly aid in all stages from chemical discovery to industrial scale implementation. It is specifically designed to assist in building processes from the ground up by enabling scientists and engineers to evaluate their concepts cost effectively and build a reactor system, truly customisable to their specific needs, rather than limiting the process to match the capabilities of a reactor.
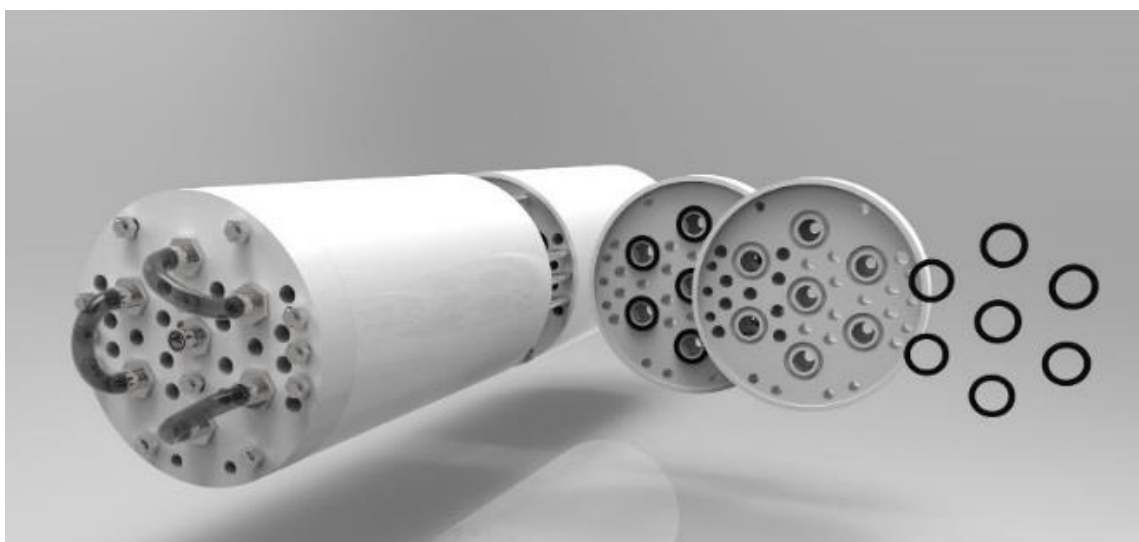
Figure 2-5 Rendering of the Centillion OBR in all Virgin PTFE material disks and Viton O-rings.

An experimentalist can therefore arrange the Centillion's core members i.e the wafer, in any arrangement they desire; by selecting between a range of wafer variants with built in monitoring probe ports, material inlet points, gas vent and injection ports and heated and cooled sections and creating a flow architecture to fit the process. The Centillion OBR can host a range of chemistries from laboratory industrial scale applications. The base component of the Centillion is

the disk (Makatsoris, Paramonov and Rakan, 2013). Each disk comprises of seven baffled segments (baffle and orifice). Six of which are radially positioned and one central. Surrounding each baffled segment, a total of 32 strategically positioned operating ports, are positioned so that they can adopt two roles; compressing the disks together or heating and cooling passages. Figure A-3 depicts the disk with geometric annotations. A baffled reactor is formed as the discs are placed in series one after the other. Scaling can be achieved either by scaling up as well as scaling out. Any length of passage can be achieved simply by adding or removing disks. In addition to that scaling up can be achieved by increasing the tube diameter, whilst all other geometric parameters and ratios constant. The Centillion technology current holds one world patent on this work (Patent Number: WO2013/050764), and one patent pending in bioprocessing (Application Number :GB2564711), (Makatsoris, Paramonov and Rakan, 2013; Makatsoris and Alissandratos, 2017).
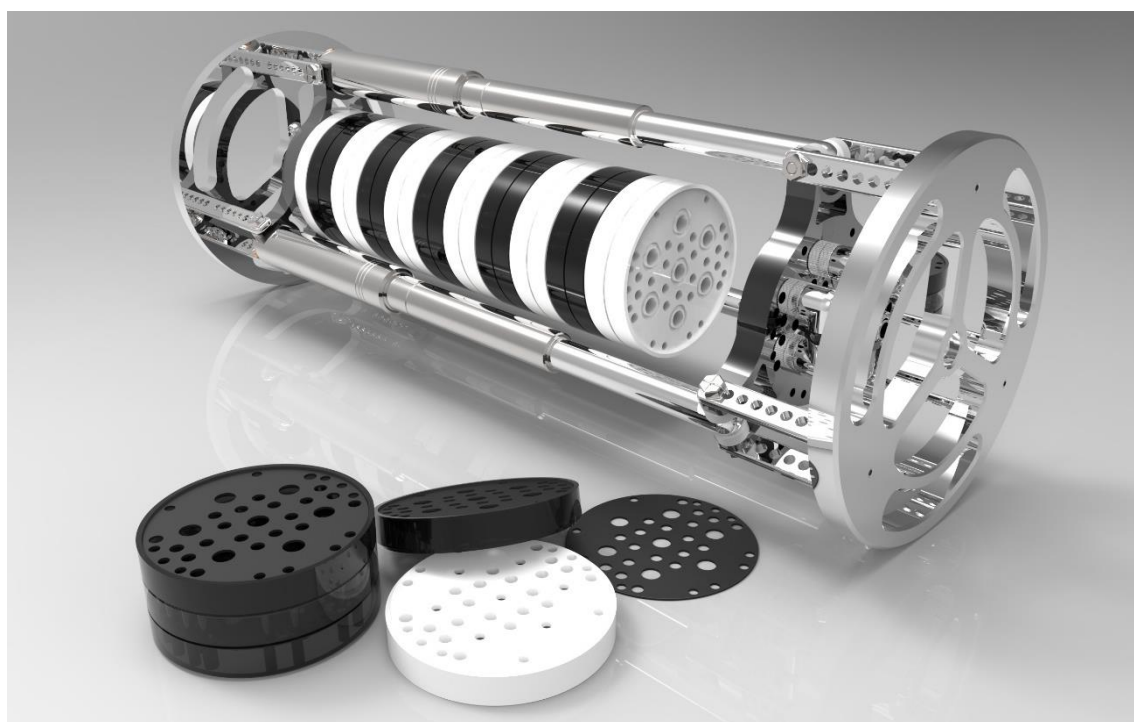
Figure 2-6: Rendering of the C-OBR, partial assembly is portrayed with black (ABS) and white(PTFE) disks, and Viton sealing gaskets. Enclosed within the electronically actuated compression system.

3 Methodology

3.1 Process

Revisiting the aims and objectives, it is clear that the major deliverable is the development of a scalable photobioreactor technology based on the continuous flow technologies, which will intensify the algae cultivation process at a balanced cost.

A suitable methodology from an engineering perspective is to first identify the PBRs technical considerations, quantify their optimum functionality in terms of bioprocess cost, sustainability and profitability. Then, link these with the unit operations of the PBR in terms of algal bioprocessing (photosynthesis, light utilisation, O_2 expulsion, CO_2 transfer). Finally produce a design which combines all at a satisfactory level.

This will be carried out in the following steps:

1. The critical design considerations are identified, these are, light (supply and utilisation), mixing (air driven agitation or pumping) , mass transfer (CO_2/O_2, and nutrient delivery), scalability, operational cost, sterility and process monitoring.

2. The critical design considerations are implemented into the design of an oscillatory baffled flow reactor, which is considered as a platform in this thesis.

    a. Implement engineering design solutions which focus on the distinct advantages OBR's that can benefit bioprocessing (continuous product output, controllable low shear mixing, high residence times, and low spatial requirements).

    b. Identify the optimum operational ranges for all design considerations, based on creating favourable and cost-effective process conditions in the reactor.

3. Once the system components are integrated and tested, the system is scaled up, from laboratory to pilot.

These are broken down to even smaller tasks and assigned to a category. With each category labelled according to the nature and discipline of the task. Operations are information-based tasks such as the development of protocols, and identification of design criteria. Biological aspects are the anything that is affiliated with the microalgal biotic operations such as the strain selection and nutrient formulation. Finally, all other tasks, design, hardware integration and testing are technical systems. This grouping allows, inspired by the work on conceptual design methodologies, carried out by Mandenius (2016), Eder (2011, 2016) and for the work to be divided into manageable segments and carried out in sequence. The complete list of tasks is shown in Table 3.1. (Eder, 2011, 2016; Mandenius, 2016)

Table 3-1 Division of objectives into smaller tasks, allocated to a number and reference system.

Ref	No.	Task
Operations	1	Identify and assimilate examples of small and large scale photobioreactor applications from past and current publications.
	2	Extract the critical design considerations as well as the benefits from each design and categorise them.
	3	Identify areas of improvement in the design and operation of small and large scale photobioreactors and categorise them.
	4	Match the critical design considerations (2) with the areas of significant improvement (3) and transform into design criteria for the photobioreactor system.
	5	Identify the biotic factors of the bioprocess and assess their significance.
Bio	6	Select a strain and optimise the media design in terms of increasing productivity at a lower cost per unit biomass

	7	Conduct batch and flow experimentation to produce an optimal set of process parameters for the photobioreactor system.
Technical	8	Design a photobioreactor system based on the design criteria from (4) that can operate within the process parameters derived from (5,6).
	9	Carry out comparative experiments to test the validity of the design and experimental work carried out and compare it with equivalent systems. Based on growth rate, biomass productivity and cost effectiveness.
Operations	10	Based on the results of (8), develop a scale up strategy of the oscillatory baffled flow photobioreactor system, using the knowledge and the technical know-how gained from the small reactor.
Technical	11.	Develop a large-scale system and evaluate its performance using identical performance metrics as the small scale.
Technical	12.	Compare the result in terms of industrial potential. In terms of scalability, bioprocess integration,

3.2 Experimental Methodologies

3.2.1 Characterisation techniques

3.2.1.1 Optical Density:

The growth of the algal culture was monitored spectrophotometrically. From each algae sample 1.42ml of it was utilised for determination of its optical density. The measurement was conducted using an Ocean Optics QE-PRO series spectrometer connected to a dH-mini UV-VIS Light Source, via 600 μm UV-Vis fibreoptic cables (Ocean-Optics, 2019). The same amount of algal sample was deposited into a quartz cuvette, and placed into a cuvette holder, and the spectra from 198 to 998nm was captured. The absorbance at 680nm, 683nm and 750nm was extracted from the data set and used to evaluate growth.

3.2.1.2 Algal Dry weight:

Algal dry weight of the samples was measured gravimetrically, by using a 10ml sample of algae and filtering it through a 0.45μm pore size cellulose acetate membrane filters, washed with DH_2O and dried at 80 °C overnight prior to use. The wet filters where placed in an oven at 80 °C overnight, taken out and placed in a desiccator to cool down, their weight measured on an analytical balance with, wind draft protectors, on antivibration mounts with measurement error of 0.1mg. The biomass productivity, in grams per litre per day, was calculated following this equation.

$$P_x = (X_2 - X_1)/t_c \qquad \textbf{(3-1)}$$

Where P_x is the biomass productivity in (gr/lit/d), X_2 and X_1 are the weight measurements on the last and first day, respectively and t_c the time in days between the last and first day. (Chia *et al.*, 2013; Rakesh R Narala *et al.*, 2016).

3.2.1.3 Ph and Temperature

The Ph of each sample was monitored using a Hannah benchtop pH, conductivity and temperature analyser. Attached to a HI-1330B glass pH multipurpose pH electrode (Hanna Instruments, 2019). The pH was taken throughout the day, and the pH meter was calibrated at the start of each day prior to measurements.

3.2.1.4 Cell Concentration:

Cellular concentration was determined through light microscopy using an improved Neubauer haemocytometer (EMS Electron Microscopy Sciences, 2019). Each culture was sampled in triplicate, and the measurement taken three times, with the average cells between measurements with error less than 100.000 cells/ml being used. Cell counting is a strenuous task; therefore, a calibration curve was created to extract the exact cellular densities from the optical density of each sample. (Sarrafzadeh *et al.*, 2015)

A matured culture of *C.vulgaris* was sampled, and serially diluted to known concentrations. Each sample was taken three time with the cells counted under the microscope an equal amount of times, the optical density at 680 was taken for each sample and the results plotted with error on the 5th decimal point. The results are shown in Figure 3-1. The cellular concentration is given by the following equation. At a confidence of $R^2 = 0.99$

$$C_{cells} = OD680 \times 10^8 + 2 \times 10^6 \qquad \textbf{(3-2)}$$

The calibration curve in Figure 3-1 was then used to correlate a samples UV-vis absorbance at 680nm with the cellular concentration at $R^2 = 99.7\%$.
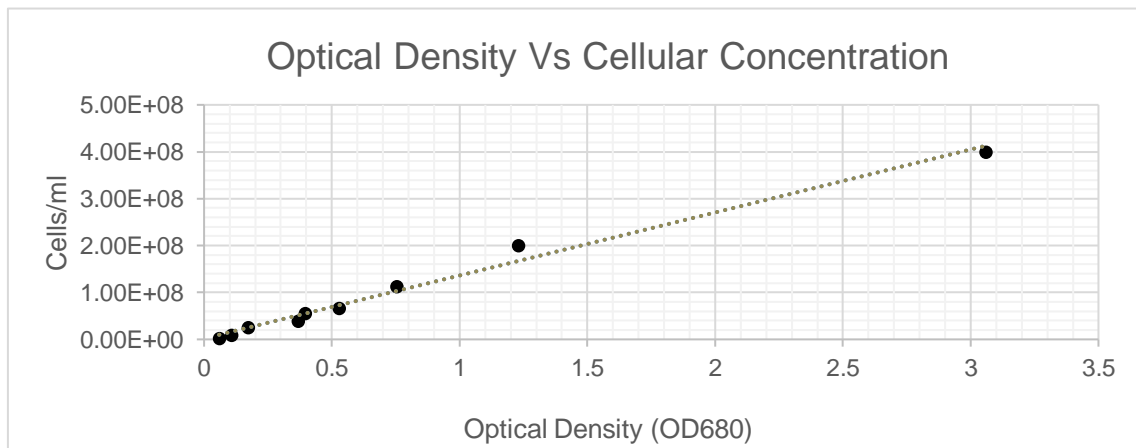
Figure 3-1 : Optical Density at 680nm wavelength vs cell count at eight difference dilutions. The calibration curve is generated by the best fit line.

3.2.1.5 Growth Rate:

The growth rate for batch systems was determined using

74

$$\mu = \ln\left(\frac{x_2}{x_1}\right)/(t_2 - t_1) \hspace{4cm} \textbf{(3-3)}$$

Where μ, the specific growth rate of the culture, x_1 t_1 are the absorbance at 683nm and time at the start of the growth phase and x_2 t_2 at the end of the growth phase (Levasseur, 1993; Madkour, Kamil and Nasr, 2012; Ammar, 2016; Rakesh R. Narala *et al.*, 2016).

In this case specific growth rate (μ) and maximum specific growth rate (μ_{max}) are equal, since the growth phase or ideal exponential growth phase, are the maximum culture rate (Doran, 2013). From the specific growth rate, assuming that the rate of growth is equal to the rate of change of cell concentration and is the only biological process affecting the change in concentration, then the doubling time is derived as below.

$$t_d = \frac{\ln(2)}{\mu} \hspace{4cm} \textbf{(3-4)}$$

Where t_d is the doubling time. (Doran, 2013).
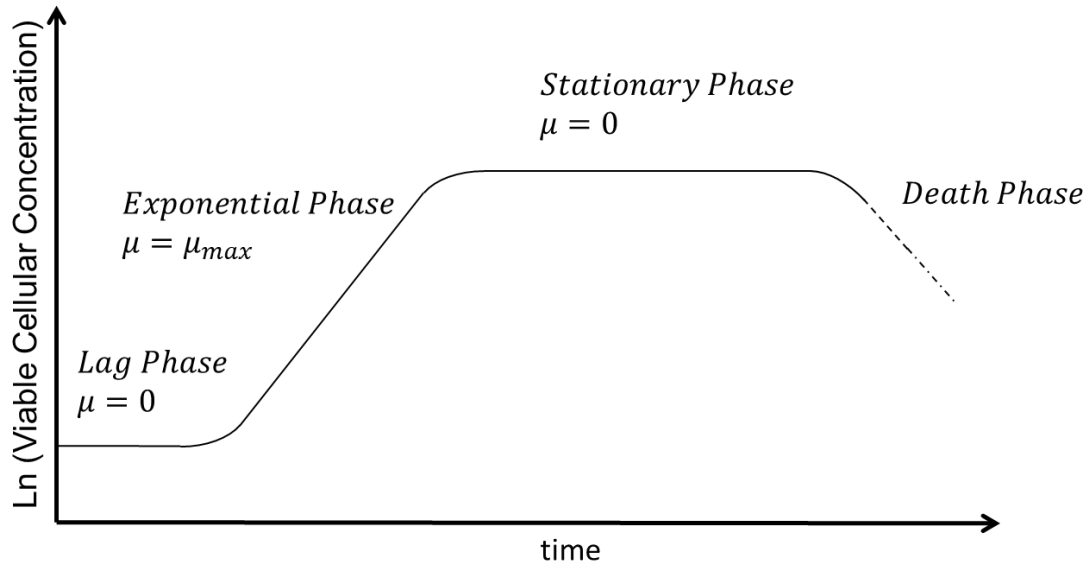
Figure 3-2 Typical Batch Growth curve for cells (adapted from Doran, (2013))

3.2.1.6 Measuring Uncertainty – Errors in measurements

Measurements in engineering are never perfect. Inaccuracies in the determination of experimental quantities due to error, lead to unreliable conclusions and wrong statements. The propagation of error is substantially escalated when multiple different types of measurements are involved (Doran, 2013).

In the case of algae culture monitoring the uncertainty margin varied considerably. In this study the analytical techniques with the lowest margin of error were the spectroscopy UV-VIS absorbance , demonstrating an absolute error of $\pm 10^{-5}$ AU between 400-600nm, and $\pm 10^{-3}$ AU in the regions of 198-399nm and 600-1000nm. The biomass concentration, with an error of ± 10mg between replicates and ± 0.1mg between repeats. The pH and temperature were carried out with errors between ± 0.05 and ± 0.1 ^{o}C respectfully. The measurement with the highest error was the manual cell count. Manual cell count error margin was demonstrated at being between 2-20 cells per measurement grid between repeats and replicates, which translate to over 10^{4} cells/ml. Furthermore, an extra level of uncertainty is added with the culture density, which influences each measurement differently. For instance, a dense culture will increase optical density, pH and cell count variations, whereas it will reduce biomass weight variation in measurement.

Since most of the measured values are used in mathematical operations, there must be an error management routine to avoid their propagation and subject the research outcomes to further systematic errors. This routine-protocol was carried on the premise of common sense and good laboratory practice.

The key measurable outcomes from the experimentation are the biomass density and concentration, these are then used to calculate the rate of biomass and concentration change, i.e. the biomass productivity and specific growth rate.

Considering the cellular concentration, error is managed similar to literature, where continuous sample cell count is replaced with optical density measurements (low error) to extrapolate the actual cell count based on a

calibration curve created using multiple points and repeats. This effectively reduces the relative error in measurement by 24%. A similar methodology is used in literature for the biomass weight, where the change in biomass is explained by a certain wavelength on the optical spectrum, however this was not found to be the case. Carrying out a partial least squares' regression methodology of 31 data sets of spectral signatures and biomass densities it was found that no specific wavelength or even group of wavelengths could robustly explain ($p<0.05$) variation in biomass weight change (data not shown).

On the other hand, as per Feng (2013) the biomass concentration of *C.vulgaris* can be found by the equation below:

$$W_{biomass} = OD658 \times 0.418 \tag{3-5}$$

Since the strain and growth medium are the same, in experiments using comparable cultivation techniques, comparing the experimental with the calibration derived biomass weights has mean error of 0.28 g/l. with the latter being consistently higher than the experimental (29 of 31 data points). A representation of the results is shown in Figure 3-3.
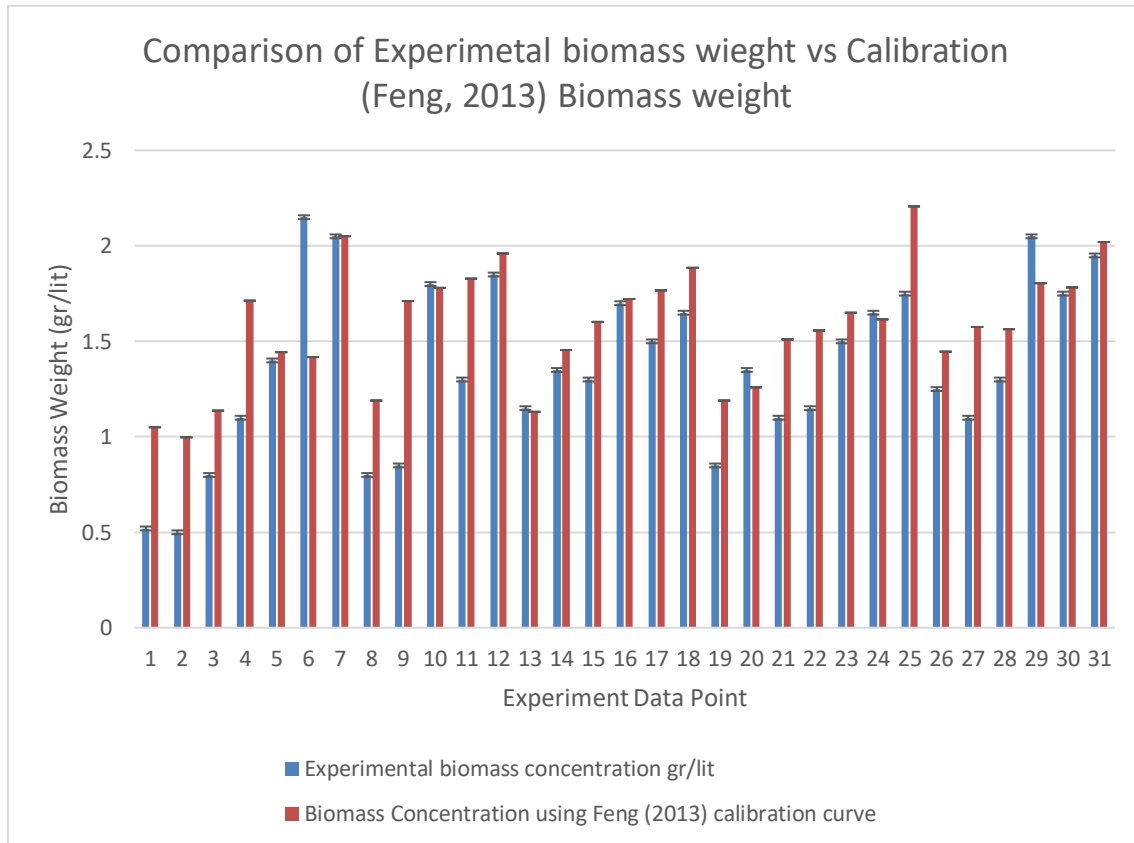
Figure 3-3 Comparison between experimental and calibration curve biomass weight, between 31 experimental data points. Error bars of both the experimental and measurement error are depicted.

Since the error between the measurements is between 0.2 and 0.37g/l, which is higher than the average biomass productivity in some instances, are all indications that such a protocol cannot be employed in this study. Therefore, the mitigation of the errors will have to be conducted carrying out the experimental procedure with care.

3.2.1.7 Data analysis tools

Contrary to empirical experimental methodologies, which are often limited to simple factorial interactors, statistical tools such as Design of Experiments (DoE) enable the development, refinement and optimisation of complex multivariate factorial relationship. (Mandenius et al., 2009; Montgomery, 2008). Design of experiment methodologies are statistical tools employed by experimentalist, which help in framing and structuring the experiments, with ultimate aim to extract the maximum amount of information from the minimal amount of experiments. (Montgomery, 2008; Lee *et al.*, 2013).

There are numerous methodologies and techniques that can be applied, in the DoE framework. In algal biotechnology however, there is an increasing trend of such a framework being used. (Ferrando *et al.*, 2015; Huesemann *et al.*, 2017; Jackson, Bahri and Moheimani, 2017)

3.2.2 Microalgae Cultivation protocols

In order to be able to carry out experimentation with a live organism a strict protocol must be in place to ensure that the algae are adequately maintained in optimum health, to standardise all procedures concerning the processing of algae, and ensure that experiments that are conducted are comparable, reliable and relatable to literature. In addition to this the fact that the continuous flow laboratories at Cranfield University host a library of difference algal strains highlights even more, the requirement of a strict protocol.

The development of such a protocol was carried out due to this project, and the result was a developed protocol currently in place in the Cranfield University Continuous flow laboratories and the Centillion technology Cranfield pilot plant. The established protocols are a result of experimentation with the methodologies outlines in Brand, Andersen and Nobles (2013), and Andersen (2005), from which Andersen is considered the seminal author in algal handling protocols. (Andersen, 2005; Brand, Andersen and Nobles, 2013).

Two protocols where developed for the bioprocessing of algae, tube to flask and flask to PBR. The former outlines the procedure of sub culturing algae from the state of receipt, to a healthy culture at a volume enough for experimentation. And the latter explains the methodology of acclimating the algae and scaling it up for large scale cultivation in a large-scale version of the PBR.

3.2.2.1 Tube to flask

The desired algae strain is supplied in two 10ml polycarbonate test tubes, containing a dense 10ml aliquot in bold basal growth media. From the time of delivery, the algae are sub-cultured within 24h.

3.2.2.1.1 Preparation stage:

Once in a laboratory environment the tubes are checked for leaks and the algae is visually inspected looking for signs of algae deterioration, such as the suspension of biomass flocs, flotation and frothing. Next a sample is examined under the microscope at x80-100 magnification looking for signs of contamination, its optical signature recorded using UV-VIS spectrophotometry. If the algae aliquots pass inspection and are accepted into the laboratory a small sample of 1.4 ml is stored in a sterile test tube in -20°C for future reference. The sub culturing protocol comprises of three stages, as shown in Figure 3-4.
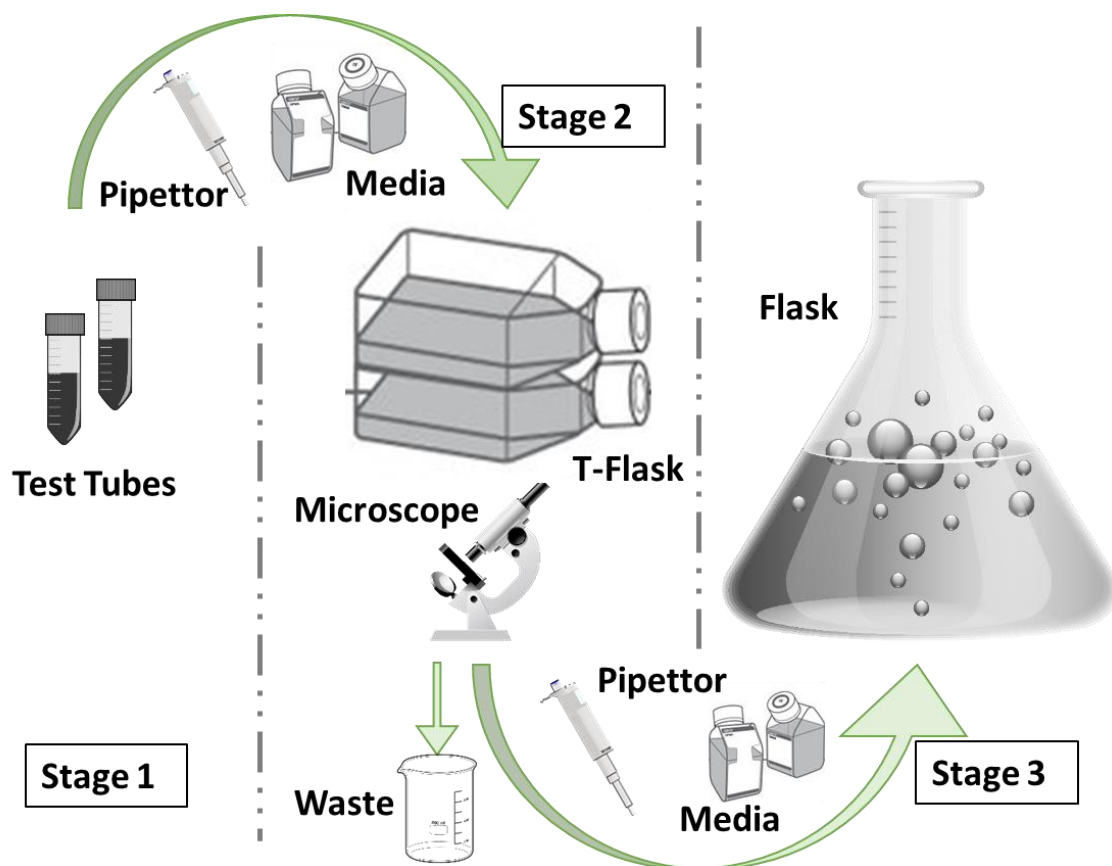
Figure 3-4 Graphical representation of the tube to flask methodology.

3.2.2.1.2 Stage 1 & 2:

Fresh media, following the Bold Basal recipe (BBM), is prepared in an autoclavable 1L borosilicate botte, with a G45 thread cap. The media was prepared as follows $NaNO_3$ 250mg/L, $MgSO_4$ 75mg/L, K_2PO_4 75mg/L, KH_2PO_4 175mg/L, NaCl 25mg/L and $CaCl_2$ 25mg/L. 6ml/L of trace metals stock solution was also added to the mix with concentration of Na_2EDTA 750mg/L, $FeCl_3$ 97mg/L, $MnCl_2$ 41mg/L, $ZnCl_2$ 5mg/L $CoCl_2$ 2mg/L and Na_2MoO_4 4mg/L. by sequential addition of the compounds in a 1L borosilicate bottle with a G45 cap.

The bottle filled to 1L by further of DH_2O. The ph. of the media is measured and regulated to a ph. of 6.9. The bottle is capped off and autoclaved for a complete cycle at 120 ^oC for 15minites.

Two sterile t-Flasks and two sterile 125 ml capacity falcon centrifuge tubes are positioned on a clean and clutter free surface. Using aseptic techniques outlines by (Andersen, 2005), each of the t-flasks are filled with 100 ml of fresh BBM

81

media, and all the contents of tubes were transferred equally between the two t-flasks, keeping a ratio of 1:10 culture to media dilution. The T-flasks are labelled and left to incubate for 5-7 days under 70-80 mmol/m^2/s fluorescent light.

3.2.2.1.3 Stage 2 & 3:

After the initial incubation period, the cellular concentrations is measured by means of optical density and cell count. Light microscopy is also used to evaluate the condition of the cultures in terms of contamination. In the unlikely event that the culture is contaminated then the t-flask and its contents are discarded, if not then the t-flask with the higher cell densities is transferred to a 1L flask. Using identical methodologies as before a clean and decontaminated Erlenmeyer flask, is filled with 900ml of fresh BBM and 100ml of algae transferred from the t-flask. The neck of the container is torched using a Bunsen burner and capped with a two 300x300mm sheet of aluminium foil, one dry and loosely covering the whole neck of the flask, and the other sprayed with a solution of 15% IPA, and covered tightly on top of the first. The remaining 20-25ml of culture left in the t-flask is sub cultured using 100ml of BBM and placed in allocated space for long term storage, with a subculture cycle of 3-4 weeks. The 1L flask is placed under a 100 mmol/m^2/s light source. After a further 5-7 days the cellular concentration in the flask should be high enough to provide algae aliquots for further culturing and experimentation.

3.2.2.2 Flask to Reactor

Unlike the tube to flask methodology, the transfer of an algal culture from a flask to a reactor is a more complex task. The complexity arises , not only due to the volumetric upscale, but also due to the acclimation challenges with light utilisation, mixing and aeration.

3.2.2.2.1 Same scale transfer:

3.2.2.2.1.1 Stage 1 & 2:

Identical to the methodology outlined above. A new Erlenmeyer flask is prepared with fresh Bold Basal media and sub cultured with an aliquot of *C.vulgaris* during

its exponential growth phase from the previous protocol. The new culture is placed on a magnetic stirrer, and a sterile PTFE magnetic stirring bar is inserted into the flask with the algae. The flask is placed under white light with similar intensity to that of the optimised light, implemented in the oscillatory baffled flow reactor system the mixing intensity of the stirrer bar (RPM) is set to a comparable intensity to the mixing conditions present in the photobioreactor.

3.2.2.2.1.2 Stage 2 & 3:

In the linear growth stage, whilst keeping all other parameters identical the light conditions were altered to be identical with those found in the reactor system. At the end of the exponential stage, the same flask is sub cultured with fresh BB media, to double its original volume and left to cultivate for an additional 4-5 days.

3.2.2.2.1.3 Stage 3 & 4:

At the end of the cultivation cycle the photobioreactor is prepared (decontaminated, sterilised and primed). The dense culture is transferred to the reactor using a pump and is left circulating through the reactor for 24hours to acclimate to the flow conditions. After the initial 24 hours in the reactor the culture is diluted with fresh BB media to approximately half the volume. After the subsequent cultivation period ends the algae in the reactor is fully acclimated and ready to commence an experimentation cycle.

Stage 2

Stage 3

Media

Pipettor

Pump

Media

White Light

Optimised Light

Flask

Stage 1

Stirrer

Microscope

Stirrer

Medium
Scale PBR
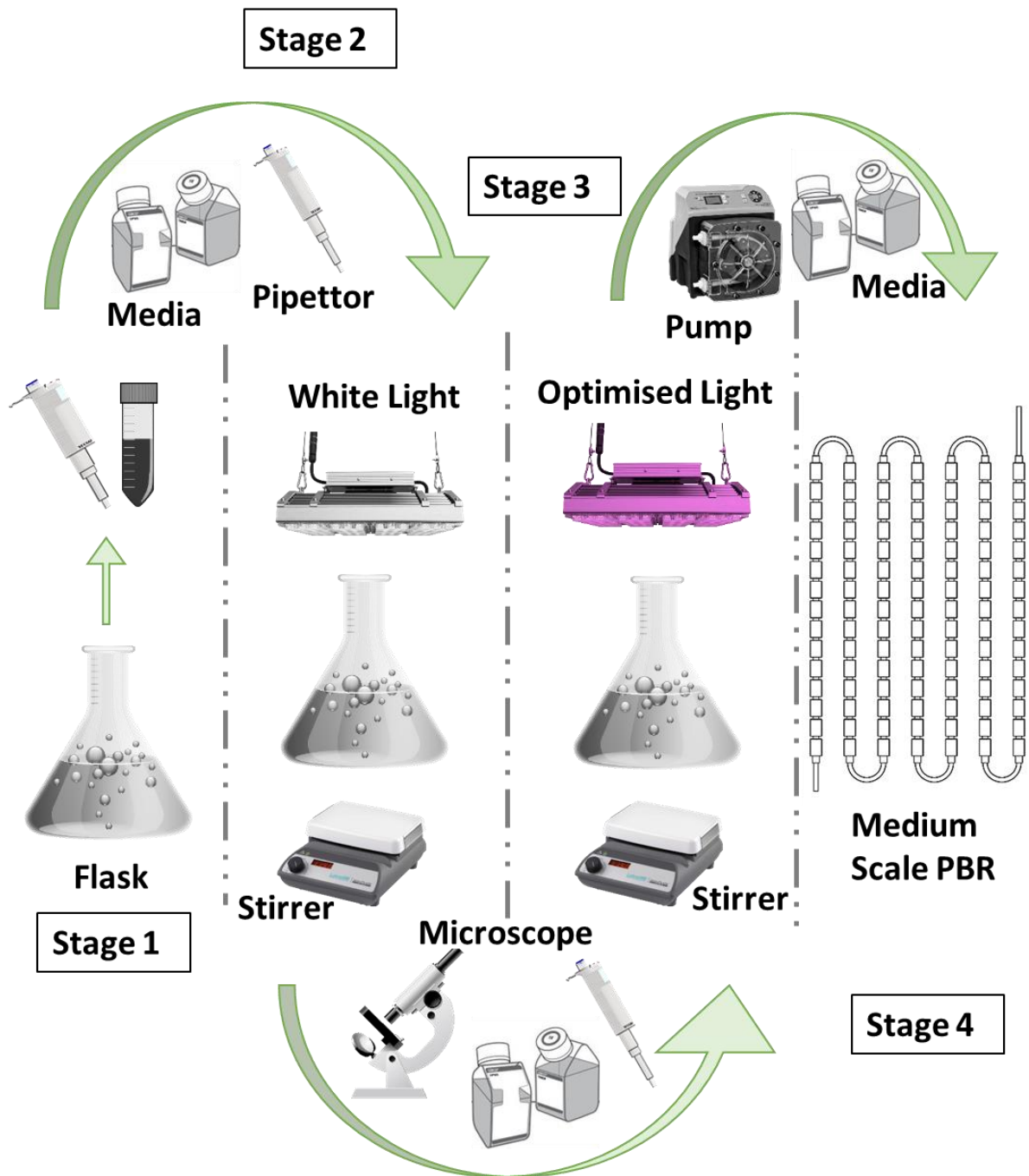
Stage 4

Figure 3-5 Same scale transfer to Reactor, Four stage methodology

3.2.2.2.2 Large Scale Transfer:

Similar to the same scale transfer the protocol for large scale transfer is carried out based on the same principle of gradually introducing new environmental conditions to the algae culture and monitoring it for change.

In the initial stages (i.e 1 & 2), the volumetric scale up to approximately 10 litres is carried out with 9 litres of fresh BB media, and 1L culture in the exponential phase. The 10 L tank is placed under intense white light and Is treated through stages 3 and 4 identical way to the protocol at the same scale, until it inoculates the large-scale reactor. The entire methodology is shown in Figure 3-7. Whereas Figure 3-8 and 3-9 show the optimised (RBW) and white light experimental rigs for acclimatising the algae. (Chia *et al.*, 2013).

Figure 3-6 Stage 1 and 2 experimental set up for same scale and large-scale protocols (LEFT to RIGHT) Day 1 to 5.
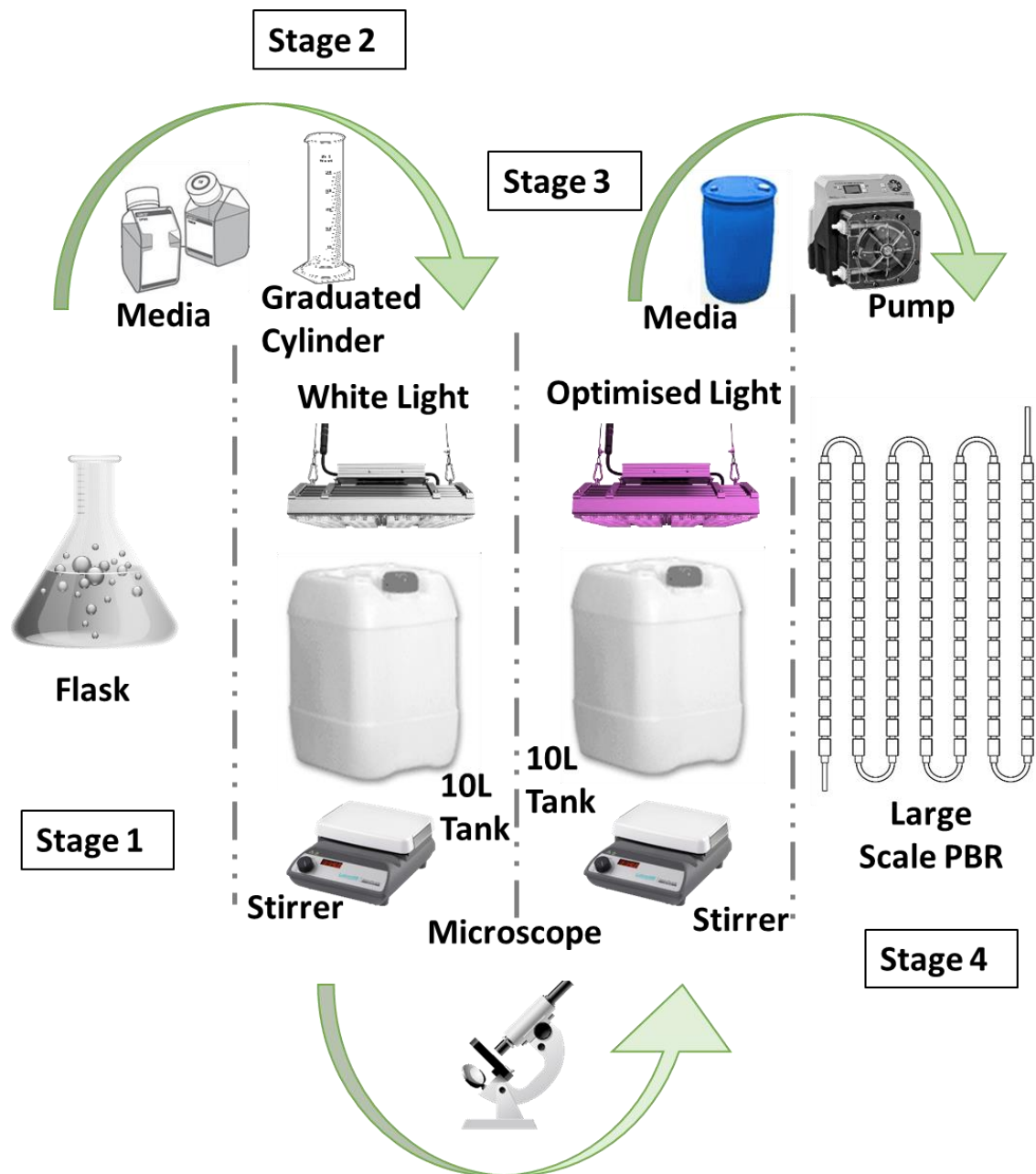
Figure 3-7: Large scale transfer to reactor, Four stage methodology

Figure 3-8 Stage 3 Growth light box, with optimised light conditions similar to those found in the reactor system.
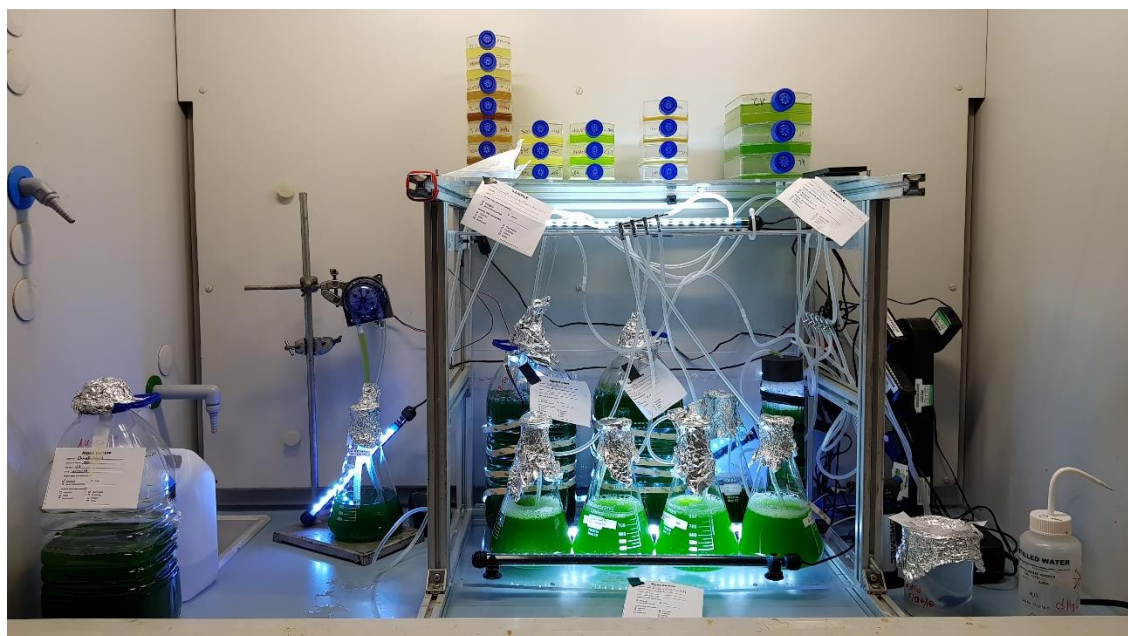
Figure 3-9 Algae strain Library and storage area (TOP) and cultivation rig in the bottom.

4 Biological System

4.1 Strain Selection

Selection of the algal species is often considered as the key criterion which will dictate the bioprocess (Kumar *et al.*, 2011) Despite their diversity, algae are highly selective, and thus suitability of a given strain for one process does not guarantee its effectiveness for another in a typical bioprocess scenario the characteristics that make an algae desirable are namely lipid concentration (oil content, % wt) , biomass productivity (g/d), lipid production (% dw/d) and CO2 requirement/sequestration (g/ml). Barclay and Apt (2013) named the action of selecting a strain based on specific criteria, which fit the suitability for commercial applications, bioprospecting (Barclay and Apt, 2013).

There is a specific pipeline of downstream processes designed for algae biofuel production and the algae strain used can be considered the primary cost factor for the overall process. Algae destined for bio-fuel must not only have a high lipid content, but also a certain intracellular biochemistry that allows for effortless and cheap extraction. A good example of this is the algae strain of *Botryococcus Braunni*, although having a lipid content of approximately 75% wt. much of it is secreted into the cellular wall making it an unviable option for a common and cost-effective lipid extraction technique (Scott et al. 2010). There is a conflicting opinion amongst researchers on whether a process must be customized to a specific algae strain or vice versa, with most scientific research based on the latter. In this specific experimental study, the laboratory environmental factors proved inhibitory to many algae strains, notably:

• 	non-Sterile Environment.

• 	the possible presence of biological contaminants.

• 	the oscillatory flow through the reactor.

• 	high stresses on the algal cellular wall.

• 	non-efficient lighting.

- Axenic Growth.

The above factors created an environment where few algal strains can survive in. Therefore, the choice of algae was based primarily on its tolerance to extreme conditions rather that its ability to generate high biomass productivities and fast growth rates. Brennan and Owende (2010) give a list of desirable algae characteristics that would be ideal for the high lipid productivities (Brennan and Owende, 2010).

- High lipid productivity.
- Robustness, tolerating high impact and shear stresses.
- Dominate over other strains of microbial contaminants.
- High CO2 sink capacity.
- Limited nutrient requirement.
- Tolerate a wide range of extreme temperatures.
- Valuable bi-product production.
- Fast production cycle.
- High photosynthetic efficiency under low light conditions.

The authors point out that the above characteristics are the main focus of genetic bioengineering on algae cells and that the 'ideal' strain does not exist yet. However, a close resemblance to the above criteria can be found in the strain *C.vulgaris*, also known as the food of the future by Shi et al (1999). (Shi *et al.*, 1999).

C. vulgaris is a blue-green alga from the *Cyanophycae* family, it is one of the few strains that has the ability to accumulate a high lipid or carbohydrate content as well as being suitable to produce desirable compounds for the nutraceutical and pharmaceutical industry (Saad H. Ammar, 2016).

C.vulgaris has been extensively used in literature. The most notable and comprehensive reviews on this strain are given by (Yamamoto, Kurihara and Kawano, 2005; Scarcella, Belotti and Filippis, 2009; Lv *et al.*, 2010; Yusof *et al.*, 2011; Kong *et al.*, 2013; Safi *et al.*, 2014; Daliry *et al.*, 2017; Wong, 2017). From relevant literature it can withstand extreme fluctuations in light intensity, high

cellular rigidity withstanding the most turbulent mixing regimes and finally is considered the only freshwater strain that can successfully grow in a non-axenic environment . For all the above reasons a strain of *C.Vulgaris* specifically CCAP 211/11B (CCAP, Oban, Scotland) was chosen as the experimental culture for all subsequent experimentation.

4.2 Growth Media Design

This section uses the systems biology approach to carry out experimentation following a Design of Experiments (DoE) and subsequent analysis of data to generate assumptions which will lead to further experiments.

The section starts with quantifying the growth and productivity of existing media recipe cited in literature. Subsequently carries out a screening experiment prior to a DoE based and based on the findings follows steps to reduce the price and number of components in the media. Thus, aiding the technical aspects of the design process.

4.2.1 Media Formulation

Growth media formulations are designed to cover the requirements and accommodate many microalgal species. Therefore, they contain compounds and elements in excess. This results in increasing the price of algae biomass production and subsequently the cost and complexity of water and media recycling.

Specifically, for *C.vulgaris* it is reported that it can be successfully cultivated in most growth media formulations (Chia *et al.*, 2013; Wong, 2017) with greatest success in Bold Basal media (Wong, 2017). However BG11 and N8 also report consistently high biomass productivities (Mandalam and Palsson, 1998). Table 4-1 specifies each of the above media recipes contents and concentrations.

Table 4-1 : BBM, BG-11 and N-8 Media Formulation Contents List (UTEX, 2019)

BBM		BG-11		N8	
Macro Nutrient	Mass per Unit Volume (mg/l)	**Macro Nutrient**	Mass per Unit Volume (mg/l)	**Macro Nutrient**	Mass per Unit Volume (mg/l)
NaNO3	249.87	NaNO3	1495.8	KNO3	1000
CaCl2·2 H2O	24.99	K2HPO4	40.06	KH2PO4	740
MgSO4· 7H2O	73.94	MgSO4·7 H2O	73.94	Na2HPO 4 2H2O	260
K2HPO 4	74.906	CaCl2·2H 2O	35.28	CaCl2 2H2O	13
KH2PO 4	175.55	Citric Acid·H2O	6.51	Fe EDTA	10
NaCl	25.11	C6H8O7x Fe3+yNH 3	5.501	MgSO4 7H2O	50
		Na2EDTA •2H2O	1.00		
		Na2CO3	20.13		
Trace metals		**Trace metals**		**Trace metals**	
Na2ED TA•2H2 O	4.5	H3BO3	2.84	Al2(SO4)3 18H2O	3.58
FeCl3 6H2O	0.58	MnCl2•4H 2O	1.78	MnCl2 4H2O	12.98

MnCl2•4H2O	2.46	ZnSO4•7H2O	0.22	CuSO4 5H2O	1.83
ZnCl2	0.03	Na2MoO4•2H2O	0.38	ZnSO4 7H2O	3.2
CoCl2•6H2O	0.012	CuSO4•5H2O	0.047		
Na2MoO4•2H2O	0.024	Co(NO3)2•6H2O	0.031		

BBM, BG-11 and N-8 are high performance growth formulations, they contain all major elements such as N, P, K, Mg, Mn, Fe in the form of salts. Nitrogen in both BBM and BG-11 is supplied in the form of NaNO3, the situation is similar for Magnesium (MgSO4·7H2O), Manganese (MnCl2•4H2O), Calcium (CaCl2·2H2O), Chloride (MnCl2•4H2O & CaCl2·2H2O), Phosphorus and Potassium (K2HPO4). whereas in N-8 is it supplied as KNO3. There is also a substantial difference in the quantities (mg/l) supplied for each salt. For example, nitrogen is supplied in BBM nearly 6 times lower than in BG-11. Similarly, the N8 medium has a potassium and phosphorus supply of 1000mg/lit whereas BBM and BG-11 supply P and K 240mg/l and 40mg/l. In terms of micronutrients (trace metals), all three medias contain Mn, Mg Na, Zn, in different forms. However, BBM and BG-11 contain cobalt whereas BG-11 and N-8 contain copper in the same form. The composition of a growth media and its ability in enabling growth is highly correlated. Matching the elemental requirements of the algal cell is key in order to avoid growth inhibitions due to nutrient depletion.   The elemental composition of *C.vulgaris* is presented in

Table 4-2 (Starr, 1991; Mandalam and Palsson, 1998; Jayasurya Vijayakumar *et al.*, 2013).

Table 4-2 : *C. Vulgaris* **elemental composition in mass percentage**

Element	S.	Lower Range Values (w%)	Mid Values (w%)	Upper Range Values (w%)
Carbon	C	51.4	60	72.6
Oxygen	O	11.6	21	28.5
Hydrogen	H	7	9	10
Nitrogen	N	6.7	6.5	7.7
Phosphorus	P	1	0.8	2
Potassium	K	0.85	1	1.72
Magnesium	Mg	0.36	0.8	0.8
Sulphur	S	0.28	0.3	0.39
Iron	Fe	0.04	0.5	0.55
Calcium	Ca	0.005	0.08	0.08
Zinc	Zn	0.0006	0.005	0.005
Copper	Cu	0.001	0.004	0.004
Manganese	Mn	0.002	0.01	0.01

Since BBM is the best performing according to Wong (2017), it is selected as the baseline media for all future experimentation. Based on the elemental composition of C. *vulgaris* and the quantity of the corresponding element in BBM, it is possible to calculate the potential biomass capacity that each media can generate. The maximum biomass capacity of each element was determined by considering the amount (g) of each element in 1L media (from above table) and the fraction of that element in the dry weight of the cell.

$$Biomass \% (v.v) \tag{4-1}$$

$$= \left(\frac{mass\ of\ element\ in\ unit\ volume\ of\ medium}{Fraction\ of\ dry\ weight\ of\ the\ element}\right)$$

$$\times \left(\frac{1}{(\ dry\ weight\ fraction\ of\ cell}\right)$$

$$\times \left(\frac{1}{(density\ of\ fresh\ cells)}\right) \times 100$$

Where the capacity in terms of cells/mL can be obtained by diving the biomass by the volume of each fresh cell. The dry weight of the cell is taken as 25% of the fresh weight and the density of the fresh cells as 1.01 g/mL The average Cell volume was found to be 40 Femtoliters (fL = 10^{-15} Litres or 1 cubic microliter) (Mandalam and Palsson, 1998).

The mass of element in unit volume of medium composition can be calculated by the following equation,

$$Mass\ of\ element\ in\ unit\ volume\ of\ medium = \tag{4-2}$$

$$\frac{Atomic\ Weight\ \times No.\ Molecules\ of\ element \times Mass\ of\ salt\ in\ Media}{Molar\ Mass\ of\ the\ Salt}$$

Where the information on molar mass and molecules of each element in the media shown in Table B-1. In similar fashion the mass of each element in media and the biomass capacity of *C. vulgaris*, can be calculated for the rest of the elements for both BG-11 and BBM. For N-8 no calculations were performed, the values were taken from (Mandalam and Palsson, 1998). Carbon, oxygen and hydrogen are supplied externally and in excess therefore they are omitted from the analysis.

Table 4-3 Biomass capacity of BG-11, BBM and N-8 for C.Vulgaris (Limiting elements ar indicated with an asterisk).

Element	Symbol	BG-11	BBM	N-8
		Biomass Capacity % v/v	Biomass Capacity % v/v	Biomass Capacity % v/v
Nitrogen	N	15.038	2.530	0.69
Phosphorus	P	3.527	26.374	4.24
Potassium	K	7.123	33.292	14.42
Magnesium	Mg	3.610	3.610	0.25*
Sulphur	S	12.744	12.699	0.7
Iron	Fe	0.929*	0.096*	0.11*
Calcium	Ca	47.617	33.729	1.78
Zinc	Zn	3.988	1.150	5.78
Copper	Cu	1.888	0.000	4.55
Manganese	Mn	19.582	2.741	14.26

Examination of the above, shows that in both BG-11 and BBM media compositions the limiting element is Iron. For N-8 there are multiple limiting elements such as Magnesium, Iron, Sulphur and Nitrogen. Also notable is the imbalanced elemental distribution in terms of biomass capacity. Focus given to the three macronutrients nitrogen, potassium and phosphorus, shows that in BBM and N-8 the nitrogen is undersupplied, severely limiting growth. In the example of BG-11, phosphorus and potassium are supplied at similar levels where nitrogen is given in excess of what can be utilised by the algae.

In similar fashion with Danquah and Harun (2010), a procedure was implemented for the growth media optimisation based on *C.vulgaris* CCAP 211/11B. The procedure aimed at rebalancing the elemental composition of the medium to suit a specific strain and to increase the media's cost effectiveness (Starr, 1991; Mandalam and Palsson, 1998; Danquah and Harun, 2010).

4.2.2 Experimental Section

To optimise the media, a design of experiments methodology was implemented in order to aid in identify the key nutrients, their interactions and their effects on the growth. From relevant literature (Grobbelaar, 2003)it is clear that nitrogen (N) and phosphorus (P) and are critical elements. As suggested by Grobbelaar (2003) there is an adequate supply zone with respect to N, P and carbon (C). With growth retardation occurring in the deficient zone, and excessive stresses when supply is luxurious. Although this zone is mentioned it is not defined, therefore experimentation to identify the limits of this phenomenon must be carried out.

Since no reference on the adequate amount of biomass capacity is given for each element, screening experiments are carried out based on literature. Specifically, Danquah and Harun (2010) which cultivated a different strain in a custom medium by modifying the supply of all macronutrients and micronutrients to correspond to a biomass capacity of $\varphi = 10\%$ and 5% respectively.

In a similar fashion for *C.vulgaris* using BBM, a series of experiments will be carried out prior to establishing the DoE matrix.

4.2.2.1 Experimental Setup

The experimental setup was similar to that shown in Figure 4-3, *C.vulgaris* CCAP 211/11B (CCAP, Oban 2018), was cultivated in 1 litre Erlenmeyer flasks, under 200 mmol/m^2/s fluorescent light. Soft agitation was provided by air pumped (Hailea V-30) supplied at 50 l/h, through a 0.22 µm disposable syringe filter connected to a 1cm sparging cylinder.

Each Erlenmeyer flask used to cultivate algae, was cleaned and decontaminated using a hand-held steam cleaner. Each bottle cleaned thoroughly with a mixture of deionised water (diH2O) and Iso-propyl alcohol (IPA), and then flushed with diH$_2$O. following that each flask was then inverted and clamped so that its nozzle was placed over the pressure steamer outlet. The steam cleaner was turned on and oriented so that steam was uniformly spread throughout the vessel, until surface temperature reached above 100C^o at the base of the vessel. Using waterproof and heat resistant gloves, the neck of the vessel was covered in a layer of sterile gauge and aluminium foil (previously sprayed with IPA 70% solution). The covered bottle was inverted and placed under UV-C light to cool down to room temperature. The procedure was repeated for all the vessels used in the experiment.

The flasks were filled with 500ml of diH$_2$O. Using an analytical balance with resolution 10^{-4} g. Each of the chemicals indicated in the formulation recipe was weighed and inserted into the flask. The pH of each media was set to 6.9 using 0.5M hydrochloric acid (HCL) solution. The flasks where capped off with aluminium foil and autoclaved for 15 minutes. The flasks were placed in a clean and clear area in the fume hood and inoculated with 50ml aliquots of *C.vulgaris*, taken in the exponential phase. Each of the flask was connected to a Hailea V-30 pump supplying 50 l/h to each of the flasks. All cultures were left to cultivate, with their optical density being monitored every 24h. When their respective optical density at 680nm, reached above <3.00 AU, the cultures were diluted with their respective freshly prepared media, to 800ml. A sample was taken and the initial optical density, cell count and biomass density measurement were taken, and the experiment was initiated.

4.2.2.2 Screening experiments

Prior to conducting a factorial DoE, evaluating the effects and interactions between selected factors (macronutrients) and response (growth), an experimental design acting as a screening using the best guess approach methodology (Montgomery, 2008). This methodology aims at establishing whether a change in formulations results in quantifiable change. It is a quick and

cost-effective method to reach a conclusion, by conducting a single comparative experiment between a baseline formulation and further modifications. In this case a nitrogen deficient media and a formulation designed based on the maximum biomass capacity, following the same methodology with (Mandalam and Palsson, 1998; Danquah and Harun, 2010). The new media called BBM R1 is formulated based on the original BBM, but enriched in nitrogen, potassium and phosphate, and reduced trace metals. Specifically changing N, P, K to a biomass capacity $\varphi=10\%$ and all others Mg, Mn, S, Fe, Ca, Zn, Cu, Mn to $\varphi=5\%$. changes to the new media are and evident increase in Nitrogen and Iron content, reduction in K, P, Na, Cl, and removal of EDTA, Cobalt and Molybdenum, since they are not required from *C.vulgaris.*

The experiments between three different subcultures of BBM, BBM -N and BBM R1, where left to cultivate for 8 days, where all cultures went into their stationary phase. Their optical density, cell count, specific growth rate as well as doubling time are shown in Table 4-4.

During the exponential phase all three medias grew to an OD680 between 2-2.5AU this translates to cellular densities between 2.19E+08 and 2.84E+08. Looking at maximum productivities the standard BB media did not perform as well as the N-deficient and the revised media (R1). With both performing surprisingly similar with comparable final cellular densities achieved. However, looking at the specific growth rate the R1 outperforms the N-deficient and by 30%.

Table 4-4 : The results of 8 days cultivation of BBM 1N, 0N and R1.

	BBM 1N		BBM 0N		BBM R1	
Days	OD680	Cells/ml	OD680	cells/ml	OD680	Cells/ml
1	1.08	1.10E+08	0.91	9.34E+07	0.46	4.81E+07
2	1.85	1.87E+08	1.26	1.28E+08	0.63	6.55E+07
4	2.43	2.45E+08	2.05	2.07E+08	1.50	1.52E+08
6	2.38	2.40E+08	2.28	2.30E+08	2.23	2.25E+08
7	2.65	2.67E+08	2.79	2.81E+08	2.53	2.55E+08
8	2.17	2.19E+08	2.82	2.84E+08	2.64	2.66E+08
μ	0.12		0.16		0.24	
t_d	5.77		4.33		2.88	

An additional area where the R1 formulation outperforms its counterparts is biomass concentration. The final biomass concentrations recorded for the three cultures at the end of the culture period, were 1.15 g/l, 1.3g/l and 1.25g/l for BB, BBM-0N and BBM-R1 respectively. In terms of productivity the redesign of the media was successful.

Algae nutrition is one of the biggest financial inhibitions of algae cultivation. As explained in the sections above. One of the objectives of re-designing the formulation was to make the media more cost effective. Based on the elemental analysis of the *C.Vulgaris* strain, the new formulation (R1) was designed with fewer components, in majority lesser amounts of nutrients but with excess N and P. This resulted in higher growth rate, albeit at a much higher price.
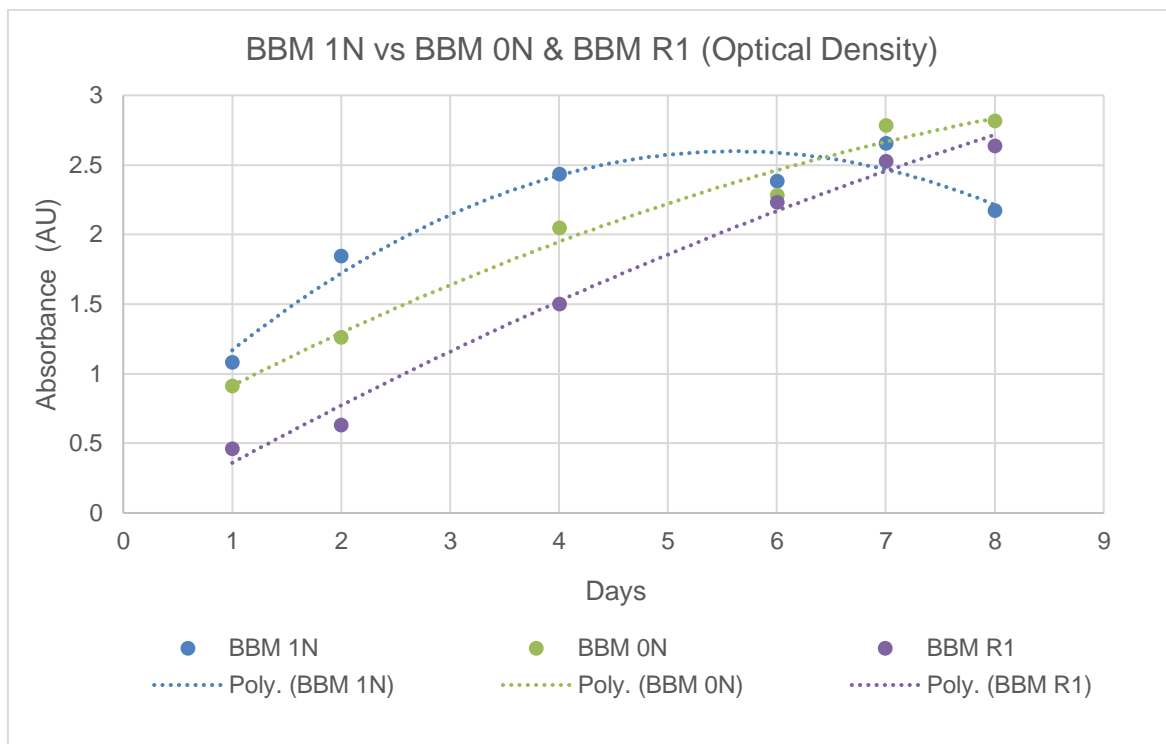
Figure 4-1 Absorbance (OD680) time line of the three experiments (Subcultures) with best fitted line.
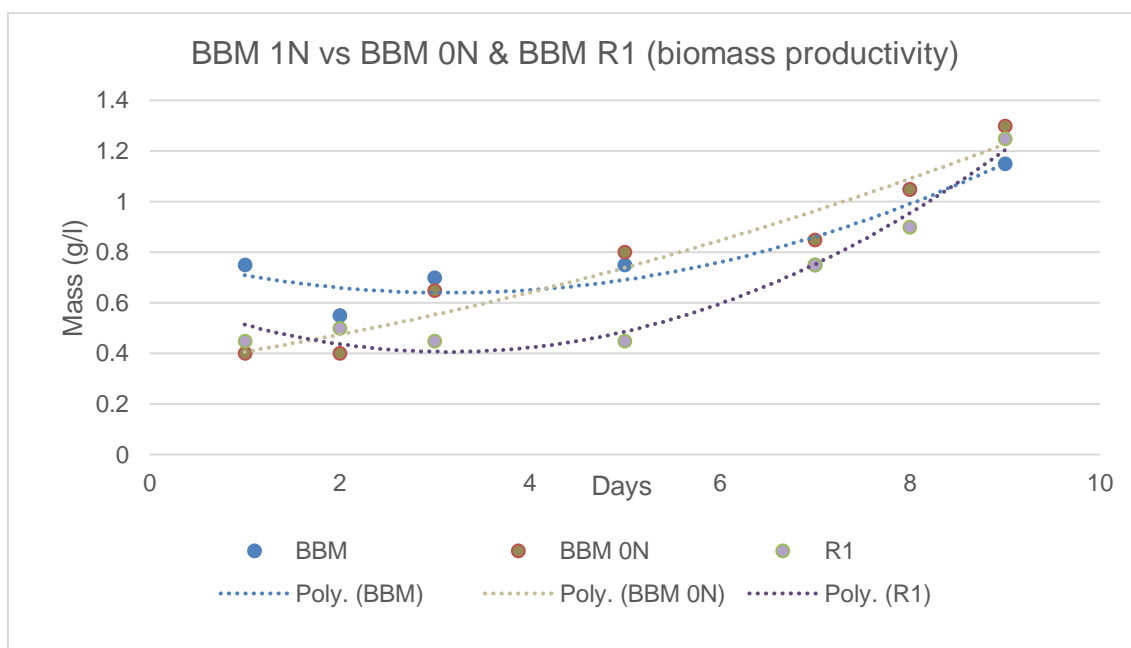
Figure 4-2 Biomass Density (g/l) timeline for the three experiments (subcultures), with best fitted line.

Looking at Table B-2 all three experimental media formulation are shown according to their cost input per component. Standard BBM is approximately 4 p/l, as expected N-deficient BBM is lower, at 3 p/l since nitrogen which is expensive is the heaviest attribute of cost, BBM-R1 on the other hand costs 10 p/lit, this cost increase is primarily due to the increase of N,P and Fe.

Based on the experimentation it is logical to deduct that all things being equal, the cost per gr of biomass is 8p/g for BBM R1, 2.3 p/g for BBM-0N and 3.47 p/g for standard BBM, based on the experiment conducted.

The most cost-effective growth solution per unit biomass is nitrogen deficient media, however this formulation cannot sustain growth long term, since it lacks the most important nutrient which accelerates division of the cells within the culture. The growth demonstrated by the media here, is most likely due to the algal cells using stored nitrogen deposits from the previous subculture, and thus driving the culture towards maturing and growing lipids rather than growing more cells.

Figure 4-3: Experimental setup of the three cultures (please note that RBW light was turned off due to interference with the camera).

4.2.2.3 Design of experiments

Overall the screening experiments between the standard, and revised BBM R1 and N-deficient BBM, showed that there is a clear difference in growth rates and biomass concentration between traditional and rebalanced (Figure 4-1 and Figure 4-2). Based on this it seems that a biomass concentration between $\varphi = 10\%$. and 5% for macro and micronutrients respectively works well with *C.vulgaris* and BBM, producing a quantifiable difference.

Therefore, a Design of experiments (DoE) matrix based on a full factorial methodology of measuring three factors, nitrogen (N), phosphorus (P) and carbon (C) concentration, at two levels was selected.

The choice of phosphate, nitrate and carbon as the factors under investigation are due to the following biotic and process driven reasons. The effect of nitrate is well investigated, however in previous experimentation, the results did not correlate with literature (Lv *et al.*, 2010; Paes *et al.*, 2016). Another reason is that nitrogen in all its forms is amongst the most expensive nutrient, considering the quantities it is consumed in. As cited by Li et al (2011) the cost of nitrogen is approximately $500 per tonne (Li *et al.*, 2011). Furthermore the investigation of nitrogen as a factor enables the new designed formulation to be a little future proof, since different sources of nitrogen are under scrutiny and have gathered major scientific interest in recent years (Ledda *et al.*, 2013b).

Phosphorus (P) is a key ingredient in growth medias. In the previous experimentation between standard BB media and BB R1 media the biomass capacity difference between phosphorus levels was 21%. Since higher growth rates were found in the media with lower phosphorus levels. It created a clear reasoning to study it more closely. Furthermore it was chosen for its importance as a nutrient and its interaction with nitrogen, which have been shown to enhance lipid production in algae and specifically in *C.vulgaris* (Chu *et al.*, 2013; Shen *et al.*, 2015; Paes *et al.*, 2016).

Carbon (C), is perhaps the most important ingredient, and contributor of algae growth. As explained in chapter 2, the selection of carbon type and source,

enables and restricts algae cultivation in more ways than the media formulation. Mainly carbon can be supplied in the form of gas CO_2 or solid $NaHCO_3$, Glucose $C_6H_{12}O_6$, or glycerol $C_3H_8O_3$. It is acknowledged that CO_2 use as a carbon source, although a very important benefit of algal use, and a main contributor to the scientific advancement of algal research, has limited algal research to applications of carbon mitigation, and is ineffective since up to 70% is lost to the atmosphere when sparged (Chisti, 2016). This has implications far beyond the nutrient formulation, but also in PBR design, scaling, algae usage, pharmaceutical use of algae, et cetera. Also, from an academic research point of view, algae research with CO_2 as a carbon input, infers that PBR design will undoubtably be based on multiphase gas-liquid gas transfer, where in both domains, scientific and engineering, the area is saturated and little space for novelty is likely. Therefore, it was decided that the use of alternative carbon sources and research into mixotrophic growth would be carried out.

Glycerol was selected as the carbon source. This decision was made for several reasons. Firstly, to give the media formulation some extra flexibility in its application, and secondly for the formulation to have the potential to be applied in the reactor without the introduction to bubbling, which is the hardest parameter to scale. Furthermore the choice of glycerol as alternative carbon source was made due to its performance (Liang, Sarkany and Cui, 2009; Yeh and Chang, 2012). And its abundance and cost considering bioprocessing strategies and the applications of recycling pathways, glycerol is a biproduct of many bioprocesses and its recycling would be the most cost-effective solutions to its utilisation.

Moreover, a critical point in the media synthesis was the source of phosphorus. According to the BBM recipe, phosphorus is contained in both K_2HPO_4 and KH_2PO_4, with mass fraction of %17 and 22% respectively. Similarly, Potassium (K) is also contained in this compound at a mass fraction of 44.9 and 28.73%. Therefore, only changing the P levels would inevitably change the K levels as well. Therefore, the levels of phosphorus that each compound contributed was split to accommodate the potassium levels in the range of previous experiments. The mass of all other nutrients was kept identical to BB. (Even the Fe levels,

since the previous experiment did not show such a difference as to justify the cost).

The experimental matrix is seen below. The experimental design focused on combining all elements required by algae to successfully cultivate. The media recipes would be custom made based on the experimental run, where the level of P, N and C would be dictated by the DoE matrix, and all other elements would remain constant and at identical levels as in BBM. The following experiments were carried out by Cox (2018).

Table 4-5: DoE Matrix, Full Factorial 2x2x2 (Cox, 2018)

Experiment Number	Pattern	Nitrogen (N)	Phosphorus (P)	Carbon (C)
		Biomass Capacity (φ)	Biomass Capacity (φ)	Biomass Capacity (φ)
1	+++	4.95	4.95	4.95
2	-++	0.99	4.95	4.95
3	+-+	4.95	0.99	4.95
4	--+	0.99	0.99	4.95
5	++-	4.95	4.95	0.99
6	-+-	0.99	4.95	0.99
7	+--	4.95	0.99	0.99
8	---	0.99	0.99	0.99

Having the factors selected, each factor had two levels set by the biomass capacity, the minimum level was set to 1, and the max level was set to 5. All other nutrients were set to the identical concentrations as with BBM. The biomass capacity of each element in the media is shown in Table 4-5

Eight experiments were designed to carry out an investigation on the effect of growth media's phosphate, nitrate and carbon levels. The complete list of ingredients can be found in Table B-3 and Table B-4 in the appendix.

The *C.vulgaris* cultures growing under the 8 different media were cultivated for a total of 8 days before reaching the stationary phase. As per protocol an equal sample was extracted every day and tested using optical density, light microscopy and biomass weight. Figure 4-4 depicts the cellular concentration trend per day of all eight cultures, with imposed pictures showing the colour difference of 4 cultures. The trend of the growth curve followed a predictable trajectory, in spite of a sudden spike in the P+N+C+ sample which spiked during day 6.

The biomass concentration trend as well as the trend of the pH are shown in Figure B-2 and Figure B-1. The results from the experiments are summarised in Table 4-6 whereas the complete data set is shown in Table B-5.

The growth curve is as expected. With 1 days as a lag phase and 5-6 days as exponential / linear growth, then levelling out into stationary. The only inconsistency on the 5th experiment where there is a sudden spike in biomass concentration, the response could be considered an error in measurement, however the same spike is observed during cell count, biomass measurements and pH as well.

The aim of the DoE was not to establish a predictive model, but to evaluate the influence of each of the factors of interest. In Table 4-7, the factors are ranked according to their suitability as a predictor. With (+) being low and (+++) being high the results indicate that nitrogen is key for the growth rate, and secondary for biomass production, whereas using $NaNO_3$ as the N source is the cheapest and thus non-influential. Phosphorus on the other hand is ranked highly across

all three Reponses with biomass concentration being the most influences by change in the phosphorus levels. The carbon content only seemed to influence the price as change in the concentration of carbon didn't affect the growth rate nor the biomass concentration. In terms of biomass concentration, and growth rate the best media formulation was P-N+C-, P+N+C+ P+N+C- and P-N+C+. In terms of price, the best medias are P-N-C+, and P-N-C-.

Table 4-6 Summarised Results of the DoE with Responses being Growth rate, maximum biomass concentration and price per litres of media.

Pattern	N (φ)	P (φ)	C (φ)	Growth Rate (μ)	Biomass (g/l)	Price (p)
+++	5	5	5	0.59	5.67	5.78
−++	1	5	5	0.61	1.32	4.8
+−+	5	1	5	0.57	1.05	2.8
++−	5	5	1	0.55	1.09	1.87
−−+	1	1	5	0.59	2.92	5.78
−+−	1	5	1	0.64	5.94	4.83
+−−	5	1	1	0.55	0.45	2.82
−−−	1	1	1	0.55	0.94	1.87

Taking and step back and evaluating the media formulations potential and applicability, it is deducted that P+N+C+, P+N+C- , P-N+C-, P-N+C+, are the better performing formulations, in terms of price per gram of biomass produced they perform better with the results shown below in Table 4-8.

Table 4-7 Factor's ranking as a predictor of each response, based on the results.

Predictor	price (p)		growth rate (μ)		biomass concentration (g/lit)	
	Portion	Rank	Portion	Rank	Portion	Rank
Nitrogen (mg)	0.18	+	0.45	+++	0.30	++
Phosphorus (mg)	0.27	++	0.39	++	0.46	+++
Carbon (mg)	0.54	+++	0.15	+	0.23	+

Table 4-8: The four best media formulations against their price per biomass productivity

Name	Media	Pence per gram of biomass
CV1	P+N+C+	1.01
CV2	P-N+C+	3.63
CV5	P+N+C-	1.97
CV6	P-N+C-	0.81

To validate the above, using a completely fresh batch of *C.vulgaris* under identical conditions the above 4 media formulations were replicated with the specific growth rate derived from the optical density at 680nm as the only measured metric. The results are as follows:

Table 4-9 Validation experiment on the four best performing medias.

Name	Media	Specific growth rate μ	Duplication rate (t_d)
CV1	P+N+C+	0.106	6.50
CV2	P-N+C+	0.105	6.56
CV5	P+N+C-	0.133	5.20
CV6	P-N+C-	0.157	4.38

Although the replicates have a lower specific growth rate, the same trend exists with CV6 being the highest performing media.
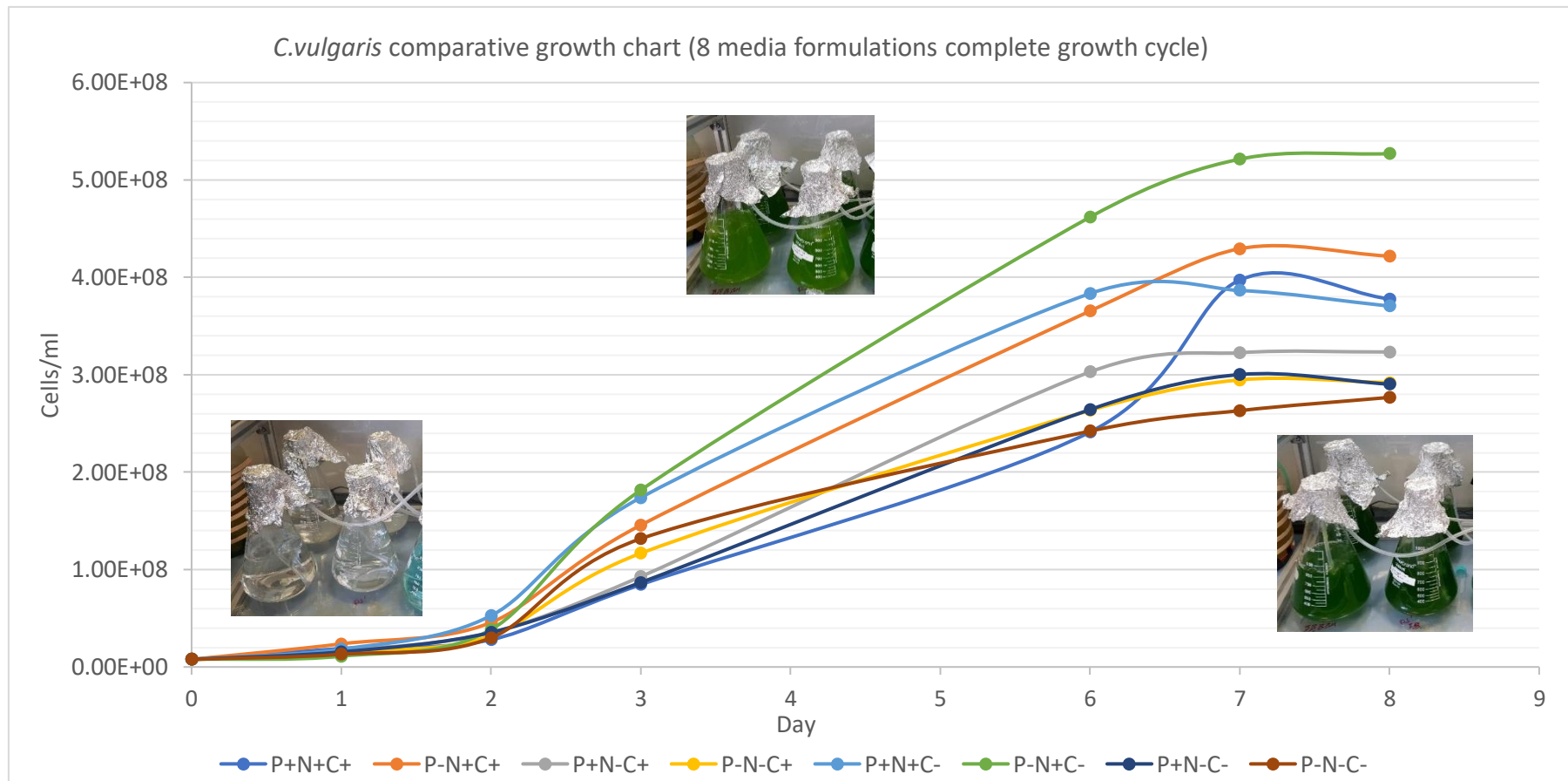
Figure 4-4 : Concentration of cells, trend between 8 medias through 8 days of cultivation. With pictures indicating the colour from day 0

4.2.3 Reducing the cost of the Formulation

Growth medium supply is considered the greatest obstacle to algae's economic viability (Ledda et al., 2013a). Reducing the cost of the media can occur in three ways. By utilising the nutrients from waste sources such as anaerobic digestate, from agricultural or food industry waste, (Ledda *et al.*, 2013a). Optimising the nutrient formulation based on the elemental capacity of the processed algal strain, as with the work presented here. And third by reducing the cost of the nutrients themselves. (Madkour, Kamil and Nasr, 2012). The work carried out in this section relates to the optimisation of the growth media which aims to reduce the price per unit biomass to as low as possible.

In literature the cost of nutrients per kilogram biomass ranges between approximately $2.95-3.8/kg (Chisti, 2007) and $20 – 200/kg (Gupta and Choi, 2015). From the experiments carried out the previous section the cost of the media for the 8 media formulations is shown on Table B-7. In trying to reduce the cost of the nutrients, it will be assumed that glycerol is sourced for free, either as recovered material or sourced externally. The cost is between £8-36, which is closer to the value cited by Gupta and Choi (2015) than Chisti (2007). The major cost difference between the latter figure and the experimental ones, is primarily depended on the quality of the nutrients.

NPK fertiliser as a source of macro and micronutrients, replacing expensive laboratory-based chemicals, with very promising results (Chia *et al.*, 2013; Saad H. Ammar, 2016; Schneider *et al.*, 2018). The benefit of NPK is cost, on the other hand, purity, quality and limitation in growth media customisation, may prove to be inhibitory.

Commercial fertilisers are commonly available, in a range of prices, quality and ingredients. The most popular and commercially available fertilisers are listed in Table B-8. They are selected based on their availability and their ingredient mix being in the range that it will be beneficial to algae.

Miracle grow® (MG) is a formulation stating 24-3.5-16 NPK, containing also manganese (Mn) and traces of iron (Fe) and copper (Cu). Comparing it with algae

growth media formulations (developed and marketed), it contains the main macronutrients however lacks majorly many of the elements required for the growth of *C.vulgaris,* specifically Mg, Cl, and Na. It proved to be difficult to find a single NPK fertiliser that contains all the elements that algae require. Therefore, a combination of commercial NPK fertilisers is considered. The addition of Bone meal, Epsom Salts and Sulphate of Iron, is also crucial since each one delivers an element which is lacking in MG. Bone meal is a source of phosphorus, Epsom salts is a form of magnesium, and sulphate of iron is a source of iron.

To ensure that the exact elemental composition of the fertilisers is known, it was crucial that they were analysed by electron diffraction EDX to identify the exact makeup of the media. And most importantly evaluate whether the fertiliser is suitable for algae culture.

The Table B-9 is the Energy Dispersive X-ray Spectroscopy (EDX) results of the media above, in addition to a commercial acid and alkaline buffer that is required due to the influence on pH the above fertilisers have.

Which as expected was different to what is advertised. For one miracle grow NPK fertiliser contains much more than what is stated, including aluminium. chloride, carbon, oxygen, and sulphur, whereas copper is not picked up by the EDX but is advertised. The same trend is found in the other fertilisers as well. Using Table B-8 and Table B-9, combined an elemental picture of each of the commercial fertilisers was made, which all subsequent calculations were based on.

Taking the best media formulations from the previous section, a similar methodology was used to match each elements concentration using the commercial fertilisers as ingredients instead substituting the high purity chemicals. Table B-10 shows the concentration of each fertiliser in the mix as well as the biomass capacity of each element in them. As is evident, the addition of the alkaline and acid buffers were included, for two reasons. First to approximate reality, and second because fertilisers such as bone meal is extremely acidic and is typically used for pH regulation. Therefore, where the high purity chemical equivalent typically was synthesised with a pH of 5.9 the low cost

fertiliser media has a pH of 4.8, which required balancing with the buffers. The buffer cost was added to the total media cost calculations to reflect reality.

Using identical experimental methodology as detailed in section 4.2.2, four media formulations were prepared and equal aliquots of *C.vulgaris* in their exponential phase were used for inoculation. The results are shown in the Table 4-10, and the growth curves for both subcultures are show in Figure 4-5 and 4-6.

Table 4-10 Two subcultures of CV1, 2,5,6 using commercial fertilisers.

1st	P+N+C+	P-N+C+	P+N+C-	P-N+C-
	CV1	CV2	CV5	CV6
Specific Growth Rate (μ)	0.31	0.36	0.36	0.37
Duplication Rate (t_d)	2.26	1.95	1.91	1.87
P_x	0.22	0.21	0.25	0.23
Max Cell count (cells/ml)	6.94E+07	1.04E+08	1.69E+08	3.49E+08
Final Biomass concentration (g/lit)	1.40	1.35	1.60	1.50
2nd				
Specific Growth Rate (μ)	0.25	0.24	0.24	0.28
Duplication Rate (td)	2.76	2.94	2.83	2.47
Px	0.20	0.32	0.22	0.25
Max Cell count (cells/ml)	1.29E+08	2.80E+08	6.29E+08	6.88E+08
Final Biomass concentration (g/lit)	1.45	2.00	1.40	1.60
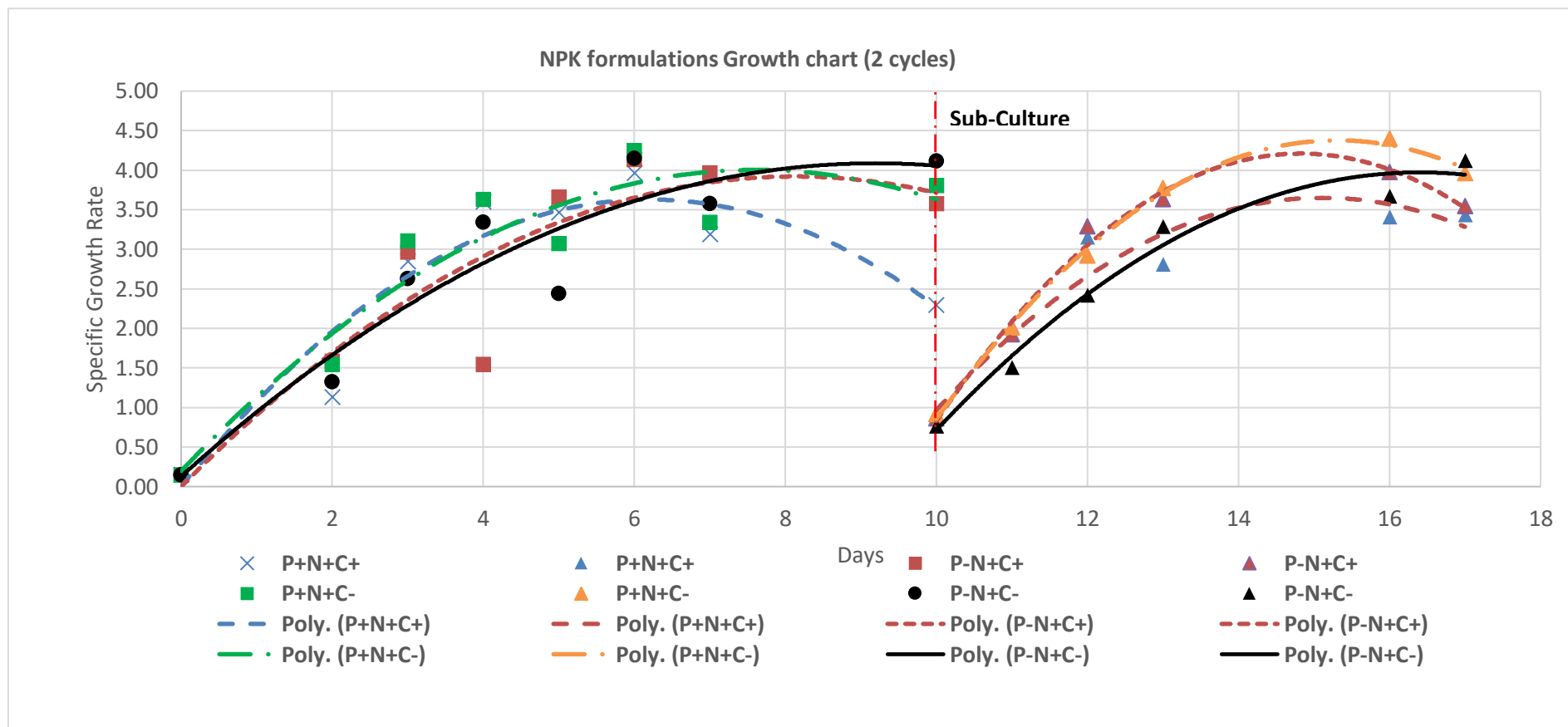
Figure 4-5 CV1,2,5,6   Using Commercial fertilisers, growth curves during two subcultures. (Day 10 being the subculture point).

113
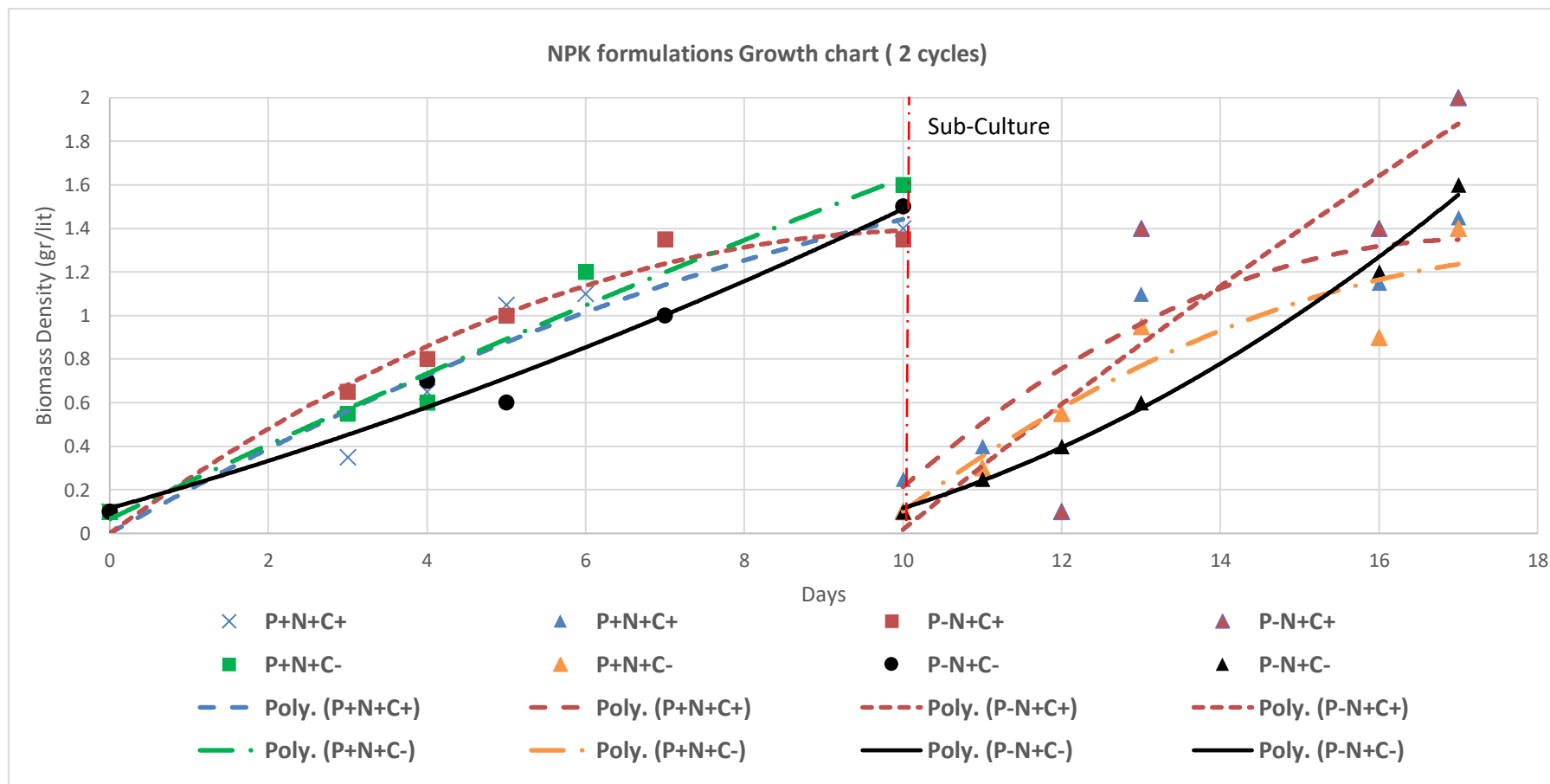
Figure 4-6 CV1,2,5,6   Using Commercial fertilisers, growth curves during two subcultures

During the first subculture, it took all four cultures approximately 8 days to reach stationary phase, at which point the highest biomass density was recorded by CV5, whereas the highest cellular concentration was in C6. The productivities of both CV5 and CV6 where similar at 0.25 and 0.26 gr/L/d. During the second subculture which lasted 7 days until reaching stationary phase, CV2 and CV6 were the best performing medias, with biomass concentrations of 2 and 1.6gr/lit and productivities of 320 and 250 mg/l/day respectively. In terms of cellular concentration, the CV5 and CV6 recorded the highest in the range of 6 x 10^8 cells/ml.

The price of each of the cost per litre of each of the medias, as shown in Table B-11 the cost per litre for CV1,2,5,6 is 2.08, 2.10, 0.47 and 0.50 p/lit including the cost of glycerol, and 0.47, 0.46,0.47 and 0.46 p/lit considering that glycerol is recovered or sourced for free. Which drops the cost of a gram of biomass to 0.32, 0.23, 0.43,0.29 p/g, which translates to 2.34 and 2.93 £/kg of biomass for the two best performing medias CV2 and CV6, which are the potassium deficient and nitrogen enriched medias, beating the potassium and nitrogen replete.

According to literature the reason why the nitrogen replete cultures reached stationary phase faster is due because P uptake is up to 3.8 times faster in N-conditions, such as CV2 and CV6, whereas biomass concentrations were similar, with N,P replete conditions (Chu *et al.*, 2013).

The interesting fact is that all 4 media formulations both N+P+ and N-P+ variants are the best performing media formulation. Between the two the one with the lower carbon content it the faster growing is due to the C/N interaction kinetics which under Nitrogen constant environments organic carbon enriched cause a degradation to the growth rate of the culture,, albeit it produced a higher biomass concentration, which is due to the glycerol concentration (Liang, Sarkany and Cui, 2009; Daliry *et al.*, 2017). Furthermore the two above formulation are the only ones that can produce a kilogram of biomass for under £2.30 which is much lower than the figures found in literature. Comparing these values with the standard BB media and the CV variants with high purity chemicals it is found that

4.3 Chapter Conclusion
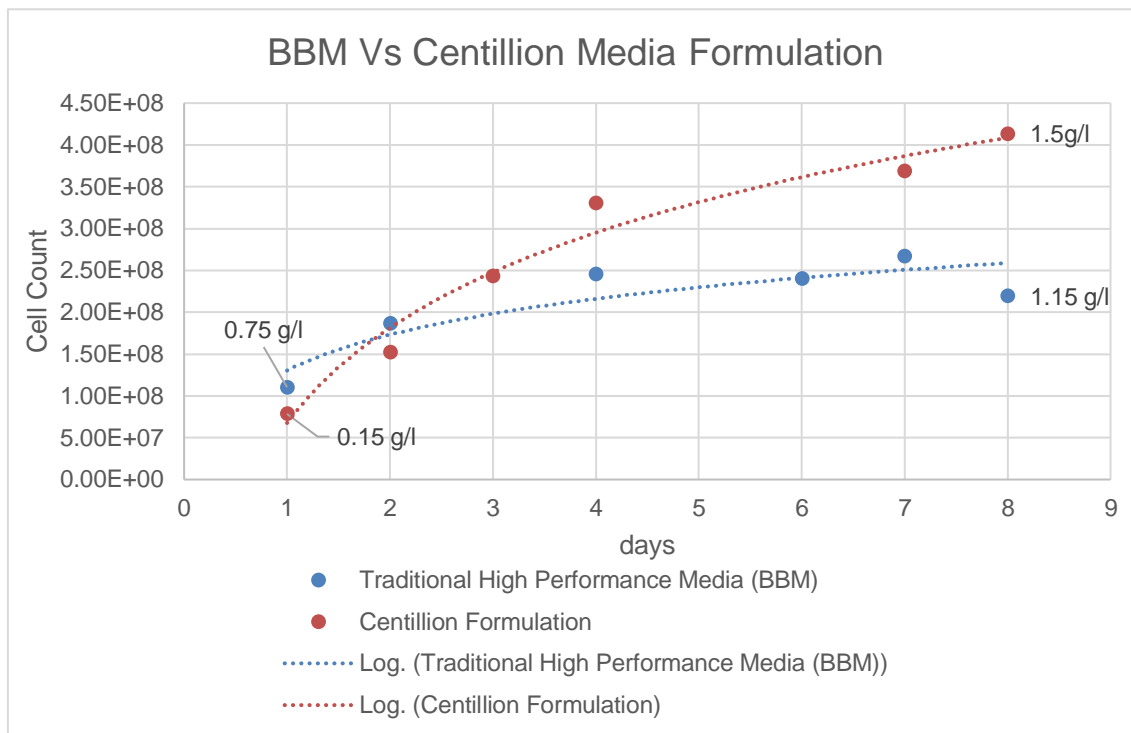
Figure 4-7 C.vulgaris growth curve, in BBM and Centillion Formulation. Final Biomass densities are labelled.

The media formulations developed using MG were named Centillion Media (CM). As can be seen in the figure above, the CM formulation achieved 1.5 g/l at day 7 (196h), comparing this to the best performing media formulation, the Bold Basal (Wong, 2017). It shows that at the same rate of time the *C.vulgaris* subculture the algae produced approximately 0.350 g/l more, dry biomass. Also comparing the Centillion media result with literature The same strain grown under similar conditions reached a higher cell count of 4×10^8 cells/ml in 196h, compared to Mendalam and Palsson (1998), whose custom media formulation achieved just over 3×10^8 cells/ml in 288h (12 days). Similarly comparing with literature using the exact same strain in both species and taxonomy (*C.vulgaris* CCAP 211/11B), the Centillion media outperformed the five highest performing media formulations (Bold Basal, M-8,BG-11, Modified Spirulina, N-8). Both in terms of biomass and cellular densities, with the highest reported being 1.4 g/l and 3.2×10^8 cells/ml of BB media. Finally comparing the biomass productivities, the overall biomass

116

productivities achieved are 0.114 g/l/d, whereas the Centillion media achieved 0.230g/l/da (Wong, 2017).

In terms of economics, the performance of the media is harder to directly compare with literature, since price is a factor not studied much in academic journals. Having said that the price of bold basal media using conventional chemicals from commercial suppliers is approximately £0.04/lit of culture. This compared to the Centillion media which costs £0.0046 /lit. According to Figure 4-7 the price per gram of biomass produced for each of the medias final biomass densities are £0.037 /gr for the BBM and £0.003 /gr for the Centillion media, grown in conventional cultivation techniques comparable to literature.

Looking at a large-scale, the media is considered the most expensive aspect. A reliable figure is hard to come by, as reported in highly regarded publications they are not uncommon to reach or $20 to $200 / kg of biomass.(Gupta and Choi, 2015). However there have been reports of media at $3.8 / kg of biomass when production rises beyond 100 tonne/year (Chisti, 2007). In this case the cost per biomass is approximately £3 /kg using the CM, in contrast to £37 /kg using the standard BBM. Considering economies of scale, the price of both will be considerably less for large cultivation volumes.

The key advantages in the new media, is the reduced dependencies on high purity and expensive laboratory grade chemicals, and their replacement to off the shelf common sources of fertiliser. Secondly the nutrient selection and mix, are designed so that they work in a highly dynamic environment in both batch and flow systems, and reduced dependency to CO_2 due to its inclusion of glycerol as a carbon source. This is a key scientific achievement, since there is no published evidence of media recipes that incorporate a source of carbon into the formulation. This disassociates the deployment of potential algae cultivations sites to locations adjacent to CO_2 and other urban pollutant sources. On the other hand, there are risks with using glycerol as a carbon source, as the culture will requires additional levels of control, as well as additional measures from predation and contamination.

5 Technical Systems

A critical aim of the project is to develop and implement the Centillion oscillatory baffled flow reactor into the bioprocess of cultivation algae. By doing so three main design errors of photobioreactors are challenged, namely mixing, scalability and process continuity. Albeit the latter is a term which subject to the biological limitations of the organism. Revisiting tasks identified in the previous section the technical system is mainly defined by elements that entail reactor design and component selection. Of which the functional elements specify the mixing, light supply and systems monitoring.

5.1 Light

As with every photosynthetic organism light is a crucial parameter. As highlighted by literature ineffective light supply has detrimental effects to the organism and by association to the process. As suggested by Huang et al., (2017) light is a multivariate parameter (e.g Light cycle, Light Intensity, light fraction, duty cycle). Considering it is one of the most important factors in algal growth, very little has been done in terms of technical advancements. (Richmond, 2004)

The work pertaining to light and its utilisation, in terms of PBR system design, will be carried out in two fields. As per Carvalho (2011), both of which aim at optimisation and control of light (Carvalho *et al.*, 2011).

1. Focus will be given in exploiting the particular design features which the Centillion OBR offers and associate it with light implementation utilisation and modulation.
2. Light from an equipment standpoint will be examined, in terms of supply (power output), intensity (photon flux density), positioning (effective coverage) and cost.

5.1.1 Light Implementation

The cylindrical shape of the reactor, and the equispaced operating holes, positioned close to the reactor surface, create a favourable environment for the algae to cultivate. In terms of light each baffled conduit, has an illuminated surface

to volume ratio of 0.52, whereas when assembled in a reactor system the surface to volume ratio increased to 0.9. Furthermore, given the flexibility on material selection, the reactor system can be assembled with all transparent materials such as acrylic, polycarbonate and even glass; thus, increasing light utilisation along the whole length of the reactor. Mutual shading from each passage, although kept to a minimum by design, can be further reduced by consideration in positioning of the lights.
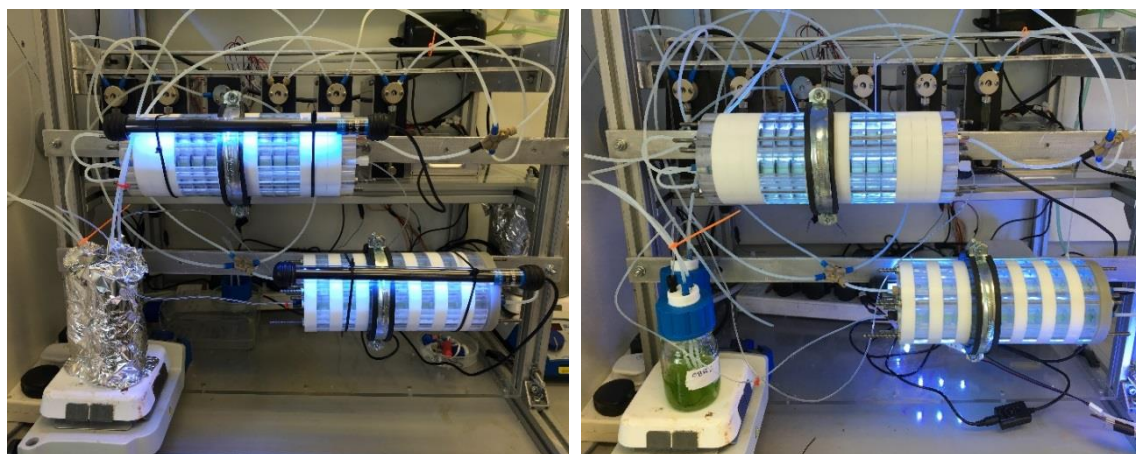
Figure 5-1: Example of examined light arrangements on the Centillion Meso Scale OBR-V1. (LHS - Using Aquarium 6W White LED columns, positioned radially at a set distance. RHS – A 6W White LED (Warm) light placed 150mm behind the reactor illuminating the reactors.
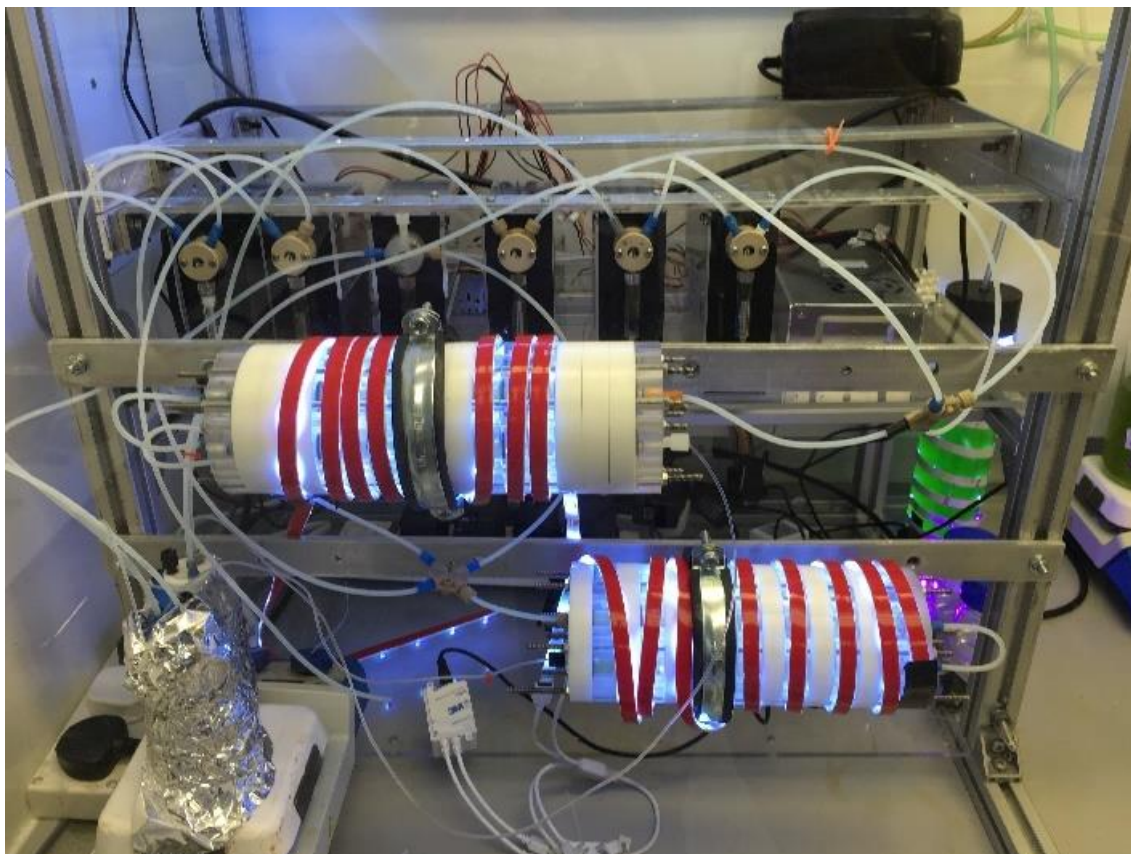
Figure 5-2 Light arrangement used for the experimentation of C.Vulgaris in the Centillion OBR-V1. A single 1m length of 5V 100 LED strip, wound around the reactor.

The shape and spatial footprint of the light harvesting unit, are the key drivers of light type selection. State of the art in light engineering, is the use of LEDs. Economical, flexible in application, waterproof and controllable in terms of intensity and colour, LEDs have become a safe choice of applications in aquaculture and indoor horticulture. The cylindrical shape of the reactor has demonstrated to work well with several very cost-effective light arrangements. The most practical and cost effective was found in this application, using a high intensity 1 metre LED strip which produced an average of 4000 Lx of light on the reactor surface.

Figure 5-1 and 5-2, show the light arrangements evaluated for use the with the Centillion. For this scale the compact size allowed a range of options to be considered and evaluated. Between white light LED bars positioned either in a

single strip or multiple unit arrangement, versus a flexible LED strip; the latter was found to be more appropriate, allowing for stronger PAR to reach the reactor surface. In addition to that, considering the arrangement of the reactor and its modular shape, means that this light arrangement can accommodate a change in length, diameter and lighting architecture (localised high intensity points, variable light intensity passages, etc).

5.1.2 Control of Light

Light cycle time is a very important parameter in the study of light (Richmond, 2013; Simionato *et al.*, 2013; Huang *et al.*, 2017b). Light cycle as the name suggests is the time segment between an algal cell entering a photic and exiting a dark zone. In all conventional designs of photobioreactors, the photic and dark zones of the reactor are defined by the depth to which light reaches. Thus, the light cycle is determined by the cyclic rotation and frequency an algal cell resides between these two zones, i.e. between the centre and outer edges of the reactor surface. As suggested by the definition, the light cycle is strongly dependent on the culture density, the light source intensity and the overall surface to volume ratio of the reactor. The control of the light cycle therefore can only occur by establishing a turbulent mixing regime which will increase the probability of the cells residing between the two zones in a more regular fashion rather than just chance. These high mixing regimes are both costly and can harm microalgal cells. Control of the light cycle via mixing is a complex task in conventional reactors and therefore the benefits of light cycle manipulation are not exploited at industrial scales, for two reasons. First at large scales light supply is given by solar radiation, thus light supply is fixed during the daylight hours (Kumar *et al.*, 2011), and second due to the large volumes of algae required indoor PBRs become notoriously difficult to scale which regards to light (Gupta and Choi, 2015). These issues create additional complications such as photooxidation, a phenomenon where an algal culture collapses under high light intensity, coupled with high temperatures during times of peak solar intensity; specifically, in PBR variants who are predominantly batch processes (e.g. column PBRs).

On the other hand, the Centillion OBR can offer two distinct advantages. The ability to combine a highly controllable flow regime, in a system which is modular, customisable and scalable. This creates the unique opportunity to redefine and fully exploit the advantages of light cycle in algae cultivation.

Light cycle manipulation in the C-OBR occurs in two ways:

1. Via the physical manipulation of the reactor architecture. This means by configuring a reactor with transparent (light) and opaque (dark) disks. A flow path can be created which physically creates a dark section in the photobioreactor (Figure 5-3). Taking advantage of the reactors dimensional and geometrical characteristics, this means that a reactor system can be configured to control the following
    a. Light and dark period path length: By placing a series of consecutive transparent disks.
    b. Light/Dark Fraction: Combining a series of dark and light regions in the reactor.
2. By controlling the flow characteristics of the reactor, namely the axial velocity (m/s), frequency (Hz) and amplitude (mm) of oscillations. This was given a reactor with fixed light and dark reactor architecture control of light supply can be extended with control of:
    a. Light cycle time (t_c) and Flash time (t_l): Combination of physical configuration of light and dark disks, in combination with the axial velocity.
    b. Individual control of the duration of each cycle time (t_d) and (t_l), flash frequency (v) and Duty Cycle (ϕ): Changing the amount of transparent and opaque disks, whilst maintain a fixed axial velocity.

The combination of the two, and their synergistic effect enables the algae to controllably cycle between the photic and dark zone of the reactor and can accommodate very short and long light cycle duration without inducing highly turbulent flow regimes to the culture. In addition to the considerable level of control this offers, the major impact that the factors of light and mixing are completely disassociated. This is a key output of this work as it is completely

novel and has never been achieved with conventional cultivation techniques nor any current PBR designs. The implementation of light on the centillion OBR and the control of light characteristics is part of an international patent WO/2019/016575 (Makatsoris and Alissandratos, 2019).
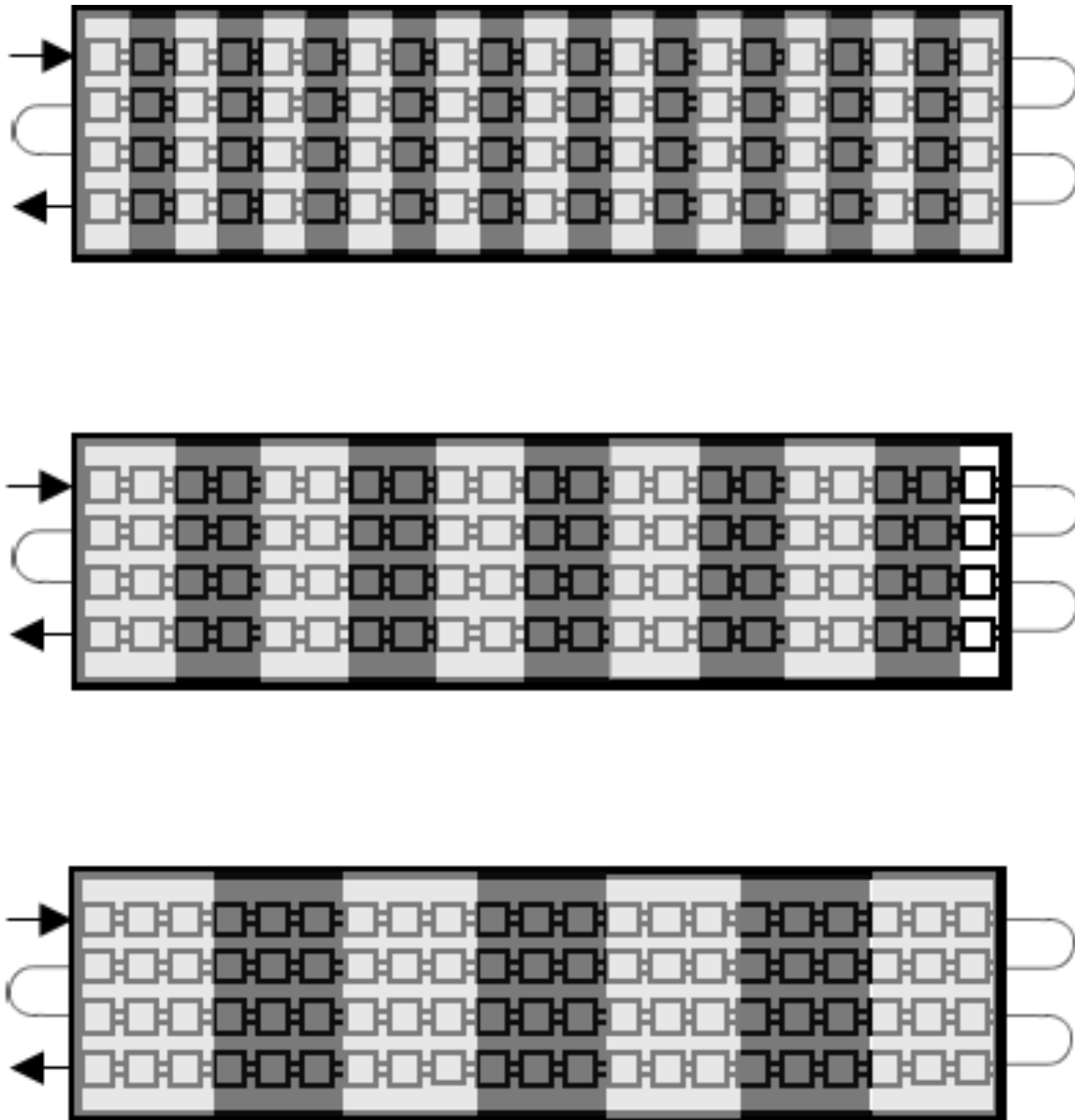
Figure 5-3 Three examples of OBR disk arrangements ("architectures")

5.1.2.1 Experimental Set up and procedure.

In the C-OBR, these two cycle times can be achieved by either assembling a reactor with a large dark section (i.e. high number of disks), in order to keep the mixing intensity low, or a small dark section whilst keeping high mixing intensity. In both cases, the culture density and high stress consideration does not play a

role since oscillatory flow, creates controllable toroidal vortices and other micro-mixing zones which alternate algal cells between the centre of the reactor and the edges of the tube, regardless of the net flow.

In order to test this hypothesis a series of experiments was set up in order to test this theory. The experimental procedure was set up with two objectives. First to evaluate what effect oscillatory flow has on algae, and secondly whether physical manipulation of the light cycle has any effect on the growth of the algae in the OBR compared with conventional and comparable systems.

The algal strain *C.vulgaris* and BBM growth medium was supplied by CCAP (Oban, Scotland). The cultivation conditions and culture transfer protocols used in this section are specified in 3.2, section 3.2.2.1 and 3.2.2.2.

The experimental setup for the growth experiments consisted of the Centillion OBR connected to six syringe pumps; four for continuous flow and two to induce oscillations. As a light source two LED light strips were positioned above the OBR's flow path, illuminating them with an average light intensity of 70 μmol/m^2/s, measured using a conventional light meter. As shown in Figure 5-4 and Figure 5-5 , the experimental set-up was different for the two-experiment series. For the experiment series examining the effect of oscillatory flow, a single reactor was used to carry out two experiments in situ using two passages per experiments. Each experiment required two syringe pumps for continuous flow of the algae through the reactor whilst the third was used to induce oscillatory flow. The physical hardware was directed via a custom build interface which set the desired process parameters ($f, \dot{f}, X_o$).
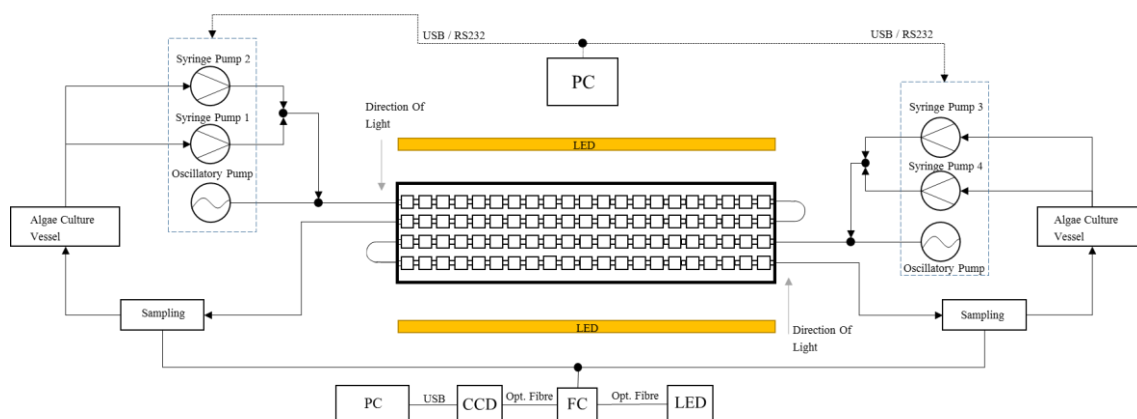
Figure 5-4 Clear Dolby experimentation Centillion OBR set up schematic. Syringe pumps on the left and right of the reactor

For the light experiment series, two reactors were assembled in two configurations of equal volume. One with a pattern of one disk per phase (one clear and one opaque), and the other with 3 disk per phase (3 clear and 3 non-transparent). As previously stated, the reason why these two arrangements are used are to establish whether the growth behaviour is due to the light cycle or the flow characteristics. The system was set up as shown in Figure 5-5. Light cycle manipulation was achieved in two ways, first by changes to the physical hardware, and secondly by fine tuning the process parameters (i.e. flowrate, oscillatory frequency and amplitude). In the former case, due to the modular reactor consecutive disk design by selecting the disk material as acrylic (transparent) and PTFE (opaque) it was possible to assemble the reactor in configurations that would create light and dark regions along the reactor length thus allowing a higher-level optical path length control. On the other hand, controlling the process parameters in conjunction with a flexible light cycle path allows for greater range of light cycle and phase residence times implementation, without inhibiting the flow regime.

A full factorial design of experiment matrix was generated for the first series experiments having as variables the number of consecutive identical disks, for each light cycle and configuration. For the light cycle 4 levels were chosen, 7, 20, 50, 150 seconds, against the disk number (i.e. configuration) of two levels 1D and 3D. Specifically, for the light cycles the duration ranges are chosen based on

Barbosa et al (2002) definition of the medium light cycle being between 10-100 seconds long, deducing that short light cycles are below 10 seconds whilst long light cycles are above 100 seconds, therefore the choice of 7 and 150 as the lower and upper limits in conjunction with the 1 and 3 disk configuration allow for the largest defined search space allowed by the operating hardware limits, whilst 20 and 50 seconds points ensure that a narrow spread between experimental parameter points. The combination of light cycle durations and disk number enables the investigation of the behaviour of the algae at a range of net Reynolds numbers and velocity ratios. Which as indicated by the tank in series (TiS) analysis and predictive model development conducted in the previous sections, can give an indication of the plug flow conditions (Barbosa *et al.*, 2002). The table below shows the equivalent dimensionless numbers against the cycle times and disk numbers The complete list of DoE factors and their levels is shown in Table 5-1, whereas the complete DoE matrix, with additional information of the dimensionless parameters, is shown in Table 5-2

Table 5-1 DoE parameters and their levels for the investigation of light cycles and number of disks per phase.

<table>
<tr><td rowspan="2"></td><td rowspan="2"></td><td colspan="4">Levels</td></tr>
<tr><td>1</td><td>2</td><td>3</td><td>4</td></tr>
<tr><td rowspan="2">Parameters</td><td>Number of Disks per Phase</td><td>1</td><td>3</td><td></td><td></td></tr>
<tr><td>Light cycle Time (sec)</td><td>7.9</td><td>23</td><td>56.3</td><td>168</td></tr>
</table>
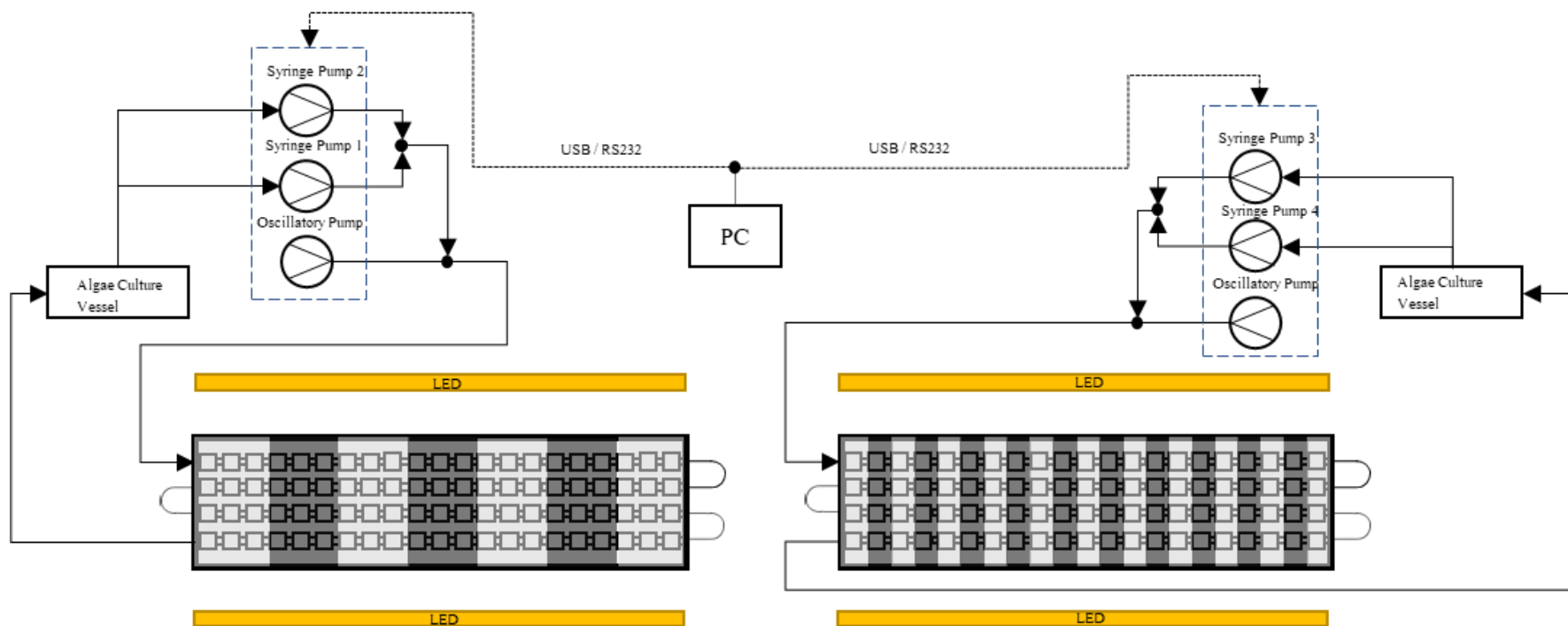
Figure 5-5 Light parameter experimentation set up schematic. Two reactors with their optical path configurations, each linked to pumps and separate algae vessel.

Table 5-2 Light Cycle DoE Table. (Main factors : light cycle, disk number / optical path length, responses specific growth rate.

Run Order	Light Cycle (sec)	Disk Number	Net Flow (ml/min)	Net Velocity (m/s)	Reynold No	Osc. Reynolds No	Velocity Ratio
1	23	3	32	0.0106	84.9	1508	17.8
2	23	1	11	0.0036	29.2	1508	51.7
3	56.3	3	4.5	0.0015	11.9	1508	126.3
4	7.9	3	1.5	0.0005	4	1508	379
5	56.3	1	11	0.0036	29.2	1508	51.7
6	168	1	3.5	0.0012	9.3	1508	162.4
7	7.9	1	1.5	0.0005	4	1508	379
8	168	3	0.5	0.0002	1.3	1508	1137

5.1.2.2 Results

Prior to carrying out the experiments indicated in Table 5-2. Screening experimentations were carried out in order to identify a suitable oscillatory flow regime for the experiments. As per literature (Abbott *et al.*, 2012), the effect of frequency doesn't play an important role in the growth of algae. This may be true in the oscillating column the author was using it, however in a flow system such as the Centillion, the regime is much more controlled. Therefore, a series of experiments were carried out as indicated by Table 5-3, to establish an appropriate oscillation conditions for the algae culture in the subsequent light experiments. Table 5-3, contains experimental process parameters $(f, \dot{f}, Re, Re_o, \psi)$ with the response being the algae growth characterisation metrics μ, t_d as specified in chapter 3.2.1 specifically in section 3.2.1.1 and 3.2.1.5. The results suggest that higher oscillatory frequencies (f) produce higher growth rates (μ), regardless of the net flow $(\dot{f})$, whereas mid-range oscillatory frequencies would produce even higher specific growth rates when coupled with higher flowrates.

To accommodate the flowrates required for the light cycle analysis, the parameter space investigated was outside the limits of the regression model presented in the previous section. Therefore, TiS number could not be derived for the complete data set. During experimentation it was found that high frequencies provided higher agitations throughout the whole of the reactor length, also such conditions worked favourably in ejecting trapped bubbles, therefore for the light experiments a high frequency was selected for the oscillatory flow. Corelating this with the mixing characterisation model from section 5.2.2, it is found that the TiS numbers are in the same range. However more experiments are required to validate this.

Table 5-3 Experimental parameters sets on the clear reactor.

Exp No.	Frequency (Hz)	Net Flow (ml/min)	Re	Re_o	ψ	μ	t_d	Max Cell productivity (cells/ml)
1	1.50	1.50	3.98	753.98	189.50	0.05	12.74	2.66E+06
2	1.50	25.00	66.31	753.98	11.37	0.41	1.71	1.98E+07
3	3.00	1.50	3.98	1507.96	378.99	0.22	3.15	1.08E+07
4	3.00	25.00	66.31	1507.96	22.74	0.20	3.39	9.98E+06
5	0.25	15.00	39.79	125.66	3.16	0.06	12.49	2.71E+06
6	0.25	10.00	26.53	125.66	4.74	0.21	3.27	1.04E+07

The experimental results are presented in the Table 5-5. Analysis of the results finds that there is a strong correlation between light cycle time and specific growth rate. As shown in Figure 5-6, there is a pattern across both optical path lengths i.e. disk numbers, with higher growth rates and maximum cellular productivities in the late medium light cycle range of approximately 50 seconds. Secondly the data show that the shorter light path at cycle times or 7.9 to 23 and 168 seconds, was more favourable for growth than the longer light path.

Therefore, the trend is most prominent in the 3-disk arrangement as shown in Figure 5-6. Overall the growth rates between the 7.9 and 56 second light cycle produced higher cellular densities
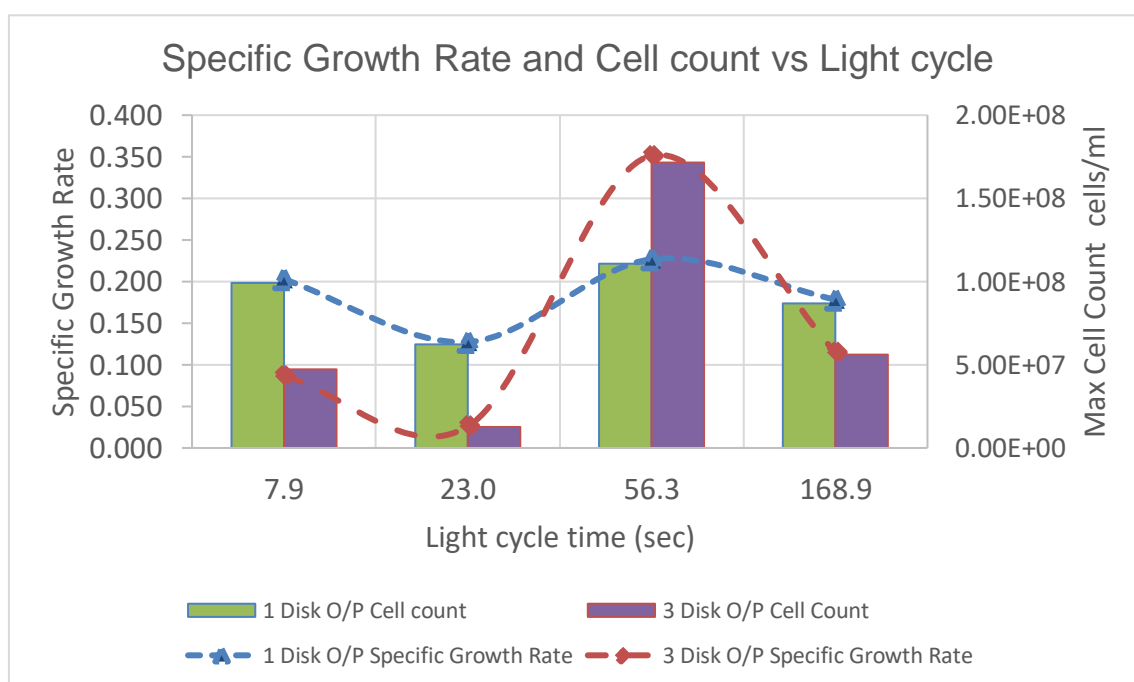
Figure 5-6 Specific growth rate and maximum cellular densities achieved according to light cycle time.

To establish the whether the correlation between algal growth and light cycle was a valid phenomenon, a second series of experiments was conducted to evaluate whether the pattern produced by the initial experiment, could be reproduced. An empirical design of experiments was devised with aim to study the effect of the light cycles whilst keeping the flow regime as limited as possible

Table 5-4 Validation experimental series. Showing the identical mixing conditions between two light cycles.

Experiment Number	Disk Number	Light Cycle time (sec)	Flash Frequency (1/sec)	Reynolds Number (Re)	Velocity Ratio ψ
1	1	7.9	0.13	29.17	51.68
2	3	23	0.04	29.17	51.68
3	1	56	0.017	3.9	378
4	3	168	0.0059	3.9	378

In the table 5.4 the experimental parameter sets are shown. As per the experimental design, the mixing conditions are identical between 7.9 and 23 seconds, and 56.3 and 168 seconds. The results from the experiment are presented in table 5.6.

Table 5-5 Light Cycle Experimental DoE results.

Experiment Number	Optical Path length (Disk Number)	Light Cycle (sec)	Reynolds number (Re)	Velocity ratio ψ	μ	t_d	Max Cell productivity (cells/ml)
1	1	7.9	29.17	51.68	0.087	7.99	4.71E+07
2	1	23	11.93	162.42	0.026	26.6	1.27E+07
3	1	56	3.97	378.992	0.351	1.97	1.72E+08
4	1	168	1.32	1136.98	0.115	6.04	5.60E+07
5	3	7.9	84.88	17.76	0.203	3.41	9.91E+07
6	3	23	29.17	51.68	0.127	5.44	6.22E+07
7	3	56.3	11.93	126.33	0.227	3.05	1.11E+08
8	3	168.9	3.97	378.992	0.178	3.89	8.70E+07

Table 5-6 Validation experiments Results

Experiment Number	Disk Number	Light Cycle time (sec)	Specific Growth Rate	Doubling time	Cellular productivity (cells/ml/day)
1	1	7.9	0.338	2.046	1.80E+07
2	3	23	0.074	9.278	2.91E+07
3	1	56	0.835	0.830	2.00E+07
4	3	168	0.318	2.179	3.11E+07
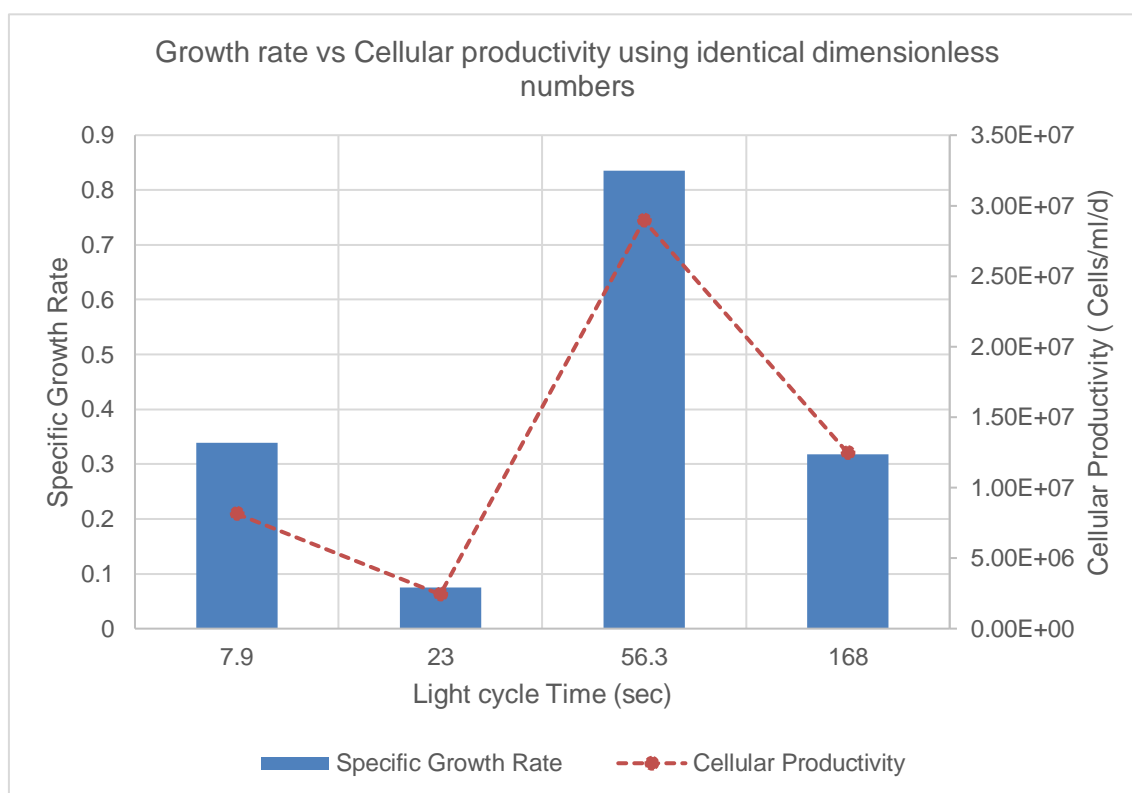
Figure 5-7 Validation experiment results, showing the same pattern as before.

The experimental results tabulated in the table 5.6 and in the figure 5.7, show than the same pattern as before is produced, with much higher specific growth rates. The 56.3 second range of light cycle produces the highest growth rate and as expected the highest cellular concentration, with a doubling time of just under a day.

To provide a better fit to the model and extend the range an additional two experiments were ran, using the same conditions as above. With 2.6 and 5.6 second light cycle using the short optical path length. The results are shown in Figure 5-8.
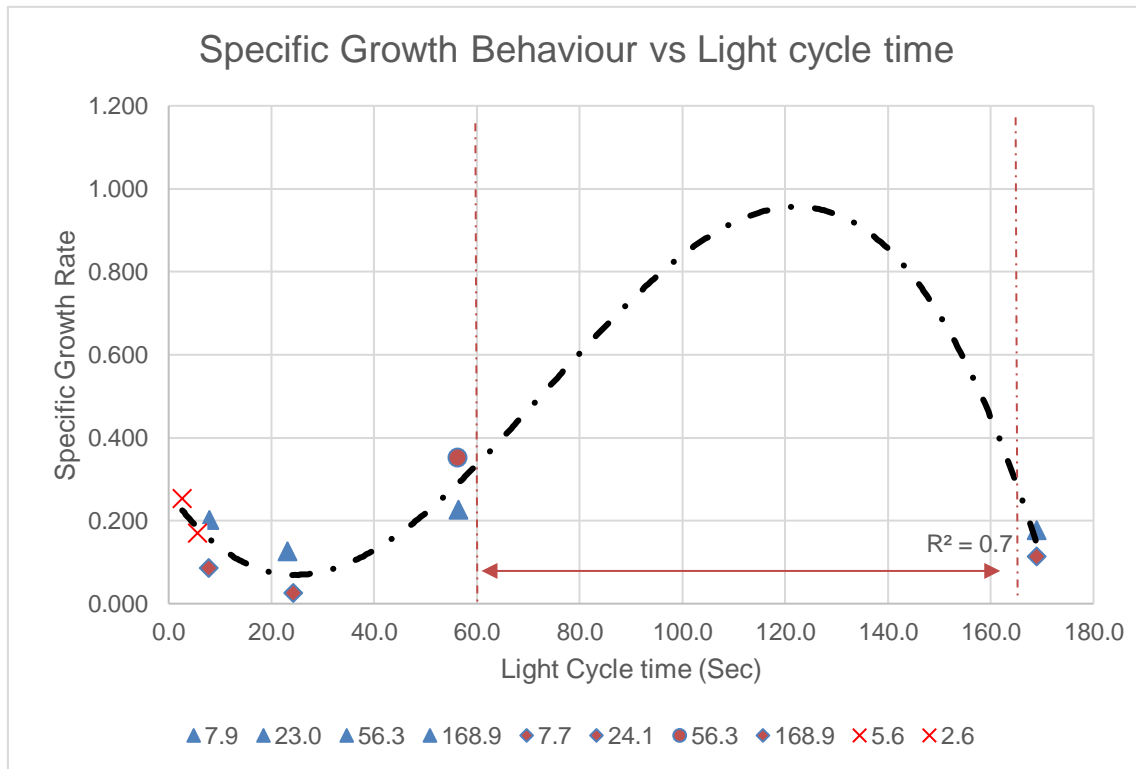
Figure 5-8 All light cycle results across both optical path lengths. Red line indicated the predictive zone, which contains a feature with no data points to validate.

Where fitting model derived from the above is:

$$\mu_{1.5-168} = -2 \times 10^{-6} \times t_{cycle}{}^3 + 4 \times 10^{-4} \times t_{cycle}{}^2 - 0.17 \times t_{cycle} \qquad \textbf{(5-1)}$$
$$+ 0.267$$

Whereas for light cycle times up to 60 seconds the model is reduced to a 2nd order polynomial fit, described by

$$\mu_{1.5-60} = 3 \times 10^{-4} \times t_{cycle}^2 - 0.14 \times t_{cycle} + 0.254 \qquad \textbf{(5-2)}$$

The two models perform equally well, despite them being data fitting models. However due to the nature and definition of the L/C time as a factor, the large variance between medium and long L/C's are unavoidable. The cubic equation's parabolic feature from 60 to 160 seconds includes a feature, which height is based on prediction. Therefore, a second quadratic model was developed to depict the relationship of the growth rate with the light cycle time from 1.5 to 60 seconds approximately.

5.1.3 Optimising the Light (Source/Cost/Reliability)

The cylindrical shape of the reactor favours the implementation of LED strips, as demonstrated in previous sections. Their cost vs utility is maybe attractive, on the other hand their low reliability and large variations in their emitted wavelengths, force the photobioreactor design to consider alternative options. Inspiration for the light architecture was drawn from the aquaculture industry, where both the light arrangement and LED emitted wavelength customisation proved advantageous in their respective application.

Transferring this concept to algae cultivation is not novel. There are examples where of the shelf aquaculture lights being applied to algae cultivation. Doing the same for the Centillion system would defeat the aim of its development and reduce the systems flexibility. On the other hand, manufacturing a custom LED light bar, with interchangeable and dimmable LED lights at a fixed spacing achieves a high level of controllability, thus maintaining a high degree of customisation and flexibility on the system..

Each light bar has a fixed length of 850mm and a width of 40mm, 24 fixed colour 3W LED chips, are equispaced along the length of the aluminium bar. The

compatible LED chips are supplied in the colour gamut show in Table 5-7. for this application the selected light pattern is BWRRiR. This pattern

As part of Quality Control, the output of a random LED light bar was measured according to its intensity and specific wavelength. Each LED chip's wavelength was measured using a spectrometer (Ocean Optics QE-PRO) and a fibre optic cable (600nm Dia.). Each LED's spectrum was captured by mounting the light bar on supports inside a dark hydroponic grow tent and placing the probe at 30cm away from the LED. To ensure that the LED's spectra is not influenced by the other and ambient light flooding the spectrum, an opaque PVC tube, taped with adhesive aluminium foil, with dimensions 22mm i.d. x 310mm, was placed between LED and absorbance probe; acting as a measurement tunnel. The blue lights emitted a region between 407-465nm, the red emit at 640-660nm, the ir emit at 740nm, and the white light emit from 480-650nm.

Table 5-7 LED light chip colour option, with minimum and maximum range of wavelength from quality control carried out in house.

LED Colour	Symbol	Min Intensity (nm)	Max Intensity (nm)
Red	R	640	660
Blue	B	410	465
White	W	480-650	
IR	iR	439	741

In order to obtain the spectral response of the light which reaches the reactor, the average spectral response was captured. Similarly, the average light intensity was recorded. using a compact handheld light meter, the average intensity in Lux (Lx) In order to convert lux to photosynthetically active radiation (PAR), a PAR meter was used to measure the PAR on the surface of an acrylic 1000x1000mm square, when illuminated from a range of distances. The results of the measurements are shown in the table Table 5-8.

Table 5-8 LED light bar light measurements Distance vs Area, Intensity and PAR.

Distance (mm)	Area (m2)	Intensity (Lx)	PAR
200	0.32	11840	283
500	0.77	4060	105
1000	1.65	1340	37
1500	3.36	550	17
2000	5.2	330	8
2500	7.2	240	5

The following six fitting equations are derived from the experimental data to establish the performance of the LED light array. The equivalent data fitting curves are presented in Appendix C.

$$Area_I = 7 \times 10^{-7} \times D^2 + 0.001 \times D + 0.04 \qquad \text{(5-3)}$$

$$I = 7 \times 10^7 \times D^{-1.6} \qquad \text{(5-4)}$$

$$PAR = 2 \times 10^6 \times D^{-1.61} \qquad \text{(5-5)}$$

$$PAR = 0.0238 \times D + 2.94 \qquad \text{(5-6)}$$

$$I_{Lux} = 0.25 \times D_{LAT}{}^2 - 129.8\, D_{LAT} + 16926 \qquad \text{(5-7)}$$

$$I_{PAR} = 0.059 \times D_{LAT}{}^2 - 3.08\, D_{LAT} + 405.7 \qquad \text{(5-8)}$$

Where equations (5-3) relate illumination distance of sensor from bar, to illuminated area, at an error of 750Lx. Equations ((5-4) to ((5-6) relate distance to illumination intensity in lux and PAR. And finally equations ((5-7), ((5-8) measure the drop in intensity on either side of the LED light bar from its longitudinal centre (across B-B' in Figure 5-9). It is noteworthy to mention that based on measurements variation in performance between light bars was negligible.
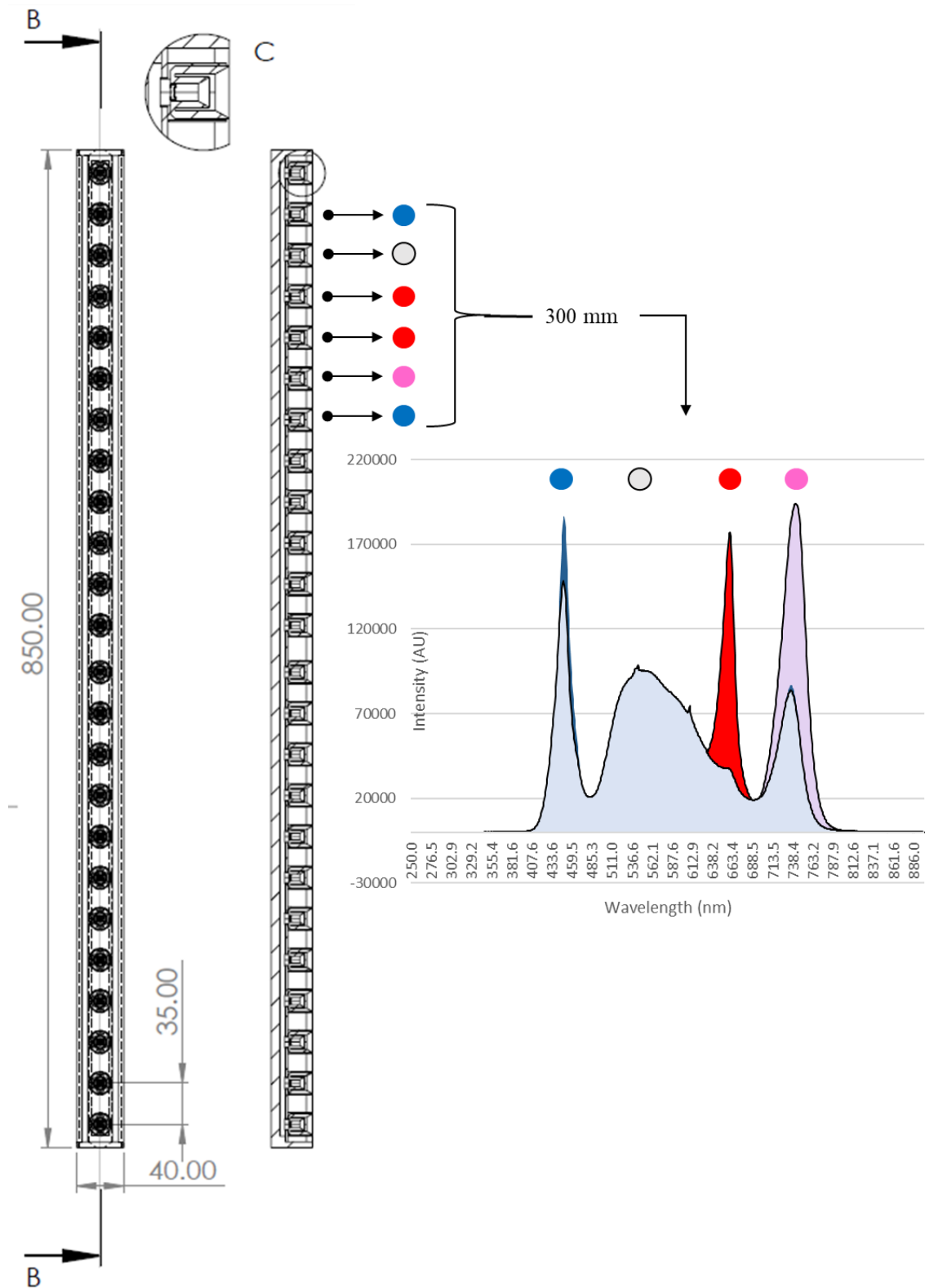
Figure 5-9 LED light bar front and side view (Annotated), Light pattern and captured spectral response from 300mm depicted as well.

C/S View LED
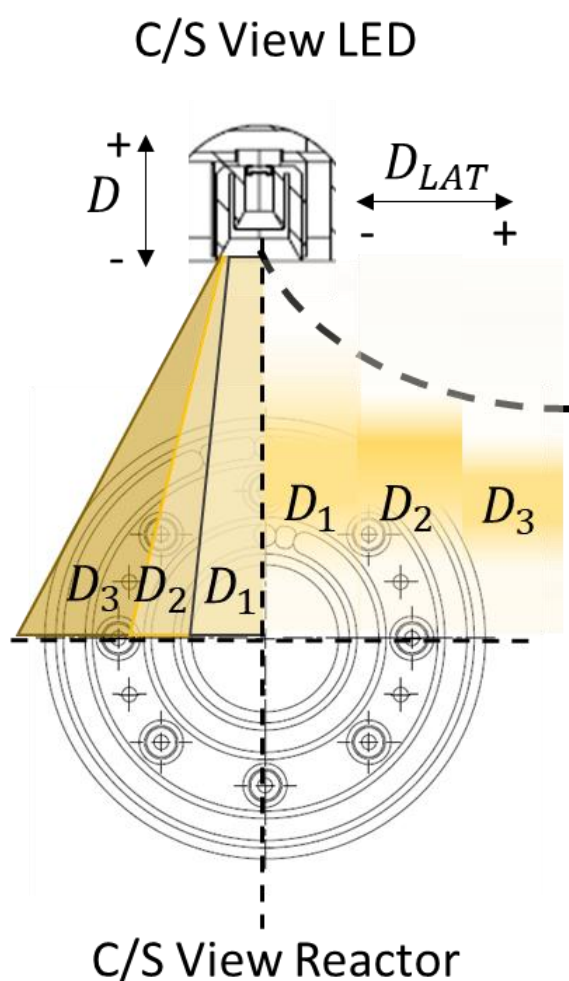
Figure 5-10 Cross Sectional (S/C) view of the reactor disk with the light arrangement. At distance D1,D2,D3 (D1<D2<D3), and the effect of the light intensity distribution (RHS D_{LAT}) and Light intensity and illuminated area (LHS D).

The light's illumination intensity profile in conjunction with the light requirements of the algal strain dictate the placement of the lights in relation to the reactor. Therefore, the quantitative evaluation of its performance increases the accuracy in matching the light characteristics with the culture requirements.

In positioning the light, assuming the light bar is set at a distance (D) from the reactor, there are three points to consider. Increasing the distance between light and reactor results in a reduction in overall intensity and reduction in the size of illuminated area. In addition to that there is also a reduction of illumination intensity along the lateral distance of the illuminated area. The final factor plays a crucial role in the positioning of additional units since their overlap changes the illumination profile considerably. Since one unit cannot provide the required light profile the addition of multiple units must be considered, as well as their arrangement.

The most important constraint with increasing the number of light units is cost. The light unit arrangement shown below, portrays two light units placed at 180° apart at equal distance from the reactor (h_p). This arrangement ensures reduction

in excessive light overlap as well as supplementing light to naturally occurring low photic zones, such as those mentioned above. With this configuration the most uniform light distribution across the reactor was achieved.
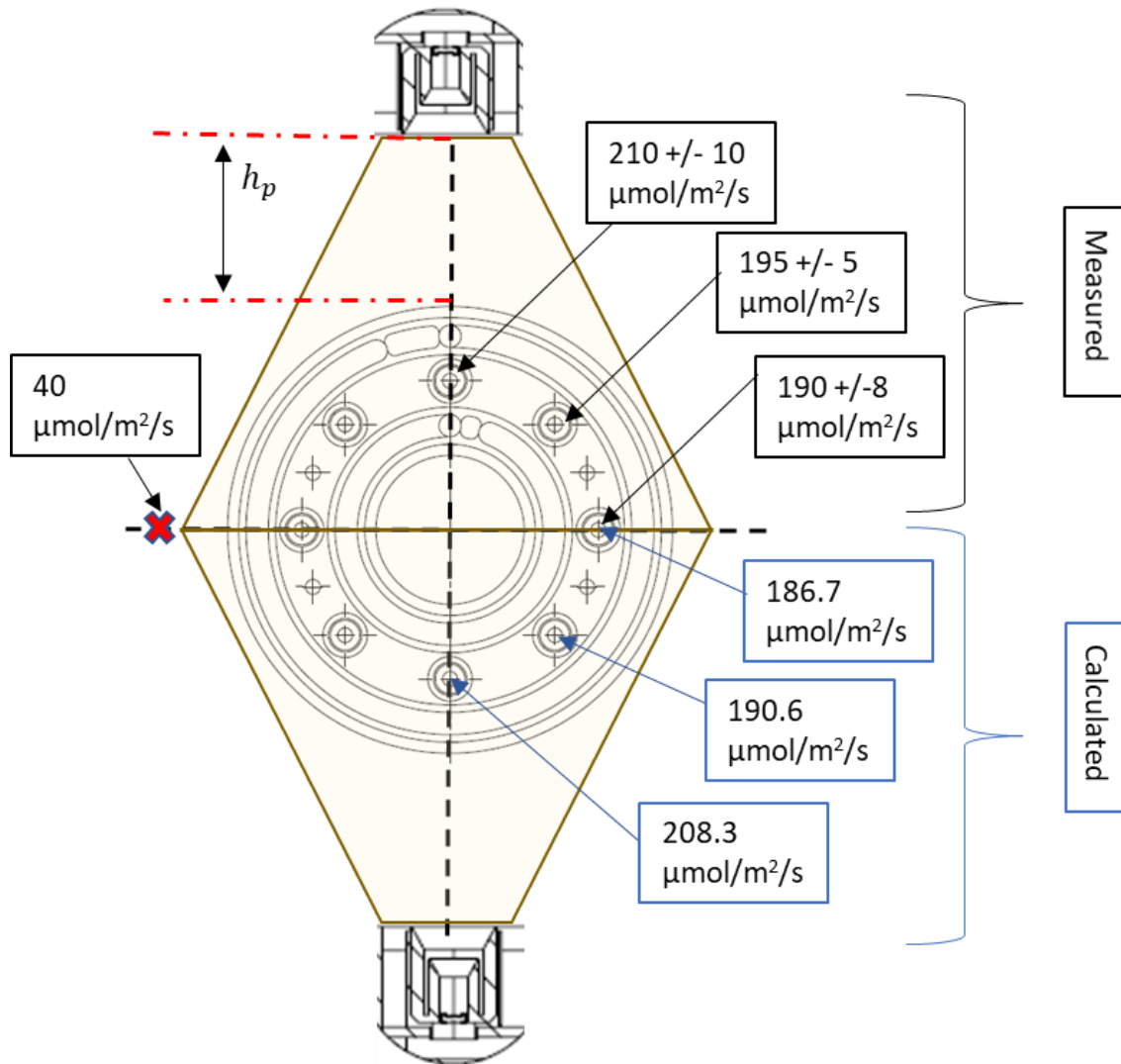
Figure 5-11 Light Supply Schematic: Experimental Set up

As per literature, the light intensity in the range of 200 µmol/m²/s, has demonstrated the ability to promote high biomass productivities and growth rates, in both freshwater and marine microalgae, with little evident benefit at higher intensities (Qiang, Richmond and Zarmi, 1998; Janssen *et al.*, 1999; Simionato *et al.*, 2013) In order to achieve such an intensity in this system the light bar must

be placed at 300mm from the reactor surface. At his distance, based on the fitting equations, the reactor baffled passages are illuminated as per Figure 5-11, specifically 208.3, 190.6 and 186.7 µmol/m^2/s, from closest to farthest. These values are taking into consideration 30% loss of transparency measured between the inner and outer surface of the reactor. For validation these values were cross checked with the same PAR meter and found to be slightly higher as shown in Figure 5-11. Finally, a random set of locations at a midpoint between the two LED light bars were selected to establish whether there was any light bleed, the average reading was approximately 40 µmol/m^2/s.

5.1.4 Discussion

As previously mentioned, the Centillion reactor was designed as a chemical reactor. To establish the feasibility of algae cultivation in a continuous oscillatory baffled reactor system, modifications were carried out in the system for it to act as a photobioreactor. Prior to that taking place the original system was not optimised for algae cultivation, initial factorial experimentation conducted using *C.vulgaris*, to establish the importance oscillatory mixing as a factor required more experimentation, however high growth rates were achieved, regardless of the mixing characteristics.

In literature, light modulation and dark and light cycling of algae plays an important role in the cell's function (Grobbelaar, 1991), shown to promote photosynthesis and overall productivity (Vejrazka *et al.*, 2013). Up to this point however no equipment had been developed that integrated and utilised this very important feature, despite being considered a significant advance worth pursuing (Chisti, 2007). Due to the modular design of the Centillion OBR the implementation of such a feature was an intuitive step towards transforming the chemical reactor to a photobioreactor. Arranging the disk members based on their material, enables flexible manipulation of the optical light path; which when combined with the inherent mixing characteristics of plug flow, it allows for complete disassociation of mixing from the light cycle frequency and duration. This facilitates both parameters be manipulated separately, mixing by amplitude and oscillatory frequency, and light and day cycle by optical path length and linear

velocity of the plug. Experimenting with equal light cycles under different optical path arrangements and velocities, demonstrated that growth is accelerated during medium light cycles of 50 seconds, in both high mixing and low mixing intensity regimes. In order to replicate the result a similar experimental series was initiated with the addition of glycerol to the media, which resulted in similar growth patterns. From the analysis, it was clear that more data were required for a regression model, therefore in lieu of that, an empirical model was developed in equation (5-1), using data fitting methodologies, with a fitting accuracy of R^2=0.7. Due to the long distance between data values (60 seconds and 160 seconds), the model was reduced to predict between 1.5 and 60 seconds (5-2).

During several weeks of cultivation, the reactor was disassembled for maintenance and cleaning. As is depicted in Figure 5-12, both reactor disk material has not fouled nor permanently stained the acrylic material, the green biofilm that formed in the reactor baffled passage was easily removed by flushing some diH$_2$O, indicating that it would have been cleaned with a cleaning cycle, between cultivation processes, rather than disassembly and cleaning. Furthermore, that baffle passage connected to the oscillatory mechanism had little to no evident, biofilm formation, which provides evidence that either the oscillatory regime is strongest, at its start, i.e. before the first u-bend. Or that plug flow diminishes after the first u-bend, as fact with holds little merit, since the TiS numbers indicate the opposite for most parameter combinations used in cultivation.
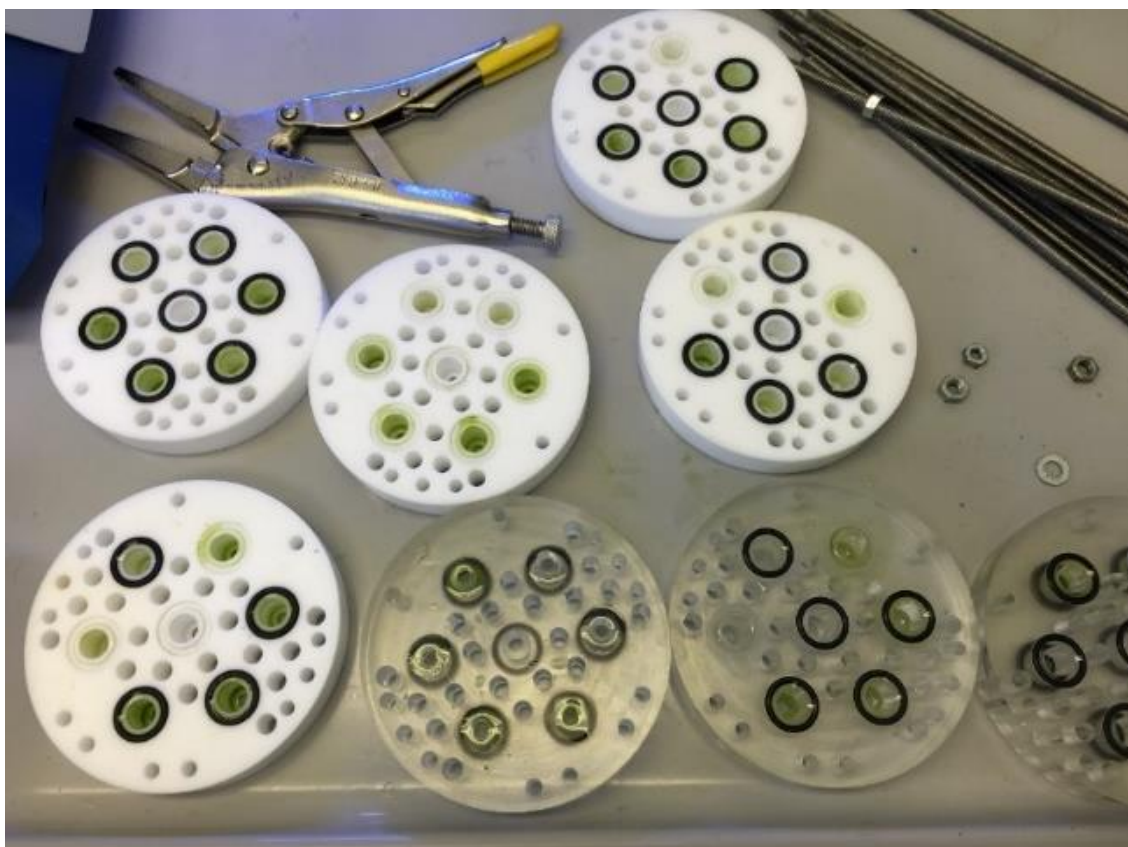
Figure 5-12:PTFE and Acrylic Disks, after disassembly during monthly maintenance cycle.

The performance of the reactor system, during several weeks of experimentation was promising. As a photobioreactor, it creates a closed system which protects the algal culture from predation and contamination, it enables effective photosynthesis and controllable L/D cycle, and finally highly selective control. In comparison with other conventional photobioreactors, which rely on their mixing and light modulation on bubbling and/or pumping. The oscillatory baffled flow reactor implements a mixing regime novel to cultivating aerobic photosynthetic organisms, which as has shown can compete with conventional techniques in terms of growth rate.

5.2 Vessel Design (Containment)

5.2.1 Centillion Reactor

As mentioned previously the Centillion oscillatory baffled flow reactor, was originally intended for use as a modular scalable chemical micro factory. Which was modified to work as a PBR by implementing transparent disks, thus transforming the reactor into a light harvesting unit. This enabled the Centillion reactor, as a vessel, to host algae (oscillatory mechanism, pumping, online monitoring, material input tanks, material output tanks, pipping network, etc) was still set up in the framework of a chemical platform.

Due to their reported benefits, OBRs have demonstrated their bioprocessing potential. In industry there is no industrial application of OBR and algae, and outside of the laboratory there are very few real scales up applications of OBRs. For the cultivation of algae in OBR technology, the Centillion OBR reactor (PCT WO2013/050764 A1) was used (Makatsoris, Paramonov and Rakan, 2013). The Centillion OBR key design features are modularity and flexibility. Microalgae bioprocessing in the Centillion benefits from both the design and the operational flow regime the Centillion possesses and is capable of seven baffled passages with six radially positioned around the circumference in a hexagonal pattern allow for maximum light penetration (depending on disk material) from all angles to reach the flow passages, in combination with approximately 10.6:1 diameter ratio of the disk to the baffle ensure that mutual shading caused by the baffles is kept at low levels.
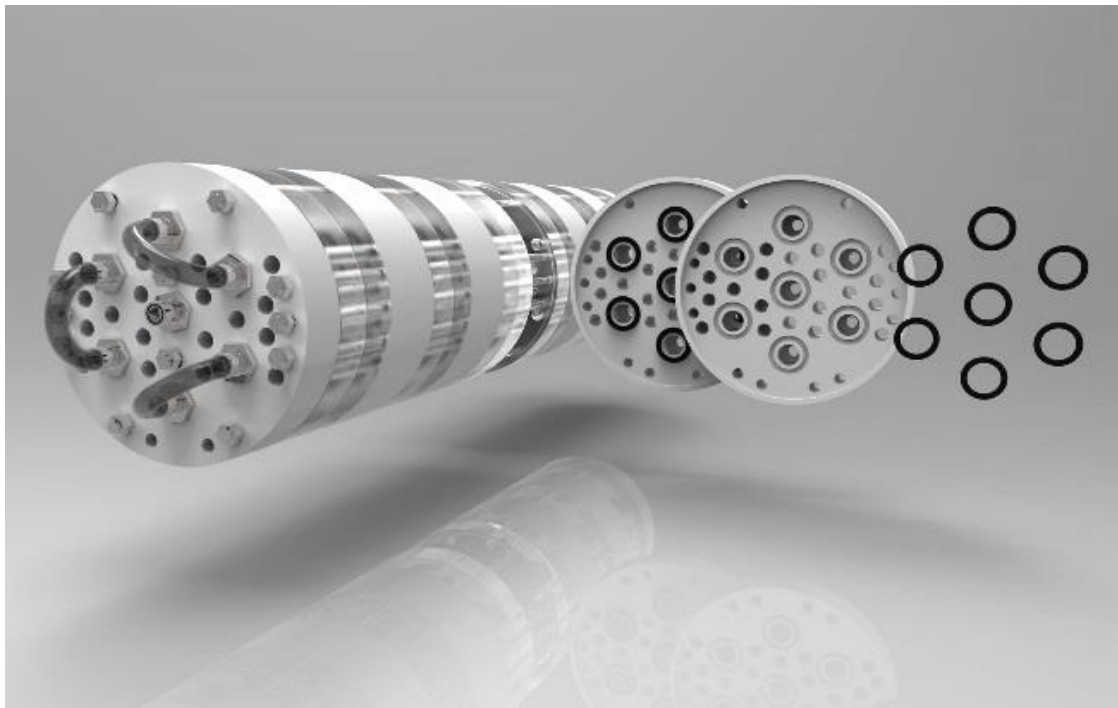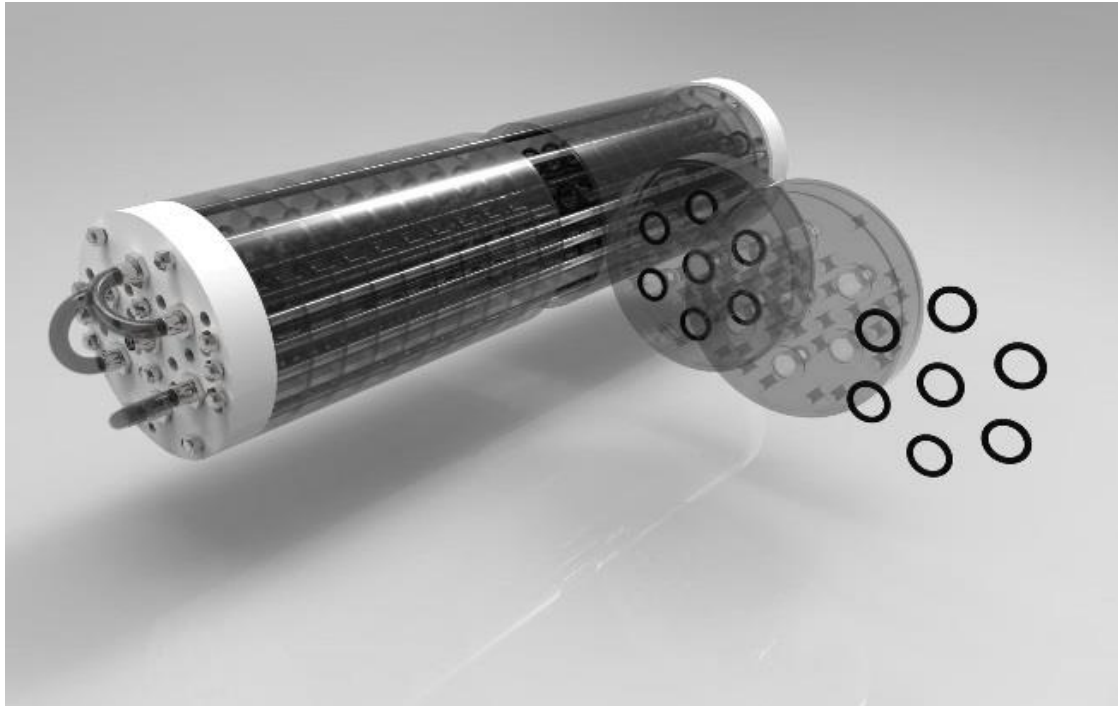
Figure 5-13 Three versions of the Centillion OBR, Opaque, clear, combined (top to bottom).

The Centillion's disk based modular design offers flexibility in disk configuration being capable of producing any length of optical paths as well as the light fraction ratios depending on the disk configuration and material. The disks utilised in this experiment are non-transparent PTFE disks and transparent acrylic, however any material can be utilised to manufacture disks proving that the Centillion can be implemented very easily in diverse production processes, that require the use of corrosive chemicals as found in biofuel processing, or FDA approved as in food product and pharmaceuticals processes.

The Centillion OBR operates a highly controllable oscillatory flow regime. Oscillatory flow as mentioned above enforces oscillation between the orifices that causes the formation of toroidal vortices in the baffle thus increasing mixing efficiency, Oscillatory motion in OBRs' is characterized by the Reynolds, Oscillatory Reynolds and Strouhal number, such degree of parametrization characterizing the flow follows that the flow in the Centillion is highly controllable, The flow regime can alter immediately and conform with new flow requirements, this can be done by the intervention of the operator, or by an automated system, when for example an online measurement device such as a spectrophotometer senses the culture cell density providing online monitoring and on line characterisation of algae.

Figure 5-14 Reactor disks, transparent on the left and opaque on the right.

Based on current research outputs as well as critical design considerations laid out in past sections, make the Centillion OBR a desirable candidate for algae bioprocessing

5.2.2 Optimising the technology's core.

Although the Centillion OBR has demonstrated efficacy in cultivating algae, there are features which limit its true potential as an OBpbR. These issues are specifically associated with the design of the disk, and are outlined below: The main points identified are:

1. **Heating/Cooling:**

   Not a requirement for *C.vulgaris*. However, to maintain the flexibility of the system to be able to host an array of cells, a method of temperature control is necessary.

2. **Baffled hole feature position:**

   As a chemical reactor spatial footprint is a key consideration, therefore the placement of a baffled passage in the middle of the reactor enables it to add operational volume whilst maintaining the same spatial profile. In the cultivation of algae however the baffle in the middle is mutually shaded and thus suffers reduced light penetration.
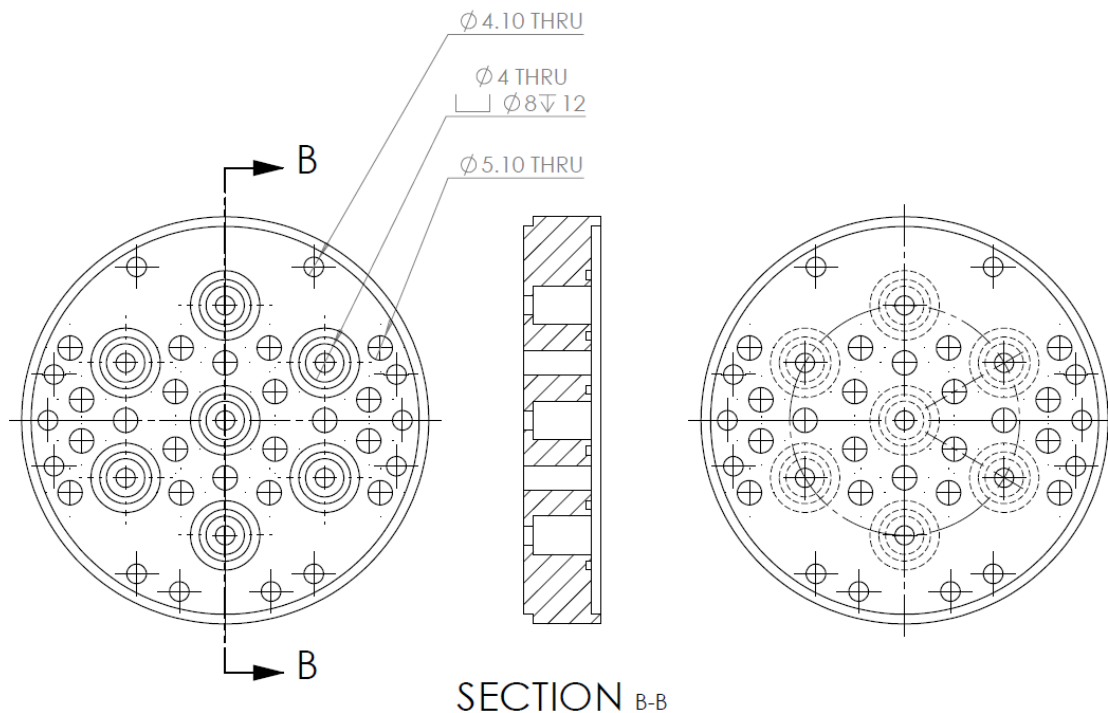
Figure 5-15: Original Version 1 mesoscale reactor disk (Makatsoris, Paramonon and Rakan , 2013).

At the core of the Centillion reactor system in the disk. The original reactor member is shown below. It consists of seven counter bored holes, and 32 multipurpose through holes, which primary role is aligning the disks and housing the threaded rods which compress the system, when assembled. The form factor of the disk is 85mm diameter by 14mm thickness, and total volume per single disk is 4.39ml. The design criteria for the new disk is outlined in the table below.

Table 5-9 Design Criteria for the Bioprocessing Disk

Design Criteria	Elaborate	Action
Increase the volume per disk.	*By increasing the volume per member, the unit cost per volume of the OBR increases*	Increase the number of counter bored features per disk.

Re-arrange the baffle spacing and architecture so that every baffled hole is equidistant from the internal and external surface of the reactor system.	*Minimise shaded areas so that there are no growth inhibitory effects due to light.*	Reduce the material thickness between passage and light.
Implement the capability of internal illumination	*Increase light intensity and enable increased light utilisation leading to higher photosynthetic efficiency.*	Make an internal non-wetted, ventilated area for internal illumination.
Implement temperature control channels	*Allow the reactor to successfully cultivate algae in extreme temperatures and enable the reactor to work with many algal strains that require different temperatures for optimal growth.*	Make a heating/cooling channel around the baffled passages. And alter the reactor shape to maintain a larger

The above requirements were translated to design specifications that led to the design as shown in the adjacent figures. The first feature that stands out is the shape of the new disk. Changing the shape to a "halo" from a "wafer" was achieved by removing the central baffle, and by position all baffled holes on the same radial, equispaced at 22º. This satisfied design criteria 2 nd 3 and made way for criteria number 4, i.e. the implementation of heating and cooling capabilities. Heating and cooling were introduced via two separate loops on the internal and external circumference of the disk. When placed in sequence the two

disk variations form a series of clockwise and anticlockwise spiral pathways which completely enclose the baffled passages.
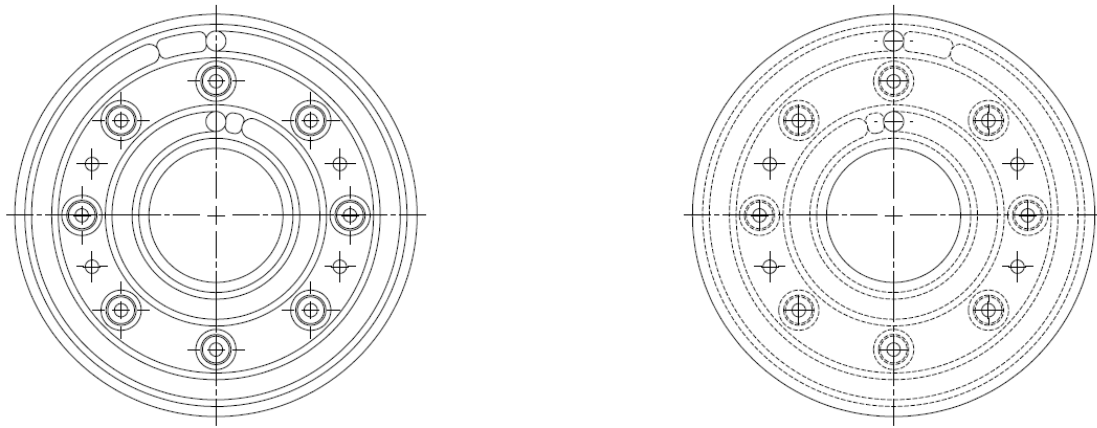
Figure 5-16: Algal bioprocessing optimised disk. Version 2. Due to the temperature control channels, two identical disks are designed with the channel holes mirrored (Makatsoris and Alissandratos, 2019).

SECTION c-c
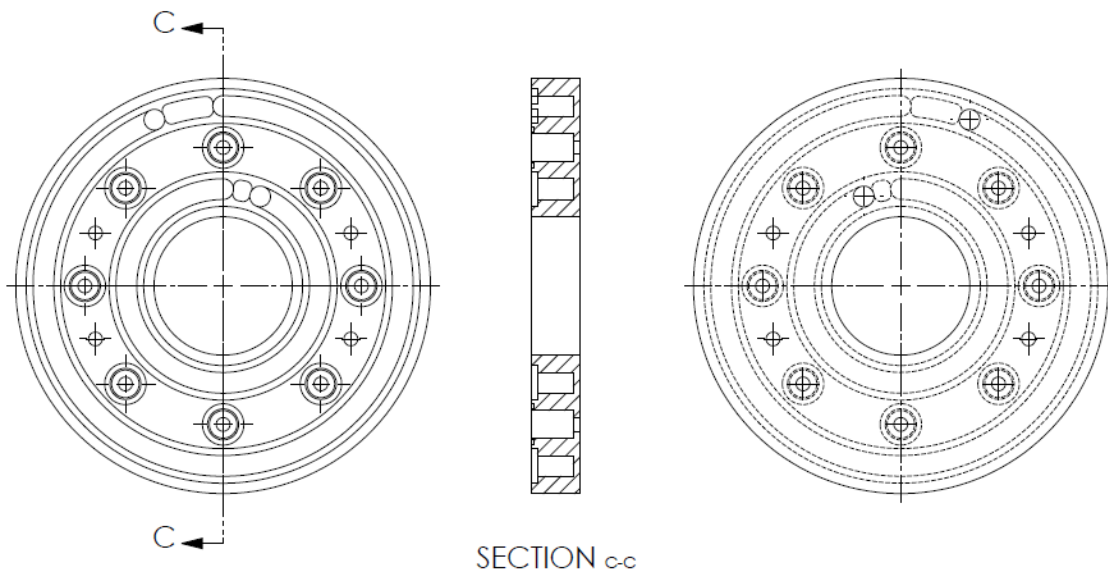
Figure 5-17 Algal bioprocessing optimised disk. Version 2, Disk A OLIR (outer left, internal right) (Makatsoris and Alissandratos, 2019).

SECTION D-D
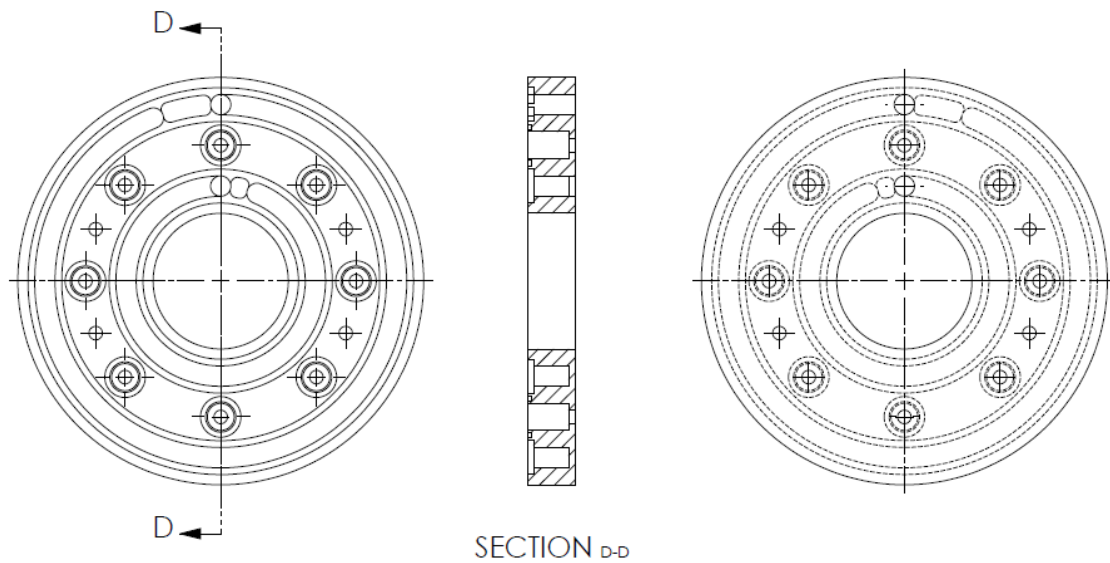
Figure 5-18 Algal bioprocessing optimised disk. Version 2 Disk B COCI (Central outer, central interior) (Makatsoris and Alissandratos, 2019).

The internal and external channels are both independent of each other, however can form a continuous loop if required by connecting the ones outlet to the others inlet. Functionality and flexibility were the key criteria in choosing to keep them separate, implemented into the reactor disk and positioned internally and externally. By doing so they also can act as operating passages for an array of applications. Such as hosting algae cultivation (identical or different strain) or acting as a growth media containment and mixing section. The volumetric capacity of the baffled section of the disk was increase as well by the addition of an extra baffled hole making the number of baffled holes increase to eight from the previous seven; increasing the volume of the disk to 5ml. This off course satisfied the first criteria, but also offers extra advantages in the control of plug flow conditions, which are introduced in the next section.

5.3 Mixing

Mixing is a crucial parameter in the cultivation of microalgae. It has been highlighted as a key consideration, and most importantly a major design flaw of current state of the art pbs. Mixing's importance as a parameter has been highlighted in the CDM where it has been ranked highly and categorised as a key technical subsystem and function of the design. Revisiting literature, mixing in traditional PBR's has never been technically revised, and still relies on pumping large volumes of liquid through a complex series of channels, or by agitating a column using gas. Both of which are costly, non-scalable, and have demonstrated to be ineffective.

As proposed in this thesis, the use of an oscillatory baffled flow reactor, allows for a completely novel and scalable way of mixing to be trialled and tested. The bioprocessing benefits of oscillatory baffled flow reactors mentioned by Abbott et al., (2012) are amplified and promoted by the modular design of the Centillion OBR which enhances light modulation and implements heating and cooling. (Abbott *et al.*, 2012).

The implementation of mixing entails the design of equipment to enable the oscillations to occur. And secondly to characterise the flow, thereby identifying key influencing variables which control the quality of the plug, as well as the regions in the parameter set map which the desired mixing is accomplished.

Therefore, the work in this section entails design and modelling. The design the work carried out to design a mechanism which induces oscillatory motion in the liquid using two different approaches, a scotch-yoke type mechanism and cam shaft mechanism. The Scotch Yoke mechanism is presented here. However the Cam-shaft type (CAM) system is included in the appendix section 7.3D.1.

The modelling aspect of the work follows a similar methodology with literature (Levenspiel, 1998), where tracer experiments are carried out to characterise the dispersion of the tracer in the flow.

5.3.1 Designing an Oscillation Mechanism.

Control of the flow is done with the use of external pumps. As elaborated in the previous section, the pumping considerations were pressure, pump duty, controllability and price. In terms of mixing the one directional net flow, in the absence of oscillations, will create a flow regime, which depending on the flowrate will either be laminar or turbulent.

In past designs of the Centillion reactor, the oscillatory flow was imposed with the use of a Tricontinent syringe pump, which was manually programmed so that it would create oscillatory motion. However as explained in the corresponding section there were limitations. The limitations where primarily that the oscillations were generated externally to the system, a fact which caused pressure losses to the flow regime, since the flow had to travel from the pump to the baffled section of the reactor system. Another issue with the current system was scalability. The current means of generating oscillations was not scalable, where a scalable system would enable higher control and transparency in predicting the flow regimes behaviour, such as the TiS number. Finally, modularity, one of the key design specifications and strengths of the Centillion OBR system. Designing an oscillatory mechanism which is bolt-on to the rest of the reactor modules would complement that design criteria and allow for even greater range of applications.

In relatable industrial examples, the use of Scotch Yoke and cam applications for oscillations are implemented. These systems create a simple harmonic motion which is transferred to a plunger section which in turn induces the oscillatory flow to the liquid. The challenge in the design of an oscillatory system was to implement the accuracy and ease in control of the frequency and amplitude of oscillations in a robust and durable system. Therefore, selection of components is the key consideration, since their specification is to endure exceedingly large operating cycles and high dynamic loads.

The Scotch Yoke mechanism's operation is based on a roller-pin (i.e. a cam roller or roller bearing) positioned on a rolling plate, at a fixed distance from the centre of rotation. Attached on the rolling pin, is a roller or coupler link, which transforms the rotational movement of the roller pin to axial harmonic sinusoidal motion of the roller link.
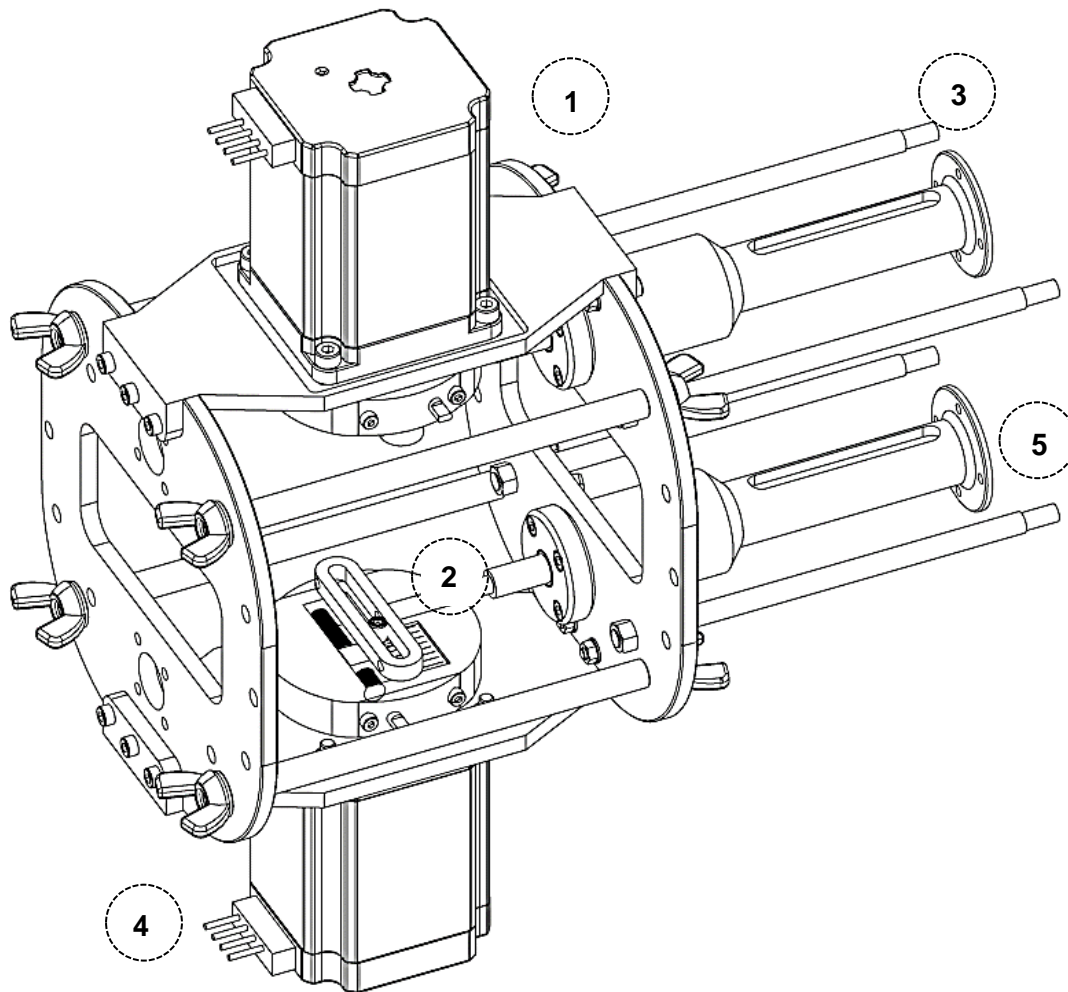
Figure 5-19 SYOM designed and built for the mesoscale Centillion reactor.

The Scotch-Yoke oscillatory mechanism (SYOM) shown in figure 5-19 to 5-21, for the Centillion reactor, was designed with simplicity and cost in mind. The whole system comprises of twelve unique parts, nine of which were purpose designed, and only three bought in. The parts where designed with manufacturing

simplicity in mind, thereby reducing the machining cost and manufacturing turnover time.

The SYOM system implements two scalable oscillatory mechanisms, which can drive one reactor using the two systems working in opposite phases, and a maximum of 4 reactors, 2 on either side, with each system driving two reactors; where the in-stroke of one would be the outstroke of the other.

From the previous schematic of the SYOM, the top-level assembly comprises of a 24V bipolar stepper motor (1), which is mounted on an aluminium frame (4) and pin is fixed on the rolling plate assembly (2). The frame comprises on the four 4mm thick aluminium plates and four 8mm diameter rods, placed for support. The system connects to the reactor's end plate using an additional found 8mm threaded rods (3), and two plunger sub assembly housings (5).

Key to the operation of the SYOM and the core of the innovation in this system is the design of the rolling plate assembly (2). The rolling plate assembly is mounted on the motor (1) pin. The rotational velocity of the motor corresponds to the oscillatory frequency, and the amplitude of oscillations is set by rotating the leadscrew pin (2a) clockwise (CW) or counter clockwise (CCW) to increase or decrease distance of the rolling pin (2b) from the centre of rotation. The oscillatory motion is transferred to the plunger (6) via a system of sequential linear guide bearings, which in turn creates the oscillatory flow regime on the processed fluid.

The innovation of the system lies in the accuracy of control. The frequency similar to other systems can be controlled by adjusting the rotational speed of the motor, on the other hand the system design offers the ability to adjust the amplitude at a resolution of 0.5mm, at a range of between 0.5 to 15mm centre to peak.
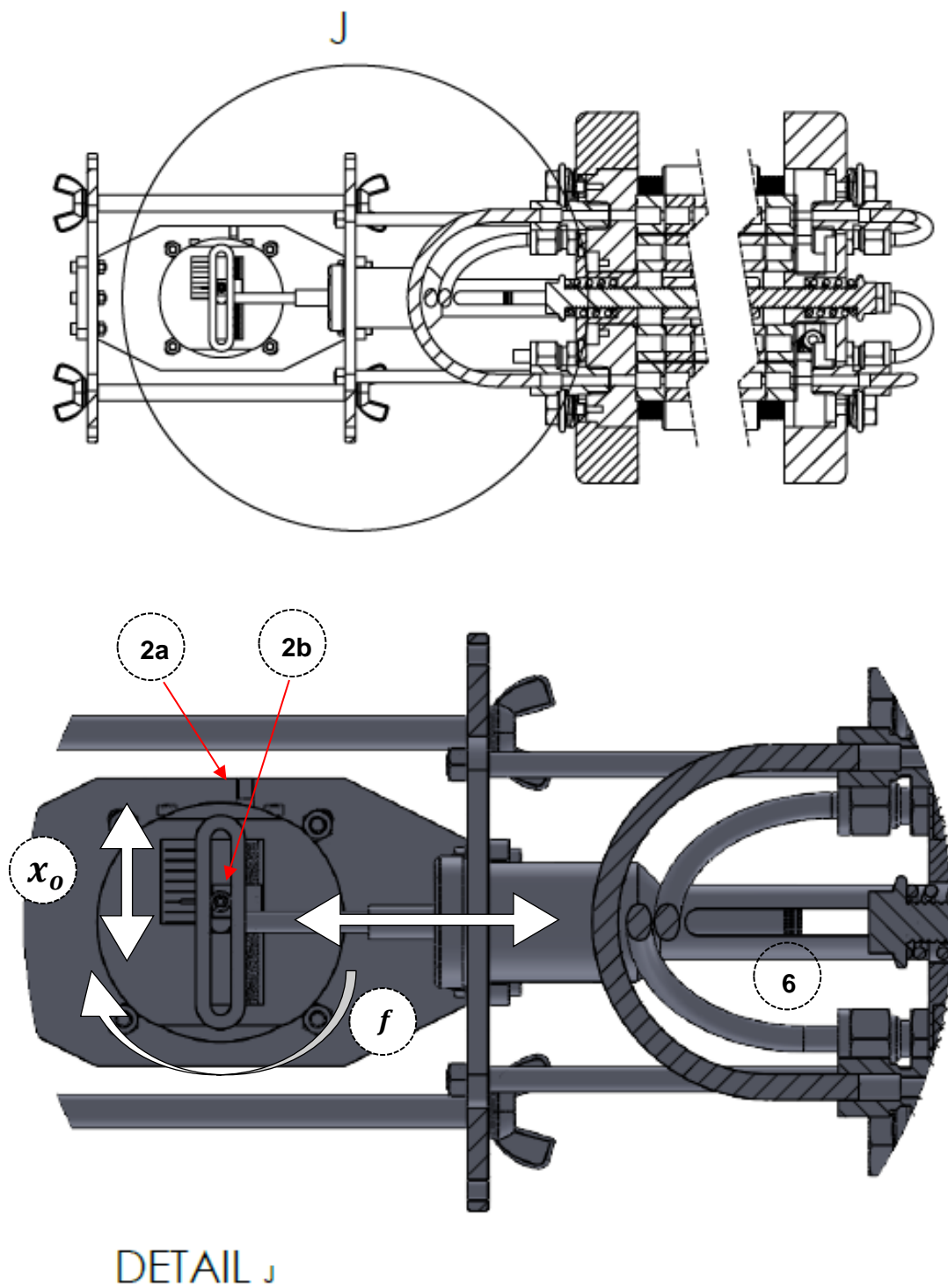
Figure 5-20 TOP: Mid-plane cross-section of the reactor system. BOTTOM: Front view of the SYOM rotating plate, with annotations.
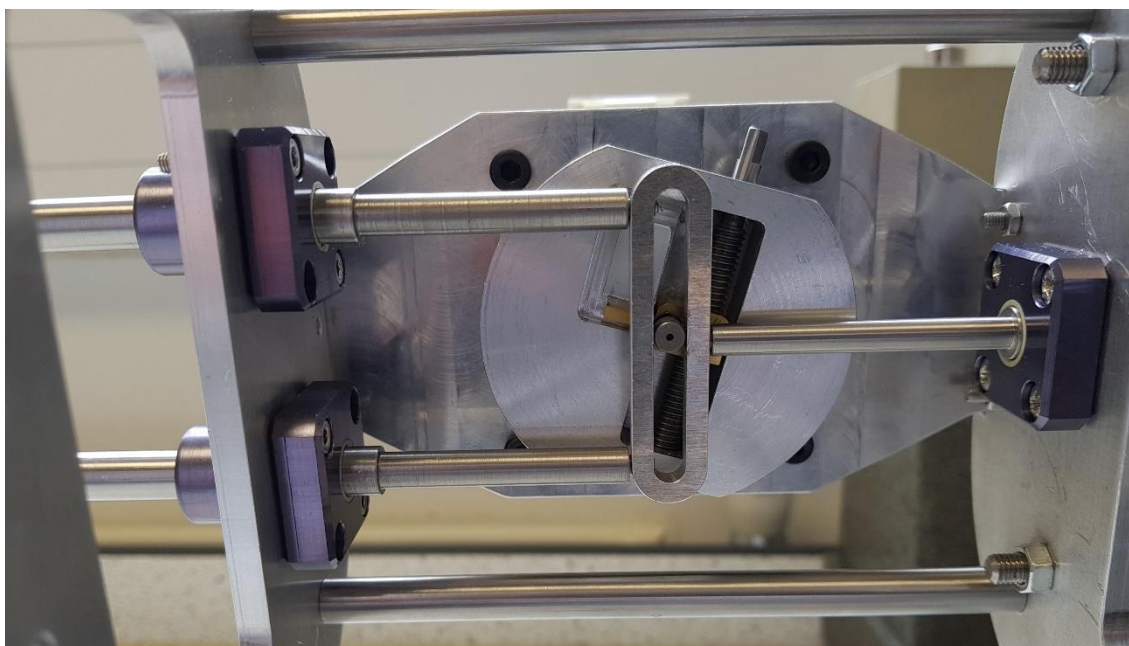
Figure 5-21 Real image of the oscilltory mechanism front face, showing the link, the front plunger rod, the rear sliding rods, the rotating late and the manually adjusted pin, on a brass threade block.

5.3.2 Characterising the flow in the Centillion Reactor.

As mentioned in the previous sections one method of evaluating the flow in an OBR is by measuring its dispersion. According to Levenspiel (1998), this enables a useful representation of the flow to be used for simply monitoring or for scale-up applications (Levenspiel, 1998).

The aim in this section is to determine the best conditions to impose on the OBR for cultivating algae. The methodology to achieve this is to develop an accurate statistical model which can work across reactor scales, this will enable the non-invasive characterisation of the flow regime, as well as assist in developing scaled up versions of the reactor in the future.

5.3.2.1 Experimental Methodology

Following similar methodology to Phan an Harvey (2010) and (2011). (Stonestreet and Van Der Veeken, 1999; Phan and Harvey, 2010, 2011). Tracer experiments were set up, in order to carry out the flow evaluation. Using the centillion oscillatory baffled flow reactor system at two scales (micro and meso

scale), two identical configurations were set up, with parameters specified in Table 5-10.
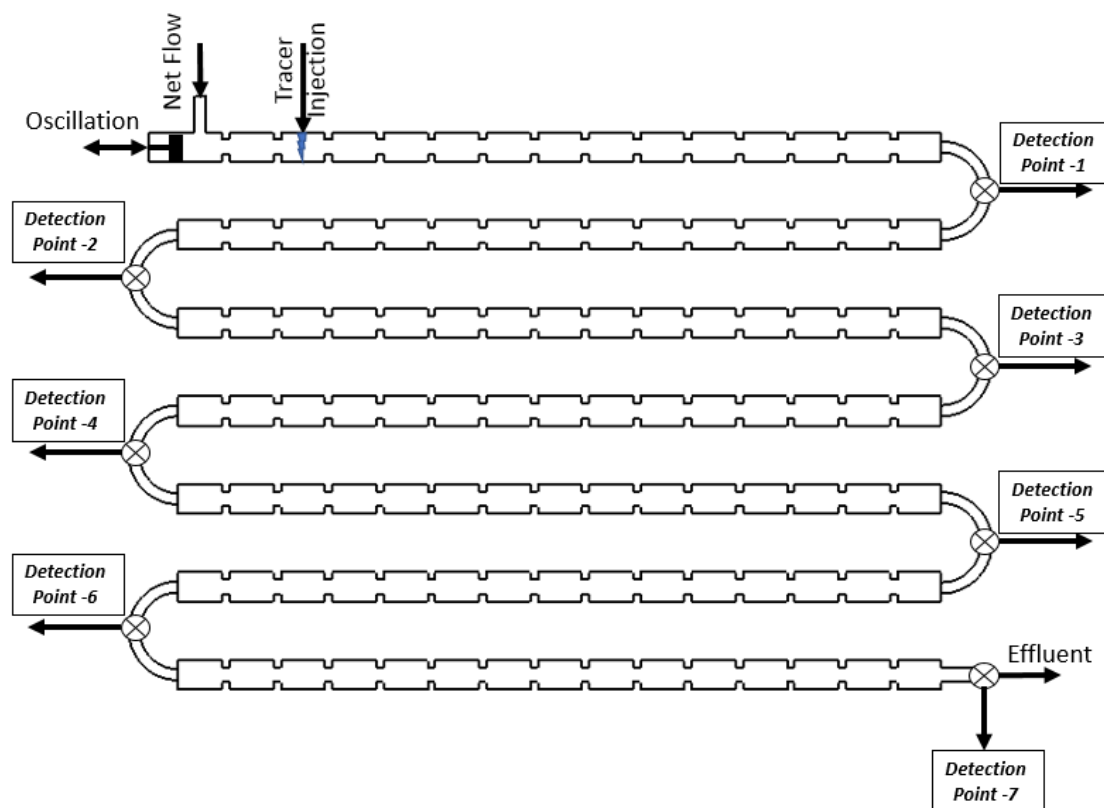
Figure 5-22 System Schematic showing the tracer injection point, and all the possible detection points through the system (Isaev, 2019).

The seven baffled lengths which are formed by the assembled reactor, where connected forming a continuous passage, using 22mm lengths of 1.8-inch FEP flexible tubing from Swagelok, with 1/8 SAE/MS PTFE ferrule-type fittings on either side. The U-bends are smooth tubes and do not contain cavities therefore their length was a consideration and was kept as low as possible, bearing in mind the minimum bend radius of the tube. Care was given when assembling in the unbends to avoid any kinks or excessive stresses which would distort the tube. At the inlet of the passage the oscillatory mechanism 4 tricontinent PVM syringe pumps with 1ml tank capacity, where connected to the inlet of the reactor, two for the continuous flow operating in opposing phases, one for the injection of tracer and one for inducing the oscillations. On the exit of the reactor an ocean optics flow cell was attached inline, at 10mm from the exit of the reactor (Detection point

159

7. Figure 5-22) baffled channel. The flow cell was connected via 600μm fibre optic cables to a QE-PRO spectrophotometer and dh-mini UV-VIS light source, both from Ocean Optics. This experimental procedure and the complete methodology from spectral signature to TiS numbers was carried out by Isaev (2019) (Isaev, 2019). In this section the work specifically entails the statistical analyses of the results, towards the development of statistical model to evaluate the flow for the algal bioprocessing .

Table 5-10 Microscale and mesoscale reactor system specification.

	Micro-Scale	**Meso-Scale**	
Parameter	**Size**	**Size**	**Unit**
Tube Diameter (D)	4	8	mm
Baffle Diameter (d)	2	4	mm
Tube Length (L)	6	12	mm
Baffle Length (l)	1	2	mm
Constriction ratio (S)	0.25	0.25	-
Reactor Parameters			
Number of Disks	24	18	-
Number of passages	7	7	-
Total Length of passage	138	252	mm
Total Length of System	780	1764	mm
Volume per passage	5.5	15.5	ml
Total Volume	19.2	100.2	ml

Using the above two setups a total of 200 tracer experiment parameter sets were developed between the two scales (100 in microscale and 100 in mesoscale). However, concerning the mesoscale, out of 100 experimental points only 50

points were carried out. The tables containing the experimental parameter sets and tank in series (TiS) numbers for both sets of experiments with micro and meso scale reactors are shown in Table D-1 and Table D-2.

Table 5-11 Micro Scale and Meso-Scale DoE parameters and their respective levels (Isaev, 2019).

Micro-Scale			Levels				
			1	**2**	**3**	**4**	**5**
Parameters	Amplitude	mm	0.5	1	1.5	2.5	
	Frequency	Hz	1	2	3	4	5
	Flowrate	ml/min	1	2	3	4	
Meso-Scale			Levels				
			1	**2**	**3**	**4**	**5**
Parameters	Amplitude	mm	1	2	3	4	5
	Frequency	Hz	0.25	0.75	1	1.25	
	Flowrate	ml/min	2	4	6	8	

5.3.2.2 Results

The aim of this analysis is to create a statistical model capable of predicting the TiS number based on a given parameter set. In order to do this the methodology followed was to first identify the key factors influencing the response (TiS). Secondly to develop a statistical model at the microscale, which has a larger experimental data set. Finally using the same methodology as with the micro scale, the analysis was relaunched to include the data from the mesoscale experimentation.

Based on the data in Table D-1 and Table D-2, a new data set comprising of 180 experimental points, nine factors and one response was developed. This data set includes the process parameters for each experiment (Xo, f, $\dot{f}, u, D$) and the dimensionless numbers (Re, Re_o, ψ, St), calculated for each data point. This data

set was used to carry out a regression analyses using the software JMP pro 14 (SAS, 2013).

Statistical analysis of the data comprised of establishing which of the input variables are the significant predictors (influencers of the TiS number), secondly the model was tested for outliers using a robust methodology which establishes outliers based on the standard deviation and quartile ranges of the distribution, and finally a fitting model needs to be established based on partial least squares regression methodologies. Using these techniques two models were developed for the microscale system. One using the process parameters as predictors and one using the dimensionless parameters; both are listed in Table 5-12.

Table 5-12 Complete List of factors for analysis of the tracer experiment datasets

Factor	Symbol	Unit
Amplitude	X_o	mm
Frequency	f	Hz
Flowrate	$\dot{f}$	ml/min
Velocity	u	m/s
Diameter	D	mm
Strouhal Number	St	-
Net Reynold Number	Re	-
Oscillatory Reynolds Number	Re_o	-
Velocity Ratio	ψ	-

The mathematical model relating factors and responses for a typical regression problem take the following form:

$$Y = \beta_0 + \sum_{i=1}^{K} \beta_i X_i + \sum_{i=1}^{K} \beta_{ii} X_c^2 + \sum_{i=1}^{K} \sum_{j>1}^{K} \beta_{ij} X_i X_j + \epsilon \qquad \textbf{(5-9)}$$

Where Y is the response, in this case the number of tanks in series as per the tracer experiments. X_i and X_j are the investigation factors where i and j are the index number for the interaction patterns K. The effects and interaction are represented by, β_i, β_{ii}, β_{ij}, where i denotes first order, ii denotes quadratic and ij the interaction effect. β_0 and ϵ are the intercept and error term respectively (Lazić, 2004; Montgomery, 2008)

To assess statistical significance in factor effects and their relationship, statistical modelling methodologies such as least squares, are employed. The accuracy of the models is evaluated based on the regression coefficient R^2 which contrary to popular belief is not an indicator of the validity, but of the degree at which the model fits the data (Nourafkan *et al.*, 2017). The lack of fit test (Fischer test) conducted by analysis of variance which assesses the significance of the regression model according to the p-value.

5.3.2.2.1 <u>Model 1</u>: Process parameters as predictors of TiS (X_o, f, $\dot{f}$)

A standard least squares regression methodology was employed to develop a model describing the relationship between the process variables and the TIS number. The model architecture was based on the full factorial methodology limited to second degree interactions between the oscillatory frequency (Hz), the oscillation amplitude (mm) and the net flowrate (ml/min). The resulting model has a fit of $R^2 = 59\%$, with RMSE = 6.36, based on 100 observations. By analysis of variance, the F-test returned a probability of F<0.001 indicated very strong correlation between factors and response in the model.

The prediction expression is shown below:

$$TIS_{No} = 42.23 - 6.68 \times X_o + 1.82 \times f - 5.90 \times \dot{f} - 0.59 \times (X_o \times f) \qquad \textbf{(5-10)}$$
$$+ 1.38 \times (X_o \times \dot{f}) + 0.39 \times (f \times \dot{f})$$

Where X_o, $\dot{f}$, f are the amplitude of oscillations (mm), net flowrate (ml/min), and the frequency of oscillations (Hz). Table 5-13, displays the parameters and their interactions according to their significance, set by the p-Value. A p-Value of below 0.05 is considered significant enough and should be included in the model. It is evident from Table 5-13 that the X_o and its interaction with f and $\dot{f}$ as well as the f, play a crucial role in predicting the tank in series number.

Whereas the X_o interaction with f, and the f interaction with $\dot{f}$ as well as the $\dot{f}$ alone, do not play any significant role in influencing change in the TIS number.

Table 5-13: Parameter significance rating by p-Factor. (asterisk [*] denotes significance, the caret [^] indicated parameter being used in significant correlation).

Parameter		P-Value
Amplitude	X_o	<0.001*
Amplitude × Flowrate	$X_o \times \dot{f}$	0.001*
Frequency	f	0.032*
Amplitude × Frequency	$X_o \times f$	0.071
Frequency × Flowrate	$f \times \dot{f}$	0.34
Flowrate	$\dot{f}$	0.37

5.3.2.2.2 *Model 2: Dimensionless Parameters as predictors of TiS (Re, Re_o, ψ, St)*

The flow in the OBR is controlled by the process parameters, and is characterised by the nondimensional numbers, specifically the Reynolds number, the oscillatory Reynolds number and the Strouhal number (Re, Re_o, St).

The predictive expression generated in model 1, shows that there is a statistically significant correlation between dispersion characteristics (TiS) and process parameters, specifically amplitude and frequency. The limitation with this model

is that it does not consider the reactor geometry. Therefore, the parameter space from which the model is derived, restricts it from being used in experiments which flow passage geometry differ. Revisiting literature the Strouhal number is a function of the amplitude and the passage diameter, the velocity ratio is a function of the two Reynolds numbers (Re, Re_o), which include the frequency. linear velocity, amplitude and rheological parameters of the liquid in motion (density and dynamic viscosity). Therefore, a model which describes the dispersion which is based on the non-dimensional characteristics will facilitate a scaleup pathway to be easily implemented as well as be able to be used cross scale.

Using equations (2-3) and (2-6) from section 2.3.2, the dimensionless parameters (Re, Re_o, ψ, St) were calculated for each of the experimental data points. Following the same methodology as with model one, results in a model

A model based on least square methodology was developed with R^2 = 64% and RMSE=6.15. the F-test returned a probability of F<0.001 indicated very strong correlation between factors and response in the model.

The prediction expression is:

$$
\begin{aligned}
TIS_{No} = 25.42\ &+\ 93.07\ \times Re_o\ -0.26\ \times Re\ +\ 34.62\ \times St_{No} \\
&-\ 0.64 \times \psi\ -\ 0.00011\ \times Re_o \times Re\ +\ 0.64 * Re_o * St_{No} \\
&+\ 0.00079\ \times\ Re_o\ \times \psi\ -\ 2.65\ \times Re \times\ St_{No}
\end{aligned}
\tag{5-11}
$$

Similar with model one the predominant influencers of TiS change are the Strouhal number, and its interactions with the oscillatory Reynolds number and the latter's interaction with the Velocity ratio. All other interactions are of negligible significance and do not influence the TIS number. A synoptic list is shown in Table 5-14.

Table 5-14 Parameter significance rating by p-Factor. (asterisk [*] denotes significance, the caret [^] indicated parameter being used in significant correlation).

Parameter		P-Value
Strouhal Number	St	<0.001*
Strouhal Number × Oscillatory Reynolds Number	$St \times Re_o$	0.001*
Oscillatory Reynolds Number × Velocity Ratio	$Re_o \times \psi$	0.007*
Strouhal Number × Reynolds Number	$St \times Re$	0.193
Oscillatory Reynolds Number	Re_o	0.360^
Reynolds Number	Re	0.360^
Velocity Ratio	ψ	0.360^

Comparing model 1 and model 2 according to accuracy it is evident by the regression coefficients (R^2) that model 2 is a stronger predictor of TiS. The factor significance between the two models is similar, since in model 1, the amplitude is shown to be the key predictor, whereas in model 2 it's the Strouhal number. As mentioned above this is beneficial since the Strouhal number contains both the amplitude and the diameter (Equation 2.3). Consequently, since the model containing the dimensionless parameters is more accurate, the model extensions to include the data from the scaled up (mesoscale) experiments, will be carried out using the methodology followed in model 2.

5.3.2.2.3 Scale up model.

The scale up strategy that was selected for the scaling of between the microscale (D=4mm) and mesoscale (D=8mm) was based on geometric similarity. This means that the increase in tube diameter was followed by increase in other components so that that constriction ratio, and tube length to baffle diameter ratio remain identical (Equations (2-2) and (2-3)). In addition to that the mixing regime can also be scaled up in an OBR can be achieved without any negative effects, simply by maintaining a constant Strouhal number. Experimentally this is demonstrated by having identical TiS numbers (Smith, 1999; Oliva *et al.*, 2018). Therefore, for the experimental procedure on the mesoscale reactor, was based on the selection process parameters ($X_o, f, \dot{f}$) in order to achieve identical Strouhal numbers. Therefore, the design of experiments was similar with that of the 4mm reactor, keeping the Strouhal number identical (amplitudes), and the velocity ratios the same. This way the two strongest TiS influencing factors would increase the possibility of unearthing a correlation and developing an accurate model, in this application.

Table 5-15 Factor importance table. Showing the contribution of each factor and its portion in defining the TiS number from 150 experiments (JMP pro 14 , 2019).

Number of Tanks				
Predictor	**Contribution**	**Portion**		**Rank**
St	420.139	0.3447		1
X_o	380.452	0.3122		2
ψ	175.044	0.1436		3
Re_o	118.709	0.0974		4
f	61.632	0.0506		5
Re	26.105	0.0214		6
$\dot{f}$	18.456	0.0151		7
u	18.149	0.0149		8

To test whether the dimensionless parameters actually are better predictors of the TiS, the predictions were ranked according to importance, based on the 180 data points table. The results are shown in Table 5-15.

Carrying out the same methodology as in model 2, an expanded predictive model based on 150 experiments across two geometric scales is shown below. Based on least square methodology was developed with R^2 = 70% and RMSE=5.3 the F-test returned a probability of F<0.001 indicated very strong correlation between factors and response in the model.

The predictive expression is shown below:

$$
\begin{aligned}
TiS = 22.71 &+ 1.27 \times X_o + 4.57 \times D + 3.50 \times Re_o - 2.23 \times Re \qquad \textbf{(5-12)} \\
&+ 222.46 \times St - 1.366 \times \psi - 0.314 \times X_o \times D \\
&+ 0.007 \times X_o \times Re_o - 0.230 \times X_o \times Re \\
&- 79.98 \times X_o \times St - 0.021 \times X_o \times \psi \\
&- 0.0144 \times D \times Re_o + 0.863 \times D \times Re \\
&- 34.08 \times D \times St_{No} + 0.158 \times D \times \psi \\
&- 0.0005 \times Re_o \times Re + 0.3277 \times Re_o \times St \\
&+ 0.00067 \times Re_o \times \psi - 7.174 \times Re \times St \\
&- 3.479 \times Re \times \psi + 3.532 \times St \times \psi
\end{aligned}
$$

In order to test the model its predictive capability is compared with the experimental results. A summary of the comparison across 150 experiments is shown in Table D-3, whereas Figure D-5, Figure D-6 Figure D-7, compare the experimental and the predicted results across the two scales (micro and meso), based on the Strouhal number. The model performs very well, however, there are larger predictive errors, at high Strouhal numbers. To test the efficacy of the reactor system's upscale , the TiS numbers of the two scales were plotted against their corresponding Strouhal number, as per Oliva et al., (2018) and Smith (1999) in ideal plug flow reactors those two lines coincide. From Figure 5-23 it shows that although the lines do not coincide, there is a very strong similarity to the pattern these lines follow.
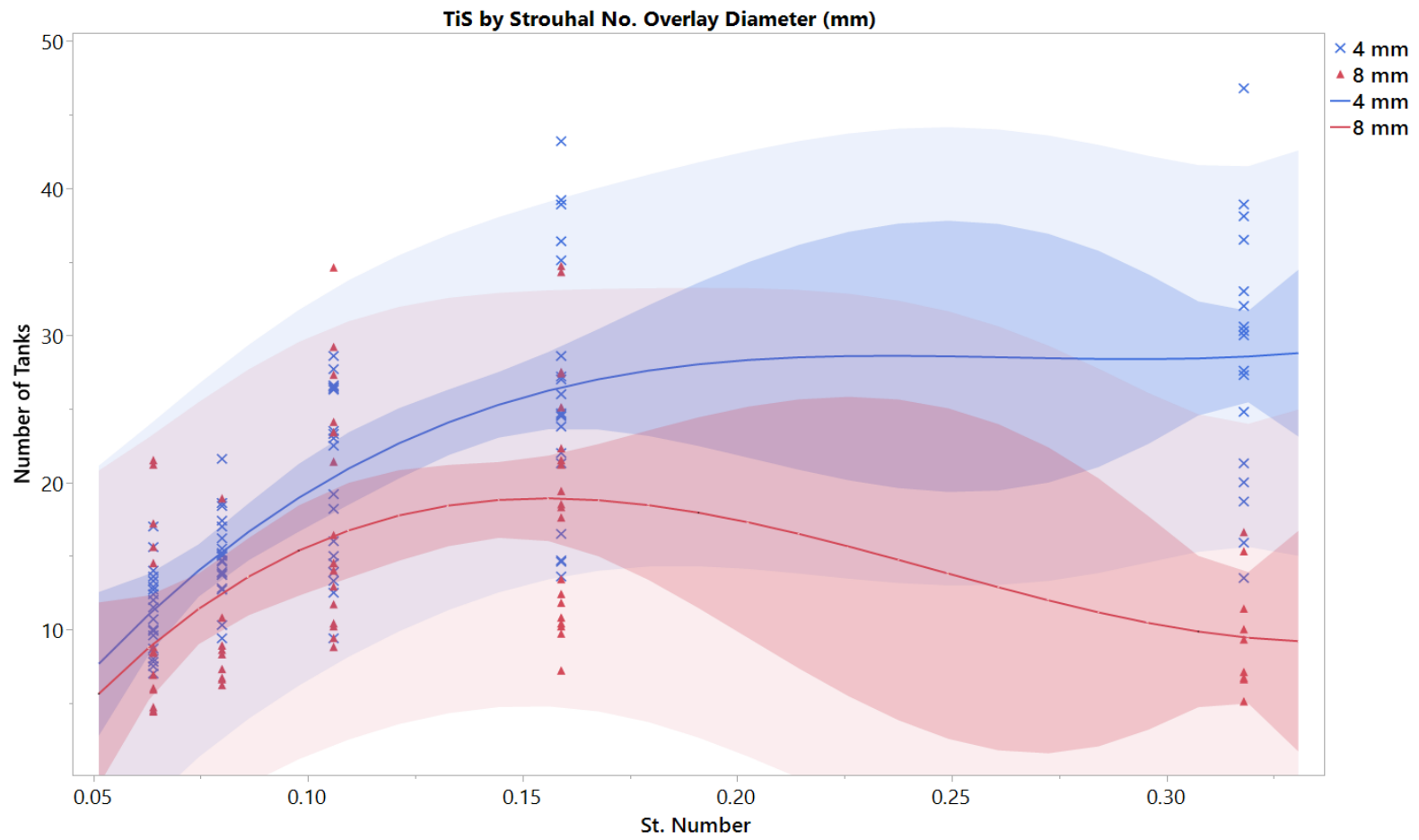
Figure 5-23 TiS number, vs St number grouped by 4mm (Blue) and 8mm (Red) best fit trend lines.

For St number in the range of $0.05 < St < 0.15$ the lines are very similar suggesting scale up is successful, On the other hand for $0.15 < St < 0.3$ the trend breaks, increasing the spread between the TiS number between the two scales. This can be explained by comparing Figure D-5and Figure D-6 with Figure D-7, where there is a larger distribution of TiS numbers; $10 < TiS < 90$ compared to $10 < TiS < 25$ and $10 < TiS < 40$ respectively.

Despite the fact that aim of the modelling is not to optimise but to characterise the flow and identify regions where the reactor performs at its best, the model was able to generate accurate predictions, therefore no further work is required. Specifically, on the performance of the model, it is indicated that it can accurately predict the dispersion for a particular parameter set between a wide range of process inputs and scales. And finally, it can be used to control and characterise the mixing regime and efficiency of the reactor in future algal bioprocessing experiments.

5.4 Monitoring and control

5.4.1 Online Sensing

Online sensing in algae cultivation is still at natal stages. Since most of the algae research is being conducted in small scale PBRs, it is easier to monitor the culture using offline methods (Spectrophotometry, colorimetry, Cell count, biomass density). On the other hand, for analysis the conditions inside the PBR, such mixing characteristics, and gas liquid mass transfer tools such as particle image velocimetry (PIV) and acoustic doppler velocimetry (ADV) are used (Vaičiulyte *et al.*, 2014; Darvehei, Bahri and Moheimani, 2018). Monitoring can be carried out in three distinct ways, offline, online and inline. Offline monitoring is already in place when monitoring algal cultures, with sampling and ph, optical density, cell counting and gravimetric weight analysis. These methods offer unparallel levels of accuracy and insight, however they are time consuming, limited to the number of samples that can be taken, and involve a contamination risk factor since physical interference with the system is involved. Online or inline monitoring enables a continuous non-invasive insight into how a system is performing, thereby increasing accuracy and making the process robust.

5.4.2 Equipment:

From section 2.2 the key considerations are, mass transfer, mixing, temperature, pH, nutrient delivery, sterility and culture density. For monitoring purposes on a photobioreactor, many are self-explanatory, (pH and temperature), some are impossible to monitor online (sterility), whilst the rest rely on the integration of strategically located physical elements (sensors, probes etc), in combination with post processing of data.
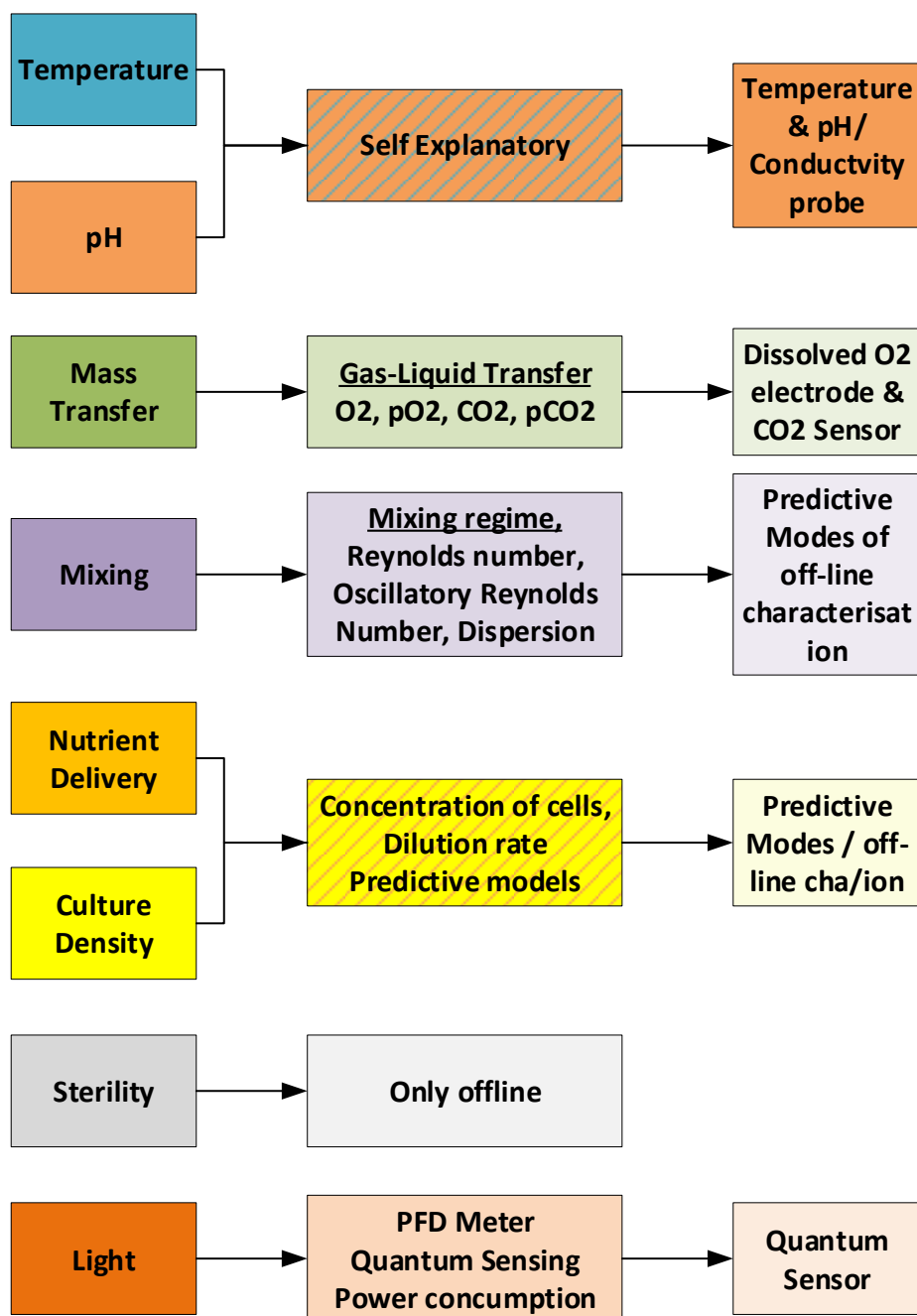
Figure 5-24 A flowchart of the systems integration mapping outlining, key considerations to monitoring outlets methodology chart.

The above eight considerations can be quantified by six measurements, which in turn are categorised into four online measurements. Light, temperature, dissolved O_2, CO_2 and concentration sensing.

Having identified the key sensing equipment types, their implementation has to be considered. Since this is a prototype application the selection of adopting Arduino based controllers, is based on price and flexibility. Comparing two equivalent systems with Arduino and PLC, which is the industrial benchmark. Arduino is found to be cost effective and much more flexible in terms of applications.

5.4.2.1 CO_2 and O_2 Sensing

Carbon dioxide and dissolved oxygen sensing can be carried out using infrared (IR) techniques. Considering the latter, oxygen can be measured in gas or liquid. In an airtight enclosure gas phase O_2 measurements are impractical and dangerous to the sensor therefore liquid O_2 is preferred. As mentioned by Havlik et al (2013), the combination of O_2 and CO_2 combinatory sensing is a great tool since it can control the pH (Havlik *et al.*, 2013). This is carried out in environments where CO_2 is supplied as a pH buffer, in the event where an organic form of carbon is supplied, liquid O_2 alone can provide information on toxic oxygen accumulation in the reactor tubes which can result in inhibitory effects on the culture at levels above 0.25g/l. A very important factor in long tubular lengths (Płaczek, Patyna and Witczak, 2017).Table E-1 outlines the key specification of two potential dissolved oxygen sensors. The preferred sensor the SEN0237-A from DF-Robot was selected for its price and range comparison. However, the low price coupled with a low service life is a compromise (DF-Robot, 2019a).

The device is a probe of 139mm in length and 12.6mm diameter. Mounting is invasive since 12-25mm of the probe must be submerged into the liquid or in the flow path. In consideration of the application mounting can occur either in flow, via a ½ inch ported T-Junction, or by simple submersion into the tank via a 13mm hole. Consideration of mounting locations must be given considering the life span and re-calibration requirements of this device.

5.4.2.2 pH and Temperature

Monitoring the pH and temperature is also a very important factor and unlike the CO_2 and O_2 sensors, both the pH and temperature must be submerged. For this application an analogue pH sensor SEN0161 by DF-Robot was used (Mouser

Electronics, 2019a). A comparative table is supply in Table E-2 For temperature sensing a NTC015H00 NTC sensor was used. Both devices are long slim cylinders, and therefore mounting options are identical to the DO probe. The pH probe is tip is 19.5mm in diameter therefore a ¾ inch port was necessary.

5.4.2.3 Optical Density

There are two methods of quantifying the optical density of a culture. spectrophotometrically and via nephelometry. The key differences are that spectrometry is a direct measurement whereas nephelometry is inferred. The significant advantage of turbimetry over the spectrometry is price. Although the inherent operation of nephelometers makes it impractical in algal applications where dense cultures is involved, it has been successfully implemented in the past for the quantification of the culture density (Chianese and Kramer, 2012; Havlik *et al.*, 2013; Ferrando *et al.*, 2015). For the measurement of turbimetry the SEN0189 Sensor (DF-Robot, 2019b) was selected due to its performance, high response time, and most importantly its compatibility with the tubing sizes used in the reactor system. Further specification and comparison with other considered systems can be found in Table E-3
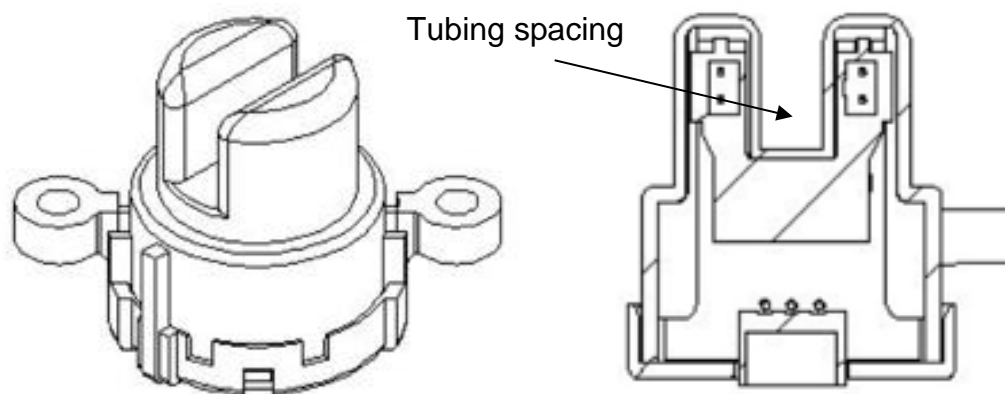
Figure 5-25 SEN0189 Isometric and cross-sectional view. Indicating the spacing for the operating tube (DF-Robot 2019b).

5.4.2.4 Motor Control

Motor control is required in three different locations. The first is the oscillatory mechanism, which motor is used to rotate the oscillating plate. The second is the main peristaltic pump used to circulate the pump and the thirst is the dosing pump used to deliver and extract material into the system. All three motors are selected to be bipolar stepper motors. The reason for the choice is the accuracy required, which can only be delivered by such a motor.

For the oscillatory mechanism a Sanyo Denki 103H7 (RS-Components, 2019) motor was selected due to its high torque output (Figure E-1). Driving the peristaltic pumps 24V OEM stepper motors where installed by the manufacturer. The purpose of which was to share the same components. Each 24V bipolar stepper motor was driven by a single B6600 stepper motor driver (3.5A 42V 160W) (DF-Robot, 2019a). All motors were powered by a Meanwell SP-200 -24, 200W 24V power supply as shown in Figure E-4 (Mouser Electronics, 2019b).

5.4.2.5 Controller interface:

As previously mentioned all equipment was controlled by Arduino. This allowed flexibility in designing circuits and cost-effective maintenance and replacement of parts or equipment.

For every system it was decided to allocate one Arduino module per function. This meant that every system would have two Arduino controllers. One dedicated to the motors and the other dedicated to the sensors. The reason behind this is very simple; Arduino cannot natively store data, therefore in the event a script was run out of schedule (i.e. media input, system flushing) it would lose all the data written on the script terminal. One method around that is to connect the Arduino to a raspberry pie module which would in turn store the data captured by the Arduino, however that was not considered here.

175

5.4.2.5.1 Pumping Dosing and Oscillation.
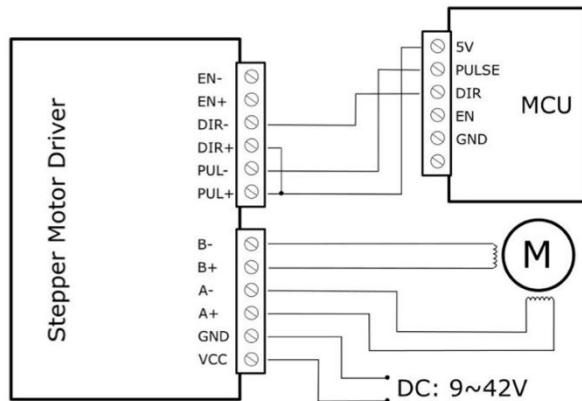
Figure 5-26 TB6600 – Stepper motor controller wiring diagram (DF-Robot, 2019b).

For each motor the system comprised of an Arduino Uno R3 (9V, 2A) microcontroller, a TB6600 stepper motor controller and a SP200 power supply.

The connection diagram Figure 5-26 indicated the connected between the controller, motor, Arduino (MCU) and power input.

Controlling the stepper motor is accurate and very precise. A stepper motor comprises of a series of magnets positioned on radially (Stator) around a shaft (Rotor). In order for the pin to move a pulse of electricity changes the poles on the stator forcing the rotor to turn a precise distance. Each pulse is a step, and each complete revolution is 24steps for the rotor and 24 pulses for the stator. The TB6600 controller can control the stepper motor to an accuracy of $0.05° – 0.45°$

To control the pumps via Arduino a purpose build code was complied. The code operated by inputting the pulse width. In order to translate pulse width settings into process parameters, a series of calibration experiments were carried out. For the oscillatory mechanism motor equations (5-13) and (5-14) were derived from the graphs Figure E-5. Where the pulse width (P_w) is corelated to the rolling disks RPM by a power curve. Frequency in RPM is then translated into Hz, by a linear relationship. In a similar fashion a relationship was determined for pulse width and flowrate for both main and dosage peristaltic pumps (5-15 to(5-18 calibrate from Figure E-6. For the dosage pump, being an identical system with a smaller peristaltic tubing, a correction factor of 1.44 was used. This was validated experimentally.

The equations are shown below:

$$P_w = 40968 \times RPM^{-0.85} \tag{5-13}$$

$$f_{hz} = 0.016 \times RPM \tag{5-14}$$

$$\dot{f}_{1200(4)} = 12591 \times P_w^{-0.85} \tag{5-15}$$

$$\dot{f}_{1200(32)} = 2098.5 \times P_w^{-0.85} \tag{5-16}$$

$$\dot{f}_{800(4)} = {\dot{f}_{1200(4)}}\Big/{1.44} \tag{5-17}$$

$$\dot{f}_{800(32)} = {\dot{f}_{1200(32)}}\Big/{1.44} \tag{5-18}$$

5.4.2.5.2 Sensor data acquisition.

To operate the sensing system a separate Arduino was set up. As per table 5.16, an Arduino Mega R3 (RS-Components, 2009) with an onboard expansions shield was set up and connected to a pH, turbidity and dissolved oxygen sensor.

Table 5-16 Product list and quantity for the Centillion sensor box.

Product name	Quantity
1.5m USB Cable Type A to B	1
Arduino Mega 2560 R3 Microcontroller	1
Arduino Power Supply - 9V 2A (Universal)	2
Breadboard	1
Breadboard Power Supply Module 3.3 V/ 5 V	1
DF-R0165 Accessories Mega IO Expansion Shield V2.4	1
DF-Robot SEN0161 Gravity: Analog pH Sensor / Meter Kit for Arduino	1
DF-Robot SEN Gravity Analogue DO Sensor	1
DF-Robot SEN0189 Gravity: Analog Turbidity Sensor for Arduino	1

Similar to the operation of the motors, the sensors operate by measuring voltage and then correlating it to legible units. For the operation of the turbidity sensor Figure E-7 and equation (5-19) correlate voltage with Nephelometric turbidity units (NTU) (DF-Robot, 2019b). Equations (5-20) is then used to correlate NTU with absorbance, where l is he optical path length, in this case the distance between the two probe and the voltmeter, within the sensor.

$$T_{NTU} = -1220.4 \times V^2 + 5742.3 \times V - 4352.9 \qquad \textbf{(5-19)}$$

$$T_{NTU} = \frac{1}{l} \times ABS \qquad \textbf{(5-20)}$$

$$pH = -59.10 \times V + 413.7 \qquad \textbf{(5-21)}$$

In a similar fashion equation (5-21) and Figure E-8 where experimentally validated to correlate voltage to the pH (Mouser Electronics, 2019a).

A code was compiled for the operation of each of the sensors. The output of the code was printed on Arduinos serial monitor. As the sensor readings were indicative only in the way they are set up, no control implementation was carried out.
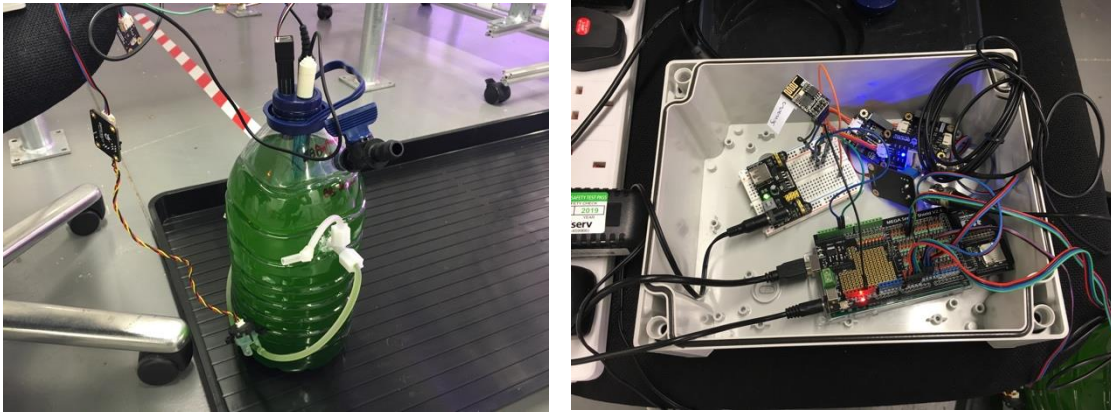
Figure 5-27 LHS – Testing all sensors mounted on a batch system with inline measurements carried out for turbidity. RHS the sensor system setup (Jegoux, 2019.

5.5 Design Systems integration

5.5.1 Centillion Oscillatory Baffled Flow system

An algae cultivation reactor system was built around the Centillion Technology oscillatory baffled flow photobioreactor (C-OBpbR). The system consisted of the following:

1. Assembled Centillion reactor system (Scotch yoke oscillatory mechanism (SYOM), a series of wafers, compression members, tube fittings and other connective elements),
2. The optimised lighting system introduced in section 5.1.3.
3. Flow control and monitoring system, as described in sections 5.4

The complete system fits on top of a benchtop as shown on Figure 5-30 and 5-31 is mounted on a frame (1) comprised of 30x30mm BOSCH-Rexroth aluminium members cut at a range of lengths. Additional items mounted on the frame are the pumping system (9), pump controls (6), lighting (4i) & (4ii), and the growth monitoring sensor (10).
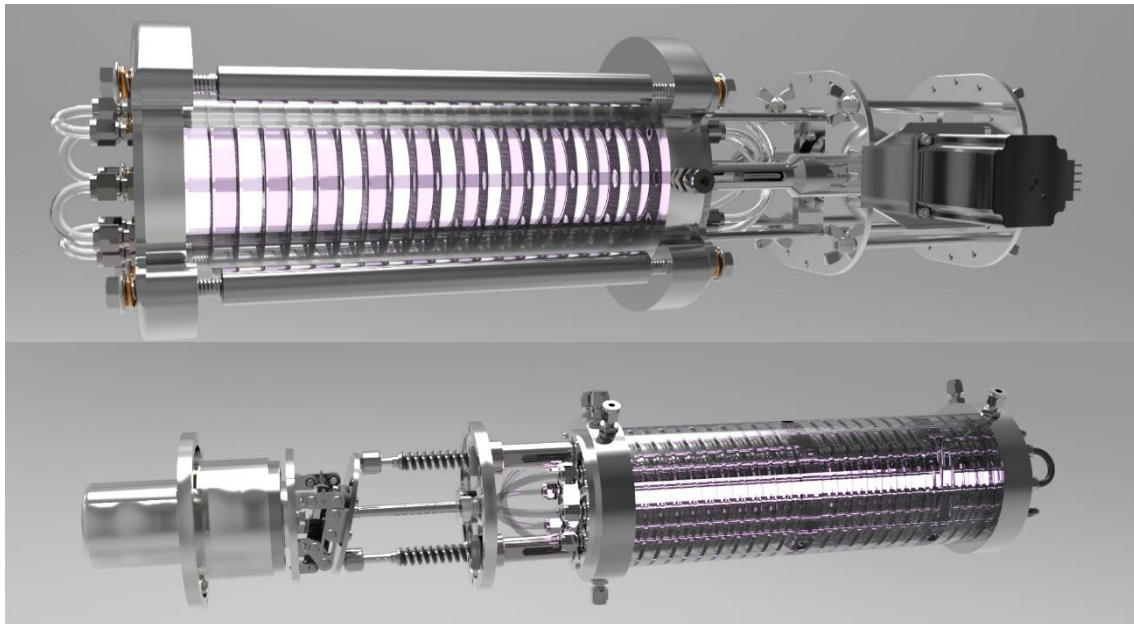
Figure 5-28 Centillion modular reactor system using the SYO mechanism and CAM mechanism on the bottom (photorealistic rendering, with internal illumination).
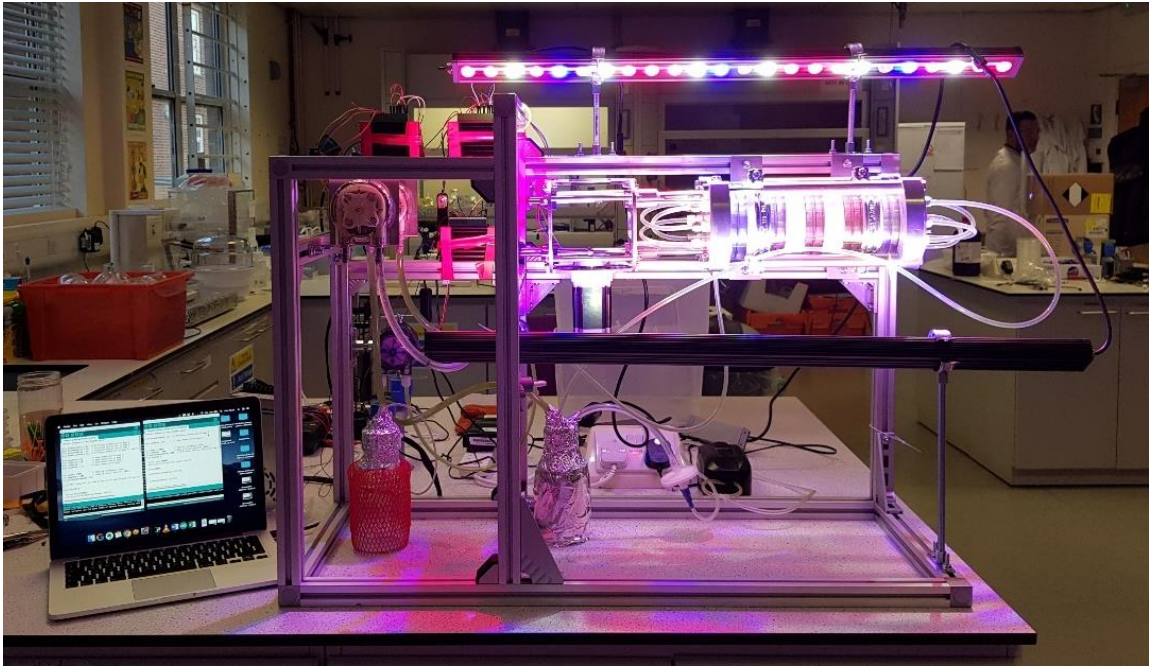
Figure 5-29 Complete system One, sitting on top of a bench In B39-G18 Continuous Flow Laboratories.
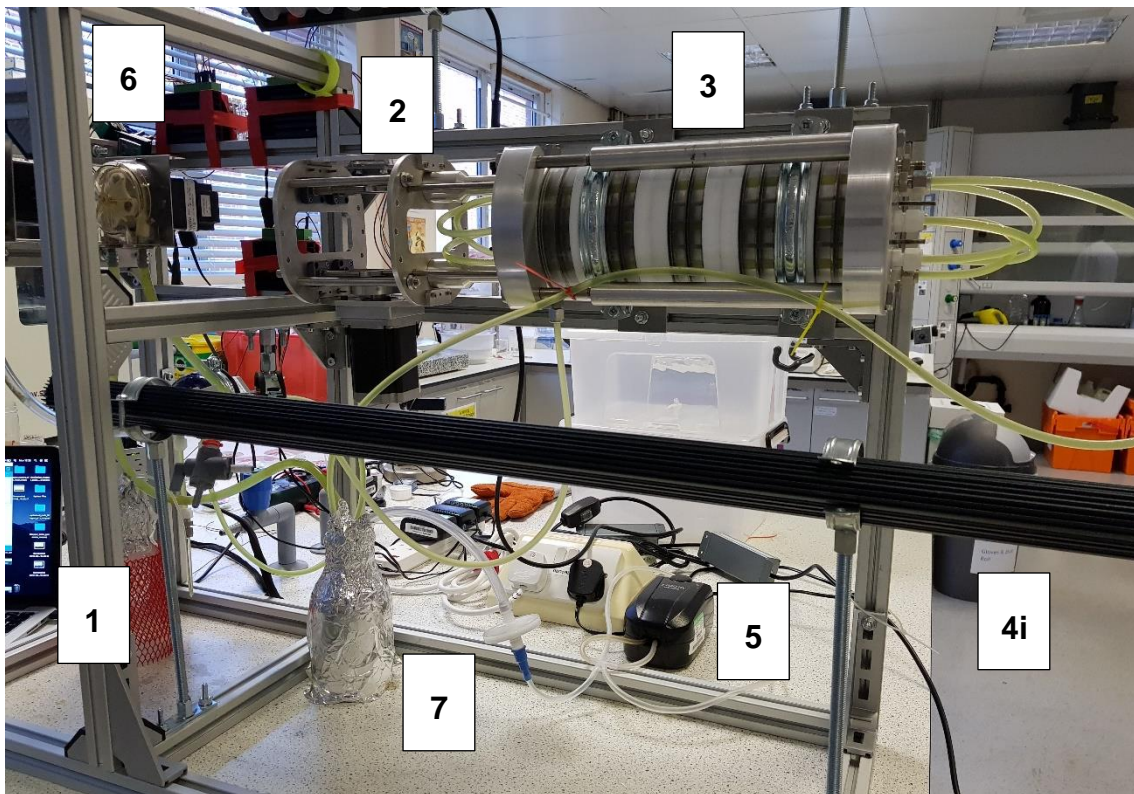
Figure 5-30 C-OBpbR system annotated
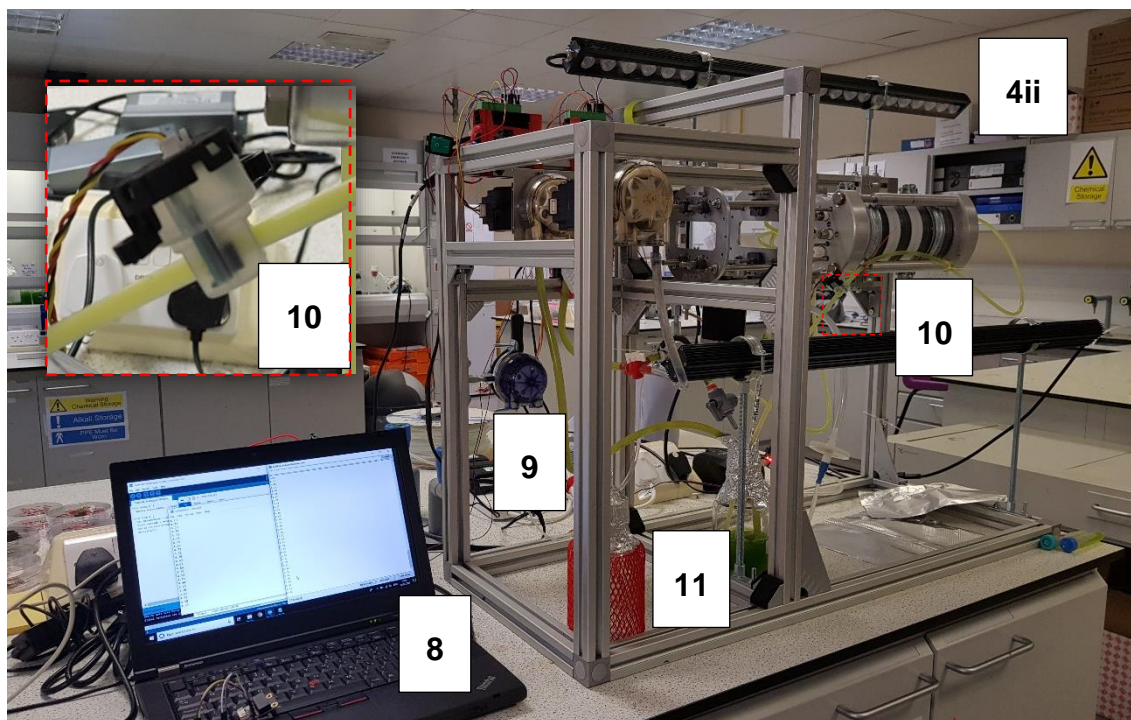
Figure 5-31 System 1 second view annotated

The C-OBpbR is assembled using 7 passages, of a total volume of 100ml. The passages were connected using St.Steel 316L Swagelok compression fittings and ¼ inch FEP tubing. Combined they formed a baffled passage of 1.8 metres in length. The net flow in the system was induced using a peristaltic pump (Welco - WP-1200) capable of a maximum flowrate of 1.4 lit/min. An additional dosing pump (Welco – PX-800) was also attached to the system to enable the injection of material (growth media, pH buffer, etc) to the cultivating algae, whilst reducing the possibility of contaminating the system. Oscillations were induced by the SYOM system which was attached to the reactor with one oscillation mechanism operational. Both net flow orientations and the generation of oscillations was on the bottom with flow going up. This was done in order to reduce the bubble build-up in the system, and enable the gas to escape quicker, thus reducing gas holdup time to a minimum.

Light was supplied to the reactor using two custom made light bars, made up of 24, 3W chips supplying RBiRW light. The bars positioned at 300mm distance from either side of the reactor. The average PFD on the reactor surface was 200 µmol/m^2/s. Light modulation was achieved by arranging the disks between

transparent and opaque forming an alternating light and dark region in the passage. In this system the light and dark region comprised of two disks forming light phase of 28mm long. Temperature control was carried out by controlling the ambient temperature to 21C°. It was observed that after 2-3 days, the temperature of the reactor increased to 23 C° while the ambient temperature in the laboratory remained stable, this was due to the LED lights.

Similar to the practices in conventional tubular reactor systems, a holding tank was implemented into the system (7). The holding tank, being equal volume of the reactor was added to the loop to aid in both biotic and abiotic operations, namely:

- To provide the system with an enclosure at which gas exchange can occur.
- To act as a buffer volume, ensuring that pumps and oscillatory frequency do not run dry during experimentation and cause damage to components.

Sterile filtered air was supplied to the system, at a flowrate of 100ml/min as per Daliry et al. (2017), directly to the holding tank, using air pump (5). Air could also be supplied into the reactor, however, in this case it was avoided due to the bubble size entering the system and interrupting the flow, as evident in Figure 5-32. As part of the monitoring was a SEN0189 nephelometer sensor (10), a SEN0237-A dissolved oxygen sensor, and a SEN0161 pH sensor, were implemented (Daliry *et al.*, 2017).

Control of the pumps, oscillatory motion and recording of the data was carried out using a PC connected. The PC was connected to each of the Arduino system as explained in section 5.4. Using the Arduino software, process parameters can be altered from the PC and communicated to the board easily and without any interruption to the operation of the system (biological and mechanical). This creates a very effective framework enabling long term continuous study of a microorganism, a critical step in establishing a new scalable bioprocess as mentioned by Da Silva (2016) and Jianye et al., (2015) since hidden limitation in the system performance, and biological mutations can only be established after several months of continuous operation (Jianye *et al.*, 2015; Reis and Da Silva, 2016; Płaczek, Patyna and Witczak, 2017).
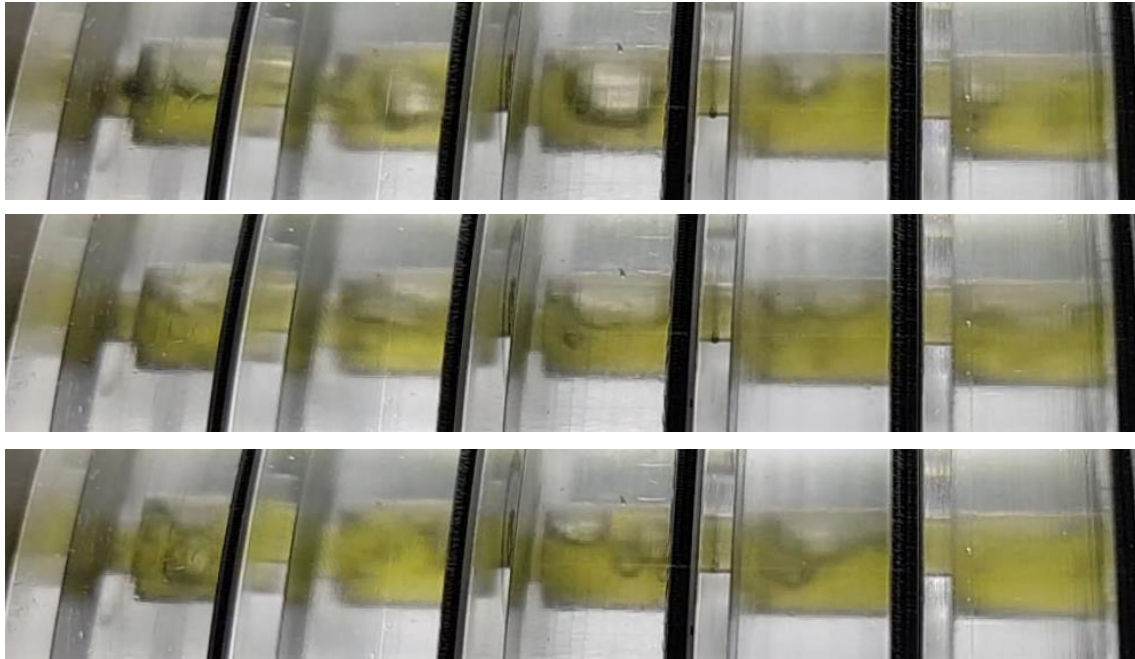
Figure 5-32 Behaviour of bubbles under oscillatory motion. Bubble injection rate of 2-5 L/h, Frequency 3Hz and amplitude 10mm. Average bubble size approximately 4mm in diameter.

5.6 Centillion Meso Scale Algae Cultivation system experimentation.

As outlined by the methodology, the biological aspects of an optimised media formulation, custom to a specific microalgae culture *(C.vulgaris)*, coupled with the development of the technical aspects of the reactor development (light, mixing characterisation and online sensing) are now combined into a novel platform for experimentation.

However as described in section 3.2, effective cultivation protocols are critical in the handling of microalgae. On the one hand culture transfer and acclimation protocols have already been developed in section 3.2.2, however reactor preparation protocols, similar to those for batch cultivation shown in 3.2.2.1, are not. Since the platform proposed in this section is a prototype, these have to be developed.

5.6.1 Experimental protocol

The Centillion mesoscale oscillatory baffled flow photobioreactor was set up identical to Figure 5-29 and Figure 5-30, In preparing the system for algae cultivation, a methodology of cleaning, decontamination, sterilisation, flushing, priming and inoculating was implemented. Since this system is a prototype, such protocols must be designed.

Cleaning: The inlets of both peristaltic pumps (9) were inserted into a steam sterilised glass bottle containing dH_2O, at room temperature. The contents of which was pumped through the reactor and collected at a separate vessel at the reactor outlet and disposed of.

Decontamination and sterilisation: A mixture of 25% IPA and DH_2O was pumped into the system using both peristaltic pumps, and collected back into the same vessel, forming a loop. The both inlets and outlets of the system were closed up with 2 layers of sterile gauge and aluminium sheets, both of which are sprayed with IPA, so that the system is closed up as much as possible. The contents were pumped through the system for 10-12 hours. after the sterilisation step, it is important that the reactor remains a closed system so that no contaminants renter

the system. Therefore, any inputs to the system must be done under ascetic conditions, and through a 0.22 µm filter.

Flushing: The system is not full of the IPA mixture. In order to remove it, a sterile bottle is connected to the secondary peristaltic pump via a 1/8 inch FEP tubing and ferrule type connectors which are pre-soaked in ethanol. DH_2O is pumped into the bottle through a 0.22 µm filter. Once the bottle is filled to approximately 200ml the contents are pumped through the reactor displacing the IPA mixture which is ejected from the reactor via the 3 way valve. This operation is carried out three times with a total of 600-700ml of DH_2O. In order to ensure that no IPA remains is in the system, a sample of the waste is collected and analysed via Raman spectroscopy. Any residual IPA can be detected via Raman through its distinctive peaks at with intensive between 100 and 750 AU, at shift wavelengths of 819, 953, 1454 and 2923nm (Wang *et al.*, 2018). If the sample still contains IPA, then the environment is not suitable for algae cultivation, therefore further flushing of the system must be carried out. Finally, a sample of the flushed volume is retained and stored in a sterile 50ml sample holder, for light microscopy evaluation, in the event that the system becomes contaminated.

Priming: Using the same methodology as before, fresh media is introduced into the system. Priming can occur in two ways. First an injection of highly concentrated media formulation can be inserted into the system and allowed to mix for approximately the duration of two residence times. A second 200ml volume of freshly made media at the appropriate concentrations can be injected using similar methodology as before and displace the existing water from the system. Using high purity chemicals does favour the first methodology, whereas lower cost media recipes are more suited to the second method. A sample of the media is retained like above for microscopic evaluation in the event that the system is contaminated.

When the system is primed and the media is completely mixed, calibration and background correction of the sensor is required for it to operate reliably. This is done electronically by simply removing or subtracting the media's signal from the background.

Inoculation: For batch reactor typical inoculum volumes are between 5-10% of the total system volume. In the case of the Centillion reactor it became best practice to prepare starter inoculums in the range of 15-20% to avoid the culture from crashing out. Calculating the volume of inoculum (ml) required for sub culturing was calculated by the following equation, where V_c the total culture volume, and OD680 is, is the final optical density required.

$$C_{Algae} = V_c \times (33.8 \times OD680 - 0.1856)/100) \qquad \textbf{(5-22)}$$

The final optical density can also calculate in terms of cellular density by the calibration curve presented in Figure 3-1. After inoculation the system was left running for approximately 1-2h prior to an initial sample being taken

With the systems set up the experimentation was ready to be initiated. The experimental protocol detailed in sections 3.2.2 and 5.6.1 were followed for all subsequent experimentation with the reactor. The aim of the experiments was to test the new cultivation system in growing *C.vulgaris*, under optimised conditions.

Selecting process parameters

The parameter set $(\dot{f}, f, X_o)$ used for the experiments, was derived following the methodology outlined in Figure 5-33. According to which, the net flow and the mixing are selected, based on the desired light cycle and maximum TiS numbers respectively.

Specifically, the net flowrate of the algae in the reactor is selected based on the length of time the plug spends in each light phase, which is correlated with the algal growth rate given by equation (5-1) and (5-2). From this the velocity u of the plug through each of the light phases is derived, which in conjunction with a known reactor geometry, results in the systems net flowrate $\dot{f}$. From a given velocity u the net Reynolds number (Re) is derived using equation (2-3). For the oscillatory parameters (f, X_o) a similar methodology is followed. Looking back at equation (5-12) and Table 5-15, the $, X_o$ is derived from the St number and the frequency f is derived by the oscillatory Reynolds number Re_o which in

conjunction with the Re provides the velocity ratio (ψ). All of the above components are input into equation (5-12) to calculate the TiS number.

To put it into context, the system used here was assembled with an optical path of 28mm, by arranging the disks by material, in sequence of AA, PP, AA, PP and so on, (A denotes acrylic and P denotes PTFE). From relevant experimentation the optimum light cycle for both short and long light paths, is 56 seconds, this translates to flowrate of 3ml/min and a net velocity of $u = 0.004\frac{m}{s}$ through the reactor.

With the flowrate set, the next task is to identify the optimum mixing conditions. These are set by the highest TiS number achieved with the flowrate set to 3ml/min. This is done by using the predictive equation (5-12) This predictive expression accurately predicts the performance of the reactor, in the form of the tank in series number as a function of the variables X_o, D, Re_o, Re, St and ψ. Since the geometry of the reactor and the set flowrate are known, the diameter (D) and the net Reynolds number (Re) are replaced with their respective values. The four remaining factors, X_o, Re_o, St_{No} and ψ which are directly related with the mixing intensity are set according to prior knowledge deriving from experimentation.

Concerning the amplitude X_o, It is shown that the maximum TiS numbers are achieved with a Strouhal number at 0.15 Figure 5-23. Given such that the diameter of the reactor is fixed, the variable which will dictate the St value is the amplitude, which in this case is 4mm centre to peak amplitude.

For f revisiting the data tables, the optimal frequency giving the highest TiS performance at 4mm amplitude is selected. Finally, all parameters and input into (5-12) and which predicts the TiS number for the parameter set. That number is compared with the equivalent TiS numbers achieved in the system and is either selected or revised. The above parameters suggest a TiS number of 81, this figure belongs to the top 25% of the TiS figures suggested by section 5.3.2, therefore the process parameters for the below experiments are presented in

Table 5-17 Experimental process parameter set for the Cultivation of C.vulgaris in the C-OBpbR. (*average velocity through baffled section of the reactor).

Factor	Symbol	Setting	Unit
Amplitude	X_o	4	mm
Frequency	f	1	Hz
Flowrate	$\dot{f}$	3	ml/min
Velocity*	u	0.004	m/s
Diameter	D	8	mm
Strouhal Number	St	0.15	-
Net Reynold Number	Re	32	-
Oscillatory Reynolds Number	Re_o	201	-
Velocity Ratio	ψ	6.2	-
Tank in series number	TiS	77	-

An investigatory experimental design was set up based on testing the long-term cultivation with the C-OBpbR, in batch and semi-continuous cultivation. The experimental procedure starts with a batch experimentation carried out with a control to establish the effect of the oscillatory mechanism. Then a long term semi-continuous cultivation experiments is carried out testing the reactor for an operational timeframe of 91 days across two media formulations and 8 subcultures.
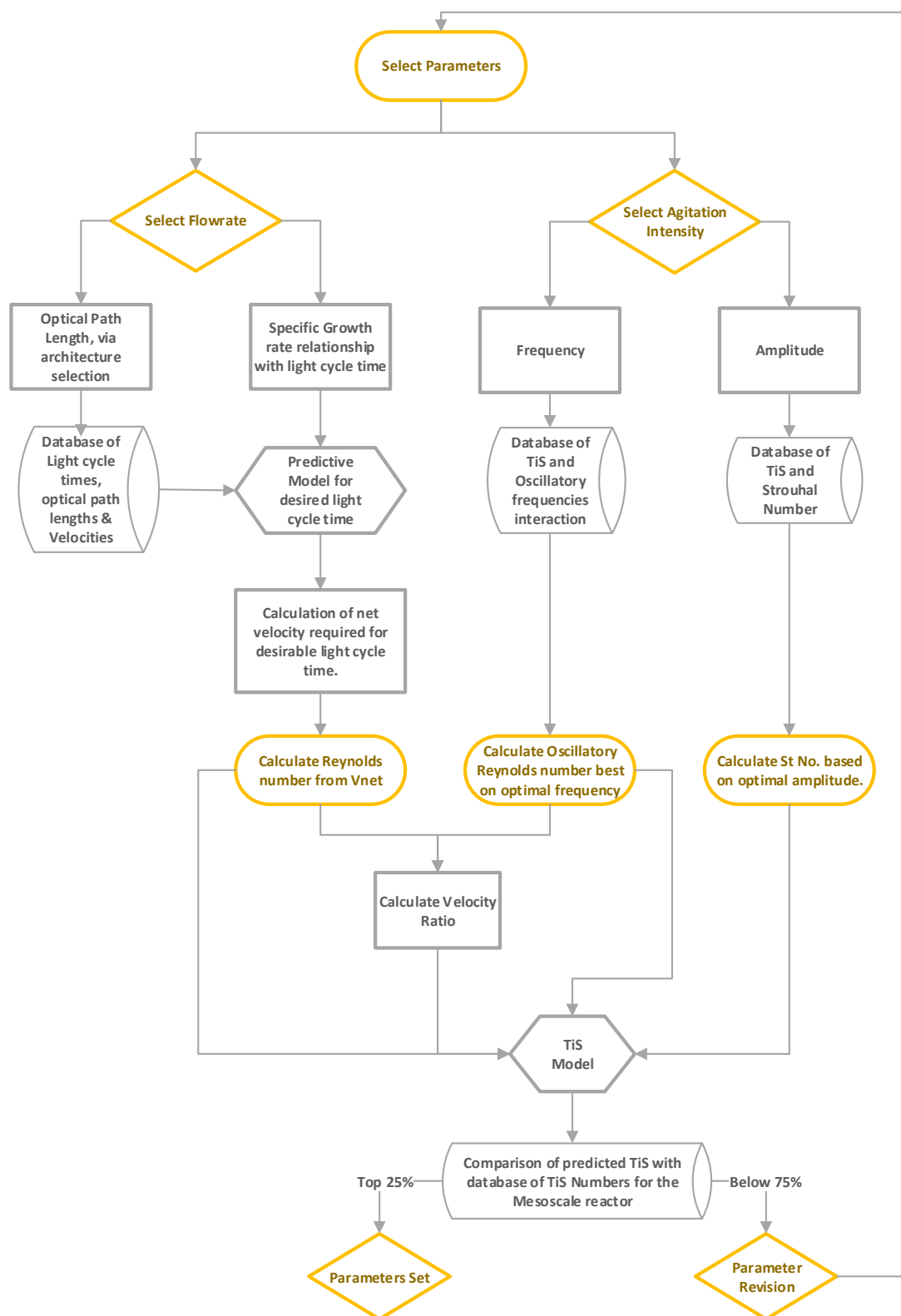
Figure 5-33: Methodology of selecting the optimal parameters for the reactor

5.7 Results and discussion.

5.7.1 Batch Cultivation in the C-OBpbR

The reactor was inoculated with an aliquot of *C.vulgaris* at a cellular density of 4 10^7 cells/ml. As a batch procedure the contents of the reactors were left circulate until the stationary phase was achieved. At that point the contents were emptied, and the reactor was re-inoculated with the same density aliquot of *C.vulgaris,* where the reactor was left to operate with only the net flow pump. The growth timeline, shown in Figure 5-35 depicts the two experiments in chronological order.

It is evident at first glance that the performance with the oscillatory mechanism is better than with mixing caused by net flow. With the oscillatory mechanism enabled, using BBM as the media with no carbon enrichment, the *C.vulgaris* culture grew from 2.50 $x10^5$ to 1.18 $x10^8$ cells/ml in 9 days, producing 0.05 g/l/d of biomass. On the other hand, without an oscillatory motion, with agitation provided merely by 3ml/min flowrate, the algae demonstrated evident lagging, with no evident change between growth phases, which indicated that there is some limitation in the system. In the first 10 days, the culture reached a cellular concentration of 5.8 x 10^7 cell/ml from an initial 1.90 x 10^7 cells/ml. With a biomass productivity of 0.025 g/l/d. Table 5-18 summarises the results of the experiments.

Table 5-18 Comparison of algal growth metrics with and without the oscillatory mechanism in batch cultivation.

	Specific Growth Rate (μ)	Doubling Rate (t_d)	P_x (g/l/d)	Cultivation time (Days)
With Oscillatory Flow	0.43	1.61	0.05	10
Without Oscillatory Flow	0.05	13.86	0.025	22
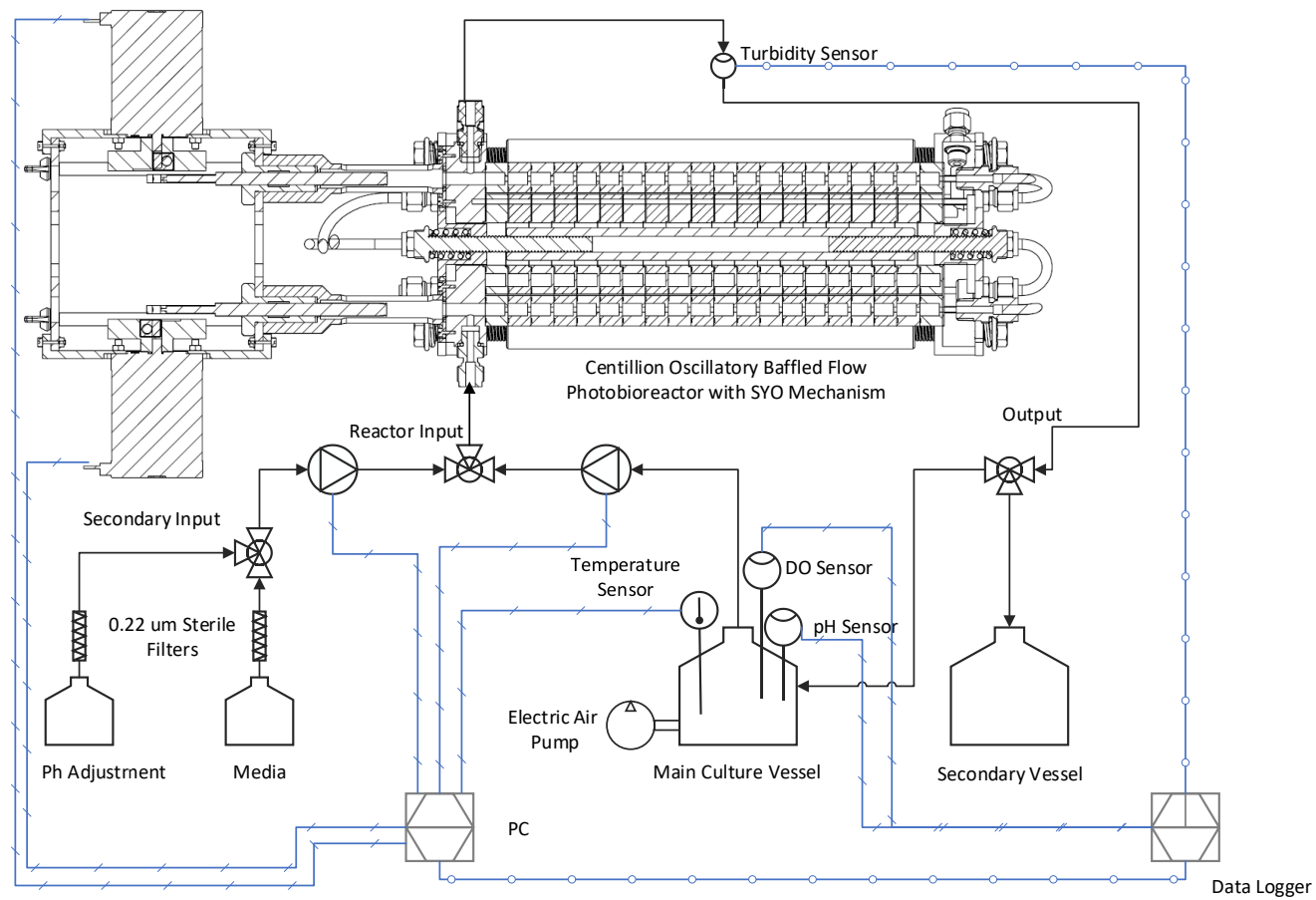
Figure 5-34 Cam Oscillatory Mechanism (COM) reactor system configuration.
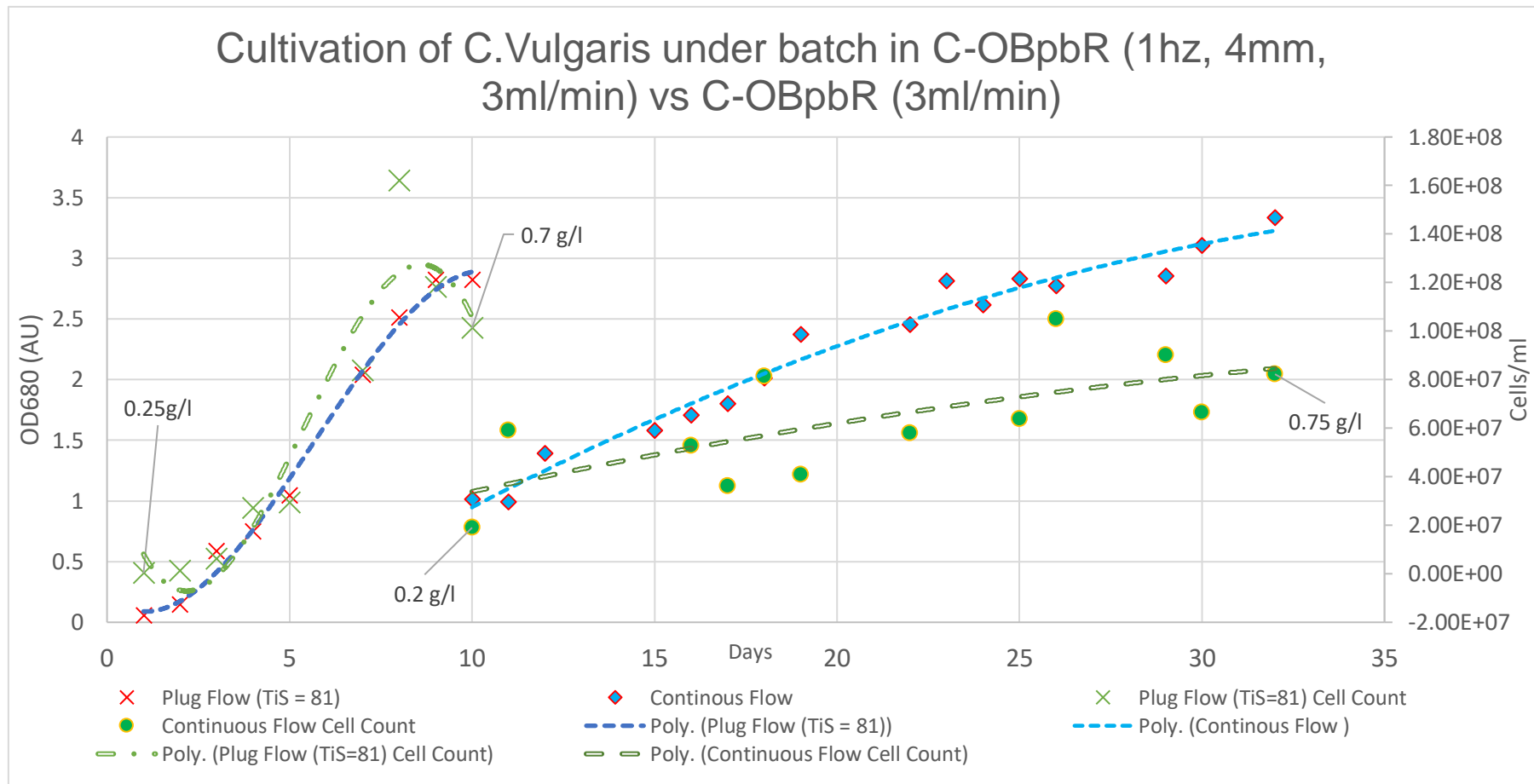
Figure 5-35:Oscillatory flow conditions vs non-oscillatory flow in the cultivation of C.vulgaris : OD680nm & Cellular Concentration vs days

5.7.2 Semi-Continuous Cultivation in the C-OBpbR

In the semi-continuous cultivation mode, the inoculated system is sub cultured multiple times, by the addition of media, and the subsequent removal of material, so that the culture returns to its starting concentration, similar to the methodology proposed by Khoo, Lam and Lee (2016) (Khoo, Lam and Lee, 2016) Using this methodology, the reactor operated for a total of 66 days continuously without fail. The first 22 days the reactor was cultivated using BBM and carbon supplied via aeration in the vessel, similar to a conventional tubular reactor. For the subsequent 44 days the algae were cultivated in the reactor using the Centillion optimised media (CV6). The purpose of the experiment was to monitor the reactor's effect on algal growth, as well as the performance of the media in dynamic conditions, such as those found in the reactor. The resulting timeline graphs of optical density, biomass concentration, pH and cellular concentration, along with a table of the growth metrics are shown in Figure 5-38, Figure 5-39, Figure 5-40, Figure 5-41 and Table 5-19.

From a design perspective the oscillatory mechanism performed uninterrupted for the duration of the experimental period, plus an additional 14 days prior which were carried out to acclimatise the algae to the new environment. From a process perspective the operation of the reactor, required minimal maintenance and oversight. Over the course of 66 days it required 30 minutes a week of allocated time to carry out sampling and sub culturing routines (including the logging and analysis of data). The 66 days experiment duration allowed for an insight into the fouling of the reactor. It was evident that all wetted areas of the reactor under oscillatory flow regime did not suffer any fouling or biofilm formation of any kind, which is a key outcome, Unlike areas such as the tubing before and after the peristaltic pump and on the outlet of the system. This infers that the reactor's internal walls did not suffer any reduction in transparency. In terms of preventing contamination, which according to Doran (2013) is a crucial reactor design consideration, the reactor maintained a sterile environment (Doran, 2013). All physical assembly and contact surfaces as well as the protocols and operational methodologies developed, demonstrated their ability to maintain a contaminant

free environment in long term cultivations on a generic bench top in a laboratory. Similarly, the performance of the online analytical tools, (pH, Turbidity and DO sensor), operated as expected with most of the values validated from simultaneous at line measurements. Specifically, the dissolved oxygen in both occasions was recorded to vary between $6.6×10^{-3}$ g/l, and $8×10^{-3}$ g/l for the cultivation in semi continuous with BBM, and $7.7×10^{-3}$ - $9.1×10^{-3}$ g/l in semi continuous mode with CM media, both of which are below the $25×10^{-3}$ g/l limitation suggested by Placzek, Patyna and Wiczak (2017).

From a cultivation perspective, during the first 22 days, the *C.vulgaris* culture was cultivated with BBM media, the average growth rate was recorded at 0.07 with a duplication rate t_d of 9.8 days. During the following 44 days the average growth was reduced to 0.046 with a duplication rate of 14.7 days. Comparing the final cellular concentrations, with the specific growth rate, as well as the final biomass productivity for each of the subcultures, the two metrics do not follow the same trend.

According Figure 5-37 the specific growth rate is compared to the final biomass concentrations, it is demonstrated that concerning the latter, the centillion media performs consistently better by achieving significantly higher cell concentrations. The same trend is observed when comparing final biomass concentration and productivity for each of the cultivation cycles (Figure 5-36), where the final biomass yield and biomass productivity exhibits a declining trend for the BBM, whereas an increasing trend is obvious for both metrics for the CM subcultures. In addition to that, similar the cellular concentration trends, the biomass densities and productivities are consistently higher for the CM than with the BBM.
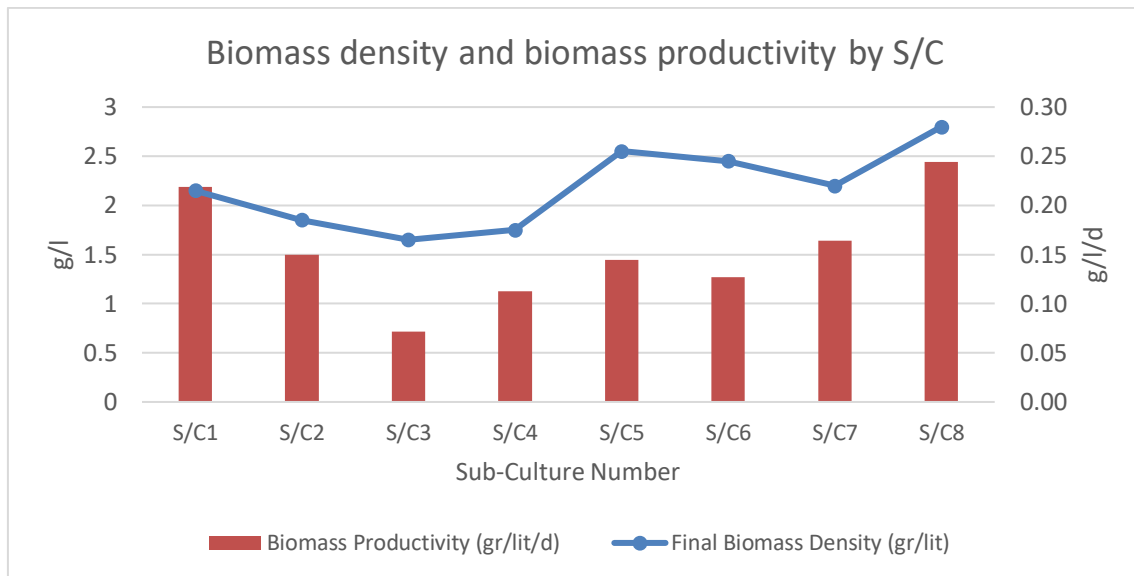
Figure 5-36: Final Biomass density compared to biomass productivity per day, by S/C
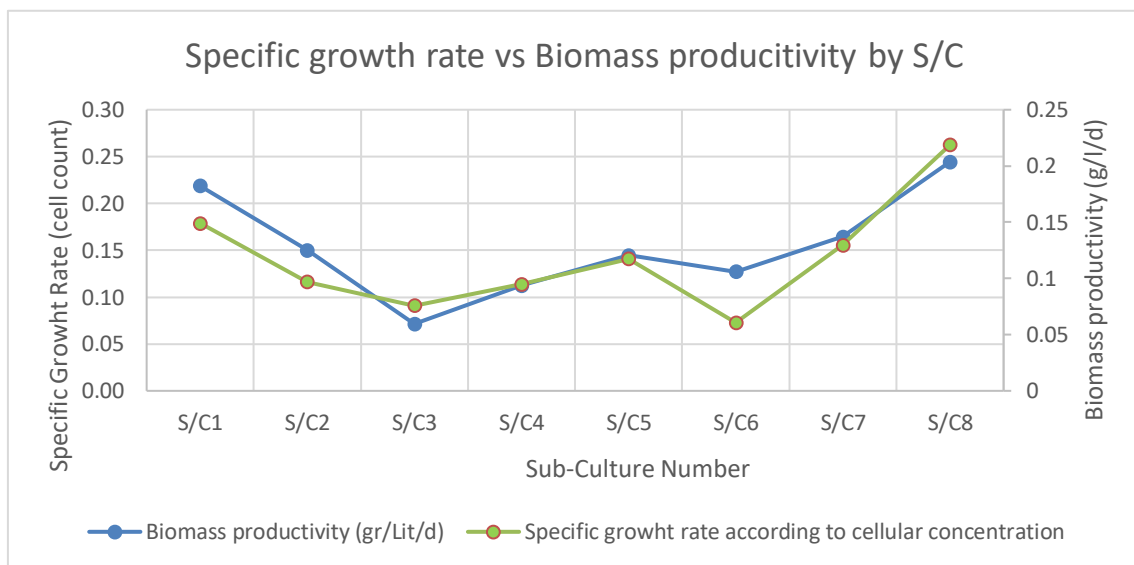
Figure 5-37: Comparison of the growth rate derived by the cell counting, versus the biomass productivity (Px).
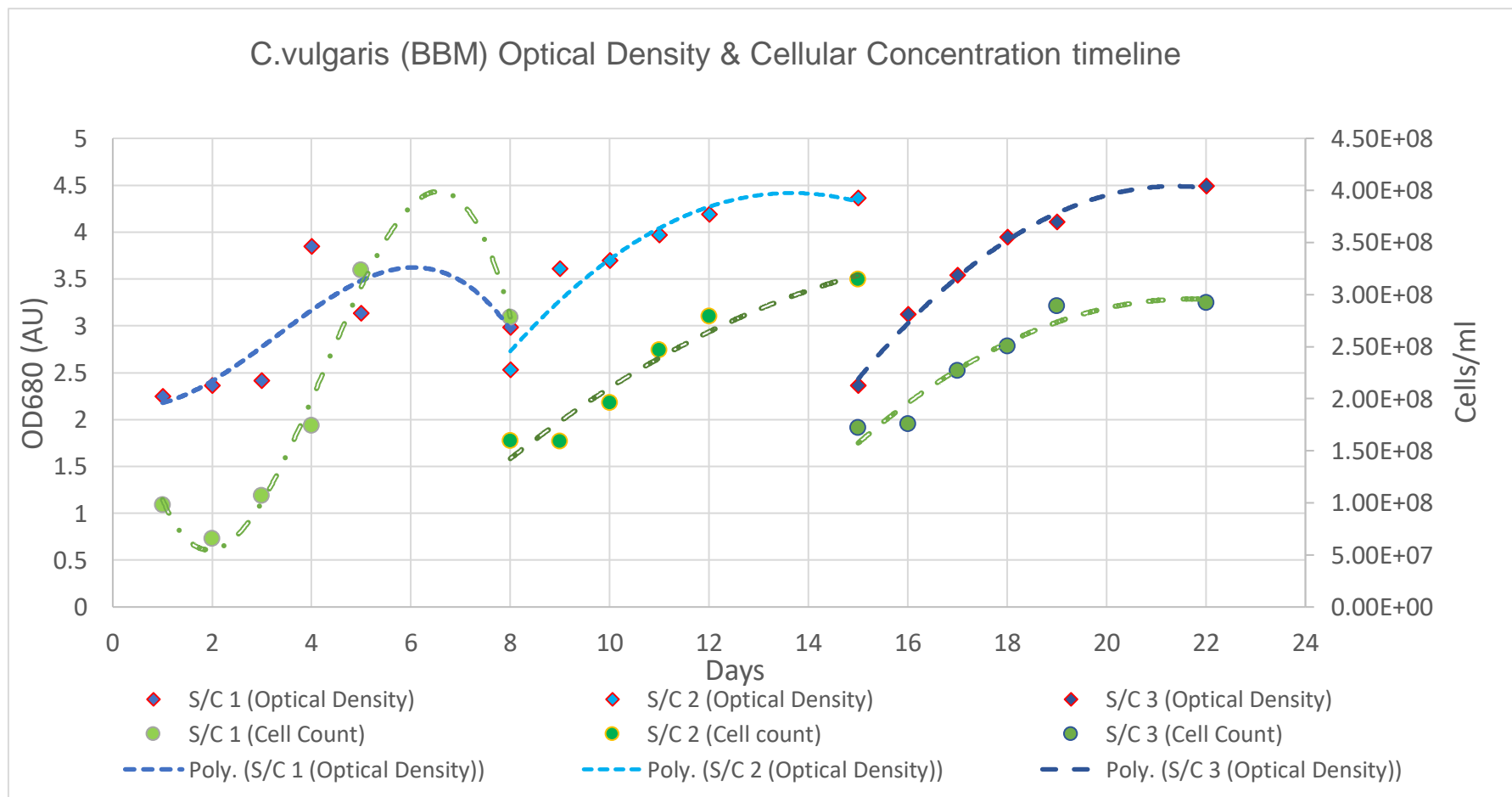
Figure 5-38 C.Vulgaris Growth time lime using Bold Basal Media. Optical density (680nm) and Cellular Concentration vs time.
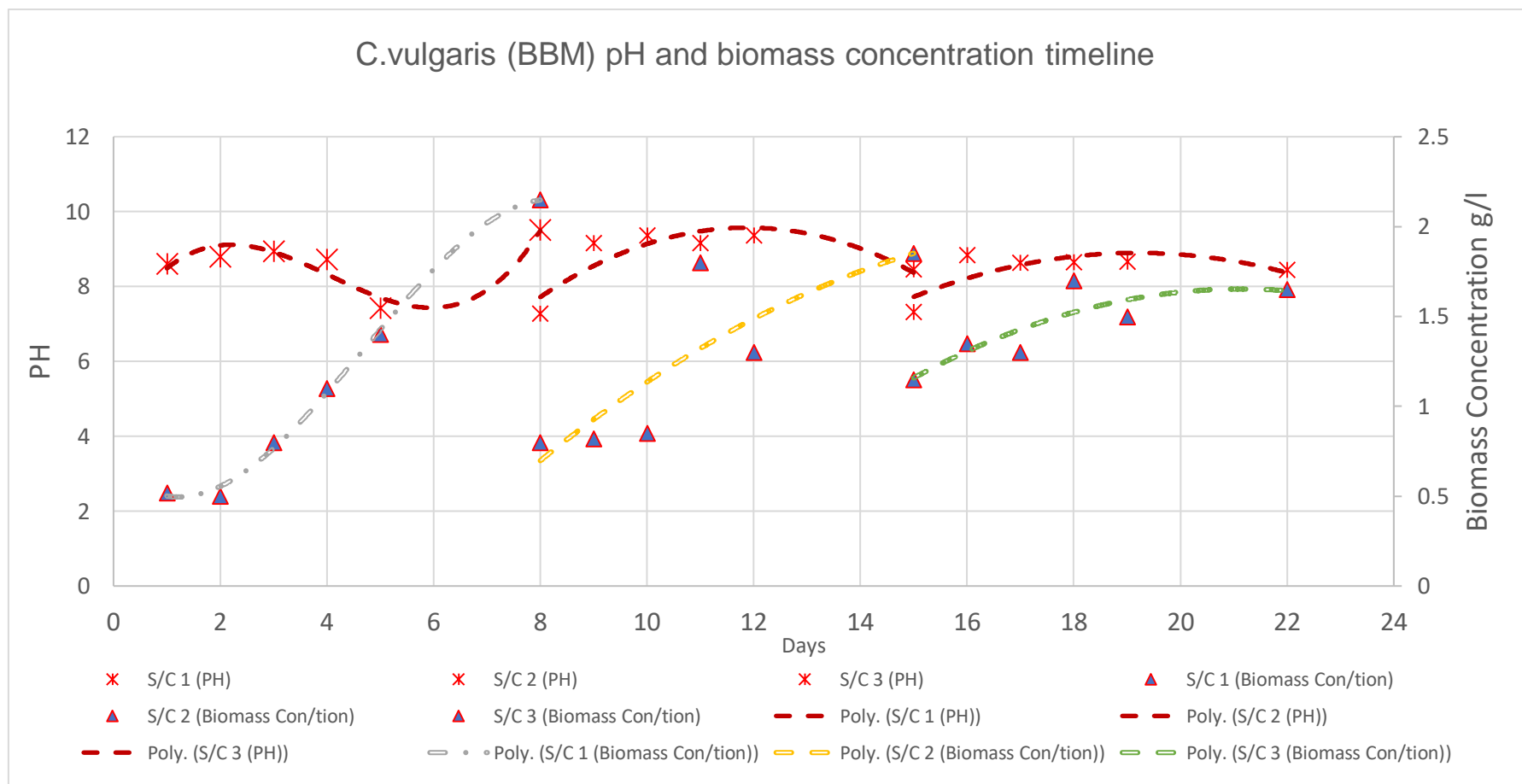
Figure 5-39 C.Vulgaris Growth time line, using Bold Basal Media. pH and Biomass density vs time.
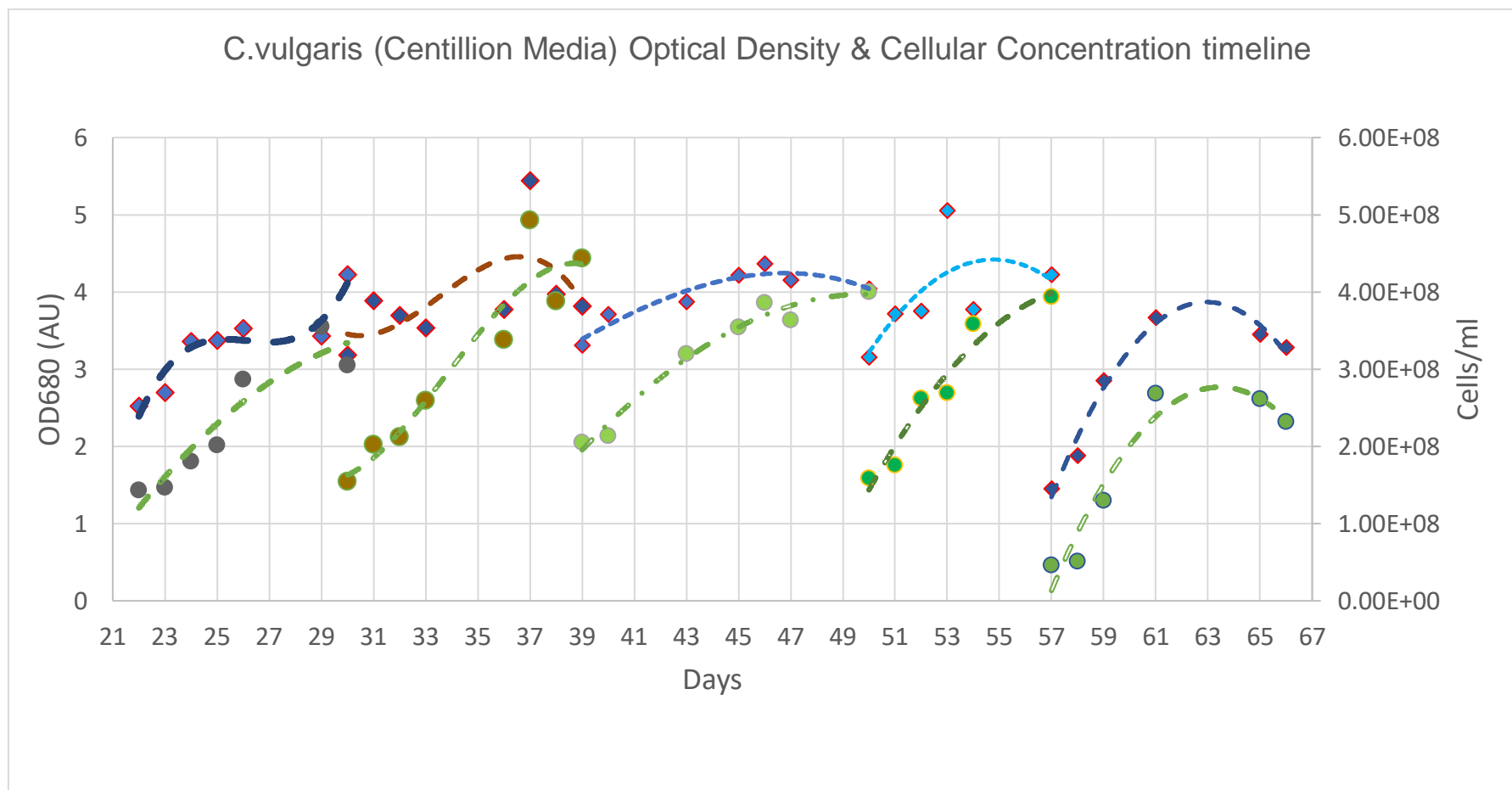
Figure 5-40: C.vulgaris growth timeline, using Centillion optimised media . Optical density (680nm) and Cellular Concentration vs time. (Diamond marker and blue solid dashed line indicate Optical Density, Round marker and hollow dashed line indicate Cellular density).
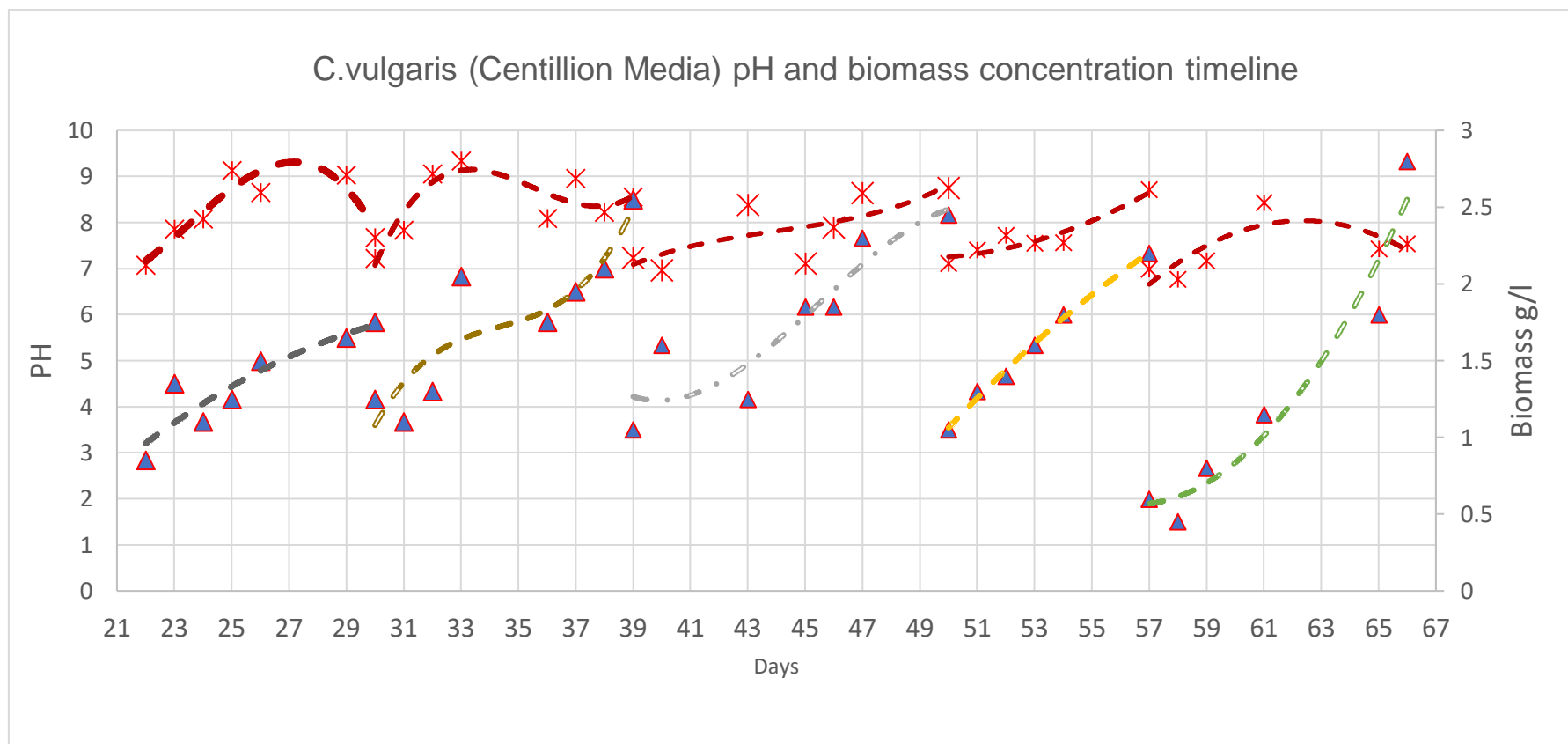
Figure 5-41 C.vulgaris growth timeline, using Centillion optimised media. pH and biomass density vs time. (Red star marker and red solid dashed line indicate ph, Blue triangle marker and hollow dashed line indicate biomass density

Table 5-19 C-OBpbR reactor Performance metrics with BBM and Centillion Optimised Media.

	BB Media			Centillion Media				
S/C No.(Cultivation Cycle)	S/C1	S/C2	S/C3	S/C4	S/C5	S/C6	S/C7	S/C8
Specific Growth Rate (μ)	0.04	0.07	0.09	0.06	0.01	0.018	0.041	0.090
Duplication Rate (td)	17.0	8.8	7.5	10.7	34.7	38.0	16.6	7.6
Px (g/l/d)	0.21	0.15	0.07	0.11	0.14	0.12	0.16	0.24
Final Cell count (cells/ml)	2.78E+08	3.14E+08	2.92E+08	3.05E+08	4.44E+08	4.00E+08	4.63E+07	2.32E+08
Final Biomass Concentration (g/l)	2.15	1.85	1.65	1.75	2.55	2.45	2.2	2.8

5.7.1 Discussion

Experiments were carried out in BBM to compare the performance between the systems, as well as comparing the performance of the CM formulation in a dynamic environment. As is evident in Figure 5-42, the C-OBpbR configuration performed better than all techniques in comparison. The C-OBpbR system consistently enabled the *C.vulgaris* to grow at faster rate and high productivities. In fact, comparing the 1st sub culture of the SYOM system with the no-oscillation experiment, shows that the oscillatory regime achieves a 237% increase in final cellular concentration in under half the duration. In comparison with a comparable bubble column of equal total volume, under identical light conditions using intermittent light of the same duration and intensity, it achieved 72% increase 6 days in advance.

Specifically looking at the batch system performance, with the oscillatory mechanism operating, the performance is evidently better than without. On the other hand, the batch system performed worse than the control experiment. Although the bubble column rig failed to accelerate growth compared to the batch growth system, it achieved a final cellular concentration 73% higher.

The CM demonstrated a marginal performance increase when cultivating *C.vulgaris* in the C-OBpbR running in semi-continuous cultivation. As is suggested from Figure 5-43 Figure 5-44, the growth curve between BBM and CM had a similar trend in the first 4 days, whereas in the end of the exponential growth phase the CM consistently picks up and overtakes the BBM performing up to 64% better cellular concentration in the same amount of days.

In contrast the biomass densities and productivity trend achieved between BBM and CM do not differ much. The biomass densities ranged between 1.65 and 2.8 g/l in 8-10 days of cultivation. On the other hand, the clear benefit with using CM is the cost of biomass production.
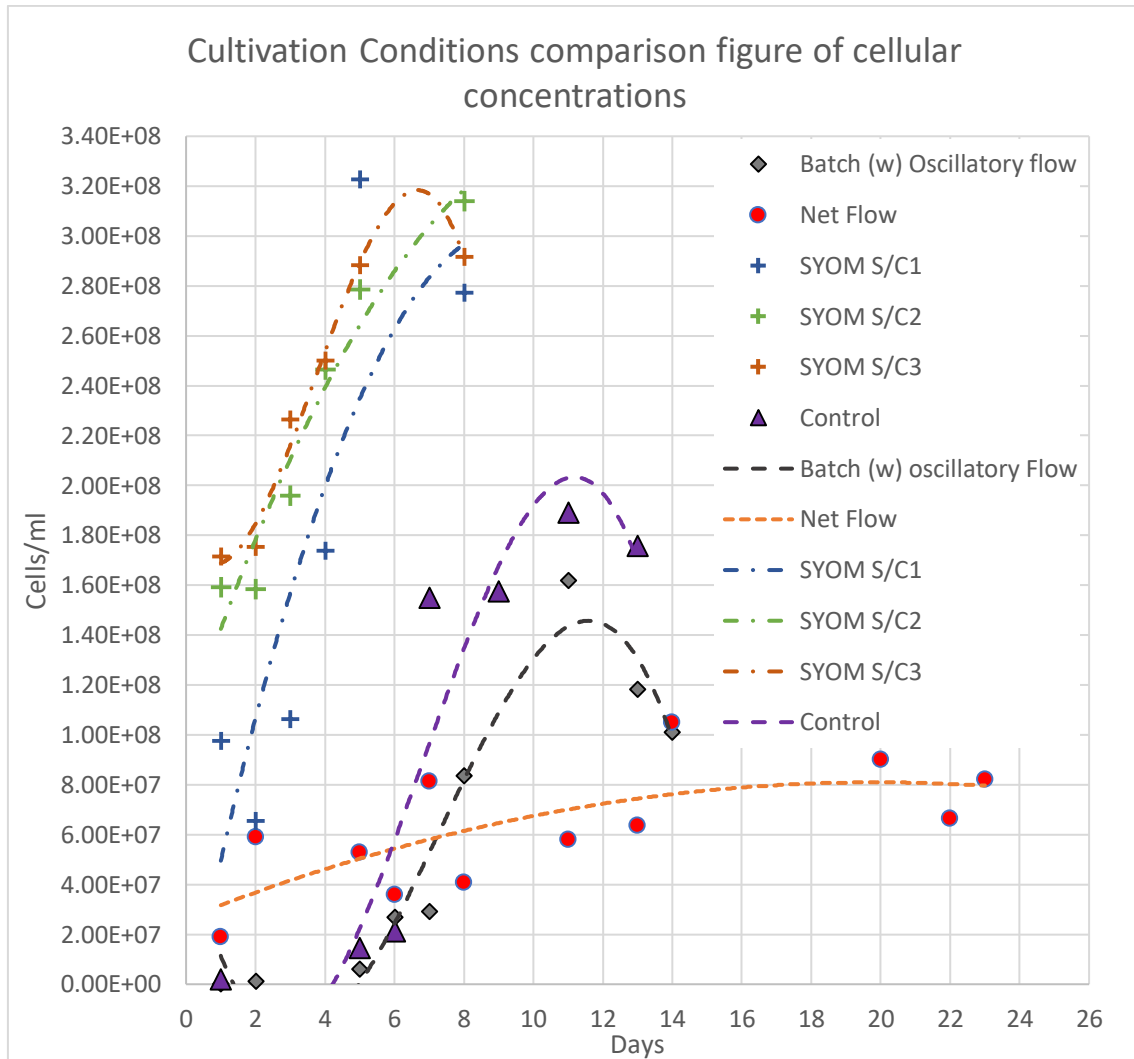
Figure 5-42 Cellular Concentration Timeline comparison between COM & SYOM systems, with No Oscillation and Control Experiments
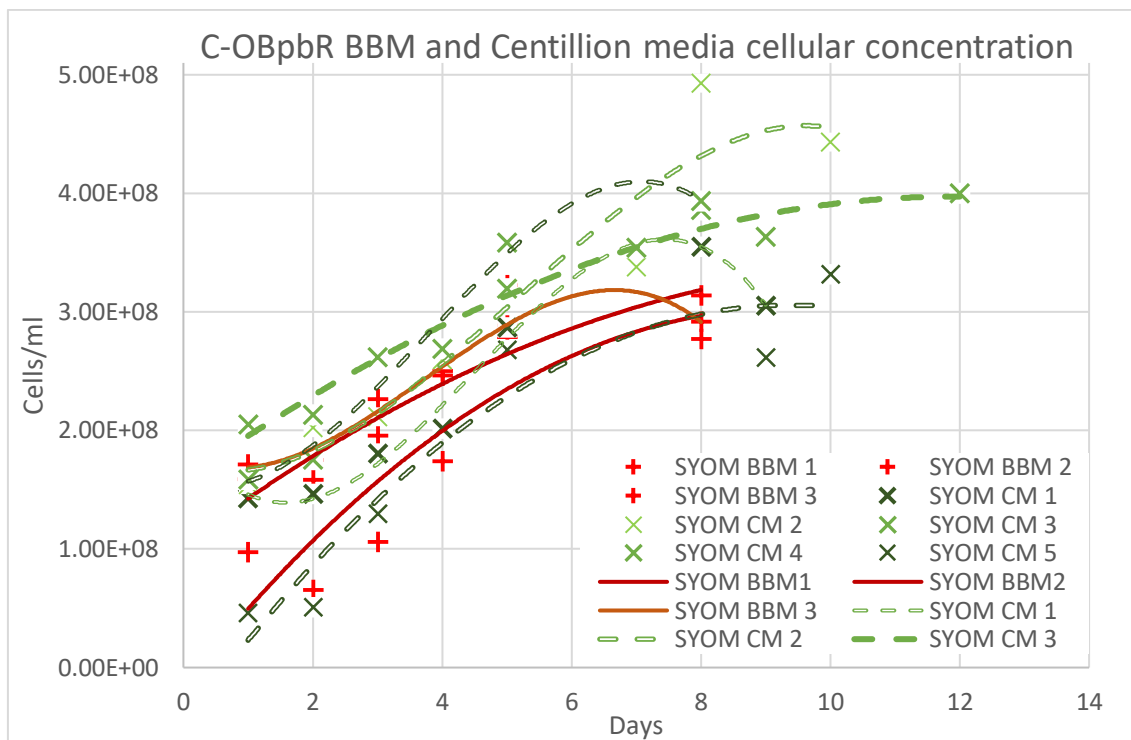
Figure 5-43 SYOM system comparative media performance figure. Cellular concentration timeline for subcultures with BBM and CM formulations.
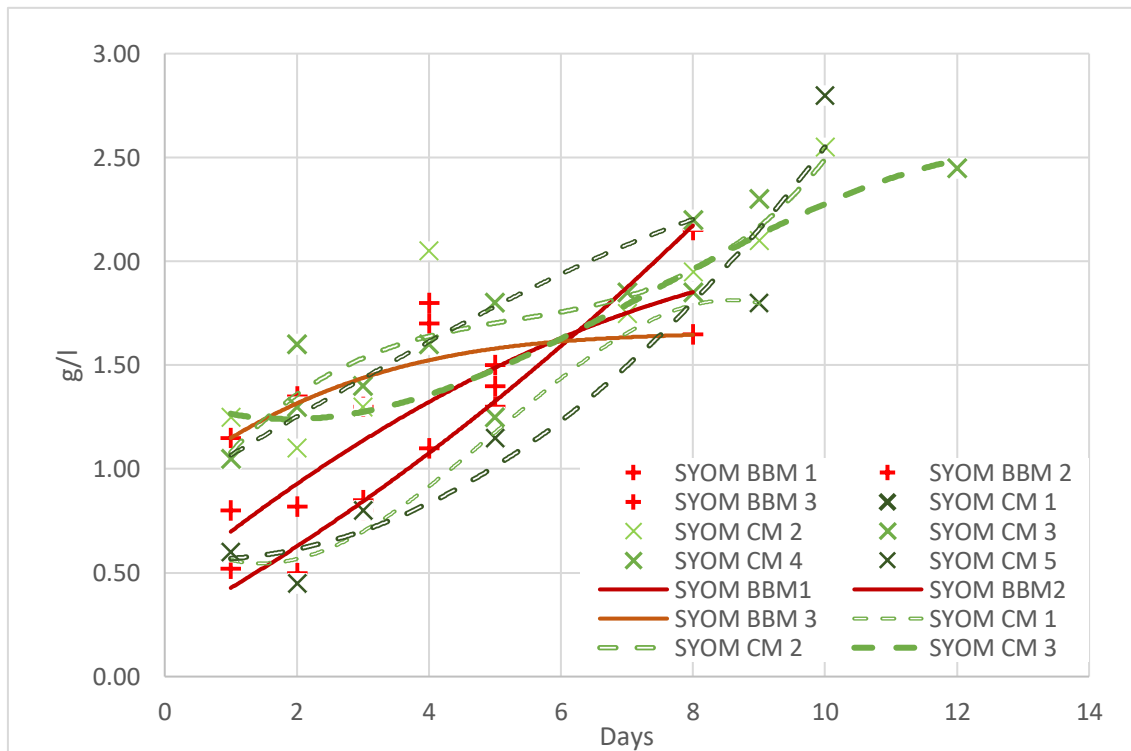
Figure 5-44 SYOM system comparative media performance figure. Biomass productivities timeline for subcultures with BBM and CM formulations.

Figure 5-45 demonstrates the clear benefit to using CM against BBM. The cost of using CM is over an order of magnitude lower than the cost of using BBM. Which is translated to a cost per unit biomass of 0.0018-0.0020 £/g in comparison to BBM which is 0.022-0.028 £/g in the oscillatory baffled flow photobioreactor.

In section 4.3, the cost per unit biomass of CM was reported as 0.3 p/g in conventional Erlenmeyer flasks, comparing this with the SYOM system the cost benefit is 34%. This translates to a price per kilogram biomass of 3£/kg for the Erlenmeyer flask bubble system compared to 1.8£/kg in C-OBpbR.
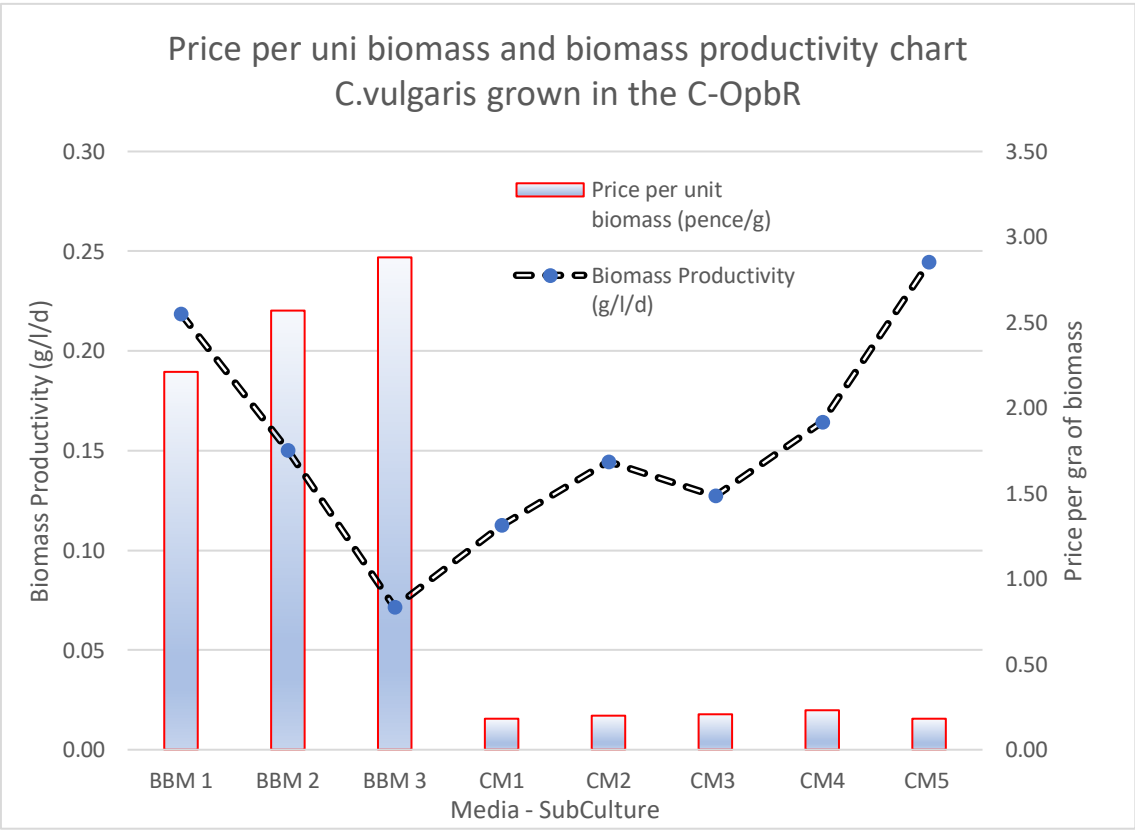
Figure 5-45: Cost per Unit biomass and the biomass density for each of the SYOM Subcultures made with BBM and CM.

The Centillion OBpbR successfully carried out batch and semi-continuous cultivation strategies. Regardless of the performance of each media, the C-OBpbR cultivating *C.vulgaris* achieved growth rates that are comparable and even surpass those in literature. In comparison with Liang et. al (2009), the performance of *C.vulgaris* under comparable heterotrophic conditions was approximately 0.25g/l in 6 days, whereas under addition of glucose this value rose to 0.72g/l at a rate of 0.102 g/l/d, under 2% or glucose dose (v/v), C-OBpbR the values achieved were 1.65 2.15 g/l under identical amount of t and 2.2-2.8 g/l with comparable glycerol addition. (Liang, Sarkany and Cui, 2009). At similar scales comparing he cultivation with one carried out on the same species *C.vulgaris* from exactly the same strain CCAP 211/11B, Rodolfi et al (2009), achieved productivities between 0.17-0.2g/l/d. Comparing these to both the BBM and CM experiments in the C-OBpbR it is found that the experiments under CM and semi-continuous regime to surpass these by 0.04g/l/d (Rodolfi *et al.*, 2009).

In addition to the growth metrics, the C-OBpbR performance as a system was also assessed, on the basis of sterility, maintaining uniform growth and in terms of usability. First, the system was successful in maintaining a sterile environment, even with the addition of organic carbon (glycerol), which is a food source of many eukaryotic predators. Secondly, during all cultivation cycles in the C-OBpbR no sudden fluctuations pH (7-9) fluctuations occurred, which indicated that the system was balanced. Finally, in terms of usability, the system did not require supervision and maintenance was zero in the 91 plus days of continuous operation during cleaning acclimation and experimental cycles. Overall the performance of algal bioprocessing in semi-continuous performed exceedingly well for the prototype.

In comparing the performance of the reactor system to comparable systems, the results suggest that the Centillion OBpbR system systematically enables faster growth rates and higher biomass concentrations to the achieved.

Figure 5-46 (left) Labfor 5 Lux system. (Right) Rendering of the Centillion C-OBpbR benchtop system concept. (Labfor, 2018).

The Centillion reactor is one of its kind. There is to this date no commercially available system that utilises oscillatory flow for mixing in algal biotechnology. Commercial examples of benchtop algal cultivators are uncommon. Examples of such systems are similar to the Labfor 5 Lux photobioreactor unit.

All systems above share the following operational benefits in common, they utilise bubbling columns with integrated external illumination capability, on board aeration and circulation potential with a pump, online monitoring and automated perfusion capability, meaning that they can operate in semi-continuous mode. Therefore, no other engineering novelty is offered in the design of the reactor. In addition to this, all systems are scale restricted, with major differences between variants in different scales. Therefore the novelty of the Centillion OBpbR system, could have great commercial appeal, since it is novel, in both engineering terms and in system design, it can handle downstream purification, offers internal and external illumination, temperature control, onboard dosing pumps, autotrophic and mixotrophic cultivation capability, reduced fouling and from a bioprocess perspective, multiscale reactor systems which can be placed in series, carrying out sequential bioprocessing operations.
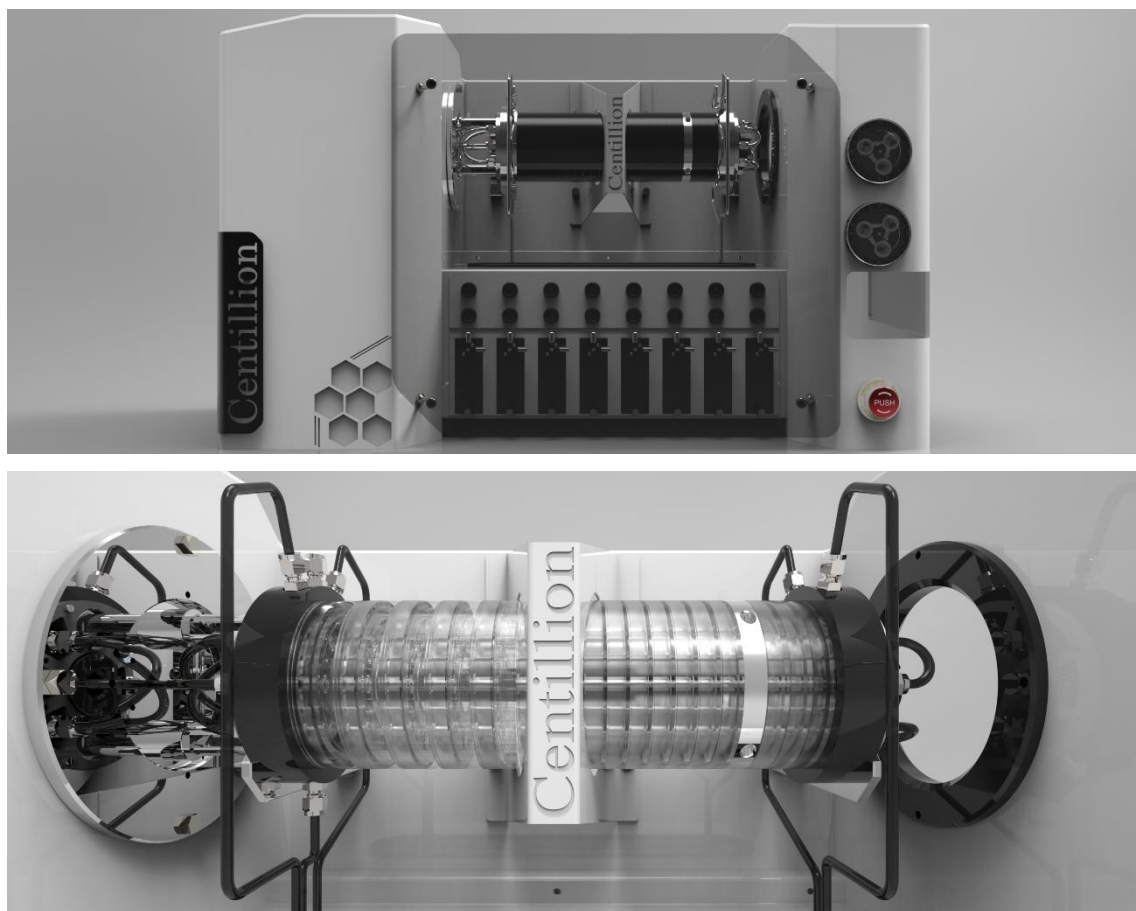
Figure 5-47 Photorealistic rendering of the Meso-Scale Centillion C-OBpbR system, encased in an open frame, complete with fixed pipe architecture, dosing and circulation pumps.(Below) closeup to the all glass reactor system.

6 Scale up

In algal research, scale up is considered a crucial step in making algae derived products viable and competitive in the market. As highlighted by Yeo et al.(2018), most of algal research into light, mass and heat transfer, nutrient delivery and cost, is typically conducted in small scale PBRs (Yeo *et al.*, 2018). In addition as cited by Reis and Da Silva (2016) after surveying publications spanning a decade, found a recurring trend; that large biomass yields at laboratory level, were systematically not achieved in outdoor full-scale culture units (Reis and Da Silva, 2016). The reason for this suggests that algal growth requirements and consistently underestimated at large scale (Reis and Da Silva, 2016). This is supported by the fact that no current PBR has been specifically designed for scale. Oscillatory baffled flow reactors on the other hand, are specifically designed with scaleup in mind.

There are no industrial nor pilot scale OBRs implemented in algal biotechnology. The Centillion Oscillatory Baffled flow reactor (C-OBpbR) has demonstrated good performance at cultivating algae in meso-scales. Therefore, scaling the C-OBpbR would determine whether OBR technology can be a viable and sustainable alternative for large scale industrial applications of algal bioprocessing. Thus, demonstrating evidence for the third objective of the thesis.

6.1 Scaling Rationale

There are three scales in the development of bioprocesses, laboratory (bench), pilot plant, and plant (industrial). In conventional bioprocessing lab scale is where screening experiments are conducted, pilot scale establishes the process parameters, and industrial scale is where economic fruition is achieved. (Ju and Chase, 1992). Although a universally applied scaling strategy does not exist, it is normal for a scaling criterion (process or physical characteristic kept constant) to be adopted to ensure a measure of similarity. Ju and Chase (1992) suggest a list of criteria which are the reactor geometry, oxygen transfer coefficient ($K_L a$), shear stress, power input per volume of liquid (P_g/V), volumetric gas flowrate

(Q/V), Superficial gas velocity (v_s), mixing time, impeller speed, or impeller Reynolds number (Re) and finally momentum factor (Ju and Chase, 1992).

Care must be taken when selecting an appropriate parameter to keep constant since it may lead to impractical solutions. For example, as cited by Plumb (2005), in scaling up to 10000 L from 100L, Oldshue (1985) discovered than when maintaining a constant blend time or a constant power per unit volume, in a non-geometric scale up would result in inhibitory power consumption approximately 50 and 10 times higher than in pilot. On the other hand, scaling to a constant tip speed would result in the lowest power consumption but also a suboptimal reaction profile, with increased reaction time (Plumb, 2005). It is common practice in bioprocessing of aerobic organisms to scale according to power per unit liquid volume and volumetric gas flow. These are typically selected since organisms are typically shear sensitive.

On the other hand, continuous OBR technology is readily scalable. As has been shown by numerous studies, most notably by Oliva et al., (2018), Smith and Mackley (2006) and Stonestreet and Harvey (2002).As has been reported, geometrical upscaling of the design features, accompanied by scaling of the process parameters whilst keeping the dimensionless numbers constant is a viable pathway for scaling an OBR

The Centillion chemical OBR has been scaled up from a micro (4mm) to meso (8mm) to kilo scale (22mm). Scaling up between those sizes was done by maintaining geometric similarity, meaning that upscaling was carried out based on keeping the diameter and length ratios between baffle and conduit the same. This meant that by keeping the same nondimensional numbers constant (St, Re, Re_o), the same mixing profile could be achieved.

As indicated by Figure 5-23 in section 5.3.2, during the scale up from 4mm to 8mm the TiS numbers followed a similar trend under the same Strouhal numbers, which indicate that scale up under geometrical similarity was achieved. Therefore, the same rationale will be adopted for scaling from meso to pilot scale.

Unlike scaling up for chemical applications, scaling the Centillion to act as a photobioreactor, engages with more critical considerations than those associated with the scale up criteria, therefore in addition to the selection of an appropriate size, consideration of all process characteristics is also required.

6.2 Scaling up the C-OBpbR

For the scale up of the reactor, three potential sizes are considered, the 22mm (A), 36mm (B) and the 51mm (C). Table 6-1 contains useful information on the geometry and volumetric capacity of the disks, the space requirements of potential reactor assemblies and finally the costs associated. Figure 6.1 portrays the complete line up of Centillion reactor scales from micro (4mm) to kilo (51mm).

Table 6-1 Table showing three potential scale up sizes (*machining costs per disk quoted by Cranfield University machine shop Q2 2019, excluding material price).

	Parameter	Lab	Pilot A	Pilot B	Pilot C
&Volumetric parameters	**Baffled Diameter [mm]**	8	22	36	51
	volume per baffle (ml)	0.62	13	57	162
	Volume per disk (ml)	5	104	458	1,302
	Volume per metre (ml)	359	2,715	7,270	14,591
Volumetric & Spatial	**No of disks per metre (unit)**	75	25	15	11
	Reactor Volumetric capacity per m^3 of space (L)	15	56	59	75
	Number of units per m^3	44	23	8	5
Cost	**Machining cost per disk (£)***	*55*	*60*	*91.9*	*160.3*
	price per metre (£)	*4125*	*1500*	*1378.5*	*1763.3*
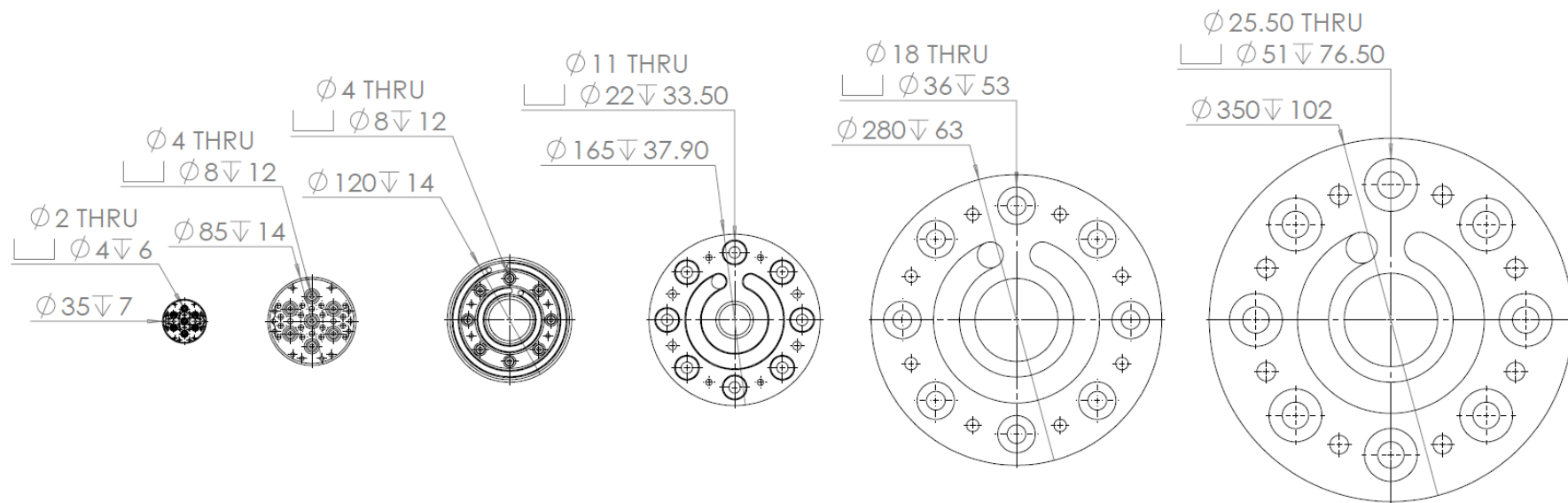
Figure 6-1 Scaling up sequence of the Centillion reactor disk. (Left to right) In ascending size, the microscale and mesoscale reactor disk (1 and 2). The optimised dual heating/cooling loop bioprocessing disk (3) , and the scaled-up version to kilo scale

In order to select a suitable pilot size, Table 6-1 contains useful information for the selection process. The wafer's volumetric capacities and the volumetric spatial requirements of the units follow an increasing trend, with increasing diameter. However, In conjunction with the cost, suggest that there is a decreasing trend up to pilot B option, where it starts to increase for the large scales Figure 6-2. This occurs in spite of increasing disks costs. Therefore, the best option based on price per spatial requirements is the size is 36mm diameter conduit option.
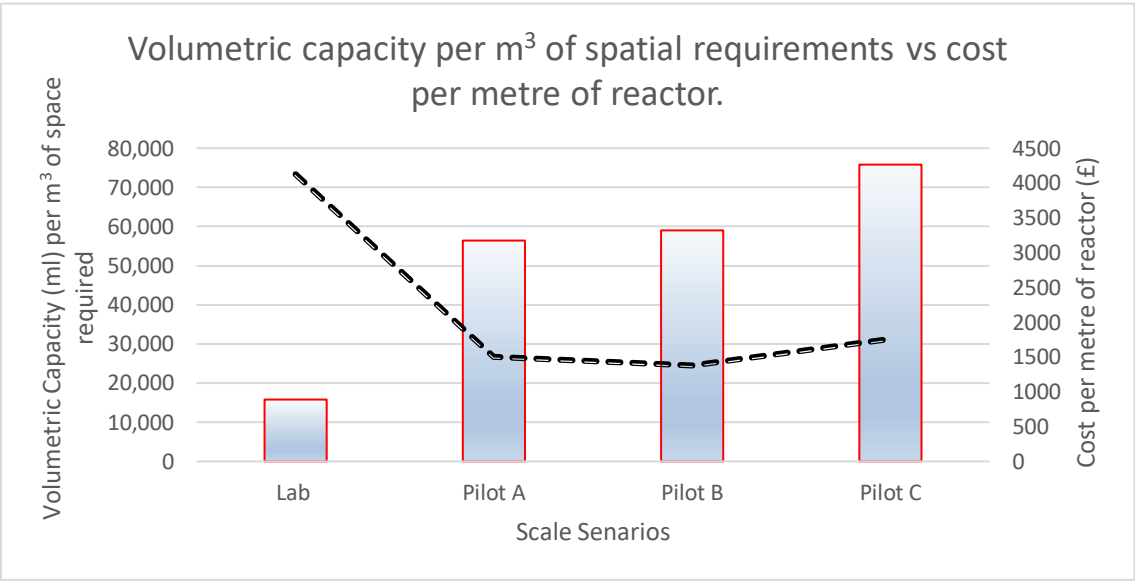
Figure 6-2 Volumetric capacity per m^3 vs cost per meter of reactor according to scale scenario.

6.2.1 Changing the Centillion members shape.
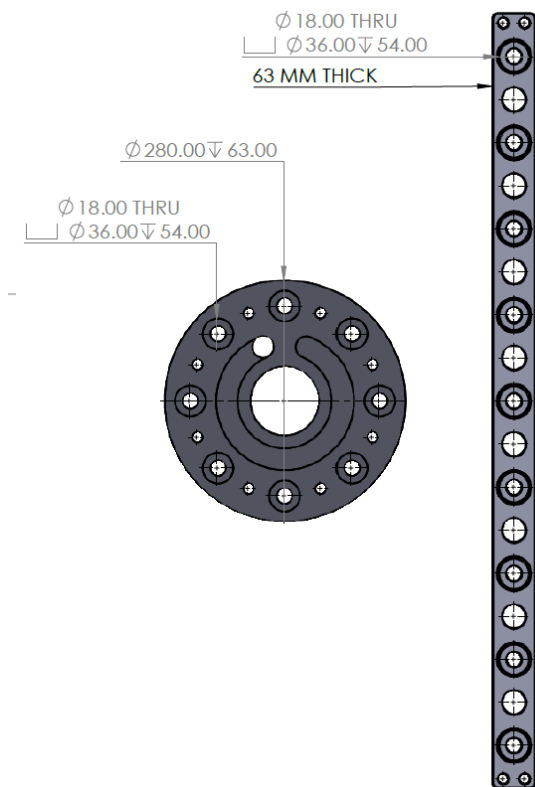
Figure 6-3 The Reshaping of the Centillion Reactor core member from Disk to Rectangular Rod.

From the previous section, Table 6-1 it is evident that one key limitation of direct geometric scale up of the trademark Centillion reactor disk is cost.

In addition to this, design complication with light arrangements and difficulties in sourcing suitable material were catalysts forcing a complete redesign of the member.

At first, a novel conceptual design stimulated by the features of tubular PBRs was developed (7.3F.1). This design introduced the helical tubular oscillatory baffled flow PBR concept, using standard tube sizes, although this is a cost-effective solution, the number of components create complications in assembly and maintenance.

Therefore, drawing inspiration from the advantages of the conceptual design (Appendix G1), as well as the benefits of flat plate photobioreactors, a common ground between functionality and cost lead to the development of an alternative design, which reshapes the member from a disk to a rectangular rod (Figure 6-3).

In the new design, the baffled passages are equispaced along the length of the rod. Large through holes are positioned midpoint, between the baffled holes for compression purposes as well as internal illumination, and 2 sets of registration holes are placed on the top and bottom end of the slice, for inline connection. The key downside of this design is the removal of the heating and cooling functionality.

213

On the other side the cost saving compared to the alternative surpassed the benefit of the temperature control utility.

The member's final design encompasses 9 baffled passages of 36mm (D) and 8mm (d) equispaced 100mm from each other, on a 900x50x63mm rectangular rod. Between the baffled passages lie 8 through holes, 28mm each in diameter, and finally, on either side of the reactor lie two 12 mm diameter location registration holes. The motivation for this design was based on maximising the operational volumetric capacity on a standard off the shelf rectangular block of transparent plastic (Acrylic or Polycarbonate), which is supplied at standard sizes of maximum thickness 50mm and 1000mm length. Considering the baffled conduit diameter, the decision with the Pilot B option, is also encouraged by this change since it is the maximum hole diameter that can comfortably fit and allow space for additional features such as a gasket mounting lips required for sealing the flow passage.

Table 6-2 Rectangular member parameters

Parameters	Rectangular member
Conduit Diameter (D)	36mm
Baffle Diameter (d)	18mm
Conduit Length (L)	54mm
Baffle Length (l)	18mm
Baffled Hole Volume	55 ml
Rectangular member volumetric capacity.	0.5 L
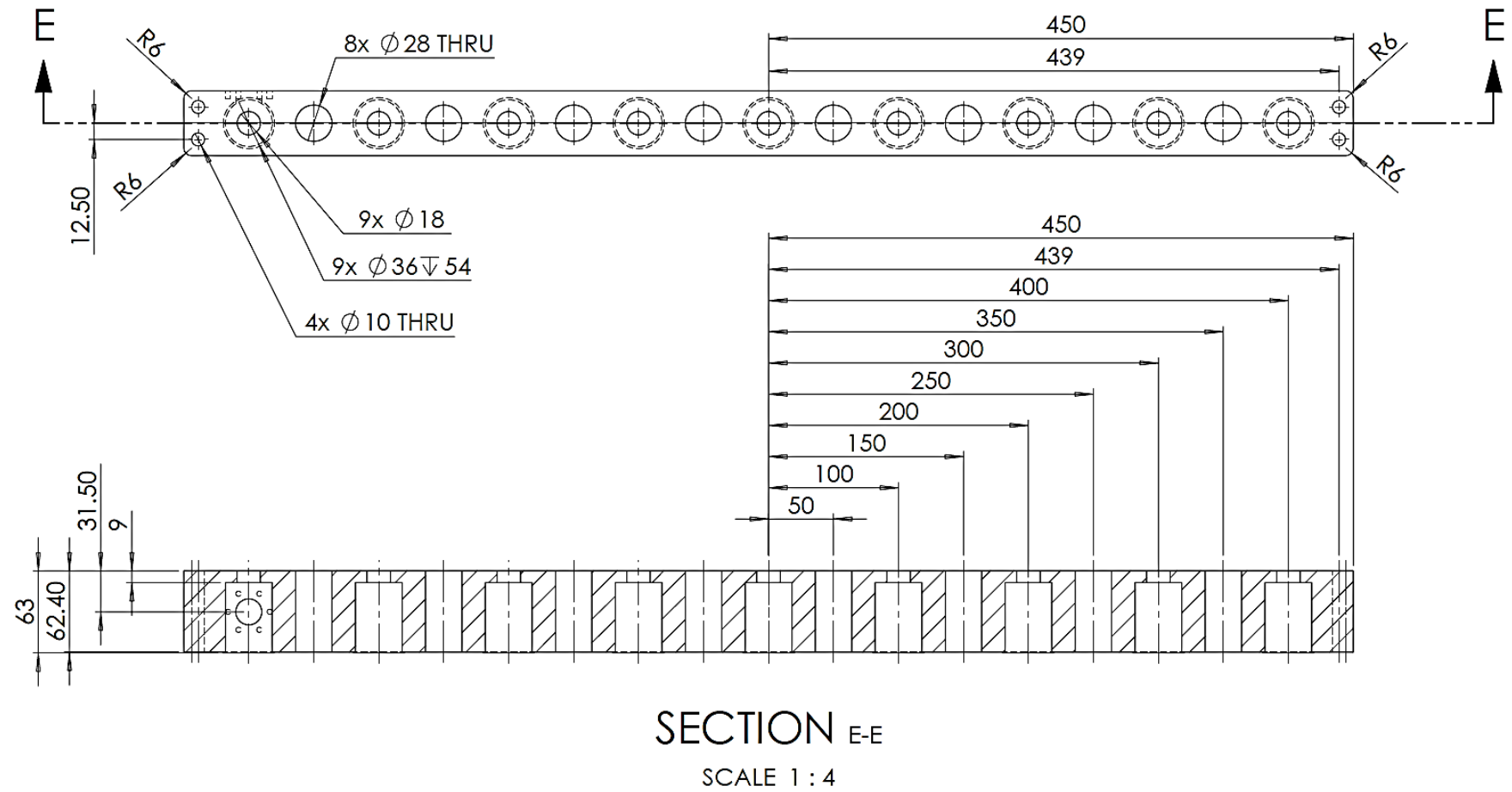
Figure 6-4 Basic Dimensional drawing of the final design of the Centillion Rectangular member

215

Assembly happens along the same lines as the original C-OBpbR. The members are positioned sequentially, forming a fat plate array of tubular passages. In between the members sealing is achieved by the inclusion of a 1mm thick Viton gaskets.. In contrast to the O-rings sealing of the previous design, the transition to gaskets sealing facilitates easier maintenance and assembly.
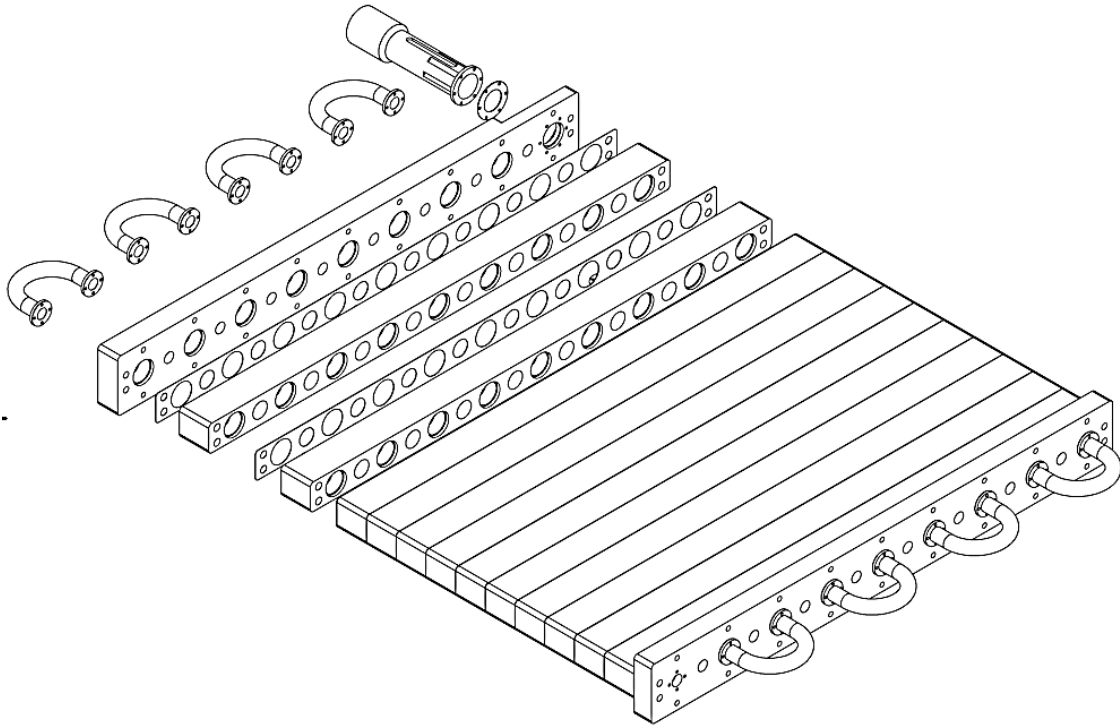
Figure 6-5 Exploded view of basic alignment assembly (Not showing assembly components). Showing the U-bend tubes, the end plates (Compression plates) and oscillatory mechanism plunger housing which connects the mechanism with the reactor, facilitating the oscillatory flow regime.

Similar with the previous design, albeit not highlighted, is the interconnecting unbend, which connects each baffled passage together. The unbend can be constructed identical to the original design, with soft tubing and threaded compression fittings, however the diameter of the tubing should be selected based on it not obstructing the flow and creating pressure fluxes.

Therefore, the u-bend is constructed by 18mm ID reinforced vinyl tubing attached to the reactor with ¾ tail-hose fittings. This however creates additional considerations since the minimum bending radius of soft tubing is critical to the

216

tubing keeping its shape on the apex of the bend. This was considered during the design phase and dictated the number of flow passages since their spacing needed to exceed the minimum bending radium of soft tubing being 50mm, at sizes larger than 3/4' (18mm approximately).

6.2.2 Oscillatory mechanism

Scaling up the reactor, required the scale up of the oscillatory mechanism as well. As mentioned this has been successfully done before, with the SYOM system which has been scaled up to accommodate a 22mm cylindrical disk reactor. In this occasion, there is an additional complication being the redesign and change of the reactor shape. This creates complications. Primarily in securing the unit, and secondly in aligning the mechanism to the reactor. To achieve both robustness and alignment, the mechanism and reactor were mounted on a common frame, where the latter was secured on the frame at points 3 and 4 (Figure 6-6), using M5 Bosch Rexroth 30x30 profile mounting screws. And aligned on the reactor via points 1 and 2 (Figure 6-6), where the reactor and mechanism are aligned via 2 x M10 rods and 1 M18 rod used for compressing the reactor members together.
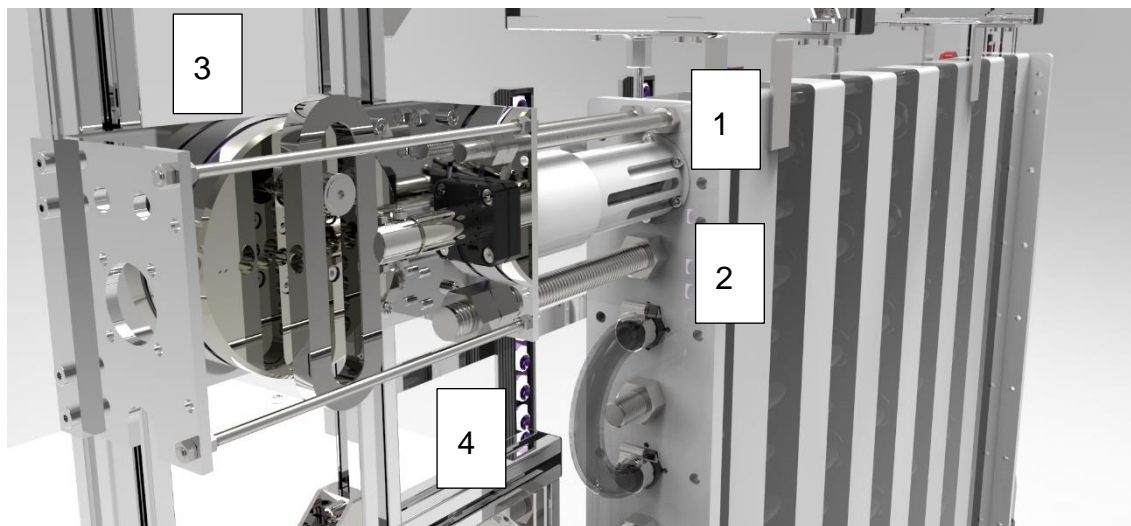
Figure 6-6 Photorealistic rendering of the oscillator mechanism mounted on the reactor and frame. With annotations showing mounting points to both the reactor and frame.

In terms of oscillatory mechanism functionality, the design follows the same philosophy with the SYOM on the mesoscale rector. As shown in Figure 6-7. A motor plate (5) is used to mount the motor and connect the front and rear support plates. A rolling plate is mounted on the motor on one side whist on the other, a M8 OD19mm track roller (1) is used to translate the angular motion of the plate to linear motion on the plunger (4), via the roller link (6) bushing (7) and plunger rod (7). A linear guide bearing (3) is placed in the path of the plunger rod to assist in smooth sinusoidal motion, when the system is aligned and assembled the oscillation of the plunger (4) are transferred to the fluid entering the reactor via port (11) in fluid path (10). The liquid oscillates throughout the reactor until it exits at (12). The opposite can also occur without any hindrance to oscillatory motion, with (12) being the reactor entry and (11) being the exit.

The key difference to the previous design is the amplitude setting method. In the mesoscale SYOM, the amplitude was set by rotating leadscrew CW or CCW, with the roller pin attached to it. In this design due to the larger range in amplitude, the leadscrew was designed with a series of threaded holes, achieving a range of 6 to 40mm in increments of 2mm. This was a more secure option considering the larger volumes of liquid being processed.
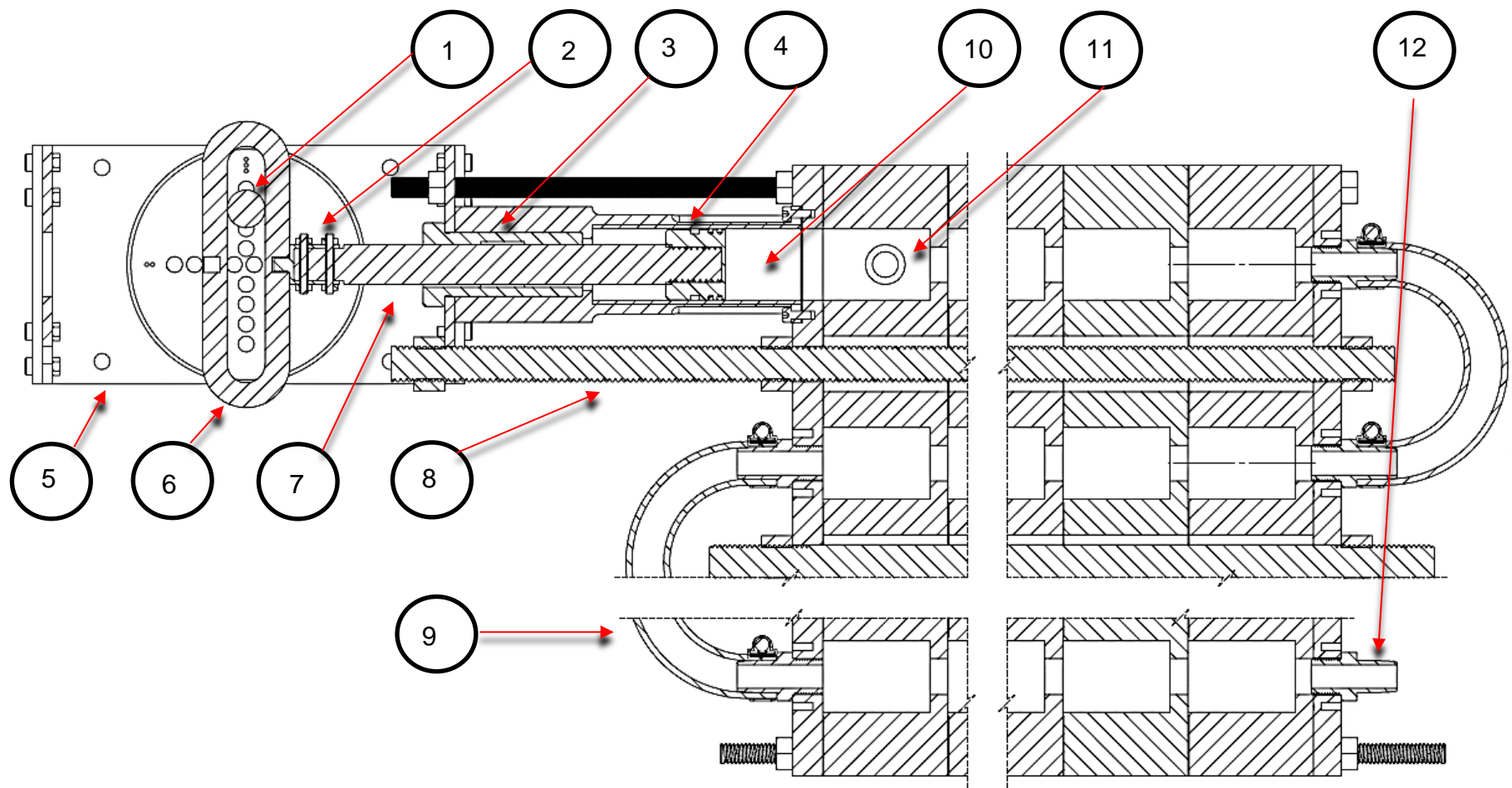
Figure 6-7 Broken cross-sectional view showing the Oscillatory mechanism attached to the reactor. Annotated are the parts of the oscillatory motion and the fluid flow pathway formed by their assembly.

6.2.3 Lights

Like the mesoscale system, light can be implemented into the system using a variety of methods. In the figure above two of which are shows. The left-hand side shows the white flexible LED light strips arranged in series on a acrylic surface forming a light panel, and of the right hand side the same LED light strips are coiled around the reactor with 10m of white lights and 20 metres red-blue lights. The average light supplied to the system was between 100 and 200 µmol/m^2/s for the one side and two sided respectfully. The intensity is within range, however considering the reactor's increased volume requiring stronger light and the flexible light strips low durability, make them an unfavourable. option.
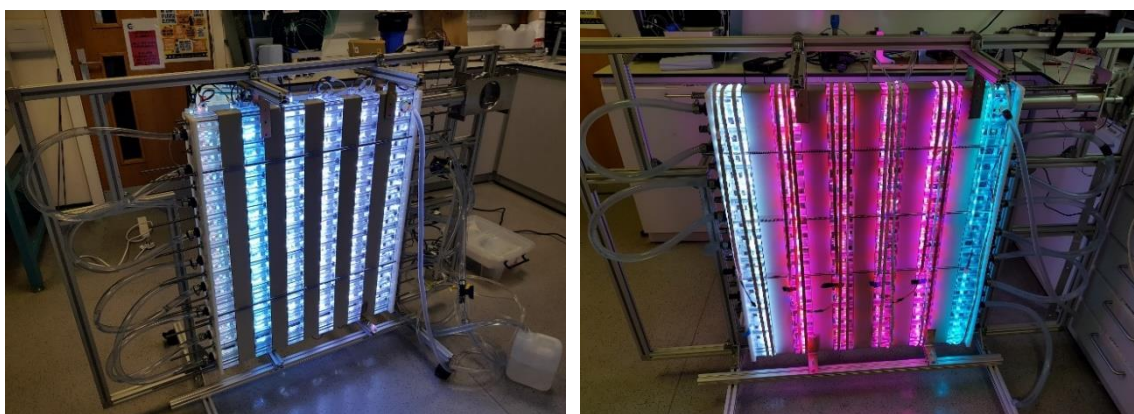
Figure 6-8 8 Different lighting configurations trailed for the large scale FPOBpbR

On the other hand, the LED light bars designed for the mesoscale system complement this design as well. Using equation (5-2), and following a similar methodology to section 5.1.3. it was derived that the best light arrangement was to use 4 LED light bar units at approximately 200mm from each other at 300mm from the reactor surface. (Table 6-3)

To optimise the positioning the reactor was sectioned in nine squares, at which the probe was held for 1 minute whilst all 4 LED light bars where active The average light intensity was captured. Using a compact handheld light meter, the average intensity in Lux (Lx) were measured over the 9 sections of the reactor.

This was done on both sides of the reactor as expected, the side in front of the LEDs had significantly higher light intensities registered than the opposite side.

20300	15346	19188
486	368	459
21000	17080	26000
481	409	621
21000	14250	19000
481	342	455
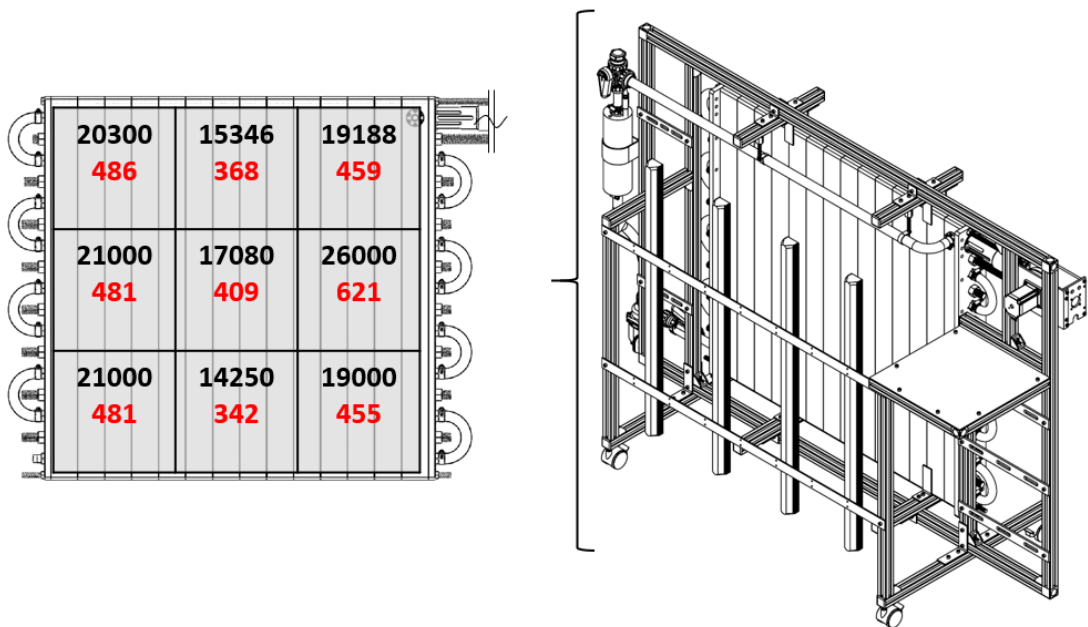
Figure 6-9 Illumination intensities on the reactor side in front of the the lights.

4305	4034	6284
105	98	152
5190	4286	5070
126	104	123
3717	3917	2900
91	96	71
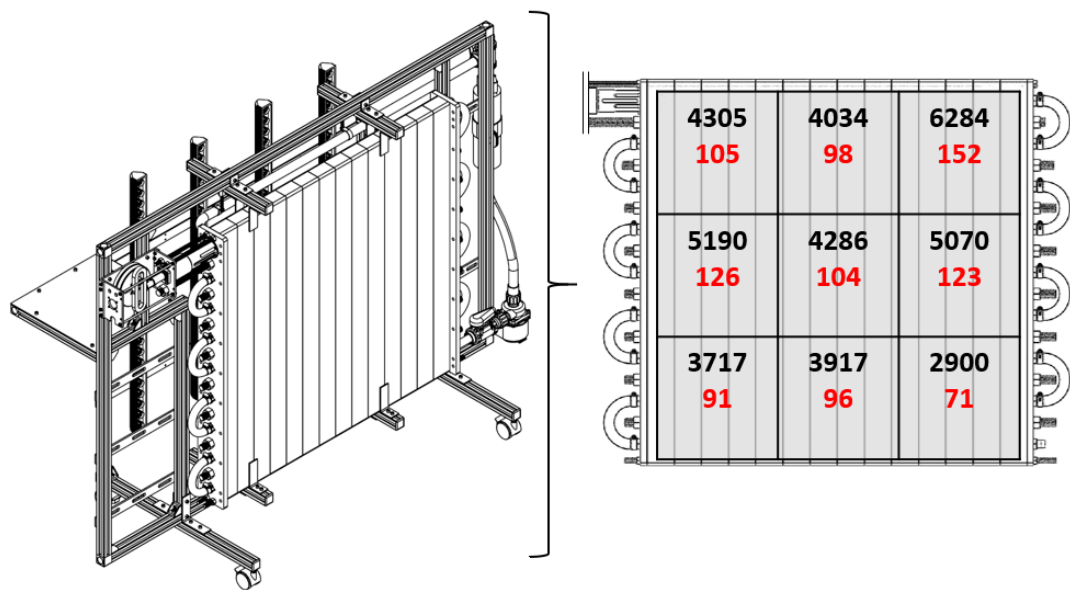
Figure 6-10 Illumintion intensity on the face behind the lights.

Table 6-3 Results from the light fitting equations

Distance (mm)	Area(m^2)	Lux (Lx)	PAR (μmol/m^2/s)
300	0.4037	7486.394	181.1223

Specifically, the original light data table shows that a single LED array emits an intensity of 11,800 Lux from 200mm, using the relationship between distance and intensity, at 300mm the intensity drops to 7,846 Lux. Using equation (1) the area one array covers is 0.4 m^2 from 300mm. From experimentation it was found that the axial drop in intensity from a single light array follows a 2nd order polynomial extinction curve, where the intensity drop until the adjacent LED array is nearly 80 times, therefore the spacing between the LED lights was set to 200mm.

6.2.4 System integration.

A flat plate oscillatory baffled flow reactor was assembled using 14 members making up 9 parallel baffled passages at 0.9 metres length each. The baffle conduit diameter was 36mm with a constriction ratio of S = 0.25, each member consisted of 9 cavities (1 baffle and 1 conduit) spaced equidistantly on a 900mm length, with 100mm spacing. When assembled one piece after another according to width. 9 parallel passages are formed. When fully assembled, each baffled passage was 0.94 metres in length, each conduit was connected to the next consecutive passage, using a u-bend of 300mm length, 16mm i.d., 25mm o.d., flexible reinforced vinyl tube, coupled with polypropylene ¾ BSP tail hose fittings. The complete flow passage length is 10.87 metres and the reactor systems total volumetric capacity is 10 litres. The oscillatory mechanism was mounted on the side of the reactor, at the highest most entry point. The location of the oscillatory mechanism coincides with the input of the reactor, which is positioned at the first conduit of the first member. The input of materials is perpendicular to the flow, whereas the exit of materials occurs axially to the flow.

Figure 6-11 Flat plate oscillatory baffled flow photobioreactor system. various views.

Oscillation is induced by a NEMA 56 bipolar stepper motor connected to a scotch-yoke mechanism, with varying amplitude from 4 – 40mm in increments of 2mm. Net flow can either be supplied by 4 peristaltic pumps working in parallel with a maximum achievable flowrate between 0.14 and 4 L/min, or 1 centrifugal pump achieving 4 to 33L/min. Table 6-4 shows the operating parameter range of the system.

Table 6-4 Operating parameters achieved with the reactor system configuration

Parameter		Min	Max
Velocity (m/s)	u	0.034	0.273
Reynolds number	Re	1228	9824
Oscillatory Reynolds number	Re_o	8	60319
Strouhal number	St	0.716	0.072
Residence times	t	2.4 minutes	14.4 seconds
Velocity Ratio	ψ	0.1	30.7

6.3 OBR Evaluating the Flow at Scale up

Similar to the work conducted in the micro and meso scale reactor, the characterisation of flow is critical for two reasons. First, the characterisation of the flow can act as a metric which indicates if scale up has been successful, and secondly to identify regions on the parameter map which offer high performance mixing.

Residence time distribution studies were performed on a FP-OBR, of nine consecutive passages, made up of 14 baffled conduits each. The complete reactor length and volume is 10.8m and 10 lit respectively.

A custom-made flow cell was attached over the exit tube of the reactor at 250mm from the reactor exit. The flow cell was designed to non-invasively integrate absorbance measurements in larger scale reactors (>1L). The flow cell has two SMA male threads on either side to accept fibre optic cables. The optical path of 12mm enables tubing of maximum OD 11.5 -12mm and i.d of 10mm, like the optical batch of the quartz cuvette used for batch measurements.

As shown in Figure 6-12and Figure 6-13 two 600um fibre optic cables were attached on either side of the flow cell at an angle of 180°. One fibre connected to a dH-mini UV-VIS light source, provided the excitation and the other connected to an Ocean Optics QE-Pro for sensing.
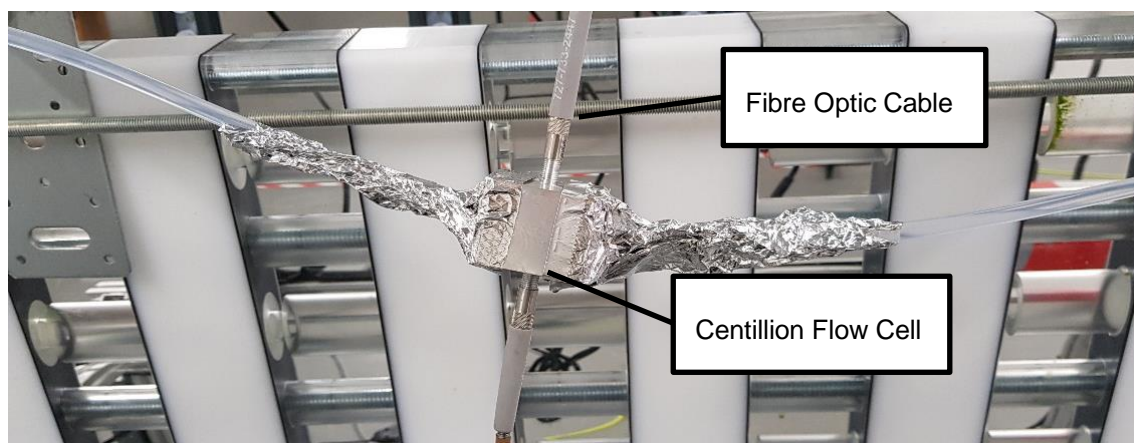
Figure 6-12 The Centillion Flow cell, shown with annotated firbe optic cables with SMA connectors. The tube passes through the flow cell, and aluminum sheets cover the entrance and exit of the optical window.

Similar to the methodology outlines in previous sections, a known concertation of blue dye was used as the tracer to characterise the flow in the reactor, and the residence time distribution model applied was that of the Tank in Series (TiS). The experimental protocol carried out as per literature, and identical to the methodology followed for the RTD studies conducted on the micro and meso scale reactor in section 5.3.2.

However, there are two main distinctions to be made for this reactor and the RTD studies.

1. First of all, the reactors operational parameters. As previously mentioned the OBR must operate in a parameter space which satisfies both the bioprocess requirements and dimensionless parameters to achieve plug flow. Considering the combined biotic and hardware parametrisation, the flow in the reactor must operate at higher net velocities to satisfy the desired light regimes.

2. Considering the previously investigated light cycles (2.5, 5, 7, 20, 50, 150 seconds). They were achieved with flowrates of 0.5 -30ml/min. In order to achieve the equivalent light cycles in the scaled-up version a flowrate of 40 – 4000 ml/min is required. This range was not achievable with the peristaltic pumps. In addition, the lower flowrates, $40 < \dot{f} < 1000 \, ml/min$ are not enough as to expel trapped air bubbles in the reactor, thus interrupting the flow. This phenomenon was only evident in low flowrates. This meant that in order attain an undisturbed plug throughout the reactor, higher flowrates $\dot{f} > 1000 \, ml/min$ were used, meaning that achievable light cycles were in the range of 2.5 and 5 seconds. The higher flowrates result in high Reynolds numbers Re, which in turn require high oscillatory Reynolds numbers to achieve flow reversal.

In literature there is no evidence of such high Reynolds numbers even being used to measure plug flow, therefore the experimental design for this series of experiments was exploratory, in order to ascertain whether it was possible to achieve high TiS numbers in these regions. The design of experiments carried out here was exploratory, with the parameters selection based on the same range of Strouhal numbers St as with the previous sets. The Strouhal number influenced the region of experimental amplitudes X_o between 8 - 27mm centre to peak, resulting in St ranging from $0.11 – 0.36$. The frequency f ranged between 0.8 and 2.5 Hz and the flowrate $\dot{f}$ was set to 4.1, 16, 33,25 L/min. This produced a velocity ratio ψ of 0.10 to 3.6. The Experiments were carried out as per the previous methodology and are detailed in 5.3.2.

In order to enable the algae to cycle at higher flowrates a centrifugal pump was used, with pump duty between 4 and 36 l/min. Flowrates lower than 4l/min where achieved by implementing a regulating valve at the exit of the reactor. By regulating the outlet size, backpressure was formed thus reducing the net velocity of the liquid in the channels. This was verified by injecting a tracer and recording the time it took to travel from one zone to the next. This measurement was carried out for each experiment using a flowrate lower that 4L/min.

Figure 6-13 : Set up for the flow experiments. (Top): FP-OBpbR system with the flow measurement area circled. (Bottom) Closeup of the UV-Vis spectral recording set-up.

6.3.1 Results:

The complete experimental parameter set along with the results are shown in Table F-1. Seventeen experiments were carried out measuring the dispersion characteristics of the flow in the oscillatory baffled tube reactor. As already expressed, the novelty in this experimentation is that first, no evidence of such high Re being tested for dispersion characteristics exist in literature, and second the length of the reactor exceeds comparable reactors.

The tank in series (TiS) numbers achieved range between 10 – 87.9. The mean TiS value of 17 experiments was 41 TiS. Reproducibility of these results are within the 5% margin. Initial indications of factor behaviours and response influencers indicate that the lower net velocities u in the range of <0.1 m/s, overall enable higher TiS numbers, whereas for velocities u between 0.15 m/s and above influence is relatively negligible. Furthermore, lower amplitudes X_o (8mm) achieve higher TiS, whereas frequency's influence on TiS is dependent on net flow.

As explained, this was a screening experiment to evaluate whether the process parameters examined in the smaller scales are transferable. Therefore, in establishing whether the scale up has been successful, as per literature, identical Strouhal St numbers musts achieve identical or similar mixing. Similar to what was done in for micro and meso scale, for the pilot plant reactor it is evident from Figure F-8 that scaling from 4mm to 36mm conduit diameter and from 3.2ml to 10Litres, the flows achieve very similar mixing characteristics for the same range of Strouhal numbers. St. Comparing this with Figure 5-23 indicates that scale up from micro to kilo, is comparable with the scale up from micro to meso scale.

Unlike the mesoscale reactor flow characterisation, the number of experiments conducted is not adequate to produce statistically significant correlations. Therefore, no models nor model extensions have been developed for the large-scale reactor yet. Having said that these results are very promising and act as a platform to which a concise DoE can be built.
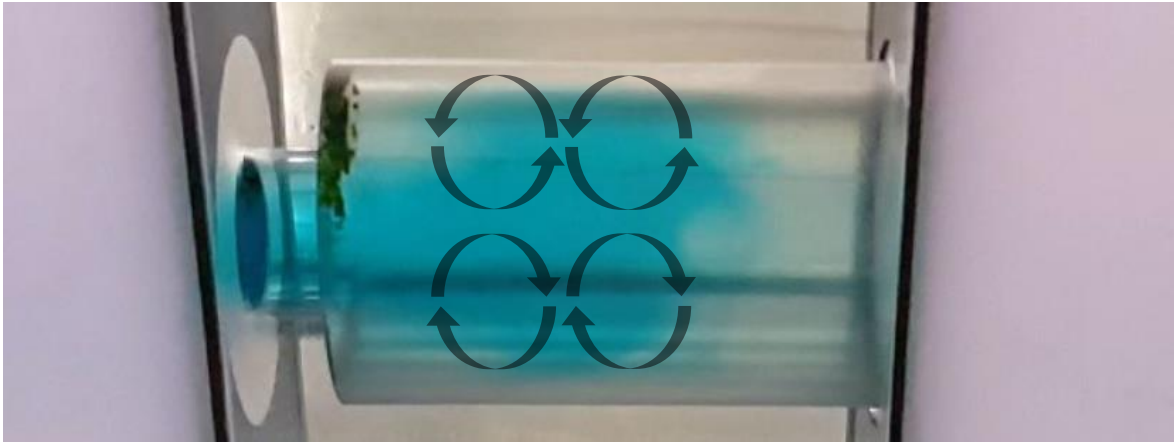
Figure 6-14 Frame capture from a 960 FPS slow motion video, showing the moment toroidal vortices enter the intrabaffle spacing.
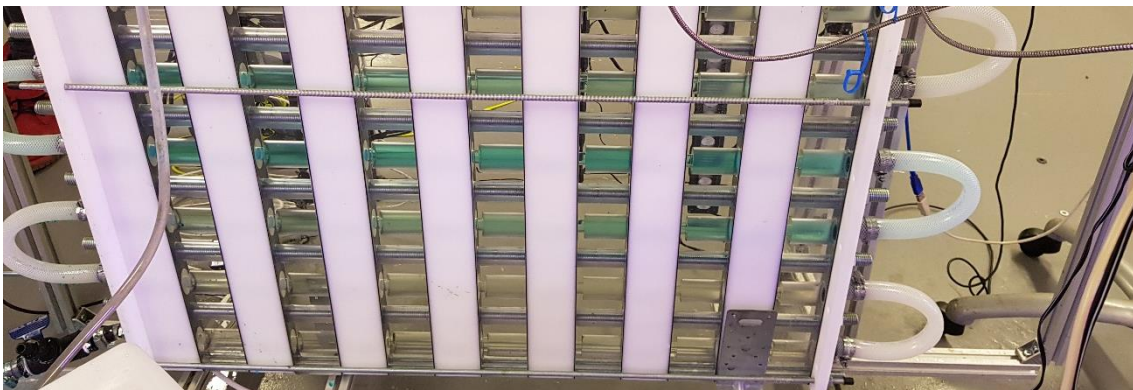
Figure 6-15 Tracer Experiments visual comparison of blue dye dispersion. Top picture showing the dye in 4 baffled channels near the entry of the reactor (TiS =10), and bottom showing the blue dye more concentrated in two baffled columns at the exit of the reactor (TiS = 87).

6.4 Experimental methodology – 10L Scale

Th experimental methodology laid out in the coming chapter, is divided into three sections. These sections are carried out in chronological order from laboratory testing of the pilot scale OBpbR to its integration into the pilot scale facility. Therefore, represent the three bioprocessing milestones in the experimentation of the large-scale C-OBpbR, herein flat plate oscillatory baffled photo bio-reactor (FP-OBpbR).

During laboratory experimentation the system was tested in a controlled environment under laboratory conditions. C.Vulgaris was transferred into the FP-OBpbR, following a three-week acclimation process. The experiment was carried out using Bold basal as the media, and flexible LED light strips spooled around the reactor. A control culture was grown under identical conditions.

The second set of experiments bring the FP-BpbR into the pilot plant facility, with four key differences.

1. The implementation of online monitoring tools,
2. the integration of optimised light,
3. the replacement of the costly peristaltic pumps to a low cost centrifugal
4. Finally, the use of the low cost Centillion media.

In the third set of experiments implement a large-scale (>50L) tank to the reactor, aiming to increase the volumetric capacity of the reactor system. This series of experimentation assesses of how much volume can a 10L light harvesting Centillion FP-OBpbR can cultivate without hindering growth rates. This is a very important point which is not covered in literature, and a crucial step to the bioprocess development. In order to do so a sequence of experimentation is carried out on the bioprocessing line developed for Centillion Technology Ltd. Pilot scale experimentation is carried out on volumes of 60, 110 160 and 260L volumes of *C.vulgaris*.

6.4.1 Laboratory experimentation

6.4.1.1 System Description

An FP-OBpbR is assembled identical to 6.2.4. The oscillatory mechanism was mounted on the side of the reactor, at the highest most entry point. The location of the oscillatory mechanism coincides with the input of the reactor, which is positioned at the first conduit of the first member.

The input of materials is perpendicular to the flow, at the top of the reactor nearer the oscillatory mechanism, whereas the exit of materials occurs axially to the flow at the bottom. The input draws material from a 4 Litre capacity plastic bottle, which as shown in Figure 6-16, identical to the control vessel. Both bottles had modified tops, the reactor bottle having 5 drilled 11mm diameter holes and one 6mm hole, 4 holes for the 4 input tubes to each peristaltic pump, one as an exit and the small one for aeration. Whereas the control bottle had two, one for daily sampling and one for aeration. Both bottles had mounted lighting supplied by identical length of flexible LED light strip.

Figure 6-16 Two identical bottles containing C.vulgaris in the exponential phase.

Oscillation is induced by a NEMA 56 bipolar stepper motor connected to a scotch-yoke mechanism, with varying amplitude X_o from 4 – 40mm in increments of 2mm. Net flow was supplied by 4 peristaltic pumps working in parallel with a maximum achievable flowrate of 6L/min. Light was supplied by 40 metres of flexible LED light strips supplying an average of 4000 Lx to the reactors surface. Light cycle and photoperiods were built into the system by having one reactor member transparent and one opaque. With on optical path length of 63mm. The aeration rate was 500ml/min to both reactors, delivered by a custom sparger system, manufactured by a sterile 50ml falcon pipette tube bent using a heat gun to the shape of a hook, and a length of master flex placed as a sleeve over the whole submerged length of the tube, with a sealed end and pierced multiple times, thus forcing the air to exit the tube and flow back and out through the sleeve.

Figure 6-17 Experimental set up (simulating RBWiR light).

The algae aliquot supplied to the system was processed according to the methodology set out in section 5.6. The experimental design was devise on the premise of evaluating the scaled reactors performance versus the smaller scale at identical parameter sets. As established from experimentation, in mesoscales, *C.vulgaris* benefit from a medium light cycle, independent of the mixing and agitation. Furthermore, it was demonstrated that the oscillatory mixing intensity does not have any significant influence on the growth rate. On the other hand, selecting parameters which achieve a high TiS number, create an environment where there is evident, reduction in fouling, reduction in bubble entrapment, leading to systematically higher productivities and yields.

6.4.1.2 Experimental Parameters

Therefore, for this experiment the parameters were set as follows. The flowrate was set 120ml /min which enabled a 30.2 second light phase with 61sec light cycle. Scaling the mixing regime, was carried out by keeping the Strouhal number constant between the two scales. Based on this a Strouhal number St of 0.35 was selected with an amplitude of 8mm. The frequency was set to 1Hz with an $Re_o = 1809$ higher than the equivalent Re of 324. based on that, velocity ratio ψ of 5.5 from the fixed Re produced by the net flowrate. However, the TiS number produced by these parameters was not high enough at TiS = 19, in spite of the high velocity ratio, meaning that flow was fully reversed.

6.4.2 Pilot Plant - 10L Scale

6.4.2.1 System Description

An identical reactor as in outline in the previous section was mounted on a frame, consisting of the new LED light arrangement-, buffer tank, pump and sensors. The compete layout of which is shown in the figure below.

Similar to the arrangement of series one, a flat plate oscillatory baffled flow reactor was assembled using 14 members making up 9 parallel baffled passages at 0.9 metres length each. As shown in Figure 6-19, oscillation is induced from the mechanism at the top end of the reactor, and a centrifugal pump is placed at the lower end. The input of material occurs coaxially with the oscillation, at the

bottom of the reactor and exit occurs via the port placed on the sidewall of the first baffle. Both entry and exit point of the reactor are connected to a cylindrical vessel, with 500ml capacity. The complete flow passage length is 10.87 metres and the reactor systems total volumetric capacity is 10 litres.

The method of oscillation is identical to the previous experiments and is induced by a NEMA 56 bipolar stepper motor connected to a scotch-yoke mechanism, with varying amplitude from 4 – 40mm in increments of 2mm. Net flow was supplied by a centrifugal pump with a maximum achievable flowrate of 33L/min.

Light was supplied by 4 fixed LED light bars, which achieved an illumination intensity of approximately 400 μmol/m^2/s on the surface directly in front and 100 μmol/m^2/s on the non-illuminated side. Fixed photoperiods were built into the system by having one reactor member transparent and one opaque. With an optical path length of 63mm.

The connected tank linked the reactor exit and input and acted to form of closed loop. The tank was introduced to enable the following, to act as a gas exchange vessel which O_2 would be ejected, and not carried into the system. Secondly to act as a volume buffer, ensuring the systems smooth operation, by absorbing any variations due to evaporation, thus avoiding mechanical malfunctions or rough running due to the pump or oscillatory mechanism running dry. Lastly the tank housed the system sensing probes (DO, pH and T). The system sterilisation and inoculation were carried out, using the methodologies outlined in section 3.2.2.2.2 and 5.6.1 .

6.4.2.2 Experimental parameters

The process parameters for the experiment were set using the methodology outlined in section specifically the flowrate was set according to the light cycle, and the oscillatory flow parameters were set to achieve an optimal TiS number. For that reason, the flowrate was set to 3000ml/min thus achieving a light cycle of 2.5sec. The frequency of oscillations was set to 1Hz and amplitude of 8mm. Combined the parameter set created a plug flow of approximately 70 – 78 TiS, as tested during the RTD Studies validations shown in Table F-2.

The process parameters therefore a shown in the table below:

Table 6-5 Process parameters for the experimentation of the FP-OBpbR in the pilot plant and 10L scale, under optimised parameters

Factor	Symbol	Setting	Unit
Amplitude	X_o	8	mm
Frequency	f	1	Hz
Flowrate	$\dot{f}$	3000	ml/min
Velocity*	u	0.049	m/s
Diameter	D	8	mm
Strouhal Number	St	0.36	-
Net Reynold Number	Re	1768	-
Oscillatory Reynolds Number	Re_o	1806	-
Velocity Ratio	ψ	1.02	-
Tank in series number	TiS	74.8*	-
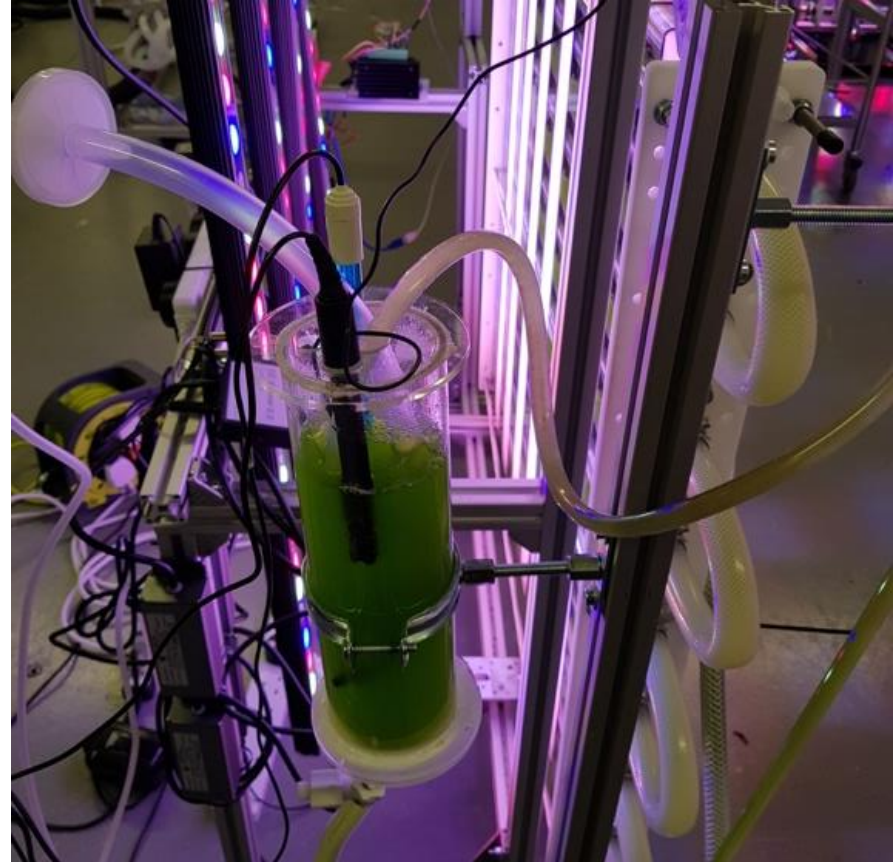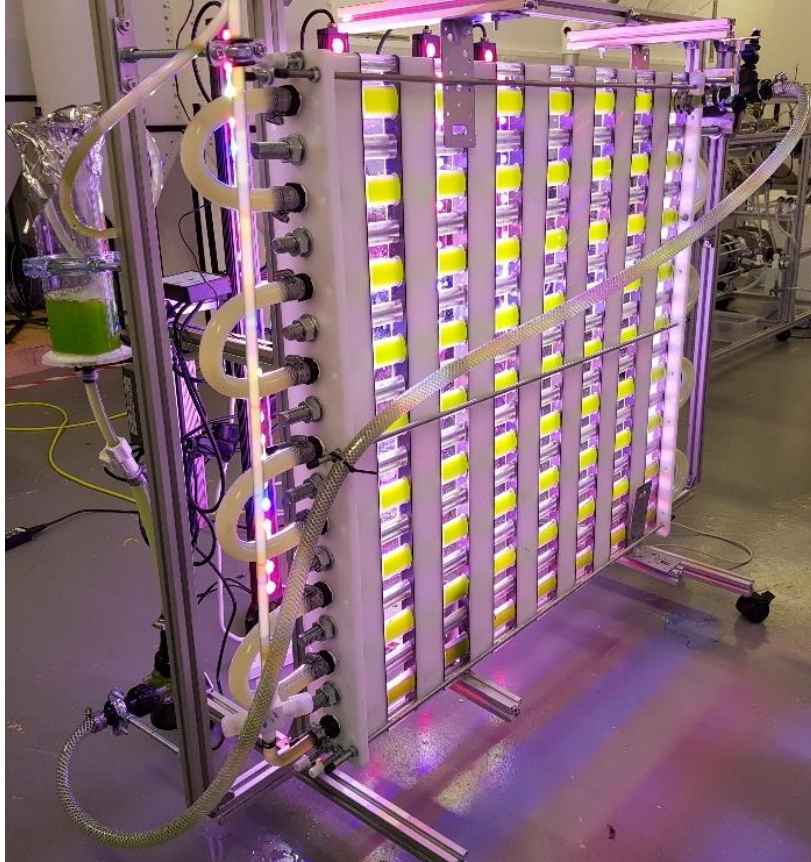
Figure 6-18 LHS: FP-OBpbR During Series two experimentation. RHS: Buffer tank shown with ph meter, DO sensor and air supply.
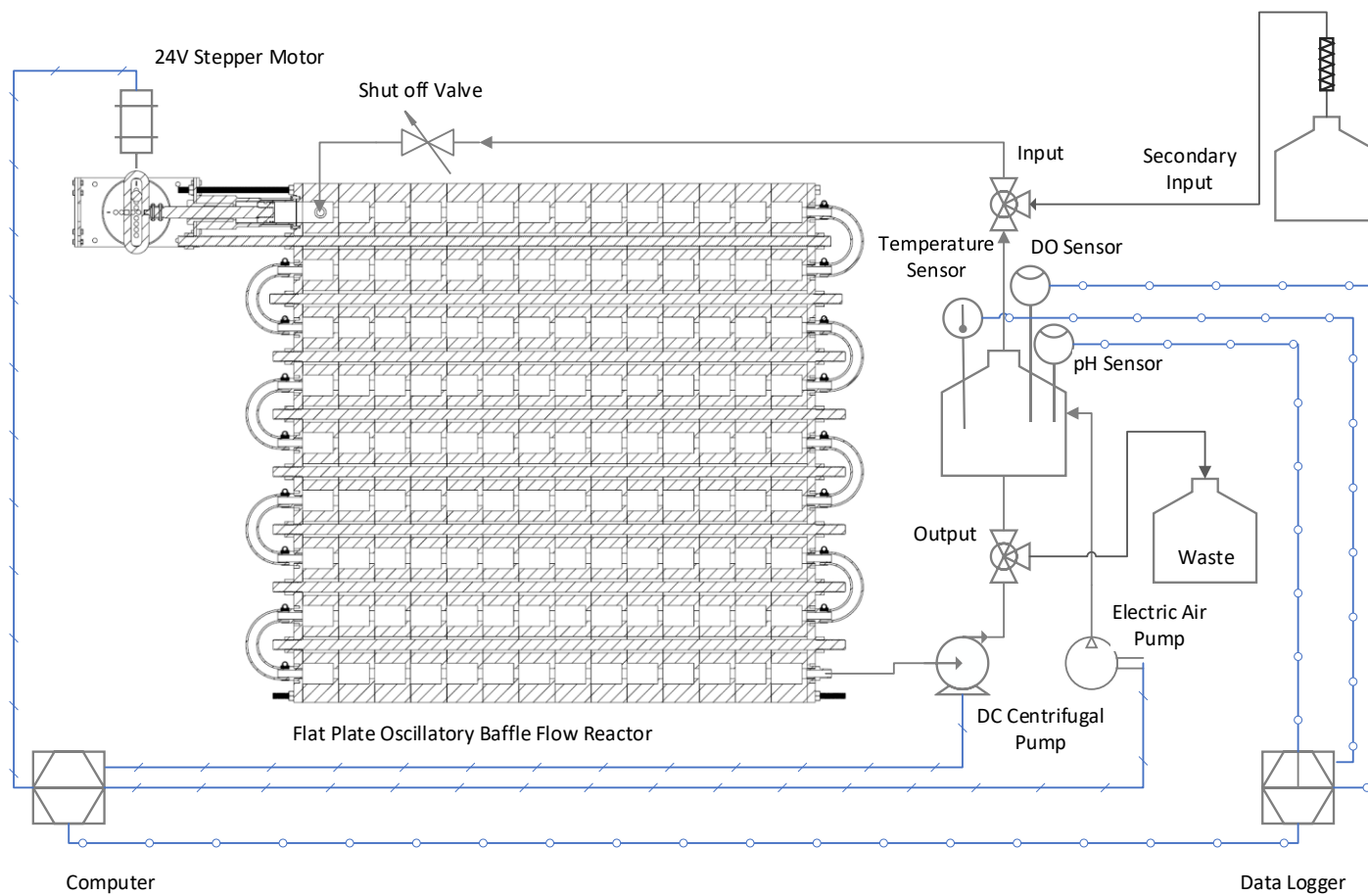
Figure 6-19 Series two experimentation system schematic

6.4.3 Pilot Scale 50-260L

In modern flow PBR's , the tubular (flow) section is linked to a tank, which acts as a feeder, buffer and gas exchange system, whereas the tubular reactor section acts as a light harvesting unit.

Up to this point, experimentation on the centillion FP-OBpbR has been to measure the effect of the reactor configuration on the algae. Therefore, a low volume buffer tank (<1L) was used so that minimal external influences, benefit or inhibit algae growth. This practice is essential when evaluating the effect of light, since any volume that remains in a holding tank, will not experience the same light cycle.

In commercial examples of microalgae tubular horizontal PBRs have equal volume tank and light harvesting unit Most prominent examples are the Varicon Aqua Bio-Fence, Phyco Lift and Phyco Flow, which report a volume of 200 to 600L, where up to 50% only comprises of the light harvesting unit (Varicon Aqua, 2019). The reasoning behind this is that the light harvesting unit and tank act as the light and dark cycle of the algae. It is noteworthy to say that this industrial practice in volumetric specification, and light modulation control is contradictory to what laboratory scale reactors specify; where reactor volumes are equal to the light harvesting unit, and light and dark cycles occur due to mutual shading.

Therefore, the FP-OBpbR ability to act as a light harvesting unit in processing much larger volumes of algae, must be evaluated. This is a crucial step in determining the scale up potential of a reactor. As it is a clear indicator of assessing the reactor's ability to integrate into much larger volume bioprocesses

.

Figure 6-20 System T1 shown with the reactor operational and T2 and T5 Tanks on the background left and right respectively.

The modularity of the Centillion FP-OBpbR enables it to increase its volume by adding more members. In order to be comparative with commercial applications, the reactor system can also increase its volume by adding a larger holding tank. The implementation of the tank makes the study of algal growth a complex task ,particularly in terms of the light cycle and mixing. Therefore, in order to study the effect, a third series of experimentation was designed to test the processing volumetric limitations of a 10L harvesting unit based on the Centillion Reactor FP-OBpbR design

6.4.3.1 System Description

To carry this out, the centillion FP-OBpbR was connected to a 1000L conical UHMWHDPE tank, as per Figure 6-22. This section of the P&ID diagram belongs to a bioprocess line developed for the Centillion Technologies pilot plant which is not in the scope of the thesis, however a brief overview will be given since parts of it are used in this set of experiments., the complete bioprocess description is given in Figure 6-25. It consists of four Centillion FP-OBpbR reactor systems with a maximum volumetric capacity of 1000L holding plus up to 50 Litres light harvesting units. These four systems are connected to a centralised clean in place (CIP) system (T4,T5 & T14), comprising of a 1000L water tank and 200L IPA tank. This enables on demand transfer of cleaning fluid to each reactor system. Cleaning in place (CIP) can occur for both tank and reactor system, tank only or reactor only, depending on the maintenance cycle (Short, Large) or unforeseen event (culture crash out). In addition to the sterilisation and decontamination line, the reactor systems are connected to a media line (T2, T3), with capacity 1000L water plus 200L concentrated media. The correct dose of media is injected from the 200L concentrated media tank into the 1000L water tank and is delivered to each system individually or all systems in parallel. Upon harvest the tanks can be either purged or a sub cultured, where dense culture flows to tanks T4 and T10.

Figure 6-21 Centillion FP-OBpbR 6000L system
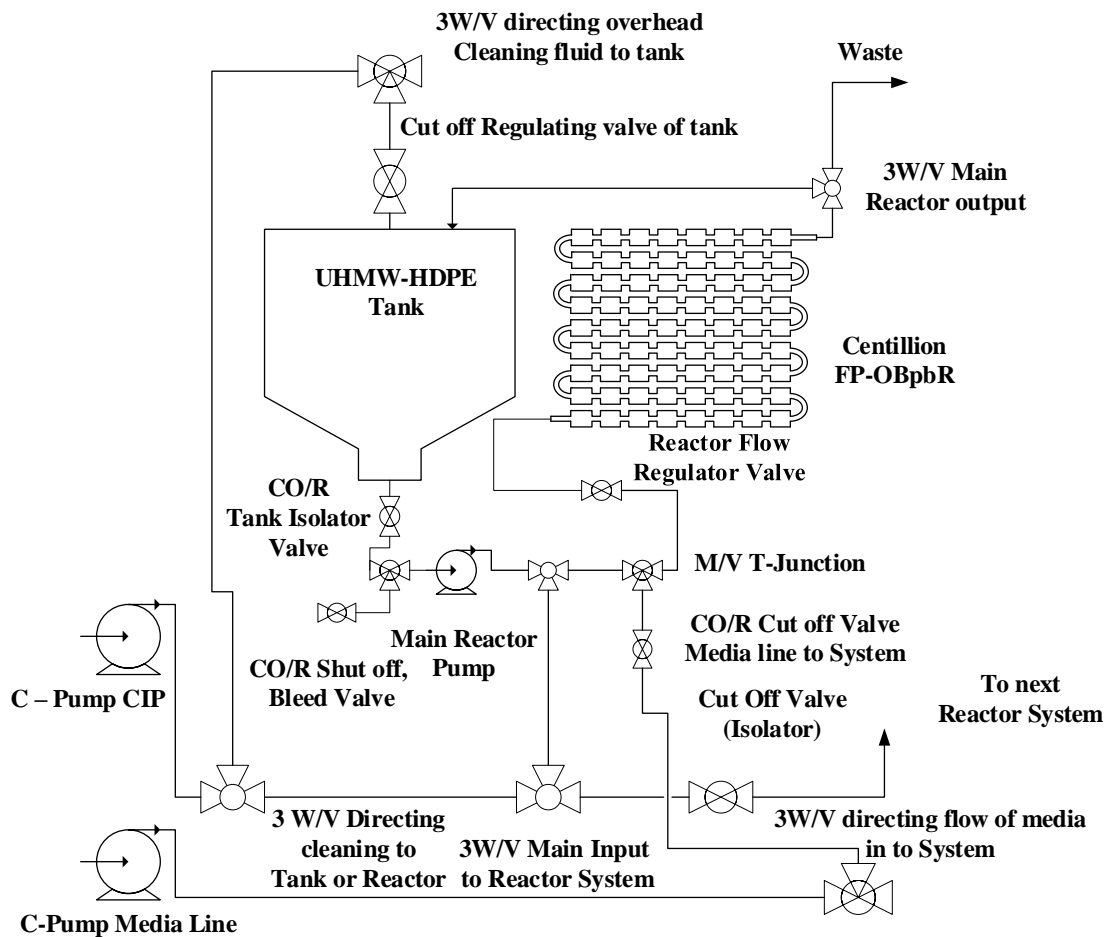
Figure 6-22 P&ID Section of One Centillion FP-OBpbR System, showing the (CIP) cleaning in place pipeline, and the continuous media feed line.

The FP-OBpbR system is connected to a 1000L tank, and a series of input and output valves, which enable cleaning and maintenance schedules, as well as deliver growth media to the systems on demand. The Bioprocessing line system, resembles the systems used in mesoscale Figure 5-34 as well as the kilo scale reactor Figure 6-19, which is clear evidence that the Centillion modular reactor can be integrated in a modern bioprocessing line without much effort or re-engineering. To operate the bioprocessing line, in a safe and effective manner, a methodology was developed for the operation of all main and auxiliary systems. A section of that methodology, covering decontamination, system priming, and inoculation is described in 7.3G.1 with additional figures of the bioprocessing line, depicting various systems and components can be seen in Figure G-1 Figure G-5.

6.4.3.2 Experimental parameters

An experimental strategy was devised to evaluate the FP-OBpbR potential in cultivating 50, 100, 150 and 250L volume in the holding tank. These indicative volumes were selected on the criteria, that if one 10L reactor can process a maximum of 250L then an arrangement similar that portrayed in 7.3F.1 with four reactor systems on each side of the IBC would, enable the production of 1000 l/m^3 with a power cost, $100W/m^3$ for pumping, $400W/m^3$ oscillating and $400W/m^3$,in lighting. which combined $900W/m^3$ is still lower than the $2000\ W/m^3$ power requirement that conventional tubular PBRs require as cited by Placzek, Patyna and Witczak (2017).

To carry out this experiment, all four tank systems from the bioprocessing line where employed. Due to biological restrictions and good bioprocessing practices, a great deal of consideration was given to develop a strategy in which experimentation was carried out in situ with volumetric ramp of the bioprocessing system. This was done to maintain the culture density high enough to prevent crash out, which as per Andersen (2005) and Brand (2013) is important to maintain the viability and axenic growth a single species at large scale (Andersen, 2013; Brand, Andersen and Nobles, 2013). Therefore, a methodology where each system would cultivate *C.Vulgaris* and inoculate the others was

implemented. Starting from T1 a 10L culture would inoculate the reactor containing 50L of media, which at the end of the exponential phase, a portion would inoculate the next system containing 85L of media. Which in turn a portion of the 110L culture would inoculate a 160L volume of media. And so forth. An accurate representation of the subculture and inoculation routine is shown in Figure 6-23.
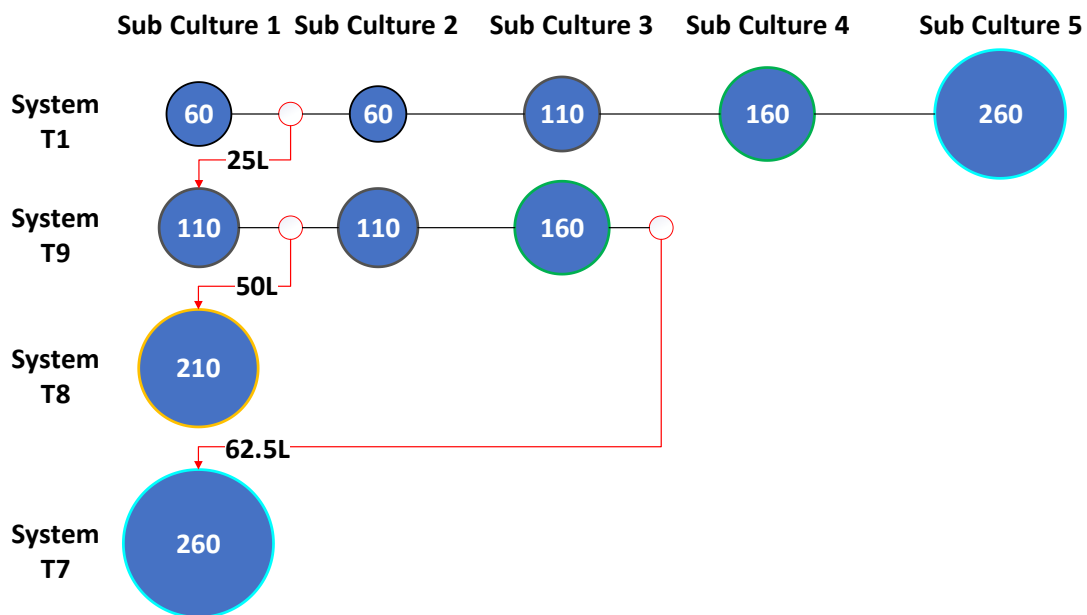
Figure 6-23 Cultivation schedule of the four tank systems T1,T9,T8,T7, Red lines indicate the inoculation pattern, and inoculant volumes.

Another important consideration in this series of experiments is the control of the light cycle. In prior experimentation a light cycle of 2.5 second was used to dictate the net flow parameter, however in this case a 2.5 second light cycle with a tank volume of 60-260L is not achievable. Therefore, for comparable flowrates of 3L/min fractions of light to dark and time under light are shown in Figure 6-24. It shows that by increasing the tank volume, i.e. the dark zone volume, the time in the light regions are severely reduced. For a volume of 60L and a net flowrate of 3L/min the light time is 4.8 h/d, whereas for 260L, at the same flowrate, the light time is under 1h/d. By increasing the volumetric flowrates, the L/D fractions remain the same, as they are disassociated with the flowrate, but rather with the volume per phase.

As suggested by Grobelaar (1989) there are cases were asynchronous light cycles are studies but are few and far between. (Grobbelaar, 1989).
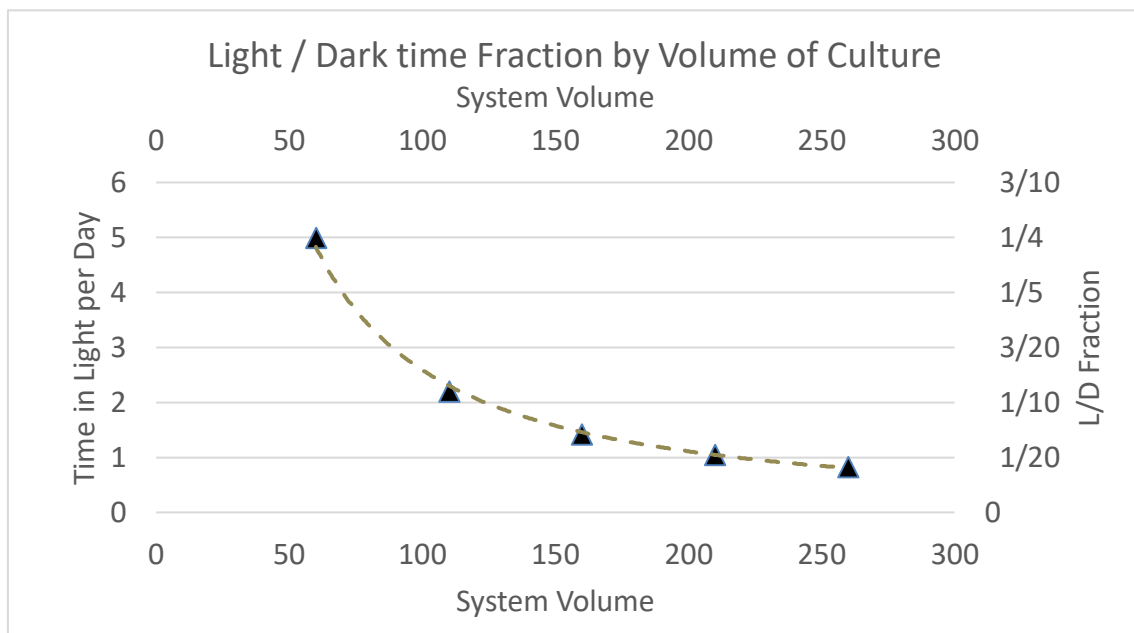
Figure 6-24 Light/Dark time fraction trend with increasing the system volume

To conclude, the purpose of this experiment is not to study the light cycle effects but to establish experimentally the limitations in increasing the holding tank in a FP-OBpbR system. Therefore, the experiments were carried out using a flowrate of 3L/min a frequency of 1Hz and an amplitude of 8mm. Therefore. The experimental duration ranges from 6 days to 43 days long. A control experiment, consisting of *C.vulgaris* cultivating in the tank, circulated by a centrifugal pump at 3l/min, was conducted to help in evaluating the true effect of FP-OBpbR.
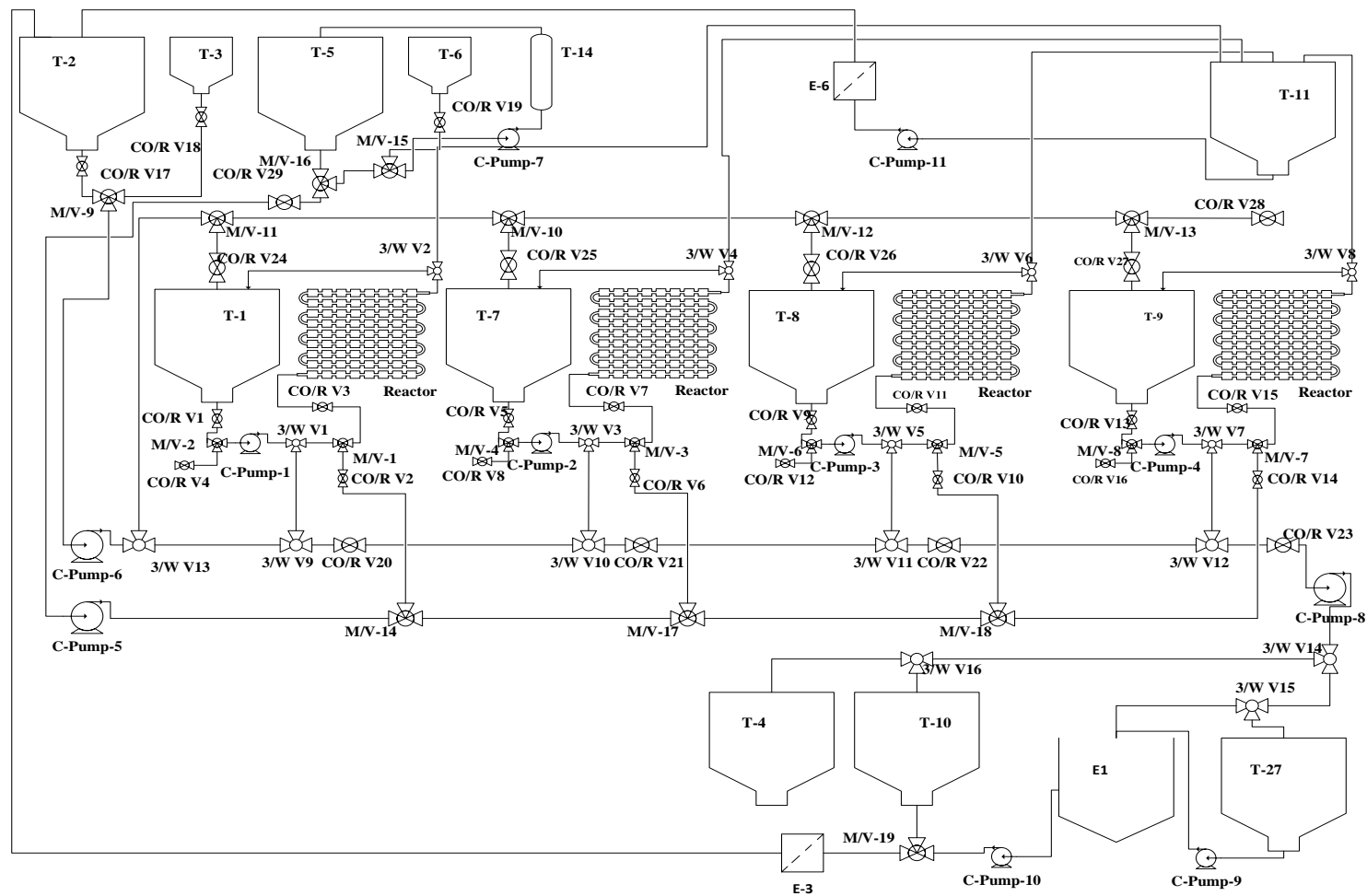
Figure 6-25 Centillion Technology Algal Cultivation bioprocessing line (Cranfield Pilot Plant).

245

6.5 Results

6.5.1 Laboratory – 10L Scale

The complete experiment ran for 17 days in operating in semi-contiguous. At which the optical density and cell count were recorded. As is shown on Figure 6-26, the first eight days the 1st subculture of the reactor system was directly compared to an identical culture growing in a batch mode. In this duration the culture started from the same density of 1.7E+08 cells/ml and produced a final yield of 2.7E+08 and 3.38E+08 cells/ml for the batch and reactor system. the reactor system performed marginally better than the batch reactor with specific growth rate being 0.089 and 0.095 respectively. The reactor was subculture at the 8th day with a dilution ratio of 0.5, with the addition of 5 litres of fresh BBM media. The consequent subculture was left to grow for 11 days, nine of which were in the exponential phase. The specific growth rate achieved for the subculture was 0.12 and the cellular productivity was 2.01E+07 cells/ml/d, and doubling time (td) was 5.3 days.
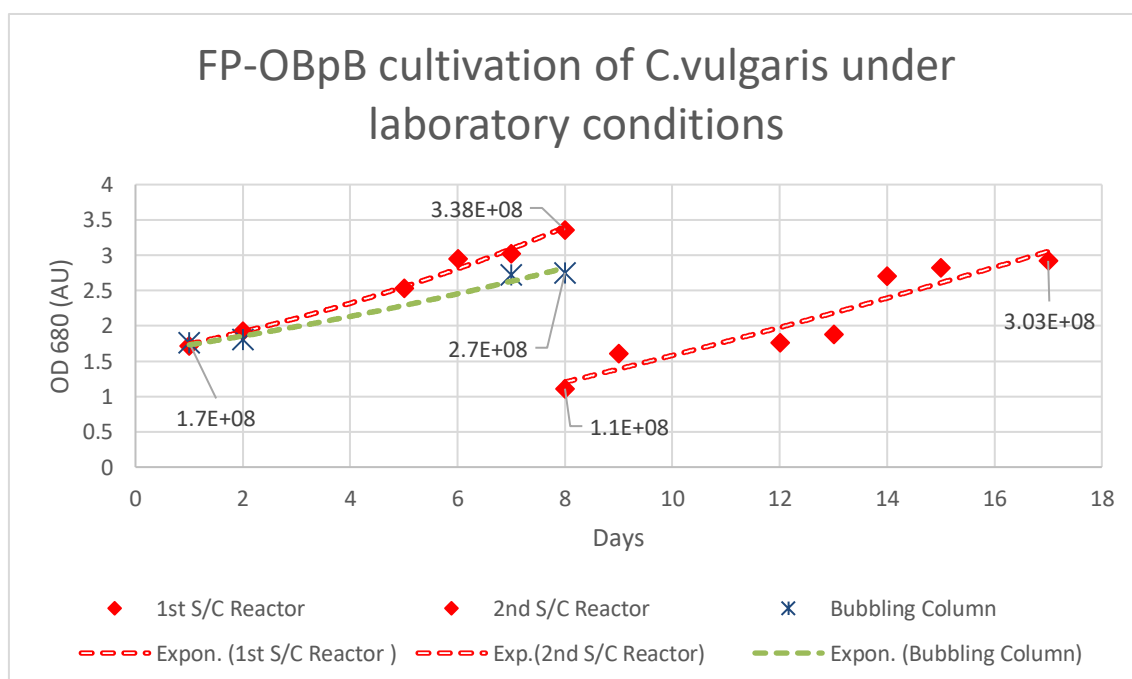
Figure 6-26 FP-OBpbR cultivation of C.Vulgaris under laboratory conditions at 10L scale, compared with control experiment.

6.5.2 Pilot Plant -10L Scale

Two experiments were set up running in semi-continuous cultivation One with BBM and the other with CM (CV6), both running optimised mixing conditions for the FP-OBpbR. Both experiments operated for 23 and 18 days respectfully.

As shown on Figure 6-27, the culture running with BBM was very slow to pick up. during the first subculture, the growth rate was negative, as the optical density and cellular productivity fell systematically throughout the 8 days, at a rate of 0.036 and 5.1E+05 cells/ml. Under light microscopy the culture was not showing any sing of microbial contamination, infestation or predation. Temperature was deemed to be the biggest issue, since the experiments were set up during early winter, where the temperature was around 14-15 C^o in the pilot plant in terms of the culture temperature, it was around 16-17C^o due to the LED lights. Space heating was implemented with the use of 1Kwh space heaters, and the experimentation process was continued.

Immediately from the 10th to 15th day, there was evident growth at a specific growth rate of 0.045, and biomass productivity of 0.015/l/d with a final culture density of 0.55 g/l. The culture was subcultures to an optical density at 680nm of approximately 1.6 AU, with 4 litres of fresh BBM media. The culture subsequently grew for another 7 days at a rate of 0.026 and a biomass productivity of 0.008 g/l/d and a final culture density of 0.4g /l.

Comparing the performance of the BBM media in the reactor between scales, it is shown that between the 100ml system and the 10L system the biomass densities are lower at kiloscale.

The system was diluted to an optical density at 680nm wavelength of 1.00 AU, with 4 litres of the Centillion media. The algae could acclimate for 5 days with serial sub culturing of smaller volumes, ensuring that the whole culture is fully acclimated to the new media, and the experiment could commence with the algae culture at the exponential phase.

As shown in Figure 6-27 and Figure 6-28. There was a significant increase in growth with the new media. For the subsequent two subcultures and 15 days experimentation. The 1st sub culture lasted for 10 days until the culture was diluted with 50% of the whole volume with freshly prepared media. During both stages the culture grew following a 2nd degree polynomial trend.

The growth rates for subculture 1 and 2 (S/C 1 and S/C 2) were 0.17 and 0.15 respectively, with productivity of 0.080 and 0.090 g/l/d. The final biomass density for both subcultures was 0.87g /l.

During the second cycle of the semi-continuous cultivation (S/C 2) reached a concentration of 2.15 g/l in7 days (see Figure 6-29). The trend of pH as is shown in the same figure, is as expected, it ranges between 6.9 and 8.6, however spikes that go beyond 9.5 and sub 6 have also been evident, where in either case pH was corrected with either 1M HCL or 1M NaOH.

Table 6-6 Combinatory table showing the all cultivation cycles in the FP-OBpbR of both experimental series. (lab and pilot plant at equal Volumes)

Exp No.	System Volume (L)	Litre holding tank (L)	Subculture no.	No Days	Biomass Density (g/lit)	Specific Growth Rate	Doubling rate
1	10	4	1	9	N/A	0.095	7.25
	10	4	2	9	N/A	0.12	5.7
2	10.2	0.2	1	8	0.4	-0.03	N/A
	10.2	0.2	2	7	0.55	0.045	15.2
	10.2	0.2	3	6	0.4	0.026	26
3	10.2	0.2	1	9	0.82	0.177	3.9
	10.2	0.2	2	6	2.15	0.153	4.5
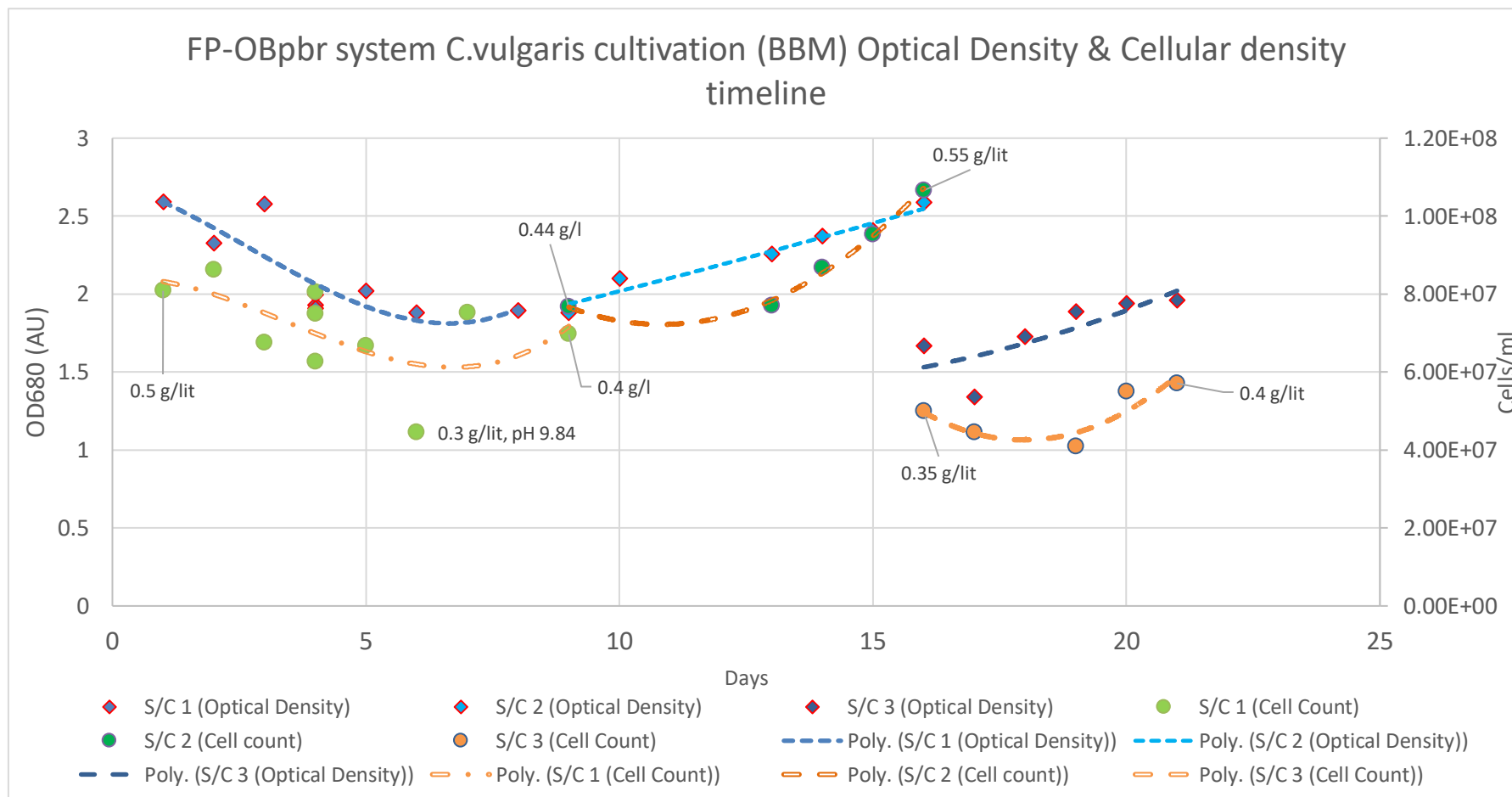
Figure 6-27 All Three subcultures, across 23 days of experimentation using the FP-OBpbR with Bold Basal Media.
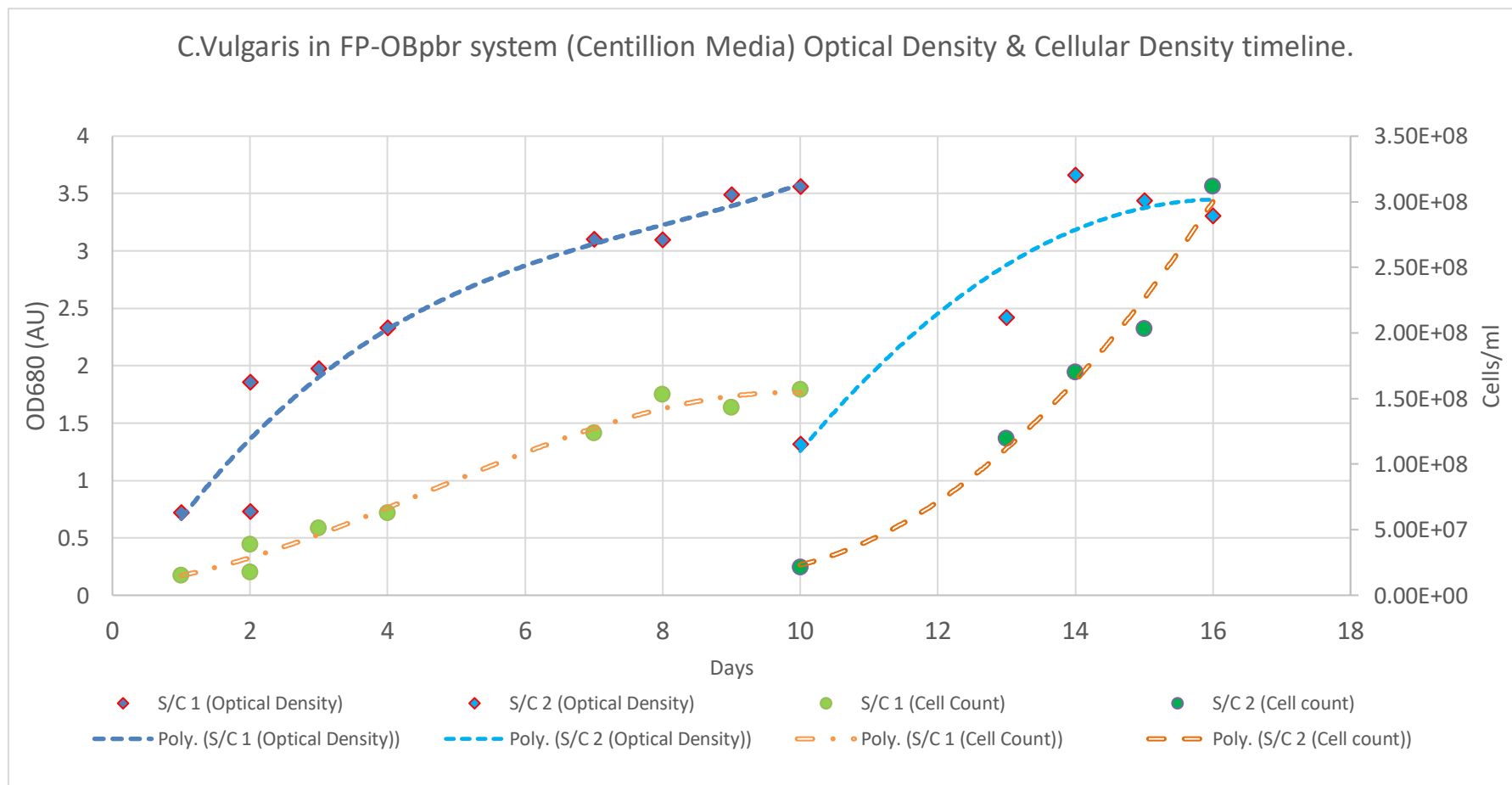
Figure 6-28 Two Subcultures of C. vulgaris across 16 days of experimentation in the FP-OBpbR, with Centillion media.
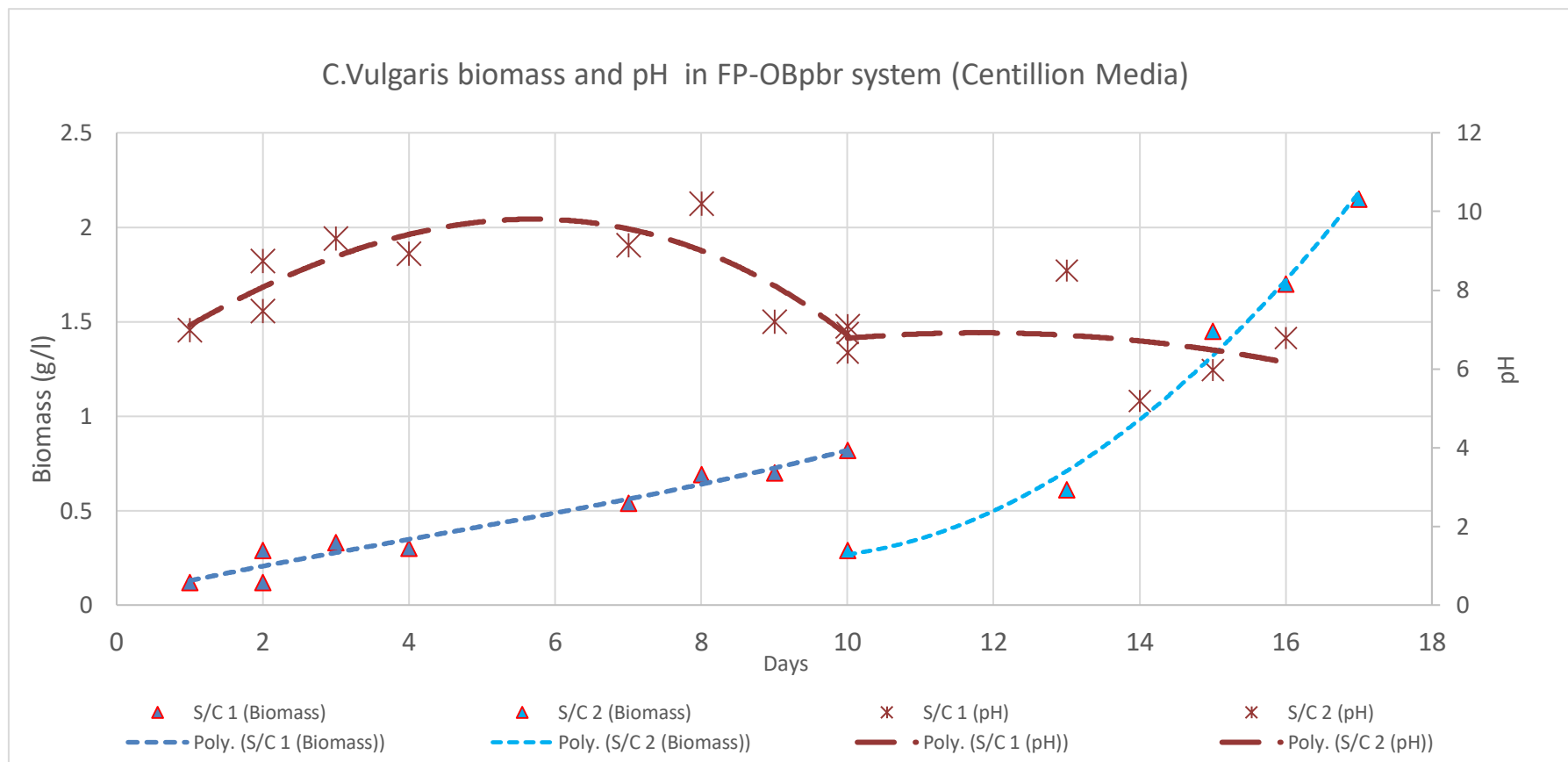
Figure 6-29 Two Subcultures of C.Vulgaris across 16 days of experimentation in the FP-OBpbr with centillion media.

6.5.3 Pilot Scale– 50-260L

The results for each of the experiments are shown in tabular form in Table 6-7. As well as showing the growth curves in Figure 6-35 to Figure 6-38.

Initially 50 litres of media were inoculated with a 10L of dense *C.Vulgaris* culture. The 60-litre culture in T1, was cultivated for 7 days until reaching stationary phase. From the 60L culture 20 litres of culture were harvested from T1 and used to inoculate 90 litres of media in tank T9. The remaining contents from T1 where sub cultured with additional 20 litres of media back to a volume of 60 litres. System T1 proceeded to cultivate for an additional 9 days at 60L then serially diluted every 5-7 days to 110, 160 and finally 260L. Similarly, system T9 after being inoculated with C.vulgaris from system T1, was cultivated at 110L for 8 days where 25L were used to inoculate T8. T9 was sub cultured back to 110L and cultivated for 7 days, and at 160L for 21 days. At the end of the 21 days, 62.5L of the culture was transferred to T7 containing approximately 190L media. T8 and T7 proceeded to cultivate for 43 and 38 days until the reaction was terminated. Finally, a control experiment of 60L C.Vulgaris culture was circulated around the UHMWHDPE 1000L tank at 4L/h, at the same environmental lighting conditions. The results are shown in Figure 6-39.

The results clearly indicate that when the system volume increases so both the biomass concentration and the specific growth rate is reduced. As can be seen from Figure 6-30 and Figure 6-31 the maximum specific growth rate achieved was at 60L in T1 (μ = 0.21), whereas system T9 with volume of 110L cultivated *C.vulgaris* with a growth rate of 0.18 and 0.19. The growth rate of the *C.vulgaris* plummeted beyond 110L volumes with T8 And T7 achieving a growth rate of 0.02 and 0.09. Biomass concentration follows a similar trend where larger biomass concentrations are systematically achieved at lower system volumes (Figure 6-37 and Figure 6-38)

All experiments performed better than the control experiment, which achieved a biomass concentration of 0.05 g/l after 26 days.
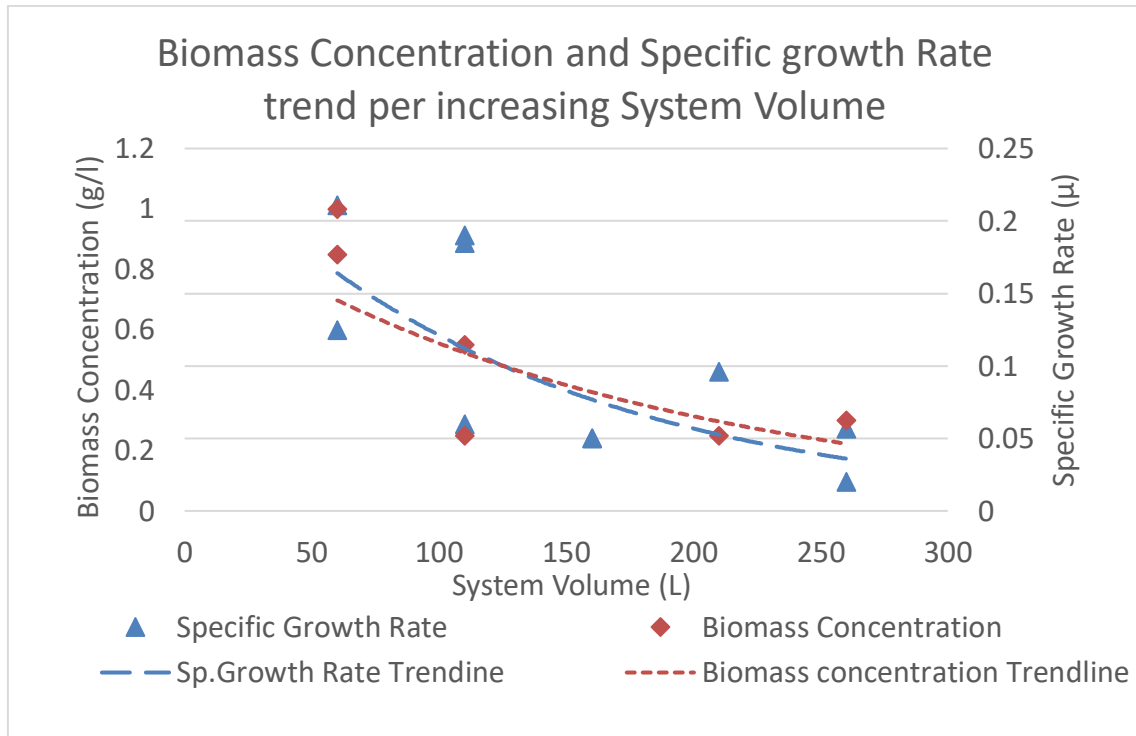
Figure 6-30 Biomass Concentration and Specific growth Rate trend per increasing System Volume (Includes Series two experiments).
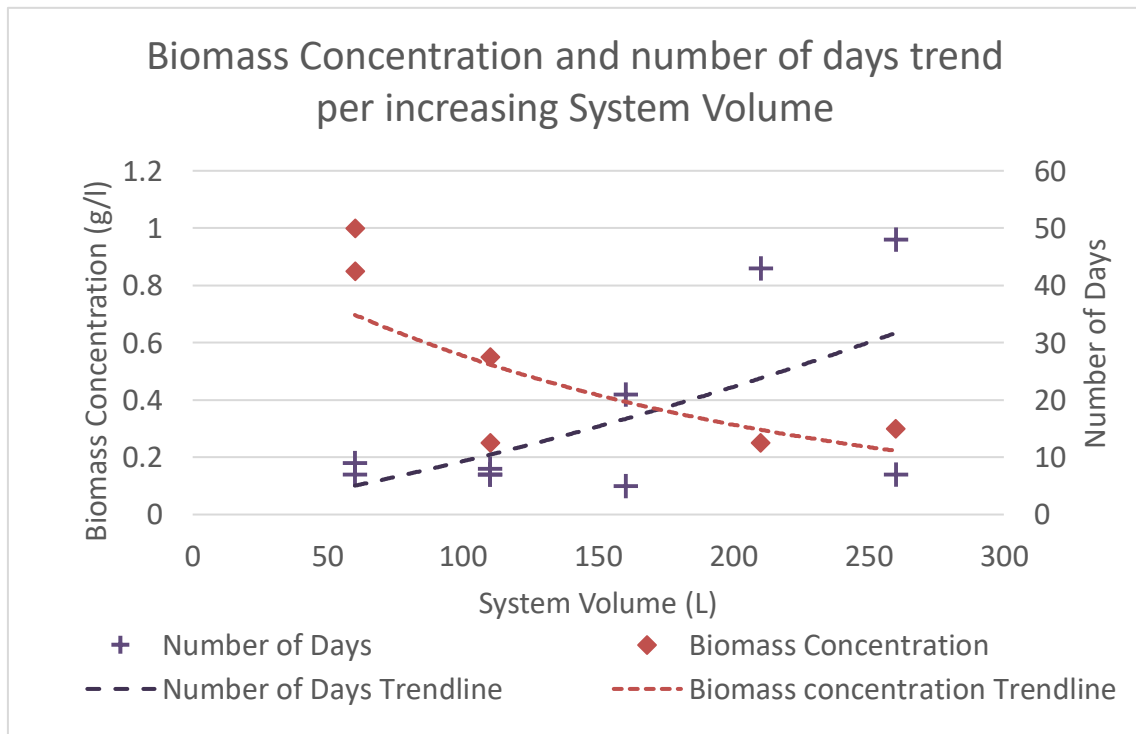
Figure 6-31 Biomass Concentration and Specific growth Rate trend per increasing System Volume

Table 6-7 Cultivation experiments results summary, showing each systems volume, the subculture number, cultivation period, biomass density, specific growth rate and doubling rate.

Tank System	System Volume (L)	Litre holding tank (L)	Subculture no.	No Days	Biomass Density (g/lit)	Specific Growth Rate	Doubling rate
Tank 1	60	50	1	7	0.85	0.211	3.27
	60	50	2	9	1	0.125	5.52
	110	100	3	7	0.25	0.06	11.3
	160	150	4	5	n/a	0.050	13.8
	260	250	5	7	n/a	0.057	12.13
Tank 9	110	100	1	8	0.55	0.185	3.7
	110	100	2	7	0.56	0.19	3.5
	160	150	3	21	n/a	0.05	13.13
Tank 8	210	200	1	43	0.25	0.096	7.19
Tank 7	260	250	1	48	0.3	0.0202	34.2
Control	60	60	1	26	0.05	0.015	46

There are two main reasons as to why the growth rate and biomass productivity rate decreases with increasing tank volume, the lack of light (cycle and intensity) and significantly reduced mixing.

Specifically, for the light, as expected the light fraction of the cultivation is reduced however comparing the average specific growth rate per volume with the

light/Dark fraction ratio, it is evident from the trend which coincides.
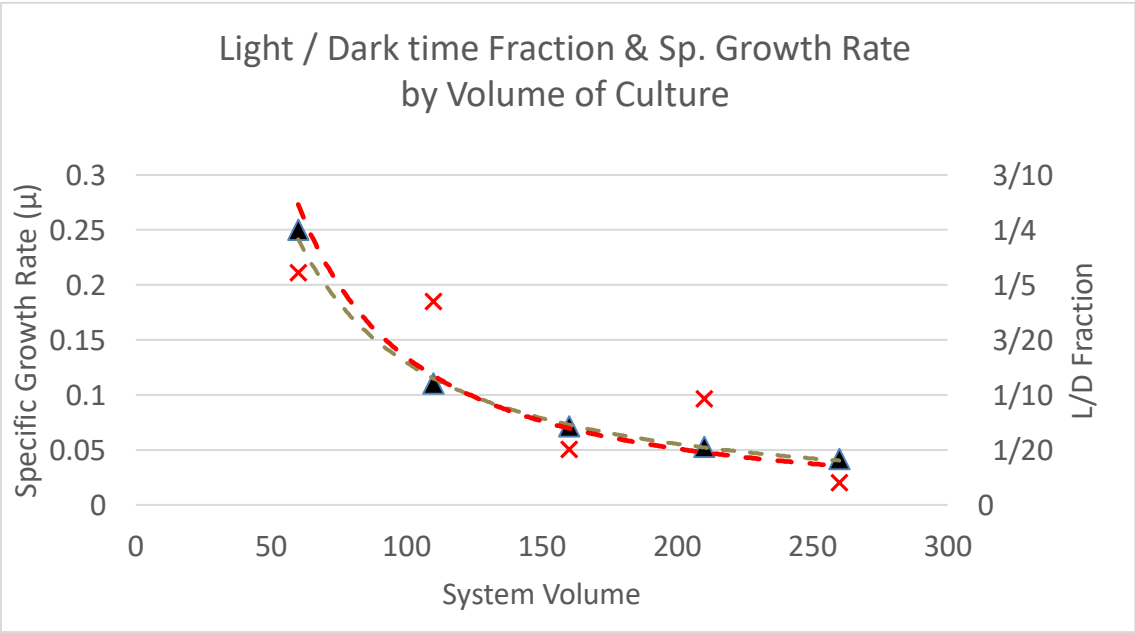
Figure 6-32 Light and Dark fraction decrease by volume, coinciding with reduction in specific growth rate.
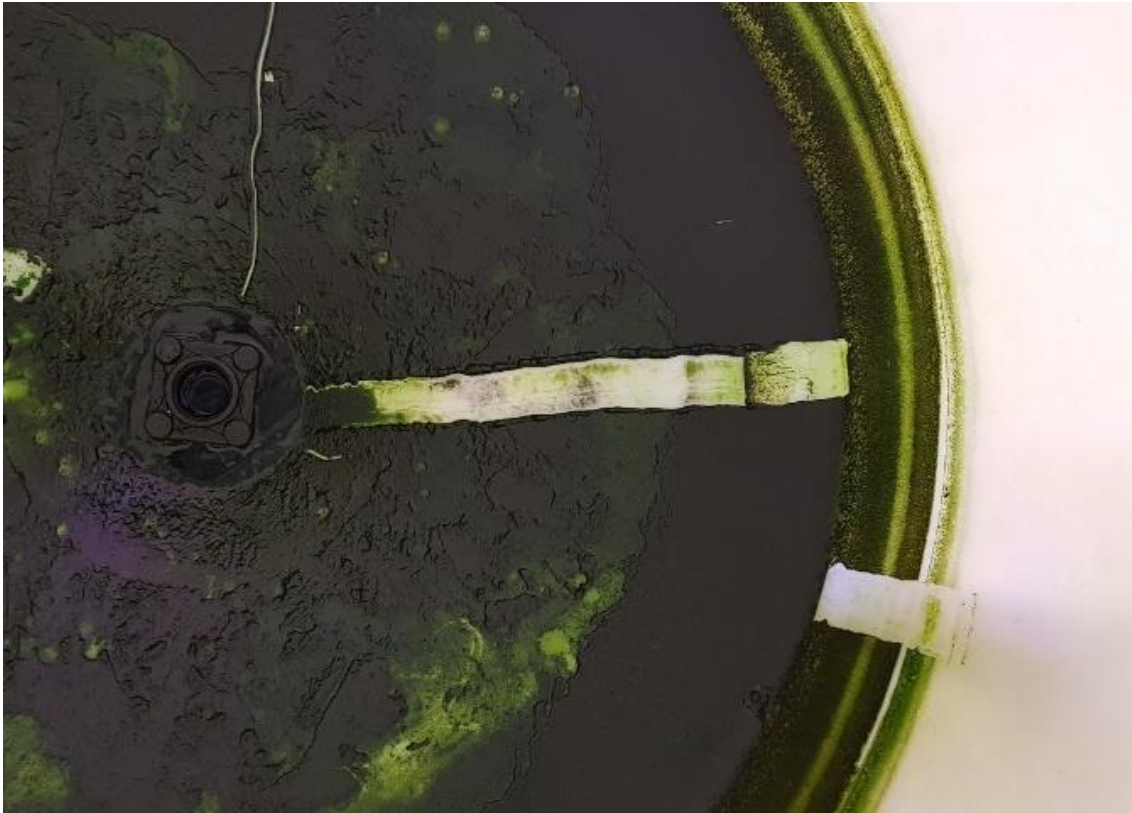
Figure 6-33 View of T1 from the top showing significant sedimentation occurring at the rim of the 60° conical section. Showing with two sampled sections.

Furthermore, mixing in the tanks occurs due to a light agitation from the reactor outflow into the tank and inflow from the tank, and sterile air being pumped at a rate of 3600L/h to all tanks by a Aqualine Hailea Aco-9820 High output air pump via a sterile 0.22μm filter, connected to a 1.5metre borosilicate rod with outlet diameter of 12mm. The rod being immersed at a depth of 1.3 metres from the tank's input, positioned at the centre of the 60^0 conical section.

The combined effect of both agitations is significantly reduced compared to the conditions in the reactor. This has resulted in significant sedimentation and settling in the reactor. Visual inspection after flushing the reactor system indicated that the mass of algae that was captured from sedimentation was significant. As seen in Figure 6-33, the top view from tank T1 at the end of experimentation there was thick paste forming on the side of the walls, localised at the joint caused by the intersection of the angled and vertical wall of the tank. In addition to that during

the flushing of the algae, there was a think biomass forming on the reactor tube walls (Figure 6-34)

To quantify this mass of algae serial sampling was carried out from tank, reactor and tube sections of known surface areas (i.e. sections of 1cm width with varying length, depending on location). It was calculated that the unobtainable biomass settled on in the system, amounted to 1082.8 gr. The identical procedure was carried out for the tank hosting the control experiment, from which a total of 16.47g was obtained.
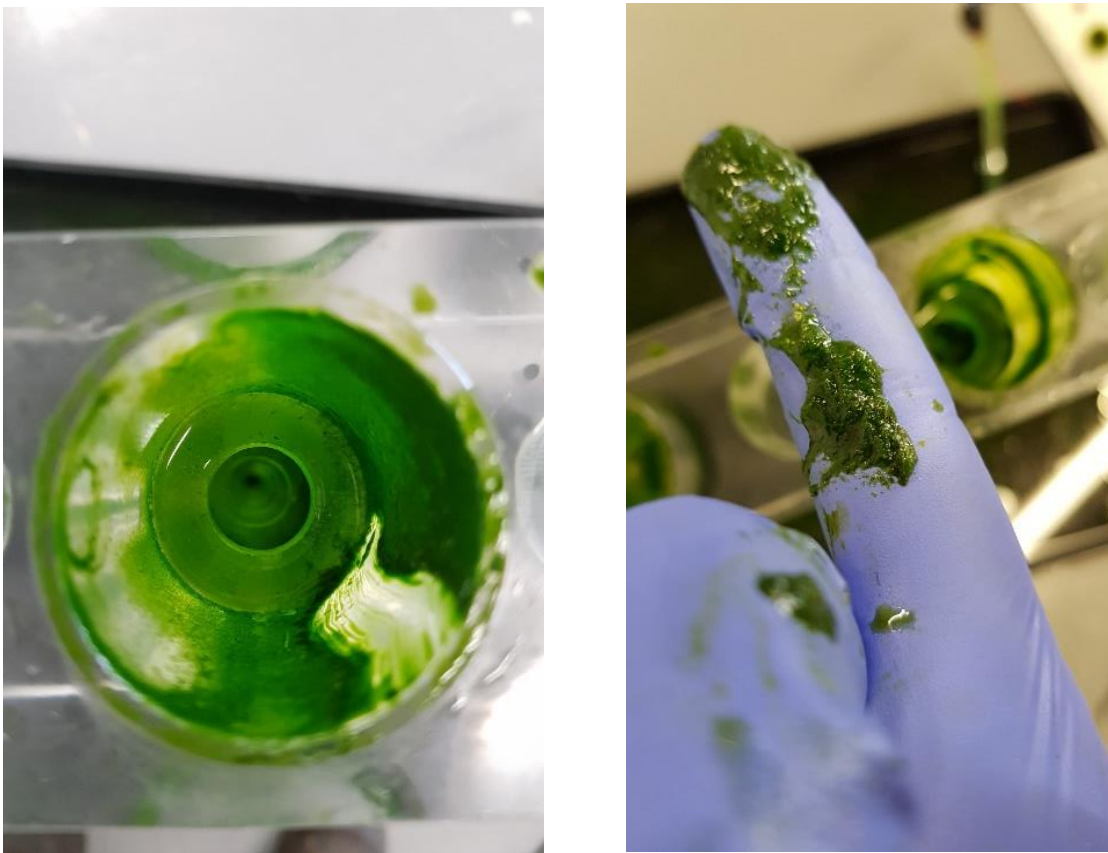
Figure 6-34 Algae biofilm forming during the flushing routine (no oscillatory flow present).

There is no practical way to determine when majority of the settling occurred. Tank T1, when through 16 days at 60L volume, 12 days at 110L volume and 9 days at 160 and 260L. Therefore, by erring on the side of caution it is assumed that uniform settling occurred throughout the whole duration of the cultivation. Which results in the generation of 23 g per day, with a culture concentration of

4.1 g/l, at a maximum productivity of 0.4g/l/d. Comparing it with the control where biomass generation is 0.24g/l/d at a concentration of 0.3g/l.
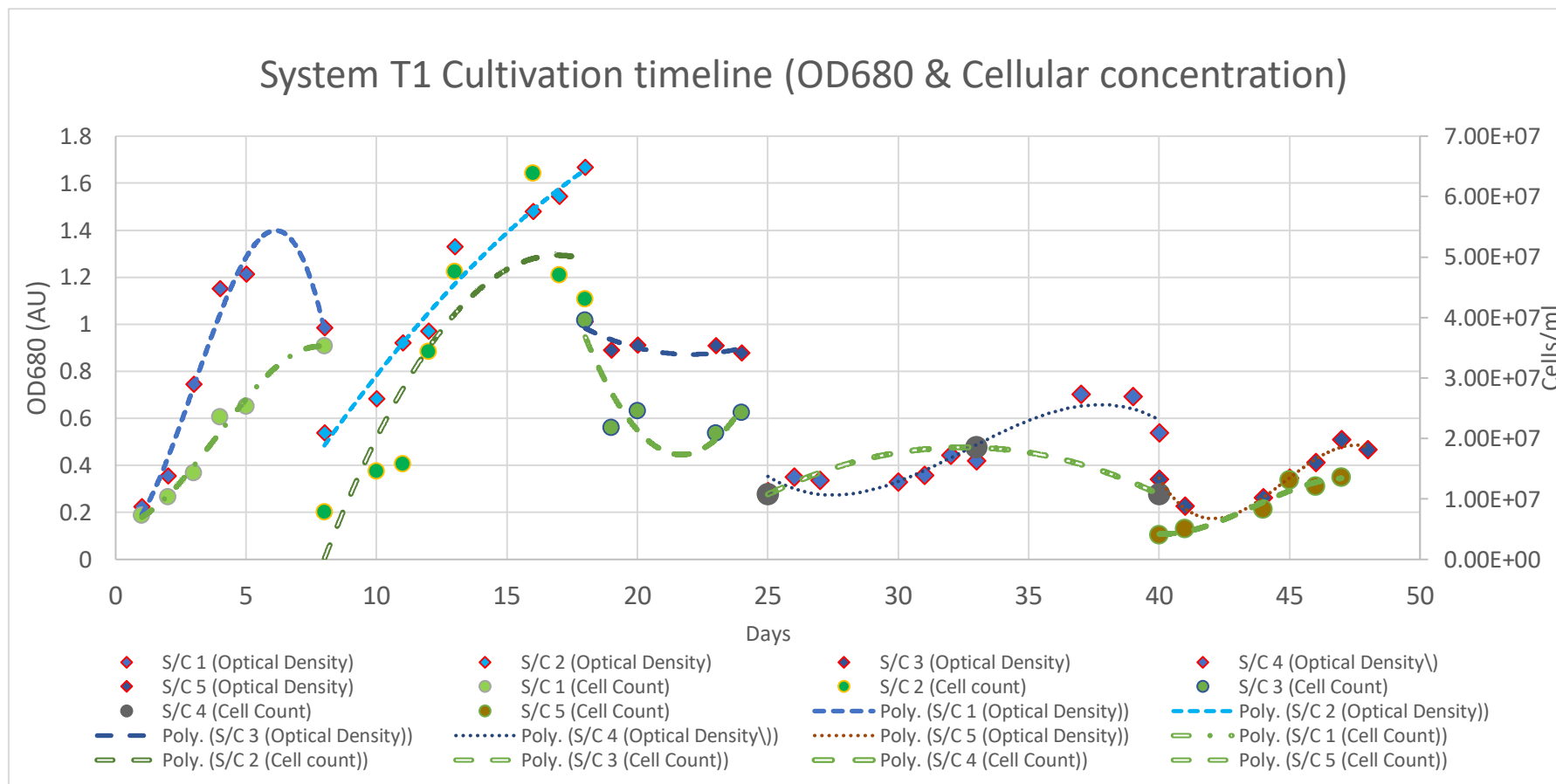
Figure 6-35 System T1 Cultivation timeline (OD and Cellular Concentration) shown for S/C1 – 5. Reduction of growth rate evident with increasing volume.
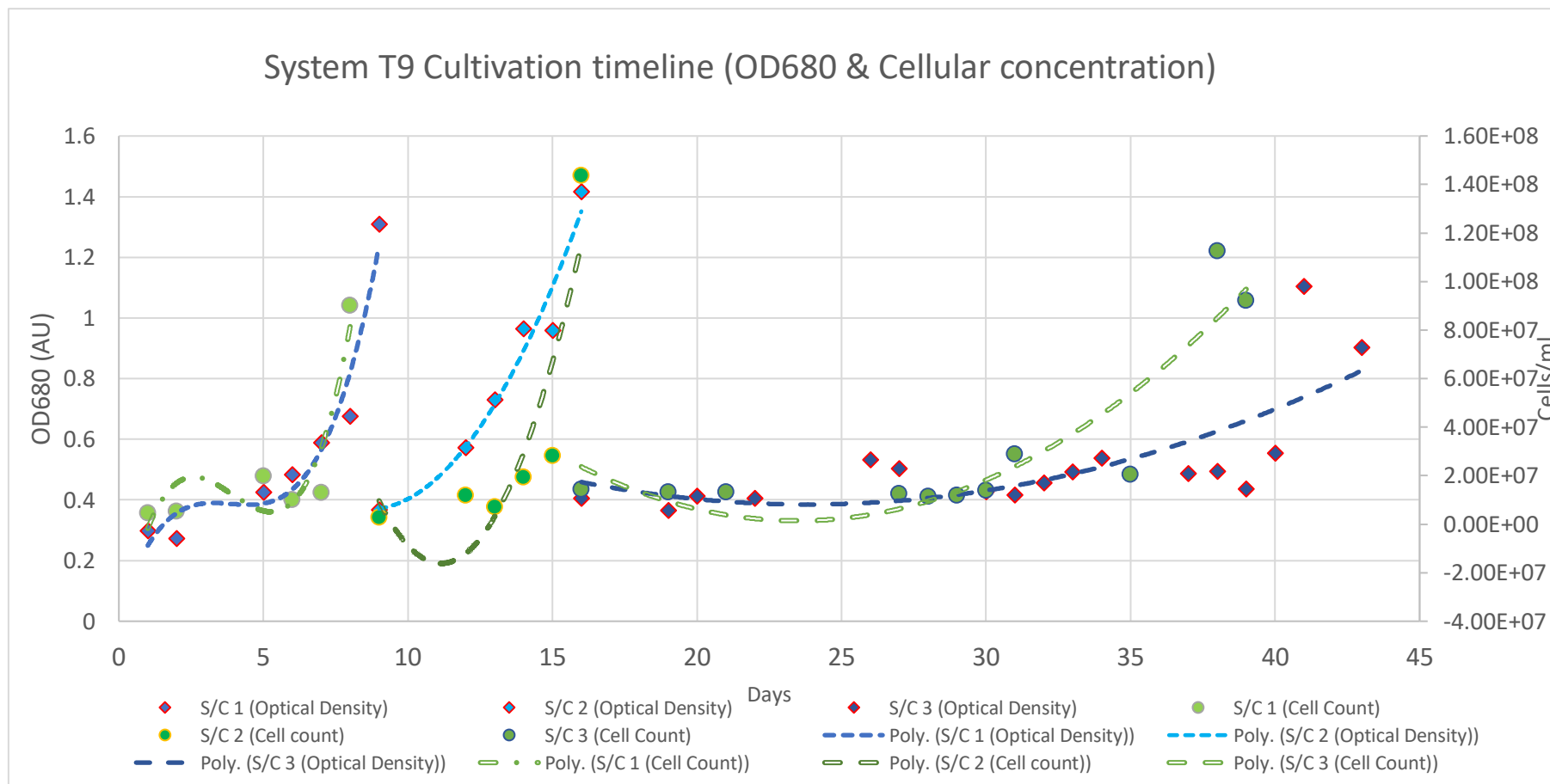
Figure 6-36 T9 cultivation timeline (OD680 and Cellular concentration) showing a clear reduction in growth rate after day 15 with increased cultivation volume.
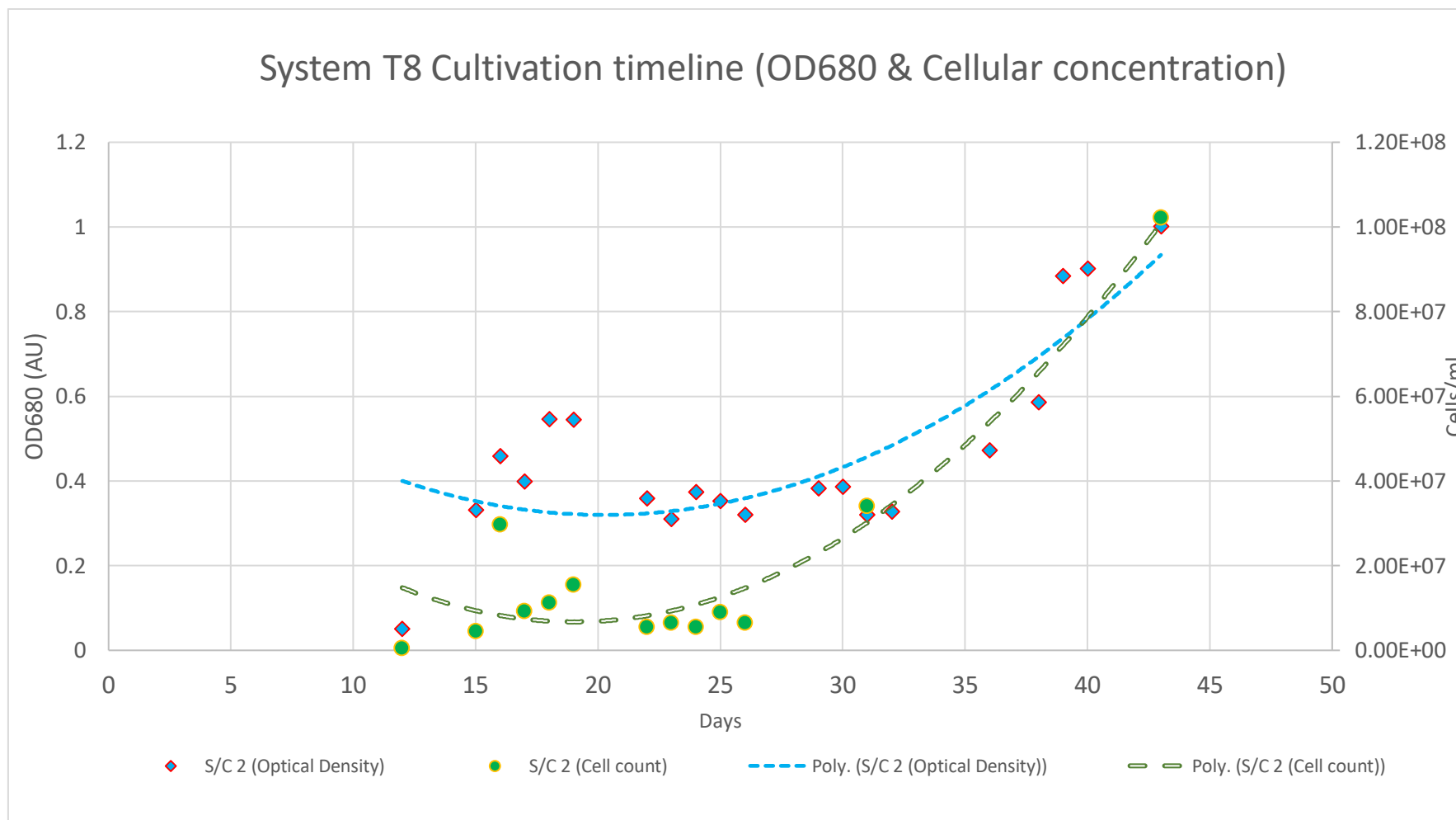
Figure 6-37 System T8 single subculture cultivation timeline showing slow growth throughout approximately 45 days.
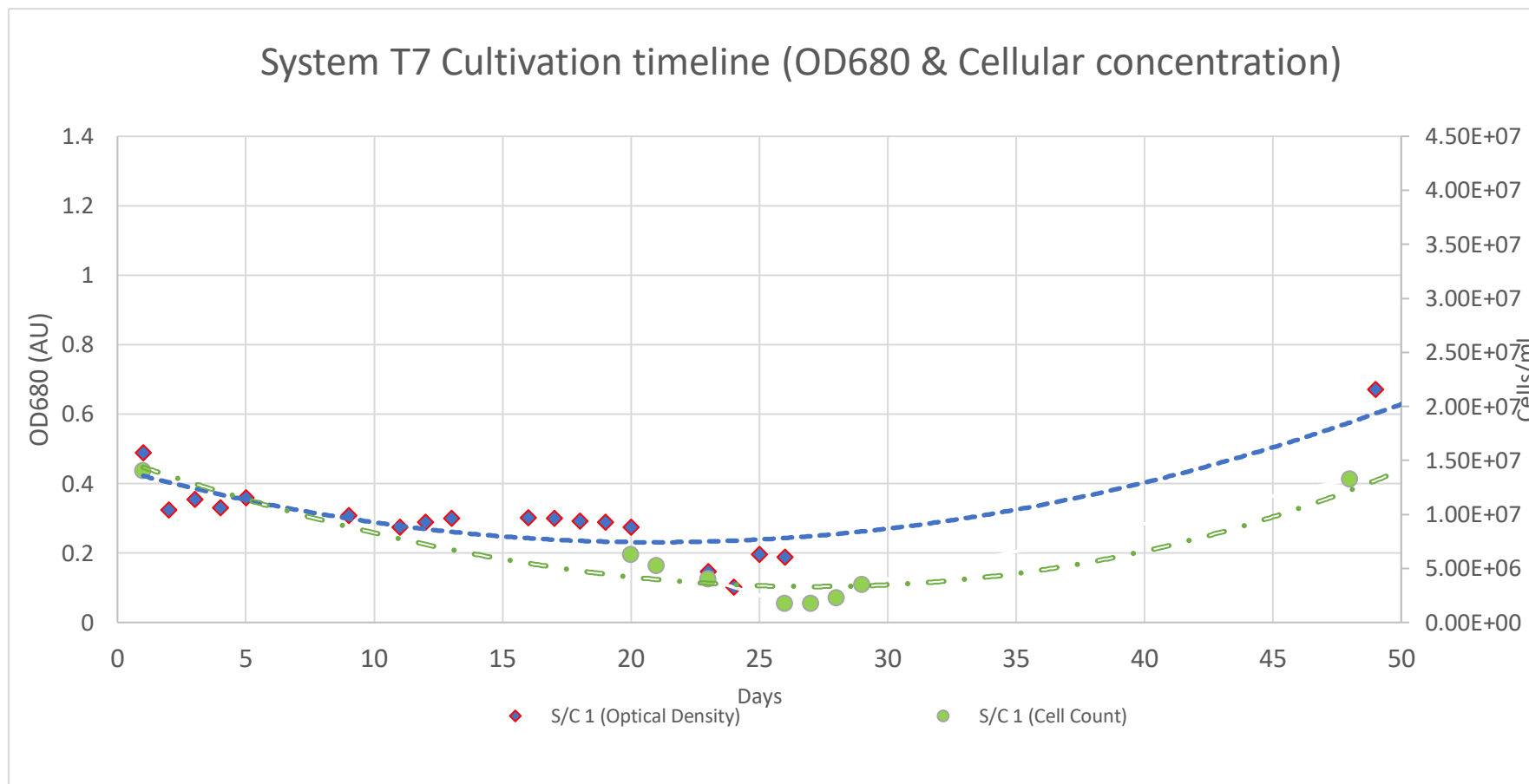
Figure 6-38 System T7 single subculture cultivation showing slow growth throughout approximately 50 days.
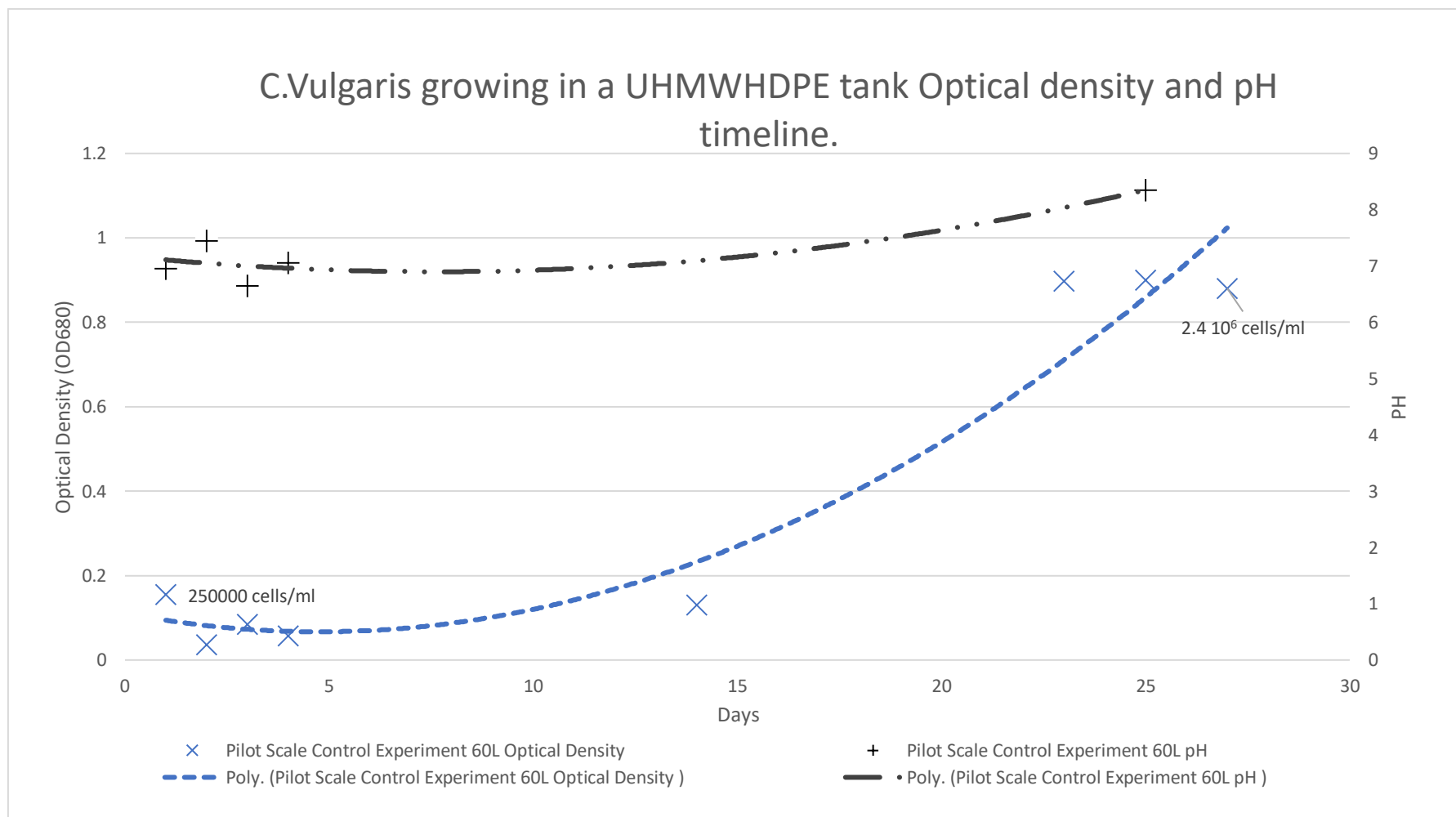
Figure 6-39 Control experiment, showing the cellular productivity of the culture in the HDPE tank without the presence of a reactor. Also showing the pH change in the reactor where no pH change indicates reduced metabolic activity from the culture

6.5.4 Discussion

As explained in section 6.4, the experiments are in chronological order of taking the technology outside the confines of a controlled environment and introducing it into a pilot plant, where system ramp up was introduced.

In summary the performance of the Centillion FP-OBpbR in cultivating *C.vulgaris* CCAP 211/11B, achieved biomass densities of 2.15 g/l and. biomass productivities averaging 0.45 g/l/d dry weight. at 10L scale. Ramping up the total cultivation volume to 60L the FP-OBpbR achieved biomass concentrations of 0.5 -1g/l.

Comparing these figures with literature at a comparable scale, using the same strain (Matos, Coeli, *et al.*, 2014) achieved a biomass productivity of 0.12 g/l/d, with a highest biomass concentration/density of 0.57 g/l. As cited by the same author, results for comparable systems, were found to be between 0.27 g/l and 0.57g/l. Similarly (Kumar *et al.*, 2011) reports biomass productivities of 0.14 g/l/d, which are lower all lower than the Centillion system.

Industrial examples of *C.vulgaris* cultivation are few and far between, therefore examples of productivities at large scale are not available. One of these examples of industrial scale cultivation of *C.vulgaris* in Klozte Germany, reports production rates of 25 $g/m^2/d$, using a serpentine reactor, the equivalent of this in volumetric terms is 0.5 g/l/d, which is very close to the centillion reactor's productivity of 0.45g/l/d. (Płaczek, Patyna and Witczak, 2017). Looking at other strains on the other hand gives an indication of biomass productivities in outdoor cultivation which range from 0.5 to 1.5 g/l/d (Chisti, 2007; Płaczek, Patyna and Witczak, 2017). A comprehensive list of studies concerning *C.vulgaris* is shown in Table 6-8.

Table 6-8 Comparison table of cultivating C.Vulgaris, at a range of scales and conditions.

Strain	Reactor Type	Scale (L)	Productivity	Yield	*Ref.*
C.vulgaris CCAP 211/11B	10L Flat Plate -Oscillatory Baffled PBR	10L	0.45 g/l/d	2.15 g/l at Day 7	Centillion Technology Ltd.
C.vulgaris (strain not specified)	6L Glass PBR (New Brunswick Bioflo 2000 Fermenter at 30C	5L	0.57 – 0.126 g/l/d	0.570 g/l max	(Matos, Torres, *et al.*, 2014)
C.vulgaris (strain not specified)	Serpentine (tube)	700,000L	0.5 g/l/d (25g/m2/d)	130t/year	(Płaczek, Patyna and Witczak, 2017)
C.vulgaris (strain not specified)	Coiled Reactor Tubular PBR (PVC Tubing - 25mm ID x 122 coils)	230l (150 Coil + 80L Holding Tub)	0.04g/l/d (Watanabe Medium) 0.024g/l/d Low N Medium	N/A	(Scragg *et al.*, 2002)
C. vulgaris F&M-M49	250ml Erlenmeyer Flasks 5% enriched CO2 at 25C, BG11 Media	100ml	0.2 g/l/d	N/A	(Rodolfi *et al.*, 2009)
C.vulgaris CCAP 211/11B	250ml Erlenmeyer Flasks 5% enriched CO2 at 25C, BG11 Media	100ml	0.17 g/l/d	N/A	(Rodolfi *et al.*, 2009)

Strain	Reactor Type	Scale (L)	Productivity	Yield	*Ref.*
C.vulgaris #259 UTEX	1L Bubbling Bottle with 200ml/min air supply under constant fluorescence light. Heterotrophic No CO2 only Air	1L	0.010-0.013 g/l/d	0.250-0.315 g/l at day 23	(Rodolfi *et al.*, 2009)
C.vulgaris #259 UTEX	1L Bubbling Bottle with 200ml/min air supply under constant fluorescence light. With 1% Glucose	1L	0.151-0.254 g/l/d	1.206-1.696 g/l at day 6	(Rodolfi *et al.*, 2009)
C.vulgaris #259 UTEX	1L Bubbling Bottle with 200ml/min air supply under constant fluorescence light. With 1% acetate	1L	0.079-0.087 g/l/d	0.898-0.987 g/l at day 12	(Rodolfi *et al.*, 2009)
C.vulgaris #259 UTEX	1L Bubbling Bottle with 200ml/min air supply under constant fluorescence light. With 1% Glucose	1L	0.151-0.254 g/l/d	1.206-1.696 g/l at day 6	(Rodolfi *et al.*, 2009)

6.6 Chapter conclusion and discussion

6.6.1 Overview

This chapter focuses on the development of a scaled-up version of the Centillion Oscillatory baffled flow photo-bioreactor. Having conducted successful experimentation with a mesoscale system, the key focus on the task was to develop a reactor form factor which would enable cheap construction, easy assembly and low-cost maintenance.

Keeping the core design feature of the reactor identical between scales, allowed the adoption of a scale up strategy based on geometric similarity. Since the reactor was still an OBR, it meant that as long as the dimensionless number is kept similar between scales mixing performance is maintained.

It was quickly evident that by keeping the same form factor, there would be challenges in material and construction. Therefore, a complete redesign of the shape of the reactor was carried out, based on progressive design criteria which were nucleated by the ethos of the newly formed company. i.e. modularity, decentralisation, and disrupting the convention. Resulting in a final design, shapes what is essentially a tubular photobioreactor, as a flat plat reactor. Thus encompassing the benefits of both systems, which coupled with the oscillatory flow regime, minimise the drawbacks (wall growth, volumetric dead zones, high energy and lighting costs).

The development of a system around the newly shaped reactor was facilitated by the development of the mesoscale system. However critical unforeseen issues did arise, which required different solutions, most importantly the pumping, where the peristaltic pump was not a cost-effective option considering the flowrates and processing volumes required. In addition to this each component was selected on the basis of maintaining a very wide field of operational parameters, which would complement the modular nature of the reactor.

Characterisation of the system was carried out based on the methodology developed for the mesoscale reactor. The purpose of the experiments where not to develop models, which would be extremely useful, but to evaluate the mixing

performance of the reactor. It was found that no comparable OBR tracer experiment study exists in literature, which utilises such high net velocities and amplitudes as this system. This was even more encouraging when the resulting performance metrics (TiS) produced for specific combinations were higher than published figures in equivalent systems.

Experimenting with the reactor produced encouraging results, outperforming most comparable systems, in growing cultures, but also having benefits from a process perspective with a very low level of fouling, coupled with high operational integrity. Where a rector system would operate for 90 days continuously and 120-160 days intermittently before requiring maintenance.

In summary, the Centillion reactor system offers a modular, flexible photobioreactor which enables the growth of axenic cultures. Due to high degree of parametrisation it can modify the environment to host a range of different algal strains. Due to its mixing regime, and smart light modulation (patent pending), it can intensify and accelerate growth, as demonstrated with a 10 Litre system. Its performance in producing biomass is consistently better in both scales in direct comparisons, and very competitive when in comparison to large scale systems, which operate other strains of algae.

From an industrial point of view the Centillion FP-OBpbR can evidently process 50L to 100L volumes per 10L reactor, without any significant inhibition to the growth rate. Comparing this configuration with a very successful commercial example, the phycoflow 400L system, demonstrates the Centillion reactor's potential spatial advantage. (Varicon Aqua, 2019). The phycoflow 400L system commands a space of $5.4m^2$ and $13.5m^3$. In this space it cultivates a maximum of 400L. Occupying the same space the Centillion system can process a total of 780L in an arrangement of 13 stackable systems as shown in Figure 6-40, clearly demonstrating its commercial appeal.
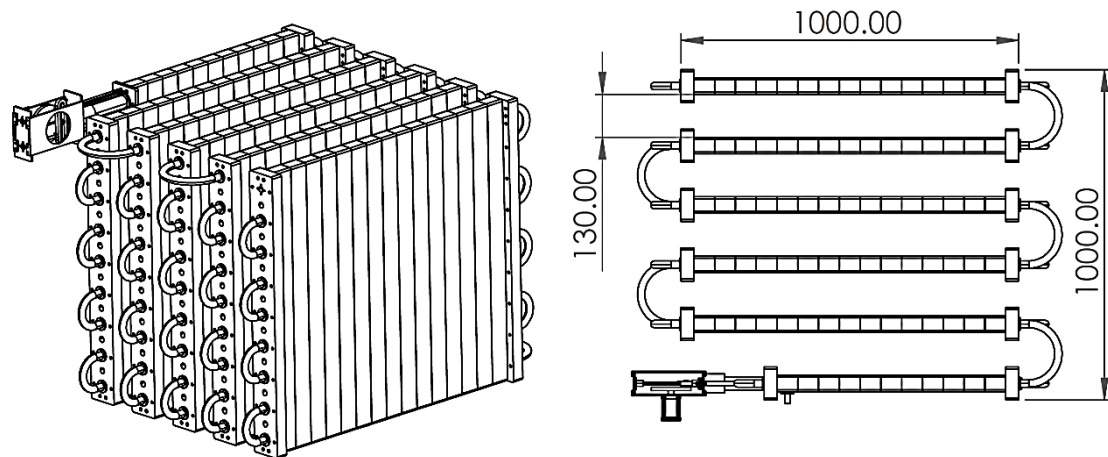
Figure 6-40 Scaling out the Centillion FP-OBpbR system to a 1m³ stackable modular system of 60L system
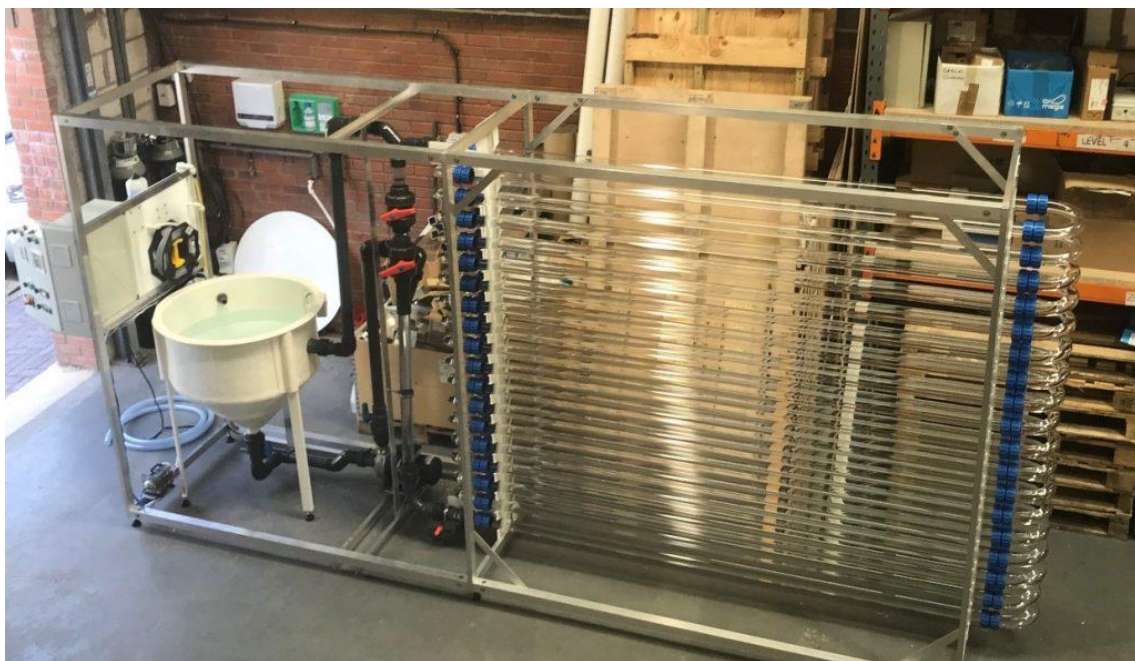
Figure 6-41: Varicon Aqua 400L phyco flow system (200L Tubular + 200L Holding Tank (Varicon Aqua, 2019).

6.6.2 Bioprocess Operational Challenges

The benefits of the system are clear, however this being a prototype there were issues that still requiring solutions an outline of the issues is given below.

6.6.2.1 Mechanical / Engineering
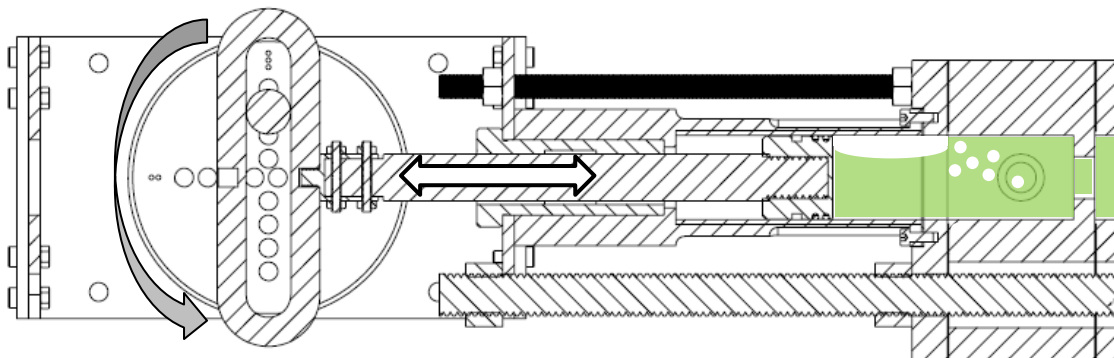
Figure 6-42: Cross Sectional View of the oscillatory mechanism and reactor inlet region. Showing in green, the bubbles coalescing on the top end of the plunger section.

The motor selected for the oscillatory mechanisms (Sanyo Denki 103H7 Bi-polar stepper motor), has a max current of 4A, and max torque of 2.1Nm. It was chosen for this system due to its performance, price, size and durability. It is used on the SYOM mechanism for the mesoscale and kilo scale chemical reactor.

Under operation it was observed that under upstroke the presence of any bubbles pulled into the system by the suction from the tank, or from the system, depending on the orientation of operation, would merge into a large bubble which created a momentary dry-spot, which increased the friction between o-ring and tube on the affected area, cause the plunger rod to misalign which caused the roller link to shudder, pushback and jam the system.

6.6.2.2 Material/ Component Failure & Deformation

The oscillatory mechanism design used for scaling was based on the SYOM, albeit modified slightly, so that it can be mounted on the narrow frame of the FP-OBpbR. The motor used to induce the oscillations was the same motor used for the SYOM system. As mentioned, its performance to price ratio was competitive, and at the time of writing its's the only NEMA 56 form factor stepper motor

capable of producing 2.1 Nm of torque. The plunger/tube assembly shown in Figure 6-43 are the only wetted parts of the oscillatory mechanism, therefore they are manufactured out of PTFE, Viton and acrylic or polycarbonate for the plunger, O-rings and tube respectively. The contact point between tube and plunger is made by three Viton O-rings. Two of which are the primary point sealing, however are designed with a small cross-sectional area to provide a small contact surface area allowing for smooth unrestricted movement, and the third o-ring is larger and placed further to the back and is primarily there for sealing. From a design point of view this is the weakest part of the system. As is evident by Figure 6-43. After approximately two months of continuous operation the tube was prone to pitting. Where the material under reciprocating contact with the o-ring would gradually abrade. Similarly, the plunger o-ring was prone to abrasion, albeit not at the same rate as the tube. For the plunger o-ring, the critical factor affecting its durability was the ratio of alcohol used during sterilisation. It was identified, that when the ratio of IPA to diH_2O increased beyond 25%, the o-ring would lose its elasticity and disintegrate.

Figure 6-43 (Left) Polycarbonate Tubing section showing evidence of pitting, (Right) Disintegrated orings on the PTFE plunger after very long periods of use.

6.6.2.3 Biological

Fouling is a very common occurrence in photobioreactors. In the mesoscale Centillion reactor the fouling was almost undetectable, in the larger scale on the other hand fouling was a growing issue.

Fouling in the scaled-up version was observed in random sites on the reactor system albeit more prevalent in the flexible silicone, and vinyl tubing as well as the polycarbonate hard tubing, than the main light harvesting section of the reactor. On the main light harvesting unit, the fouling nucleation points, were predominantly on the edge of the baffled conduit the sharp 90° area was prone to bubbles being trapped thus interrupting the flow and causing localised fouling spots. Other fouling areas would be on the polypropylene ¾ inch BSP tail hose fittings, where the often-rough edges on the fittings would protrude into flow path. And finally, sporadic biomass accumulation on the baffled conduit at random locations in the conduit itself as well as the reactor.

This is beyond reasonable expectations. As indicated by literature, when the flow regime approximates plug flow, mixing occurs only in radial direction; where mixing is localised in areas of intense micro mixing close to the walls, thus minimising areas where turbulence is close to zero causing dead spots which are prone to fouling. This means that if the oscillatory flow is dominant and thus when high TiS numbers are achieved no fouling should be observed. This is the case with the mesoscale reactor, which was the main reason fouling was evident in areas which were not under oscillatory flow (pump input and output tubes, etc).

Therefore, assuming this is valid, attempts to verify whether there are inconsistencies in the flow across the reactor, were carried out. These were conducted by slightly altering the sub culturing protocol. Upon normal operation the subculture of the reactor would encompass the gradual harvesting and fresh media input at equal volumetric flowrates over a duration approximately 10 times that of the photoperiod. The difference in protocol, was to input the complete dilution volume in one go, simulating a pulse injection of tracer. With this achieved there was an evident plug being formed and pumped through the reactor. Any disruption to the plug should coincide with the sections of the reactor which would

foul the most. As shown in Figure 6-44 the tracer did not disperse and was contained to 9 baffled sections throughout the whole reactor path, finally being disrupted at tank of the system. Further investigation showed that air may be the culprit. The system was set up with great care to avoid bubbles being injected to the system, however being a photosynthetic organism the expulsions of O_2 was carried out continuously. As shown in Table 6-9 , tracking a single section throughout showed that within 36hours bubbled would generate and transform into areas which disrupt the flow, and trapped in the corner by the net flow. The locations where this occurred the most coincided with the baffled sections with the most fouling.

Overall the methodology used in this series of experiments is identical to that carried out at smaller scale, which in turn, is inspired by already published batch protocols. In this series of experiment, operational challenges were present due to the change environmental conditions, when moving from laboratory to pilot plant, (e.g. temperature and contamination control). Despite these challenges, as the results demonstrated all cultivation operations where carried out successfully with growth occurring in each subculture.
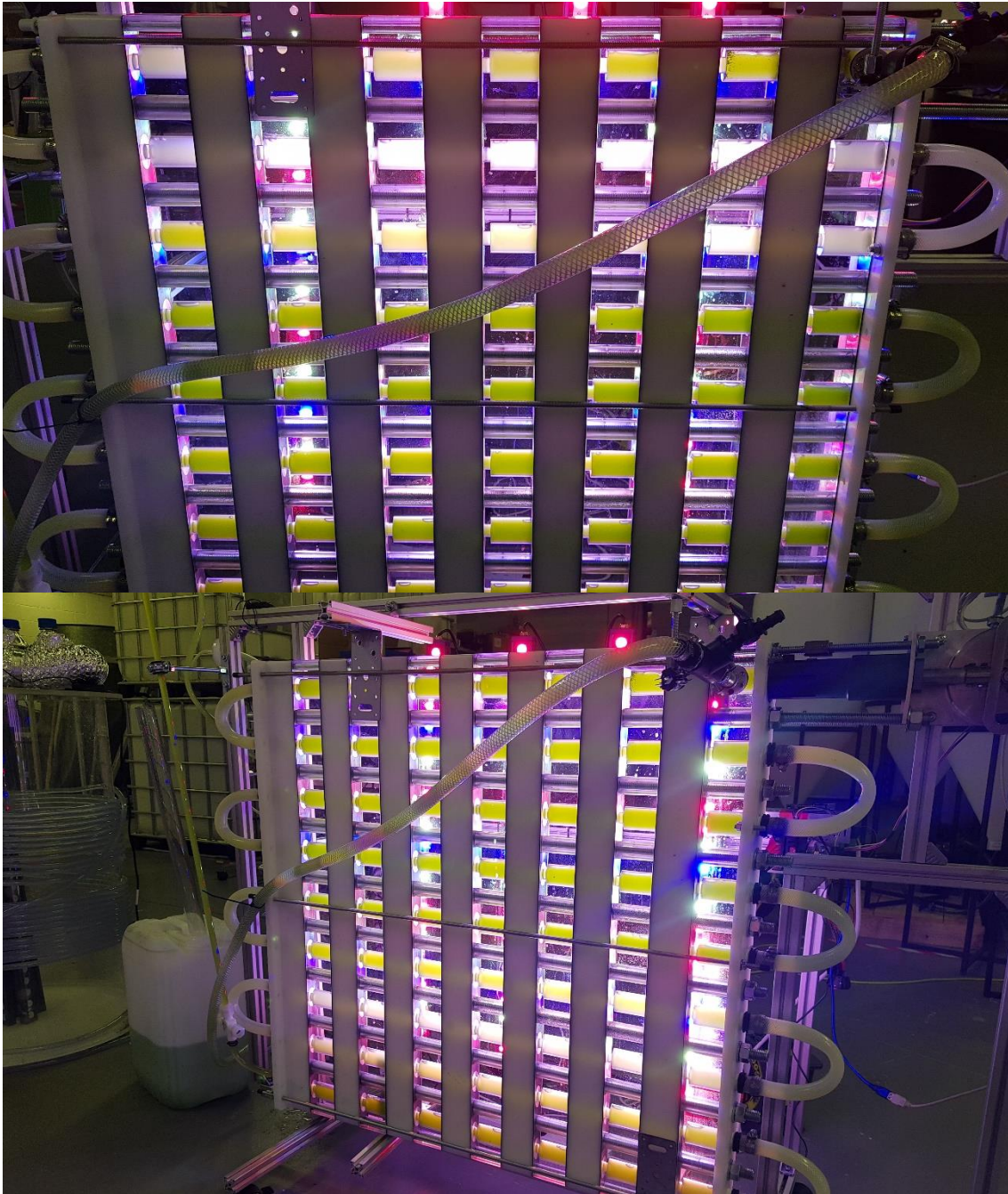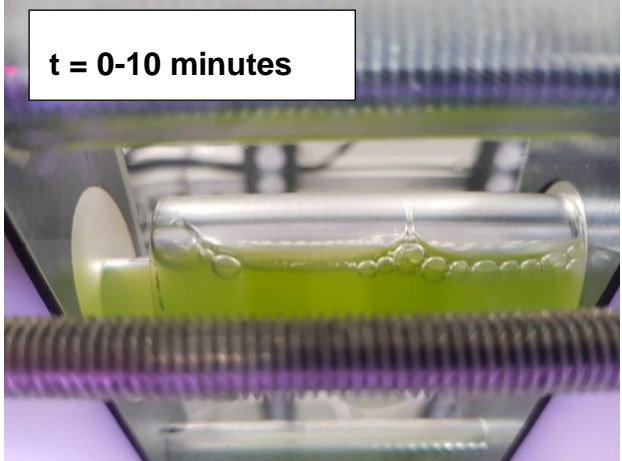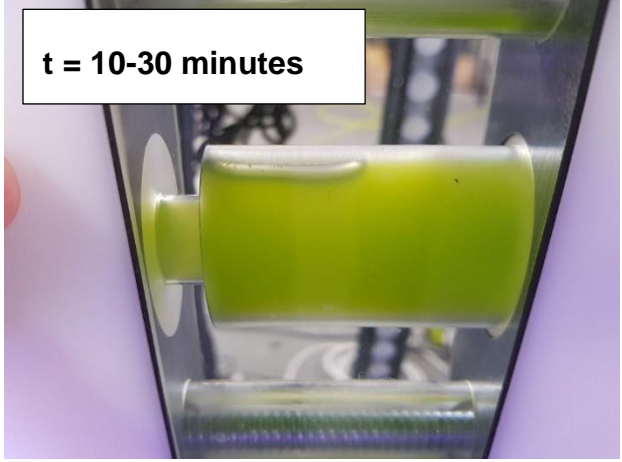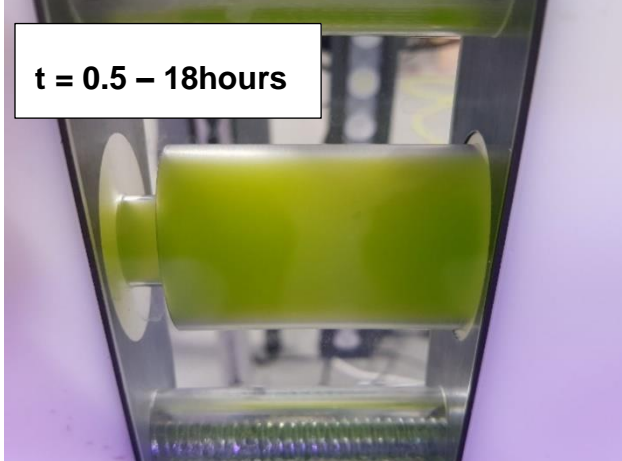
Figure 6-44 Plug flow verification during operation Flow from bottom to top, with the bottom figure showing the tracer contained at the third baffled passage, and the top picture showing the tracer at the 8th baffle

Table 6-9 Bubble coalescence timeline, from priming to bubble entrapment in the baffled area.

Picture	Description.
t = 0-10 minutes	During priming, or if for any reason air gets into the system, it pools into a baffled channel, as in the picture. This is ejected via oscillations and a net flow which pushed the bubbles towards the exit.
t = 10-30 minutes	Gradually the volume occupied by the bubble is reduced, due to compressibility of air, or due to the system ejecting bubbles effectively.
t = 0.5 – 18hours	When the system is primed, the air is ejected, and al baffles look like this.
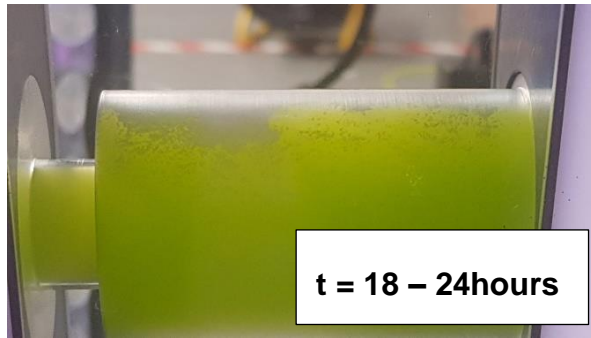
t = 18 – 24hours | After 10-14 hours (as typically observed in the morning) there are spots n the top side of the baffled tube, which are coalesced by micro bubbles which are attached the other surface of the reactor. |
|
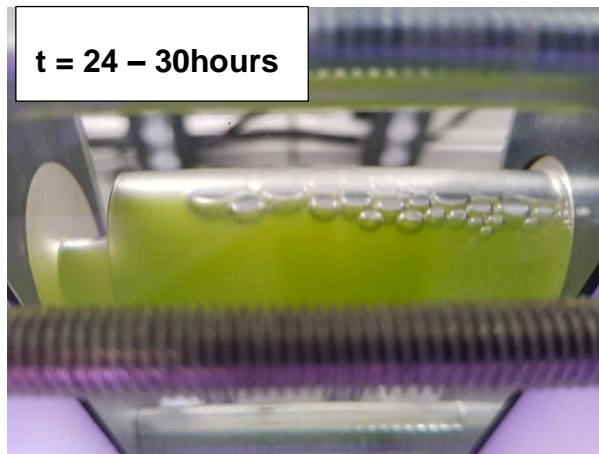
t = 24 – 30hours | After a while if the system remains under the same parameters the bubbles grow and coalesce capturing a larger volume. |

7 Conclusion

The overarching aim of this research was to develop new routes for the bioprocessing of algae in industrial scales. This was achieved with the development of a multiscale novel continuous flow photobioreactor platform which enhances and accelerates growth in *C.vulgaris* cultures as well as the development of a cost effecting media formulation which not only does it avoid growth inhibition but also enables algae to systematically achieve high culture density.

In addition to the accomplishment of the objectives, the main contributions of this research are:

1. An exhaustive review of current PBR systems, their operating benefits and limitations.
2. The generation of knowledge, specifically in identifying the critical design considerations of current lab scale and commercial PBR applications.
3. The design and development of algal handling methodologies, culture scaling and batch to flow protocols, from lab to pilot volumes, specifically tailored for flow technologies.
4. The design of a low-cost nutrient formulation for the *C.vulgaris* algal strain, which results in a ten-fold cost saving per litre of culture.
5. The design, development, characterisation of two novel flow photobioreactor systems. One at mesoscale and the other at kilo scale. Currently commissioned and operating at the Centillion Technologies Ltd. Cranfield pilot plant.
6. The identification of optimised process parameters for the cultivation of *C.vulgaris* in the Centillion OBpbR and FP-OBpbR. Developed from a combination of experimental methodologies, statistical data analyses, and predictive model development using established tools and methodologies such as DoE and Least squares regression.
7. The configuration and development of a pilot plant, operating a 9000L capacity bioprocessing line using four FP-OBpbR reactor systems for the scaled indoor cultivation of microalgae.

8. The development of a intellectual property, leading to a patent application for a novel continuous photobioreactor (Makatsoris and Alissandratos (2019).

9. This research is part of the portfolio assigned to a Cranfield spin out company and is being considered for commercialisation by the Centillion Technology Ltd.

The research was initially carried out following a set of interdisciplinary objectives, which combined manufacturing systems, process systems and reactor design and development, statistical modelling for predictions and biology considerations, and defined the scope of this work. The research was organised into two major phases, laboratory exploration and process design followed by a second phase for the design and demonstration for pathway to industrial deployment. The key findings, novelties and key contributions for each phase are going to be presented separately.

7.1 Process design at the Laboratory scale

At laboratory scale the work covered these three areas:

- The selection of a suitable algal strain and the design of media customised to the strain itself.
- The design of a scalable PBR system, based on the mesoscale continuous flow OBR reactor technology.
- The transfer of the batch cultivation protocols into flow.

The first objective was concerned with the selection of a suitable model algal strain that is relevant to industry. Other section criteria were drawn from the literature as there are no standard bioprospecting methodologies or industrial best practice at present. This resulted in the selection of *C.vulgaris* as the experimental strain. Based on the literature, its characteristics and robustness in surviving in adverse conditions made this strain a suitable candidate for this research. Then, a media formulation was developed with the aim to maximise the productivity of this strain and fit the processing technology selected. For this, the elemental makeup of the *C.vulgaris* cell was investigated using a DoE

strategy, which highlighted three critical nutritional elements. This approach led to optimisation of the media formulation that led to the following three key results.

1. A cost saving in the media from 0.04 £/l to 0.0046 £/l.
2. Accelerated growth rates (μ) and higher biomass productivities (P_x), for *C. vulgaris* grown in batch protocols using he centillion media.
3. More than ten-fold cost saving in the cost per kilogram of biomass, from 37£/kg to 2.1£/kg, compared with BBM.

In addition to the above, the optimised media, had reduced dependency on high purity chemicals and reduced number of components from 13 compounds to 6, which facilitates the hardware and process design of PBRs. In addition, the study of glycerol as part of the media formulation has not yet been reported in literature. This adds novelty to the work, since the complex interdependencies of the nutritional compounds (N,P,K,C, etc) are not understood to a degree which justifies them being studied separately. It is noteworthy, that the cost performance was consistent and validated systematically throughout the research. It is also worth noting that better productivities were observed at times, that led to even better cost performance, but these were treated as outliers as they were not systematically observed.

The design of the reactor system, followed a conceptual design approach, starting from identifying critical design considerations of the current state of the art in PBR systems. Building on technology available in the research group and combining these, a design specification for a new and novel PBR design has emerged. These steps ultimately were combined to obtain a systematic design methodology, which focussed on optimising three main design criteria, namely containment, light and mixing:

- Containment: The new photobioreactor design was based on the patented modular continuous oscillatory baffled flow chemical reactor belonging to the Makatsoris Group at Cranfield University. As described in section 5.2. The core element of the reactor was redesigned, to optimised it for bioprocessing of photosynthetic microorganisms (microalgae). This was carried out by redefining the shape of the module from a disk to a torus,

with the inclusion on additional design features which increased volume, ensured uniform light distribution and implemented internal temperature control.

- <u>Light:</u> Considered as the most important design consideration light supply and light modulation (light cycle) were studied extensively. Light cycle control was achieved by implementing light and dark sections along the fluids path. These alternating light and dark region were enabled by taking advantage of the reactor's modularity, whilst the highly controllable mixing regime (plug flow) ensured that all the culture experience uniform and periodic lighting conditions. This effect was studied by carrying out an extensive DoE which focused on studying the effect of the cycle time (s) in both high and low mixing intensities. As described in section 5.1 there was an evident increase in growth rates in the light cycles of approximately 56 second, this result was replicated with additional experiments carried out in two mixing intensity scenarios. Moreover, two fitting models (R^2=0.7) were developed from these experiments, used to predict the growth rate of *C.Vulgaris* by inputting a light cycle time. This work resulted in IP which is currently being filed for patent protection (Makatsoris and Alissandratos, 2019). In terms of light supply custom made high intensity low cost LED light bars, emitting in the red (640-660nm), blue (407-465nm), white (480-650nm), and infrared (740nm) regions of the light spectrum, was selected as the light source. As described in section 5.1.3 extensive experimentation and testing using spectrophotometry and PAR units, was carried out to identify the most suitable light arrangement. This resulted in characterising the light supply on the reactor shown in Figure 5-11.

- <u>Mixing:</u> Conventional mixing techniques in PBRs involve gas sparging agitation, and pumping. These as analysed in sections 2.2 and 2.3 are highly ineffective, costly and non-scalable. By implementing continuous flow technologies such as the OBR, into algal biotechnology introduces a new method of mixing which is inherently controllable, scalable and cost effective. Two challenges were faced in implementing this mixing regime into algal bioprocessing. First the development of a robust oscillation

mechanism capable of long-term operation, which considering the algal cultivation cycle periods, meant continuous operation for weeks and months. Secondly the characterisation of the flow in the reactor which would ensure that the appropriate parameters are selected so that flow is effective. To overcome these challenges a custom oscillatory mechanism was designed and built, based on the operation of a scotch yoke mechanism. This mechanism operated and controlled by a single stepper motor, capable of achieving robust and true sinusoidal motion, which is critical for oscillatory flow. With the mechanism in place, the characterisation of the flow was carried out using residence time distribution (RTD) studies. The actual experimentation and RTD curve analysis wat not in the scope of this thesis, however the analysis of the data produced was. The data table produced by the RTD studies comprised of 200 experiments carried out in two different reactor scales (micro and meso). Analysis of the data table was carried out aiming to create a statistical model capable of predicting the tank in series (TiS) number on a given parameter set ($Xo, f, \dot{f}, u, D$). The analyses resulted in the development of a multiscale prediction model ($R^2 = 0.71$). This study derived that, in the case of OBRs, the process parameters ($X_o, \dot{f}, f$) and the dimensionless numbers (Re, Re_o, ψ, St) are accurate mixing performance predictors, with the latter group performing marginally better. In addition to this parametric analysis concluded that the amplitude (X_o) and Strouhal number (St), where the biggest contributors to change in mixing, with the velocity ratio (ψ) and Re_o being close second and third. The predictive capability of the model was tested against the experimental values in Figure D1 to D3.

All the system subcomponents were assembled into a novel system described in section 5.5. This section comprised two major group of components, the hardware, and the control protocols. Specifically, the optimised disc, oscillatory mechanism, lights, online monitoring tools described in 5.4, and the mixing and light control protocols (models) aiming at creating appropriate process parameters that accelerate growth. Therefore, extensive experimentation was

carried out in batch and semicontiguous flow at laboratory scale, with the following key results:

1. *C.Vulgaris* grown in batch cultivation under oscillatory flow was compared to continuous circulation with only net flow, resulting in a much faster growth cycle. This conclusion was derived due to the culture reached stationary phase in 10 days compared to 22 days, without the oscillatory flow imposed. Whereas no major change in biomass concentrations were reported, with 0.05g/l difference between the two cultures.

2. The C-OBpbR system consistently enabled the *C.vulgaris* to grow at faster rates and high productivities. In fact, comparing the 1st and last cultivation cycle operating in semi-continuous mode, with the one under net flow, shows that the oscillatory regime achieves more than double the increase in biomass concentrations.

3. Comparing the growth using the BBM and CM media, shows that the latter consistently overtakes the BBM performing up to 64% better according to the cell densities, in the same time period under comparable conditions.

4. In contrast the biomass densities and productivity trend achieved between BBM and CM do not seem to differ much. The biomass densities ranged between 1.65 and 2.8 g/l in 8-10 days of cultivation.

5. The cost of using CM is over an order of magnitude lower than the cost of using BBM. Which is translated to a cost per unit biomass of 0.0018-0.0020 £/g in comparison to BBM which is 0.022-0.028 £/g in the oscillatory baffled flow photobioreactor.

6. This translates to a price per kilogram biomass of 3£/kg for the Erlenmeyer flask bubble system compared to 1.8 £/kg in C-OBpbR.

7. In comparison to similar scale experimentation in literature this system performs consistently better achieving higher growth rates (μ) and biomass concentrations.

7.2 Scale up and pathways to organism cultivation at industrial scales

Scaling up the system to pilot, was carried out by adopting a scaling rationale of maintaining geometric similarity. Three different scaling scenarios were considered (22,36 and 50mm) with the 36mm size, selected based on considerations such as cost and spatial requirement. However, during the design process of the pilot C-OBpbR, it was evident that material costs would prove to be inhibitory, considering traditional manufacturing methodologies. Therefore, a completely new design was established inspired by plate reactors. In doing so the disk shape was transformed into a rectangular shape, as shown in figure 6.3. The new reactor (FP-OBpbR) system design was carried out using the same methodology as that at laboratory scale. The light supply and light cycle were implemented using the same approaches, with the transparent and non-transparent segments, using the same scotch yoke mechanism approach a new oscillatory mechanism was developed for the larger flow path and finally a series of tracer experiments were carried out based on the same methodology as outlined in literature. Although this study was not comparable with the detail, of that carried out in smaller scale it acted only to identify suitable parameter combinations which enable high performance mixing to be achieved. The results from the study are summarised with the following points. First of all, there is a substantial increase in mixing performance, as is shown by the higher TiS numbers. Second, there is no comparison with literature as no report has been made, that carries out RTD studies with such high mixing intensities (Re, Re_o, ψ), and lastly, compared with the microscale reactor, the scale up using geometric similarity indicated to be successful, with a very similar mixing performance achieved for similar Strouhal numbers between the micro and kilo scale.

Following the development phase, extensive experimentation was carried out in the FP-OBpbR system, in three different situations. First in a laboratory environment at 10L scale, second in the pilot plant environment operating in semicontiguous mode with optimised process parameters, and finally at large scale with 60-260L volume. In summary the performance of the Centillion FP-OBpbR in cultivating *C.vulgaris* CCAP 211/11B, achieved biomass densities of

2.15 g/l and. biomass productivities averaging 0.45 g/l/d dry weight running at 10L volume. Ramping up the total cultivation volume to 60L the FP-OBpbR achieved biomass concentrations of 0.5 -1 g/l. Comparing these with literature makes the case evident that the FP-OBpbR achieved systematically higher productivities as was shown in comparison with the exhaustive list of results in Table 6.8. In addition to the performance in cultivation, the modularity of the FP-OBpbR system itself is compared with industrial examples of PBRs, at comparable scales. It is found that using the same metric for volumetric capacity per spatial footprint as they use in industry, the FP-OBpbR in a stacked configuration of 6 reactor achieves a ratio of 60L/m^2, which compared with the Varicon aqua phycoflow system at 36L/m^2 is higher. In addition to that considering the volume of space the reactor system occupies, in 13.5m^3 the Varicon Aqua achieves 400L, half of which comprise of the light harvesting unit, in comparison with the FP-OBpbR can achieve 780L light harvesting volume.

With both platforms (laboratory and pilot plant) built and assessed the aim and objectives of this study have been achieved. A novel scalable photobioreactor system has been developed based on the oscillatory baffled flow reactor technology, which has proven very effective in the low cost, controllable and highly productive cultivation of the microalgal strain *chlorella vulgaris*. From this thesis, three key pieces of technology have been developed, a meso scale C-OBpbR, a kiloscale FP-OBpbR and an algal bioprocessing line with a maximum working capacity of 9000L. In addition to that there is also substantial scientific contribution with the investigation into light cycles and the development of a high-performance cost effective mixotrophic nutrient mix.

7.3 Further work

This research has also created a platform on which multiple opportunities for future studies to take place. From an engineering perspective, considering that these reactor systems are prototypes, there is ample space for improvement, in the aspect of commercialisation at bench scale and industrial application at much larger scales than pilot. In addition, there is further work to be done in the process design, in these experiments, semi continuous cultivation is carried out in flow,

however with the system set up as a continuous flow cultivation, transitioning to continuous flow is a low hanging fruit, for future work. Moreover there is potentially further scientific work to be carried out in in the cultivation of algal strains in OBRs, as well as an in-depth study on parameters affecting growth such as light and mixing, which respect to OBR technology. The research presented here, has demonstrated that OBR technology can challenge conventional industrial and laboratory research best practice and can deliver a step change to algal biotechnology.

REFERENCES

Abbott, M. S. R. *et al.* (2012) 'Biological processing in oscillatory baffled reactors: Operation, advantages and potential', *Interface Focus*, 3(1). doi: 10.1098/rsfs.2012.0036.

Alissandratos, I. (2014) 'Continuous Flow Cultivation and Transesterification of the Microalgae Species Chlorella Vulgaris using an Oscillatory Baffled Flow Reactor', (Unpublished MSc Thesis) Brunel Univerisy London (September, 2014).

Ammar, S. H. (2016) 'Cultivation of Microalgae Chlorella vulgaris in Airlift photobioreactor for Biomass Production using commercial NPK Nutrients', *Al-Khwarizmi Engineering Journal*, 12(1), pp. 90–99.

Andersen, R. A. (2005) *Algal Culturing Techniques*. Elsevier Inc.

Andersen, R. A. (2013) 'Part 1 The Microalgal Cell with Reference', in *Handbook of Microalgal Culture: Applied Phycology and Biotechnology*.

Azma, M. *et al.* (2011) 'Improvement of medium composition for heterotrophic cultivation of green microalgae, Tetraselmis suecica, using response surface methodology', *Biochemical Engineering Journal*, 53(2), pp. 187–195. doi: 10.1016/j.bej.2010.10.010.

Bajpai, R., Prokop, A. and Zappi, M. (2014) *Algal Biorefineries Vol.1*. 1st edn. Springer.

Barbosa, M. J. *et al.* (2002) 'Microalgae cultivation in air-lift reactors: Modeling biomass yield and growth rate as a function of mixing frequency', *Biotechnology and Bioengineering*, 82(2), pp. 170–179. doi: 10.1002/bit.10563.

Barclay, W. and Apt, K. (2013) 'Strategies for Bioprospecting Microalgae for Potential Commercial Applications', in *Handbook of Microalgal Culture: Applied Phycology and Biotechnology*, pp. 69–79. doi: 10.1002/9781118567166.ch4.

Bharathiraja, B. *et al.* (2014) 'Bioethanol Production from Lignocellulosic

Materials - An Overview', 01(07).

Bosca, C., Dauta, A. and Marvalin, O. (1991) 'Intensive outdoor algal cultures: How mixing enhances the photosynthetic production rate', *Bioresource Technology*, 38(2–3), pp. 185–188. doi: 10.1016/0960-8524(91)90152-A.

Brand, J. J., Andersen, R. A. and Nobles, D. R. (2013) 'Maintenance of Microalgae in Culture Collections', in *Handbook of Microalgal Culture: Applied Phycology and Biotechnology*, pp. 80–89. doi: 10.1002/9781118567166.ch5.

Brennan, L. and Owende, P. (2010) 'Biofuels from microalgae-A review of technologies for production, processing, and extractions of biofuels and co-products', *Renewable and Sustainable Energy Reviews*, 14(2), pp. 557–577. doi: 10.1016/j.rser.2009.10.009.

Burlew, J. S. (1953) *Algal Culture: From labratory to pilot plant*.

Camacho, F. G. *et al.* (2011) 'Photobioreactor scale-up for a shear-sensitive dinoflagellate microalga', *Process Biochemistry*, 46(4), pp. 936–944. doi: 10.1016/j.procbio.2011.01.005.

Caporgno, M. P. and Mathys, A. (2018) 'Trends in Microalgae Incorporation Into Innovative Food Products With Potential Health Benefits', *Frontiers in Nutrition*, 5(July), pp. 1–10. doi: 10.3389/fnut.2018.00058.

Carvalho, A. P. *et al.* (2011) 'Light requirements in microalgal photobioreactors: An overview of biophotonic aspects', *Applied Microbiology and Biotechnology*, 89(5), pp. 1275–1288. doi: 10.1007/s00253-010-3047-8.

Chia, M. A. *et al.* (2013) 'Growth and biochemical composition of Chlorella vulgaris in different growth media', 85, pp. 1427–1438.

Chianese, A. and Kramer, H. J. . (2012) *Industrial Crystallizatin and Process Monitoring and Control*. 1st edn. Wiley-VCH.

Chisti, Y. (2007) 'Biodiesel from microalgae', *Biotechnology Advances*. Elsevier Inc., 25(3), pp. 294–306. doi: 10.1016/j.biotechadv.2007.02.001.

Chisti, Y. (2016) 'Algae Biotechnology Science', (858), p. 9351. doi: 10.1007/978-

3-319-12334-9.

Chu, F. F. *et al.* (2013) 'Phosphorus plays an important role in enhancing biodiesel productivity of Chlorella vulgaris under nitrogen deficiency', *Bioresource Technology*. Elsevier Ltd, 134, pp. 341–346. doi: 10.1016/j.biortech.2013.01.131.

Cox, R. M. (2018) *Bioprocess Engineering: Establising cell growth protocols within a novel continuous flow bioreactor*.

Daliry, S. *et al.* (2017) 'Investigation of optimal condition for Chlorella vulgaris microalgae growth', *Global Journal of Environmental Science and Management*, 3(2), pp. 217–230. doi: 10.22034/gjesm.2017.03.02.010.

Danquah, M. and Harun, R. (2010) 'Cultivation Medium Design Via Elemental Balancing for Tetraselmis suecica', *Chemical and Biochemical …*, 24(3), pp. 361–369. Available at: http://hrcak.srce.hr/index.php?show=clanak&id_clanak_jezik=89122.

Darvehei, P., Bahri, P. A. and Moheimani, N. R. (2018) 'Model development for the growth of microalgae: A review', *Renewable and Sustainable Energy Reviews*, 97(August), pp. 233–258. doi: 10.1016/j.rser.2018.08.027.

DF-Robot (2019a) *TB6600 arduino Stepper Motor Driver - DFRobot*. Available at: https://www.dfrobot.com/product-1547.html?gclid=Cj0KCQjwgezoBRDNARIsAGzEfe7VWVn9Zb-0Ka6vpVhKH36C7ubYeJvLHezHi-2lrmaSucocYfrUgxkaAm1tEALw_wcB (Accessed: 2 July 2019).

DF-Robot (2019b) *Turbidity sensor SKU SEN0189 DFRobot, DF-Robot*. Available at: https://wiki.dfrobot.com/Turbidity_sensor_SKU__SEN0189 (Accessed: 2 July 2019).

Doran, M. P. (2013) *Bioprocess engineering principles, Elsevier*. London: Elsevier Inc. doi: 10.1016/S0892-6875(96)90075-8.

Eder, E. (2011) 'Engineering design science and theory of technical systems: legacy of Vladimir Hubka', *Journal of Engineering Design*, 22(5), pp. 361–385.

doi: 10.1080/09544828.2010.522558.

Eder, E. W. (2016) 'Theory of Technical Systems - Educational Tool for Engineering', *Universal Journal of Educational Research*, 4(6), pp. 1395–1405. doi: 10.13189/ujer.2016.040617.

EMS Electron Microscopy Sciences (2019) *Neubauer Haemocytometry*. Available at: https://www.emsdiasum.com/microscopy/technical/datasheet/68052-14.aspx (Accessed: 2 July 2019).

Falkowski, P. G. *et al.* (2004) 'The evolution of modern eukaryotic phytoplankton', *Science*, 305(5682), pp. 354–360. doi: 10.1126/science.1095964.

Ferrando, N. S. *et al.* (2015) 'A quick and effective estimation of algal density by turbidimetry developed with Chlorella vulgaris cultures', 34(2), pp. 397–406. doi: 10.23818/limn.34.30.

Flandrin, P. (2019) *Developing metastable switchable materials towards scale-up production in continuous flow environment*. University of Bath.

Gordon, J. M. and Polle, J. E. W. (2007) 'Ultrahigh bioproductivity from algae. Applied Microbiology and Biotechnology, 76(5).pdf'.

Grobbelaar, J. U. (1989) 'Do light/dark cycles of medium frequency enhance phytoplankton productivity?', *Journal of Applied Phycology*, 1(4), pp. 333–340. doi: 10.1007/BF00003470.

Grobbelaar, J. U. (1991) 'The influence of light/dark cycles in mixed algal cultures on their productivity', *Bioresource Technology*, 38(2–3), pp. 189–194. doi: 10.1016/0960-8524(91)90153-B.

Grobbelaar, J. U. (2003) 'Inorganic Algal Nutrition', in *Handbook of Microalgal Culture*, pp. 123–134. doi: 10.1002/9781118567166.ch8.

Gupta, P. L. and Choi, S. L. H. (2015) 'A mini review : photobioreactors for large scale algal cultivation, *World Journal of Microbiology and Biotechnology*. Springer Netherlands, (June). doi: 10.1007/s11274-015-1892-4.

Hadj-Romdhane, F. *et al.* (2012) 'Development and validation of a minimal growth medium for recycling Chlorella vulgaris culture', *Bioresource Technology*. Elsevier Ltd, 123, pp. 366–374. doi: 10.1016/j.biortech.2012.07.085.

Halim, R., Danquah, M. K. and Webley, P. A. (2012) 'Extraction of oil from microalgae for biodiesel production: A review', *Biotechnology Advances*. Elsevier Inc., 30(3), pp. 709–732. doi: 10.1016/j.biotechadv.2012.01.001.

Hanifzadeh, M. *et al.* (2018) 'Technical, economic and energy assessment of an alternative strategy for mass production of biomass and lipid from microalgae', *Journal of Environmental Chemical Engineering*. Elsevier, 6(1), pp. 866–873. doi: 10.1016/j.jece.2018.01.008.

Hanna Instruments (2019) *HI-1330B Glass Body Refillable pH Semi-micro Electrode*. Available at: https://www.hannainstruments.co.uk/glass-body-refillable-ph-semi-micro-electrode.html (Accessed: 2 July 2019).

Havlik, I. *et al.* (2013) 'On-line monitoring of large cultivations of microalgae and cyanobacteria', *Trends in Biotechnology*. Elsevier Ltd, 31(7), pp. 406–414. doi: 10.1016/j.tibtech.2013.04.005.

Huang, J. *et al.* (2015) 'Improving performance of flat-plate photobioreactors by installation of novel internal mixers optimized with computational fluid dynamics', *Bioresource Technology*. Elsevier Ltd, 182, pp. 151–159. doi: 10.1016/j.biortech.2015.01.067.

Huang, Q. *et al.* (2017) 'Design of Photobioreactors for Mass Cultivation of Photosynthetic Organisms', *Engineering*. Elsevier LTD on behalf of Chinese Academy of Engineering and Higher Education Press Limited Company, 3(3), pp. 318–329. doi: 10.1016/J.ENG.2017.03.020.

Huesemann, M. *et al.* (2017) 'Simulation of outdoor pond cultures using indoor LED-lighted and temperature-controlled raceway ponds and Phenometrics photobioreactors', *Algal Research*. The Authors, 21, pp. 178–190. doi: 10.1016/j.algal.2016.11.016.

Isaev, S. (2019) *Advanced Flow Technologies for the controlled continuous manufacture of nanoscale materials*. Cranfield University. doi: 10.1590/s1809-98232013000400007.

Jackson, B. A., Bahri, P. A. and Moheimani, N. R. (2017) 'Repetitive non-destructive milking of hydrocarbons from Botryococcus braunii', *Renewable and Sustainable Energy Reviews*. Elsevier Ltd, 79 (May), pp. 1229–1240. doi: 10.1016/j.rser.2017.05.130.

Janssen, M. *et al.* (1999) 'Specific growth rate of Chlamydomonas reinhardtii and Chlorella sorokiniana under medium duration light / dark cycles : 13 – 87 s', 70, pp. 323–333.

Jayasurya Vijayakumar *et al.* (2013) 'Calculation of biomass capacity of Algae based on their elemental composition', *2013 Kansas City, Missouri, July 21 - July 24, 2013*, (January 2013). doi: 10.13031/aim.20131620717.

Jian, H. and Ni, X. (2005) 'A numerical study on the scale-up behaviour in oscillatory baffled columns', *Chemical Engineering Research and Design*, 83(10 A), pp. 1163–1170. doi: 10.1205/cherd.03312.

Jianye, X. *et al.* (2015) 'Advances and Practices of Bioprocess Scale-up', *Advanced Biochemical Engineering Biotechnology*, 20(1), pp. 237–247. doi: 10.1007/10_2014_293.

Ju, L. and Chase, G. G. (1992) 'Bioproess Engineering Improved scale-up strategies of bioreactors', *Bioprocess Engineering*, 8, pp. 49–53.

Khan, M. I., Shin, J. H. and Kim, J. D. (2018) 'The promising future of microalgae: Current status, challenges, and optimization of a sustainable and renewable industry for biofuels, feed, and other products', *Microbial Cell Factories*. BioMed Central, 17(1), pp. 1–21. doi: 10.1186/s12934-018-0879-x.

Khoo, C. G., Lam, M. K. and Lee, K. T. (2016) 'Pilot-scale semi-continuous cultivation of microalgae Chlorella vulgaris in bubble column photobioreactor (

BC-PBR): Hydrodynamics and gas – liquid mass transfer study', *Algal Research*. Elsevier B.V., 15, pp. 65–76. doi: 10.1016/j.algal.2016.02.001.

Kong, W. B. *et al.* (2013) 'Effect of glycerol and glucose on the enhancement of biomass, lipid and soluble carbohydrate production by Chlorella vulgaris in mixotrophic culture', *Food Technology and Biotechnology*, 51(1), pp. 62–69.

Kumar, K. *et al.* (2011) 'Development of suitable photobioreactors for CO2sequestration addressing global warming using green algae and cyanobacteria', *Bioresource Technology*. Elsevier Ltd, 102(8), pp. 4945–4953. doi: 10.1016/j.biortech.2011.01.054.

Kunjapur, A. M. and Eldridge, R. B. (2010) 'Photobioreactor Design for Biofuel Production From Marine Microalgae', *Industrial Engineering Resource,* (49), p3516-3526.

Lam, M. K., Lee, K. T. and Mohamed, A. R. (2012) 'Current status and challenges on microalgae-based carbon capture', *International Journal of Greenhouse Gas Control*. Elsevier Ltd, 10, pp. 456–469. doi: 10.1016/j.ijggc.2012.07.010.

Larroche, C. *et al.* (2016) *Current Developments in Biotechnology and Bioengineering: Bioprocesses, Bioreactors and Controls*, *Current Developments in Biotechnology and Bioengineering: Bioprocesses, Bioreactors and Controls*.

Lazić, Ž. R. (2004) *Design of Experiments in Chemical Engineering*. Wiley-VCH Wenheim, doi: 10.1002/3527604162.

Ledda, C. *et al.* (2013a) 'Nitrogen and water recovery from animal slurries by a new integrated ultrafiltration, reverse osmosis and cold stripping process: A case study', *Water Research*, 47(16), pp. 6157–6166. doi: 10.1016/j.watres.2013.07.037.

Ledda, C. *et al.* (2013b) 'Nitrogen and water recovery from animal slurries by a new integrated ultrafiltration, reverse osmosis and cold stripping process: A case study', *Water Research*, 47(16), pp. 6157–6166. doi: 10.1016/j.watres.2013.07.037.

Lee, Y. K. *et al.* (2013) 'Basic Culturing and Analytical Measurement Techniques', *Handbook of Microalgal Culture: Applied Phycology and Biotechnology*, pp. 37–68. doi: 10.1002/9781118567166.ch3.

Lee, Y. K. and Pirt, J. S. (1981) 'Energetics of Photosynthetic Algal Growth : Influence of Intermittent Illumination in short (40s) cycles, *Journal of General Microbiology* (124) p43-52', (1981).

Levasseur, M. (1993) 'Physiological acclimation of marine phytoplankton to different nitrogen sources', *Journal of Phycology*, (29) p.587-595 (September). doi: 10.1111/j.0022-3646.1993.00587.x.

Levenspiel, O. (1998) *Fluid-Particle Reactions: Kinetics*. 3rd edn, *Chemical Reaction Engineering*. 3rd edn. Edited by O. Levenspiel. New York: John Wiley& Sons Inc. doi: 10.1016/0009-2509(80)80132-1.

Li, J. *et al.* (2011) 'An economic assessment of astaxanthin production by large scale cultivation of Haematococcus pluvialis', *Biotechnology Advances*. Elsevier Inc., 29(6), pp. 568–574. doi: 10.1016/j.biotechadv.2011.04.001.

Liang, Y., Sarkany, N. and Cui, Y. (2009) 'Biomass and lipid productivities of Chlorella vulgaris under autotrophic, heterotrophic and mixotrophic growth conditions', *Biotechnology Letters*, 31(7), pp. 1043–1049. doi: 10.1007/s10529-009-9975-7.

Lv, J. M. *et al.* (2010) 'Enhanced lipid production of Chlorella vulgaris by adjustment of cultivation conditions', *Bioresource Technology*. Elsevier Ltd, 101(17), pp. 6797–6804. doi: 10.1016/j.biortech.2010.03.120.

Madkour, F. F., Kamil, A. E. W. and Nasr, H. S. (2012) 'Production and nutritive value of Spirulina platensis in reduced cost media', *Egyptian Journal of Aquatic Research*. National Institute of Oceanography and Fisheries, 38(1), pp. 51–57. doi: 10.1016/j.ejar.2012.09.003.

Makatsoris, C. and Alissandratos, I. (2017) 'Modular continuous photo-bioreactor GB2564711'. Intellectual Property Office, Concept House, Cardiff Road, Newport, NP10 8QQ. information@ipo.gov.uk. Available at:

https://www.ipo.gov.uk/p-ipsum/Case/ApplicationNumber/GB1711764.9 (Accessed: 17 June 2019).

Makatsoris, C. and Alissandratos, I. (2019) 'MODULAR CONTINUOUS PHOTOBIOCHEMICALREACTOR' .Available at: https://patentscope.wipo.int/search/en/detail.jsf?docId=WO2019016575&recNum=93&docAn=GB2018052073&queryString=FP:(algae)&maxRec=18888 (Accessed: 25 June 2019).

Makatsoris, C., Paramonov, L. and Rakan, A. (2013) 'Modular Flow Reactor WO2013/050764'.

Mandalam, R. K. and Palsson, B. (1998) 'Elemental balancing of biomass and medium composition enhances growth capacity in high-density Chlorella vulgaris cultures', *Biotechnology and Bioengineering*, 59(5), pp. 605–611. doi: 10.1002/(SICI)1097-0290(19980905)59:5<605::AID-BIT11>3.0.CO;2-8.

Mandenius, C.-F. and Bjorkman M., (2016) *Bioreactors - Design, Operation and Novel Applications* Wiley, New York, 1st Edt. doi: 10.1002/9783527683369.

Mandenius, C. *et al.* (2009) 'Quality-by-Design for biotechnology-related pharmaceuticals'*, Biotechnology Journal, (4)* pp. 600–609. doi: 10.1002/biot.200800333.

Matos, Â. P., Coeli, R., *et al.* (2014) 'Growing Chlorella vulgaris in Photobioreactor by Continuous Process Using Concentrated Desalination : Effect of Dilution Rate on Biochemical Composition', *International Journal of Chemical Engineering*, 2014.

Matos, Â. P., Torres, R. C. D. O., *et al.* (2014) 'Growing chlorella vulgaris in photobioreactor by continuous process using concentrated desalination: Effect of dilution rate on biochemical composition', *International Journal of Chemical Engineering*, 2014. doi: 10.1155/2014/310285.

McGlone, T. *et al.* (2015) 'Oscillatory Flow Reactors (OFRs) for Continuous Manufacturing and Crystallization', *Organic Process Research and Development*, 19(9), pp. 1186–1202. doi: 10.1021/acs.oprd.5b00225.

Millington, L. A., Goulding, K. H. and Adams, N. (1988) 'the influence of growth medium: Composition on the Toxicity of Chemicals To Algae', 22(12), pp. 1593–1597.

Montgomery, D. (2008) *Guidelines for Designing Experiments*. 8th edn, *Design and Analysis of Experiments*. 8th edn. Edited by D. Montgomery. London: John Wiley& Sons Inc. doi: 10.1198/tech.2006.s372.

Mouser Electronics (2019a) *SEN0161 DFRobot | Mouser United Kingdom*. Available at: https://www.mouser.co.uk/ProductDetail/DFRobot/SEN0161?qs=Zcin8yvlhnPq1 OJbBVjoIw== (Accessed: 2 July 2019).

Mouser Electronics (2019b) *SP-200-24 MEAN WELL | Mouser United Kingdom*. Available at: https://www.mouser.co.uk/ProductDetail/MEAN-WELL/SP-200-24?qs=moO%2F8p2KOt%252BxowKqCFhHzA%3D%3D&gclid=Cj0KCQjwgezo BRDNARIsAGzEfe5C3rbcb1mTXkZgtKpCd1Dqz6w7Rhk23WYQ-Gh-CWRjs_cbUmHkKVUaAj9mEALw_wcB (Accessed: 2 July 2019).

Muller-Feuga, A. (2013) 'Microalgae for Aquaculture: The Current Global Situation and Future Trends', in *Handbook of Microalgal Culture: Applied Phycology and Biotechnology*, pp. 613–627. doi: 10.1002/9781118567166.ch33.

Narala, Rakesh R *et al.* (2016) 'Comparison of Microalgae Cultivation in Photobioreactor, Open Raceway Pond, and a Two-Stage Hybrid System', 4(August), pp. 1–10. doi: 10.3389/fenrg.2016.00029.

Narala, Rakesh R. *et al.* (2016) 'Comparison of Microalgae Cultivation in Photobioreactor, Open Raceway Pond, and a Two-Stage Hybrid System', *Frontiers in Energy Research*, 4(August). doi: 10.3389/fenrg.2016.00029.

Nauman, B. E. (2002) *Chemical Reactor Design, Optimisation and Scaleup*. 1st edn. New York: McGraw-Hill.

Ni, X.-W. (2006) 'Continuous Oscillatory Baffled Reactor Technology',

Innovations in Pharmaceutical Technology, 20, pp. 90–96.

Ni, X., Jian, H. and Fitch, A. (2003) 'Column Using Large Eddy Simulation and', *Trans IChemE*, 81(September). doi: 10.1205/026387603322482086.

Nourafkan, E. *et al.* (2017) 'Formulation optimization of reverse microemulsions using design of experiments for nanoparticles synthesis', *Chemical Engineering Research and Design*. Institution of Chemical Engineers, 125, pp. 367–384. doi: 10.1016/j.cherd.2017.07.023.

Ocean-Optics (2019) *DH-mini Light Source - Ocean Optics*. Available at: https://oceanoptics.com/product/dh-mini/ (Accessed: 2 July 2019).

Oliva, J. A. *et al.* (2018) 'Experimental investigation of the effect of scale-up on mixing efficiency in oscillatory flow baffled reactors (OFBR) using principal component based image analysis as a novel noninvasive residence time distribution measurement approach', *Chemical Engineering Journal*. Elsevier, 351(March), pp. 498–505. doi: 10.1016/j.cej.2018.06.029.

Paes, C. R. P. S. *et al.* (2016) 'Growth, nutrient uptake and chemical composition of Chlorella sp. and Nannochloropsis oculata under nitrogen starvation', *Latin American Journal of Aquatic Research*, 44(2), pp. 275–292. doi: 10.3856/vol44-issue2-fulltext-9.

Phan, A. N. and Harvey, A. (2010) 'Development and evaluation of novel designs of continuous mesoscale oscillatory baffled reactors', *Chemical Engineering Journal*. Elsevier B.V., 159(1–3), pp. 212–219. doi: 10.1016/j.cej.2010.02.059.

Phan, A. N., Harvey, A. and Lavender, J. (2011) 'Characterisation of fluid mixing in novel designs of mesoscale oscillatory baffled reactors operating at low flow rates (0.3-0.6ml/min)', *Chemical Engineering and Processing: Process Intensification*. Elsevier B.V., 50(3), pp. 254–263. doi: 10.1016/j.cep.2011.02.004.

Phan, A. N. and Harvey, A. P. (2011) 'Effect of geometrical parameters on fluid mixing in novel mesoscale oscillatory helical baffled designs', *Chemical Engineering Journal*. Elsevier B.V., 169(1–3), pp. 339–347. doi:

10.1016/j.cej.2011.03.026.

Płaczek, M., Patyna, A. and Witczak, S. (2017) 'Technical evaluation of photobioreactors for microalgae cultivation', *E3S Web of Conferences*, 19, p. 02032. doi: 10.1051/e3sconf/20171902032.

Plumb, K. (2005) 'Continuous processing in the pharmaceutical industry: Changing the mind set', *Chemical Engineering Research and Design*, 83(6 A), pp. 730–738. doi: 10.1205/cherd.04359.

Qari, H., Rehan, M. and Nizami, A. S. (2017) 'Key Issues in Microalgae Biofuels: A Short Review', *Energy Procedia*. Elsevier B.V., 142(December), pp. 898–903. doi: 10.1016/j.egypro.2017.12.144.

Qiang, H., Richmond, A. and Zarmi, Y. (1998) 'Combined effects of light intensity, light-path and culture density on output rate of spirulina platensis (cyanobacteria)', *European Journal of Phycology*, 33(2), pp. 165–171. doi: 10.1080/09670269810001736663.

Reis, A. and Da Silva, T. L. (2016) 'Chapter 6 Scale-up Problems for the Large Scale Production of Algae', in Das, D. (ed.) *Algal Biorefinery: An Integrated Approach*, pp. 1–467. doi: 10.1007/978-3-319-22813-6.

Richmond, A. (2000) 'Microalgal biotechnology at the turn of the millennium : A personal view', *Journal of Applied Phycology*, pp. 441–451. doi: 10.1023/A:1008123131307.

Richmond, A. (2004) 'Principles for attaining maximal microalgal productivity in photobioreactors: An overview', *Hydrobiologia*, 512(Table 1), pp. 33–37. doi: 10.1023/B:HYDR.0000020365.06145.36.

Richmond, A. (2013) 'Biological Principles of Mass Cultivation of Photoautotrophic Microalgae', *Handbook of Microalgal Culture: Applied Phycology and Biotechnology*, pp. 169–204. doi: 10.1002/9781118567166.ch11.

Richmond, A., Cheng-Wu, Z. and Zarmi, Y. (2003) 'Efficient use of strong light for high photosynthetic productivity: Interrelationships between the optical path, the

optimal population density and cell-growth inhibition', *Biomolecular Engineering*, 20(4–6), pp. 229–236. doi: 10.1016/S1389-0344(03)00060-1.

Richmond, A. and Zou, N. (1999) 'Efficient utilisation of high photon irradiance for mass production of photoautotrophic micro-organisms', *Journal of Applied Phycology*, pp. 123–127. doi: 10.1023/A:1008033906840.

Rodolfi, L. *et al.* (2009) 'Microalgae for oil: Strain selection, induction of lipid synthesis and outdoor mass cultivation in a low-cost photobioreactor', *Biotechnology and Bioengineering*, 102(1), pp. 100–112. doi: 10.1002/bit.22033.

RS-Components (2009) *Arduino Mega 2560 Rev3 MCU Development Board A000067 | RS Components*. Available at: https://uk.rs-online.com/web/p/processor-microcontroller-development-kits/7154084/?cm_mmc=UK-PPC-DS3A-_-google-_-DSA_UK_EN_Semiconductors-_-Processor+%26+Microcontroller+Development+Kits-_-DYNAMIC+SEARCH+ADS&matchtype=b&dsa-612308665602&s_kwcid=AL!7457!3! (Accessed: 2 July 2019).

RS-Components (2019) *103H7823-1740 | Sanyo Denki Bipolar Single Shaft Stepper Motor 1.8°, 2.7Nm, 24 V dc, 4 A, 6 Wires | RS Components*. Available at: https://uk.rs-online.com/web/p/stepper-motors/8787673/ (Accessed: 2 July 2019).

Rudnicki, P. *et al.* (2017) 'A comparative study of photosynthetic unit models for algal growth rate and fluorescence prediction under light/dark cycles', *Algal Research*. Elsevier, 24(March), pp. 227–236. doi: 10.1016/j.algal.2017.03.028.

Saad H. Ammar (2016) 'Cultivation of Microalgae Chlorella vulgaris in airlift photobioreactor for Biomass Production using commercial NPK nutrients', *Al-Khwarizmi Engineering Journal*, 12(1), pp. 90–99. doi: 10.1016/j.immbio.2010.04.001.

Safi, C. *et al.* (2014) 'Morphology, composition, production, processing and applications of Chlorella vulgaris: A review', *Renewable and Sustainable Energy*

Reviews, 35, pp. 265–278. doi: 10.1016/j.rser.2014.04.007.

Sarrafzadeh, M. H. *et al.* (2015) 'Evaluation of various techniques for microalgal biomass quantification', *Journal of Biotechnology*. Elsevier B.V., 216, pp. 90–97. doi: 10.1016/j.jbiotec.2015.10.010.

Sathasivam, R. *et al.* (2017) 'Microalgae metabolites: A rich source for food and medicine', *Saudi Journal of Biological Sciences*. King Saud University, 26(4), pp. 709–722. doi: 10.1016/j.sjbs.2017.11.003.

Scarcella, M., Belotti, G. and Filippis, D. (2009) 'Study on the optimal growing conditions of Chlorella vulgaris in bubble column photobioreactors'.

Schneider, R. de C. de S. *et al.* (2018) 'Life cycle assessment of microalgae production in a raceway pond with alternative culture media', *Algal Research*. Elsevier, 32(April), pp. 280–292. doi: 10.1016/j.algal.2018.04.012.

Scragg, A. H. *et al.* (2002) 'Growth of microalgae with increased calorific values in a tubular bioreactor', *Biomass and Bioenergy*, 23(1), pp. 67–73. doi: 10.1016/S0961-9534(02)00028-4.

Shen, X. *et al.* (2015) 'Enhancement of FAME productivity of Scenedesmus obliquus by combining nitrogen deficiency with sufficient phosphorus supply in heterotrophic cultivation', *Applied Energy*. Elsevier Ltd, 158, pp. 348–354. doi: 10.1016/j.apenergy.2015.08.057.

Shi, X.-M. *et al.* (1999) 'Production of biomass and lutein by Chlorella protothecoides at various glucose concentrations in heterotrophic cultures', *Process Biochemistry*, 34, pp. 341–347. doi: 10.1016/S0032-9592(98)00101-0.

Simionato, D. *et al.* (2013) 'Optimization of light use efficiency for biofuel production in algae', 182, pp. 71–78.

Smith, K. B. (1999) 'The Scale-Up of Oscillatory Flow Mixing', *PhD Dissertation, Christ's College, University of Cambridge*, (September). Available at: https://core.ac.uk/download/pdf/1334175.pdf.

Smith, K. B. and Mackley, M. R. (2006) 'An experimental investigation into the

scale-up of oscillatory flow mixing in baffled tubes', *Chemical Engineering Research and Design*, 84(11 A), pp. 1001–1011. doi: 10.1205/cherd.05054.

Soman, A. and Shastri, Y. (2015) 'Optimization of novel photobioreactor design using computational fluid dynamics', *Applied Energy*. Elsevier Ltd, 140, pp. 246–255. doi: 10.1016/j.apenergy.2014.11.072.

Starr, C. G. (1991) 'A History of the Ancient World', *Journal of Biochemical Technology* (4)(2012), p. 742.

Stonestreet, P. and Harvey, A. P. (2002) 'A mixing-based design methodology for continuous oscillatory flow reactors', *Chemical Engineering Research and Design*, 80(1), pp. 31–44. doi: 10.1205/026387602753393204.

Stonestreet, P. and Van Der Veeken, P. M. J. (1999) 'The effects of oscillatory flow and bulk flow components on residence time distribution in baffled tube reactors', *Chemical Engineering Research and Design*, 77(8), pp. 671–684. doi: 10.1205/026387699526809.

Torzillo, G. and Seibert, M. (2013) 'Hydrogen Production by Chlamydomonas reinhardtii', in *Handbook of Microalgal Culture: Applied Phycology and Biotechnology*, pp. 417–432. doi: 10.1002/9781118567166.ch22.

Vaičiulyte, S. *et al.* (2014) 'Batch growth of Chlorella vulgaris CCALA 896 versus semi-continuous regimen for enhancing oil-rich biomass productivity', *Energies*, 7(6), pp. 3840–3857. doi: 10.3390/en7063840.

Varicon Aqua (no date) *YEAR END PROMOTIONAL OFFER - 400 L PHYCO-FLOW - Varicon Aqua - Algal photobioreactor design and aquaculture supply specialists*. Available at: http://www.variconaqua.com/news-and-case-studies/year-end-promotional-offer-400-l-phyco-flow/ (Accessed: 10 June 2019).

Vejrazka, C. *et al.* (2013) 'Photosynthetic efficiency and oxygen evolution of Chlamydomonas reinhardtii under continuous and flashing light', *Applied Microbiology and Biotechnology*, 97(4), pp. 1523–1532. doi: 10.1007/s00253-012-4390-8.

De Vree, J. H. *et al.* (2015) 'Comparison of four outdoor pilot-scale photobioreactors', *Biotechnology for Biofuels*. BioMed Central, 8(1), pp. 1–12. doi: 10.1186/s13068-015-0400-2.

Wang, B., Lan, C. Q. and Horsman, M. (2012) 'Closed photobioreactors for production of microalgal biomasses', *Biotechnology Advances*. Elsevier Inc., 30(4), pp. 904–912. doi: 10.1016/j.biotechadv.2012.01.019.

Wang, G. *et al.* (2018) 'All-Fiber Raman Biosensor by Combining Reflection and Transmission Mode', *IEEE Photonics Technology Letters*, 30(4), pp. 387–390. doi: 10.1109/lpt.2018.2792489.

Wong, Y. (2017) 'Growth Medium Screening for Chlorella vulgaris Growth and Lipid Production', *Journal of Aquaculture & Marine Biology*, 6(1), pp. 1–10. doi: 10.15406/jamb.2017.06.00143.

Yamamoto, M., Kurihara, I. and Kawano, S. (2005) 'Late type of daughter cell wall synthesis in one of the Chlorellaceae , Parachlorella kessleri (Chlorophyta , Trebouxiophyceae), pp. 766–775. doi: 10.1007/s00425-005-1486-8.

Yeh, K. and Chang, J. (2012) 'Bioresource Technology Effects of cultivation conditions and media composition on cell growth and lipid productivity of indigenous microalga Chlorella vulgaris ESP-31', *Bioresource Technology*. Elsevier Ltd, 105, pp. 120–127. doi: 10.1016/j.biortech.2011.11.103.

Yeo, U. hyeon *et al.* (2018) 'Identification of the key structural parameters for the design of a large-scale PBR', *Biosystems Engineering*. Elsevier Ltd, 171, pp. 165–178. doi: 10.1016/j.biosystemseng.2018.04.012.

Yusof, Y. A. M. *et al.* (2011) 'Chlorella vulgaris: A miracle plant?', *2011 4th International Conference on Modeling, Simulation and Applied Optimization, ICMSAO 2011*. doi: 10.1109/ICMSAO.2011.5775638.

APPENDICES

Appendix A **Literature Review Additional Information**

A.1 Algal Growth Parameters

A.1.1 Light

Algae are photosynthetic organisms, and thus require light in order to photosynthesize therefore metabolise and grow. The variable of light is crucial for all algae but parameters such as light supply quality, utilization, intensity spread, wavelength and light pigment are specific for each algae strain. Due to the complexity of PBR systems the photosynthetic efficiency does not solely depend on the wavelength and the pigment of that algal species, rather it depends on a more complex system of interdependencies amongst parameters and variables.

Photosynthesis

Photosynthesis is the process of chemically synthesizing molecules with the use of light. Carbon dioxide (CO_2) and water (H_2O) react, powered by light energy creating carbohydrates (sugars) and O_2 as products. Light energy specifically targets and enables the transfer of water electrons to carbon dioxide molecules i.e. oxidation, thus transforming the water electrons into a more energetic state in the form of a sugar molecule, Photosynthesis is an endothermic reaction as it required a heat input of approximately 2,814 kJ of energy supplied solely by incident radiation of light (Carvalho *et al.*, 2011).

Photo synthetic efficiency.

As well as depending on the wavelength and pigment, as previously referred to, photosynthetic efficiency also depends on the time duration that a single cell resides in the presence of light (light/dark cycle) and the light intensity at point of absorption (Lee and Pirt, 1980)

Light period

During a cell's exposure to a light source, a photon is captured and absorbed by the molecule chlorophyll – a, antennae's embedded in the thylakoid membranes as well as other light absorbing cellular structures create a cloud impinging the light in the cell. (Carvalho *et al.*, 2011) This light depended process where light harvesting, and charge separation occurs is called primary photochemistry reaction and has duration of only pico to nano seconds.

Dark period (light independent)

During the dark period energy harvested from the light is broken down to electrons and is transferred to the stroma of the chloroplast (electron shuttling) where the carbon molecule is broken down and sugar is formed (carbon metabolism), consuming adenosine triphosphate (ATP) reserves produced during the light phase, extracting and ejecting O2 out of the cellular walls. The dark period takes a little longer to complete, with the electron shuttling taking a couple of milliseconds, and the carbon metabolism taking up minutes due to an enzyme activation mechanism. Although the enzymatic carbon metabolism takes up the longest time, the processes can be uncoupled by providing pulsating or intermittent light making the cellular system ready to restart the process within 1-15ms.

The photosynthetic efficiency (PE) can be defined as the fraction of incident light within the solar spectrum that is stored as chemical energy in biomass and can be expressed by combining the illuminated surface area per unit volume (m^2/m^3), and the microbial growth energy equation defined by (Lee and Pirt, 1980; Janssen *et al.*, 1999)

Light intensity.

Light intensity although crucial for the photosynthetic process, like all variables there is a limit when considering algae applications. Light intensity and photosynthetic efficiency are very closely correlated factors, but too high a photonic flux can cause serious damages to the algal cell whereas too low can constrain growth and seriously inhibit the photosynthetic efficiency. The light intensity effect on the photosynthetic rate can be optimally explained by a curve showing the irradiance versus the photosynthetic rate of an algal culture in a PBR. There are three regions of interest. Between the compensation light intensity and
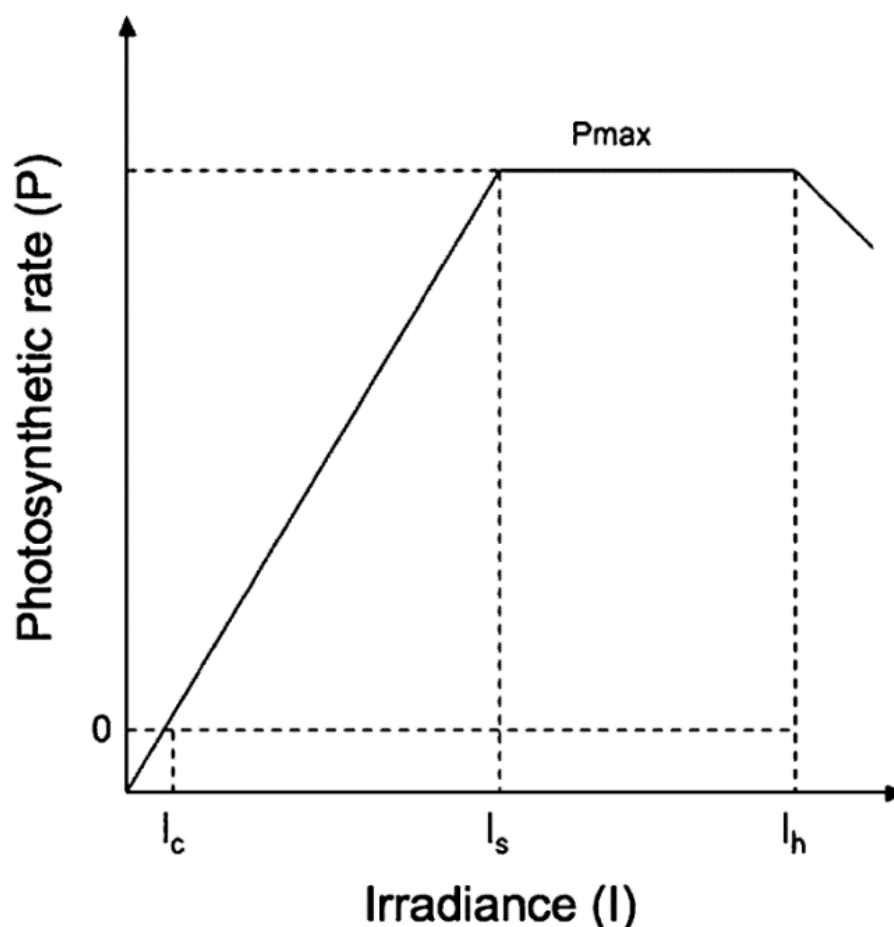
Figure A-1 Photosynthesis (P) – Irradiance (I) curve for algal cultures (Carvalho et al. 2011)

light saturation zone I_c and I_s respectively) photosynthetic efficiency increases with increasing irradiance, therefore the higher the light intensity on a unit volume of algae will increase the photosynthetic process and thus the growth. Beyond that point reaching the photo inhibition point (I_h) the algal culture has reached its

maximum photosynthetic processing capacity, therefore any increase in light intensity will exhibit itself with a brief increase in local temperature. Beyond the photo-inhibition point increase in irradiance will become dangerous for the algal cells and the photosynthetic ability will deteriorate reaching to cell termination (Grobbelaar, 1991; Qiang, Richmond and Zarmi, 1998).

Photo-inhibition has been tested to occur at 200-400 $\mu mol/m^2/s$, however it has been shown that algal cells can withstand photonic fluxes of up to 5000 $\mu mol/m^2/s$ by using an LED source with discontinuous light fluxes (Gordon and Polle, 2007). Richmond (2003) in his study on ultra high density microalgal cultures tested extreme light conditions of 8,000 $\mu mol/m^2/s$ on a flat plat reactor testing the frequencies of a light/dark cycle path; his findings give evidence to the fact that the photonic flux algae absorb is an interdependent variable taking into consideration the PBR design i.e. the tube or plate depth, the material penetrative ability of the light source and the density of the algal culture ((Richmond, Cheng-Wu and Zarmi, 2003) Richmond's findings are based on a previous study of Neidhardt et al (1998 and 1999) where they state that photo-inhibition occurs usually on the top layer on the algae culture, as it is happening in nature. The top layer of cells reach the photo-inhibition zone and due to chemical inefficiencies of the chlorophyll molecule, they discard 50-80% of the excess photonic fluxes towards the mutually shaded regions of the second and third layer providing suboptimal lighting conditions, therefore inhibiting light conversion efficiency and cellular productivity (Barbosa *et al.*, 2002; Richmond, Cheng-Wu and Zarmi, 2003)

Algal cells in a photobioreactor unit are not exposed to constant photon flux densities (PFD), their mutual shading, and agitation/mixing induced motion do not allow cells to reach dangerous levels of photon absorption beyond the photo inhibition zone. Due to the light gradient the mixing regime and the cell concentration the algae become acclimated extremely fast to their microenvironment inside the PBR and their new photo-rhythm. It is suggested by Richmond (2003) that circulation between light and dark regions leads to a photosynthetic efficiency surpassing those of constant illumination of a PFD for

long periods of time as is the case in nature. Short optical path and dark region residence times coupled with tubular depth of the PBR are all variables that are taken into consideration for the photosynthetic productivity and photon absorption efficiency, due to turnover time of the photosynthetic unit (PSU) a cycle of 1-4 seconds is preferable translating into an optical path of 1-10cm (Richmond, 2003).

A.1.2 Nutrients & Carbon:

Carbon

During the photosynthesis the algae cell sequestrates carbon dioxide and converts it into sugar through a process known as the Calvin cycle. The prime carboxylating enzyme that metabolizes the carbon molecule is Riboculose-1,5-bisphophate-carboxylase-oxygenase (RuBisCO). The importance of RuBisCo is in the fact that in situations where there is an imbalance of CO2/O2 it can regulate and utilise O_2 producing CO_2 in abundant oxygen situations. This inhibits the photosynthetic efficiency of the cell and in excessive imbalance situations dissolved intercellular oxygen concentrations are toxic to the cell, causing the development of radical reactive oxygen species (RES). Which presence is detrimental to the cytoplasmic membranes and cellular components causing wall ruptures and even the termination of the culture (Wang, Lan and Horsman, 2012). This situation almost never occurs in nature, since the carbon concentration and oxygen expulsion cycle is maintained by natural habitual phenomena, however it is a very important factor to consider during the design of a PBR.

Carbon mitigation via sequestration is the prime motivator for the research into algae industrial suitability, their capture of the heavy polluting carbon dioxide molecule and release on oxygen has placed algae amongst the forerunners of viable future energy technologies. One kilogram of algae biomass can absorb around 1.82Kg of CO_2, taking into consideration the global annual corresponding weight of 37 tonnes/hectare this figure transforms into 54.9-67.7 tonnes of CO_2 capturing per year (Brennan and Owende, 2010). There are various industrial applications other than biodiesel production that take this fact into consideration, such as flue gas mitigation. Flue gas mitigation with the use of biomass is a very

interesting topic of great scientific interest but details will be omitted due to the different nature of this thesis.

The amount of CO_2 that an algae culture can absorb depends primarily on the culture strain itself; secondary absorption factors include photobioreactor design, temperature, light intensity, mixing, culture density and carbon mass transfer.

As all variables different algal strains possess similar but intrinsically different internal biochemistries. Their native environmental factors as well as potential cell growth and carbon-fixation drive the ability for each strain to absorb a different amount of CO_2 and survive. Like all factors there are two extremes in this case, first possibility is that the algae does not have enough CO_2 in order to survive, and secondly the CO_2 amount is overwhelming making the algae stress rupture and terminate. As mentioned in Kumar et al., (2011) the algae strain *Dunianella* represents a fragile species where high levels of CO_2 can stress the cell and dissolve it, on the other hand Spirulina a marine type strain is very efficient in tolerating high levels of CO_2 sequestration without inhibiting its culture growth. Other cultures such as *Chlorella sp.* at 45 ℃ its maximum CO_2 tolerance was recorded at 40% v/v, whereas the tropical marina strain *Cyanidium caldarium* at 60 ℃ had a tolerance of 100% v/v (Ono and Cuello 2004) (Kumar *et al.*, 2011).

Enough carbon is essential for the survival and growth of a culture; low concentration would result in the same limitation in growth and even termination of the culture, too high concentration of CO_2 would result in lowered pH which would equally inhibit growth. However, provided sufficiently carbon dioxide will result in higher growth rates (Jiang et al. 2011), higher lipid contents (Sydney et al. 2010), increased culture density (Zhang et al. 2001) and a stable pH level.

The carbon molecule is usually injected into the photobioreactor in the form of carbon dioxide gas, this method of delivery although considered the most expensive and most non-sustainable but is preferred for certain PBR's. Column PBRs, airlift, adopt carbon dioxide gas delivery for the added agitation and mixing effect it delivers. However recent research has provided evidence that bubbling CO_2 causes stress to the algae cell as well as inadequate uniform distribution of carbon since the optimal absorption will only occur in the immediate vicinity of the

bubbling 'column' therefore the majority of CO_2 captured bubbles are lost to the atmosphere.

A recent study conducted by Lam M.K et al. (2012) provides information on a carbon delivery method that shows to promises to alleviate the limitations associated with carbon dioxide gas injection. Sodium bicarbonate (NaHCO3) as an alternative carbon source provides the algae with the bicarbonate ion (HCO3 -) molecule whilst the sodium molecule counteracts the pH acidation. When CO_2 is injected in gas form in order for it to be processed it must come in contact with RuBisCO and subsequently transported and stripped, whereas the HCO3- the dissociated ion from NaHCO3 due to the presence of the carbonic anhydrase enzyme on the surface of the cell is rapidly converted to CO_2 inside the cell therefore less energy is consumed during stripping and shuttling resulting in a more sustainable method of CO_2 distribution in the algal culture (Lam M.K., et al 2012).

In a recent study cited by Lam M.K et al. (2012) a culture of Chlorella vulgaris was grown using 1gr of NaHCO3 per litre of culture, yielding a final growth figure of 0.6g/L translating to 30-40% lipids, a very high number considering that particular strain of algae reports average values of 14-22%. Chi Z., et al. (2011) attributes this success to the longer retention time of HCO3- in the medium.

Nutrients

Freshwater algae's composition is CH1.7O0.4N0.15P0.0094 therefore stoichiometrically it requires carbon, nitrogen and potassium. There has been extensive research on different medium composition in order to provide various algae cultures with enough nutrients to provide optimum growth and avoid nutrient starvation inhibitions. There are two major categories of medium available, fresh water mediums and marine type mediums, the major difference is that the latter contains salts to in order to re-create a saline environment for the marine algae. Typical mediums such as Diatom Medium, Bold Basal, TG-11 and TAP contain nitrate phosphate solution, silicate, trace metal and vitamins such as thiamine and biotin in small amounts (Millington, Goulding and Adams, 1988; Mandalam and Palsson, 1998; Lv *et al.*, 2010; Hadj-Romdhane *et al.*, 2012)

Maximum growth it requires phosphate, oxygen, nitrogen, potassium and carbon as carbon dioxide at enough levels to avoid inhibiting final growth yield (Borowitzka M.A., and Moheimani N.R., 2010). Phosphorus is absorbed by the algal cells in the form of inorganic phosphate from wastewater streams or via inorganic food fertiliser. Nitrogen is supplied in forms such as ammonia, nitrate or urea, and finally carbon dioxide provides both the carbon molecule and oxygen molecule required to complete the cell's growth requirement. The algal cells ability sequestrates carbon dioxide and release oxygen back into the atmosphere whilst producing such a valuable commodity such as fuel is the prime reason why algae is currently being researched.

A.2 Pictures

Figure A-2 Lab Scale OBR column showing the glass tube and baffle train (Nitech Solutions, 2019).
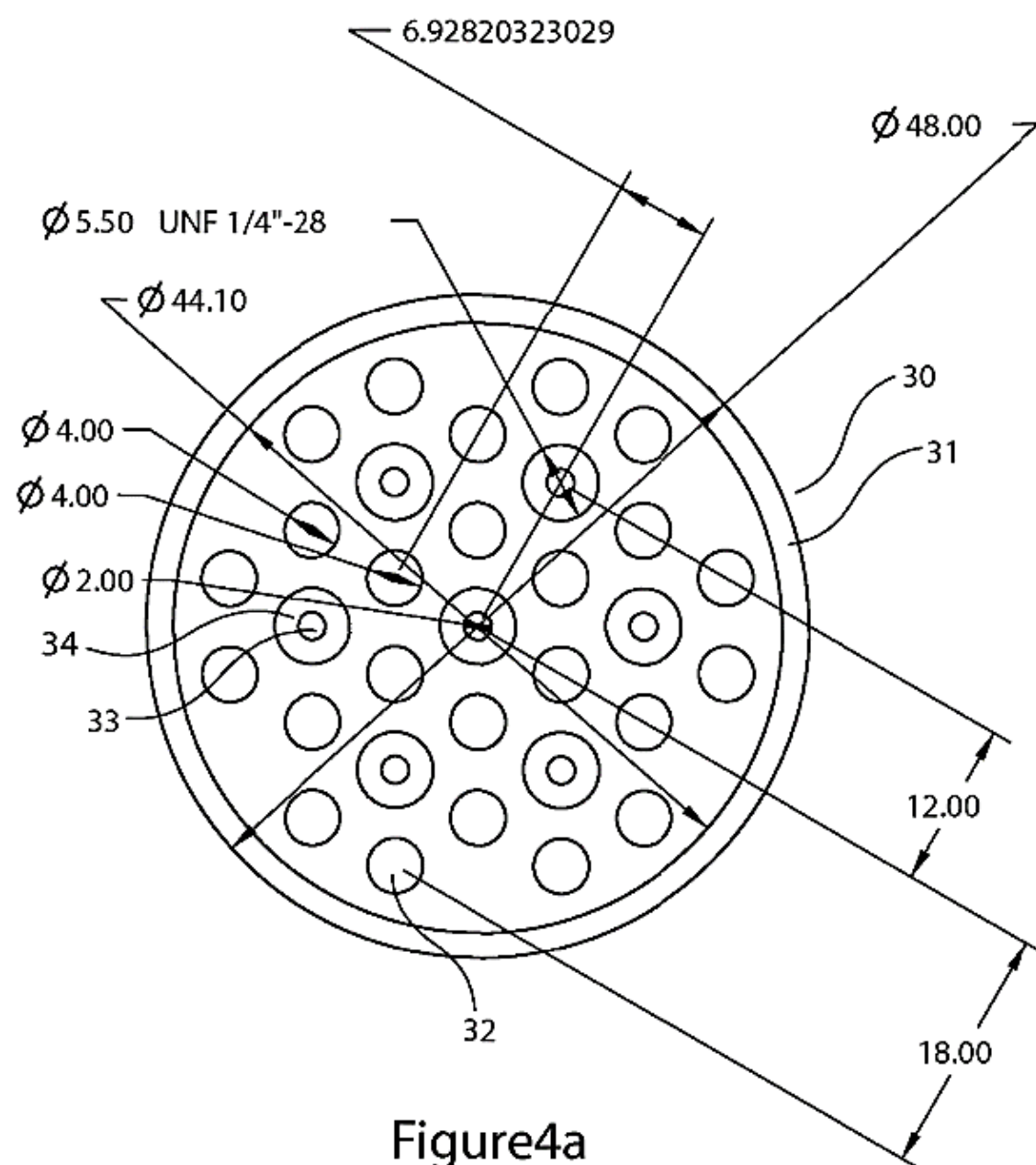
Figure A-3 WO013/050764 Patent, figure 4a. The single Disk/Wafer

Appendix B : Elemental Design of a media Formulation

Table B-1 Quantification of mass percentage of each element in the components of Bold Basal Media

Component	Element	Atomic Weight	No. Atoms	Mass percent %	Mass in BBM mg/lit
NaNO3					
	Sodium	22.99	1	27.05%	67.59
	Nitrogen	14.01	1	16.48%	41.18
	Oxygen	16.00	3	56.47%	141.11
CaCl2·2H2O					
	Calcium	40.08	1	27.26%	6.81
	Chlorine	35.45	2	48.23%	12.05
	Hydrogen	1.01	4	2.74%	0.69
	Oxygen	16.00	2	21.77%	5.44
MgSO4·7H2O					
	Magnesium	24.31	1	9.86%	7.29
	Sulfur	32.07	1	13.01%	9.62
	Oxygen	16.00	11	71.40%	52.80
	Hydrogen	1.01	14	5.73%	4.23

K2HPO4					
	Potassium	39.10	2	44.90%	33.62
	Hydrogen	1.01	1	0.58%	0.43
	Phosphorus	30.97	1	17.78%	13.32
	Oxygen	16.00	4	36.74%	27.52
KH2PO4					
	Potassium	39.10	1	28.73%	50.44
	Hydrogen	1.01	2	1.48%	2.60
	Phosphorus	30.97	1	22.76%	39.96
	Oxygen	16.00	4	47.03%	82.56
NaCl					
	Sodium	22.99	1	39.34%	9.89
	Chlorine	35.45	1	60.66%	15.24
Trace metals					
Na2EDTA•2 H2O					
	Sodium	22.99	2	12.35%	0.55

	Carbon	12.01	10	32.27%	1.44
	Hydrogen	1.01	18	4.87%	0.22
	Nitrogen	14.01	2	7.53%	0.34
	Oxygen	16.00	10	42.98%	1.92
FeCl3 6H2O					
	Iron	55.85	1	20.66%	0.12
	Chlorine	35.45	3	39.35%	0.23
	Hydrogen	1.01	12	4.47%	0.03
	Oxygen	16.00	6	35.52%	0.21
MnCl2•4H2O					
	Manganese	54.94	1	27.76%	0.07
	Chlorine	35.45	2	35.83%	0.09
	Hydrogen	1.01	8	4.07%	0.01
	Oxygen	16.00	4	32.34%	0.08
ZnCl2					
	Zinc	65.38	1	47.97%	0.01
	Chlorine	35.45	2	52.03%	0.02
CoCl2•6H2O					

	Cobalt	58.93	1	24.77%	0.00
	Chlorine	35.45	2	29.80%	0.00
	Hydrogen	1.01	12	5.08%	0.00
	Oxygen	16.00	6	40.35%	0.00
Na2MoO4•2H2O					
	Sodium	22.99	2	19.00%	0.00
	Molybdenum	95.96	1	39.66%	0.01
	Oxygen	16.00	6	39.67%	0.01
	Hydrogen	1.01	4	1.67%	0.00

Table B-2 The recipe of BBM and reformulated BBM R1, developed by applying the biomass capacity methodology as per relevant literature.

	BBM	BBM R1
	Mass per Unit Volume of Media (mg/Lit)	Mass per Unit Volume of Media (mg/Lit)
Macronutrients		
NaNO3	249.871	995.879
CaCl2·2H2O	24.992	74.098
MgSO4·7H2O	73.941	102.421
K2HPO4	74.906	102.421

KH2PO4	175.556	13.183
NaCl	25.112	16.035
Trace metals		
Na2EDTA•2H2O	4.500	0.000
FeCl3 6H2O	0.582	30.55
MnCl2•4H2O	2.460	0.455
ZnCl2	0.030	0.132
CoCl2•6H2O	0.012	0.000
Na2MoO4•2H2O	0.024	0.000

Table B-3: The media recipees developed from the 8 different combinations of high and low levels of N,P,C for the Desing of Experiments .

Compound	Amount used (mg)							
Macro Nutrients	1	2	3	4	5	6	7	8
NaNO3	530.3686	530.3686	104.4281	104.4281	530.3686	530.3686	104.4281	104.4281
CaCl2.2H2O	25	25	25	25	25	25	25	25
MgSO4.7H2O	75	75	75	75	75	75	75	75
K2HPO4	75	0	75	0	75	0	75	0
KH2PO4	24.60	16.64	24.60	16.64	24.60	16.64	24.60	16.64

NaCl	25	25	25	25	25	25	25	25
Micronutrients	╱	╱	╱	╱	╱	╱	╱	╱
EDTA	4.5	4.5	4.5	4.5	4.5	4.5	4.5	4.5
FeCl3.6H2O	0.582	0.582	0.582	0.582	0.582	0.582	0.582	0.582
MnCl2.4H2O	0.246	0.246	0.246	0.246	0.246	0.246	0.246	0.246
ZnCl2	0.03	0.03	0.03	0.03	0.03	0.03	0.03	0.03
CoCl2.6H2O	0.012	0.012	0.012	0.012	0.012	0.012	0.012	0.012
Na2MoO4.2H2O	0.024	0.024	0.024	0.024	0.024	0.024	0.024	0.024
C3H8O3	1997.1	1997.183	1997.183	1997.183	396.4673	396.4673	396.4673	396.4673

Table B-4 The Biomass capacities of all elements. C,N,P are set by the DoE at their respective levels, whereas K,Mg,S,Na,Fe,Mn,Ca and Zn are kept identical with BBM (Adapted from Cox, (2018)).

Element	Biomass capacity of each element for formula (g)							
╱	1	2	3	4	5	6	7	8
C	5.00	5.00	5.00	5.00	1.00	1.00	1.00	1.00
N	5.00	5.00	1.00	1.00	5.00	5.00	1.00	1.00

P	5.00	1.00	5.00	1.00	5.00	1.00	5.00	1.00
K	13.06	1.53	13.06	1.53	13.06	1.53	13.06	1.53
Cl	∞	∞	∞	∞	∞	∞	∞	∞
Mg	5.05	5.05	5.05	5.05	5.05	5.05	5.05	5.05
S	11.54	11.54	11.54	11.54	11.54	11.54	11.54	11.54
Na	N/A	N/A	N/A	N/A	N/A	N/A	N/A	N/A
Fe	0.16	0.16	0.16	0.16	0.16	0.16	0.16	0.16
Mn	4.51	4.51	4.51	4.51	4.51	4.51	4.51	4.51
Co	∞	∞	∞	∞	∞	∞	∞	∞
Ca	63.51	63.51	63.51	63.51	63.51	63.51	63.51	63.51
Zn	2.04	2.04	2.04	2.04	2.04	2.04	2.04	2.04
Mo	∞	∞	∞	∞	∞	∞	∞	∞

Table B-5 DoE results from the P,N,C study using 8 different media formulations.

	Experiment Run							
OD680	**P+N+C+**	**P-N+C+**	**P+N-C+**	**P-N-C+**	**P+N+C-**	**P-N+C-**	**P+N-C-**	**P-N-C-**
Day	1	2	3	4	5	6	7	8
0	0.06	0.06	0.06	0.06	0.06	0.06	0.06	0.06
1	0.17	0.22	0.15	0.13	0.16	0.09	0.13	0.11

2	0.26	0.44	0.33	0.30	0.51	0.36	0.33	0.28
3	0.83	1.44	0.91	1.15	1.72	1.80	0.85	1.30
6	2.39	3.63	3.01	2.61	3.81	4.60	2.62	2.40
7	3.95	4.27	3.21	2.93	3.85	5.19	2.98	2.61
8	3.76	4.20	3.21	2.90	3.68	5.20	2.88	2.75
cells/ml								
Day	1	2	3	4	5	6	7	8
0	7.77E+06	7.77E+06	7.77E+06	7.77E+06	7.77E+06	7.77E+06	7.77E+06	7.77E+06
1	1.89E+07	2.37E+07	1.67E+07	1.52E+07	1.82E+07	1.11E+07	1.55E+07	1.30E+07
2	2.80E+07	4.56E+07	3.53E+07	3.19E+07	5.27E+07	3.85E+07	3.55E+07	2.99E+07
3	8.46E+07	1.46E+08	9.27E+07	1.17E+08	1.74E+08	1.82E+08	8.67E+07	1.32E+08
6	2.41E+08	3.65E+08	3.03E+08	2.63E+08	3.83E+08	4.62E+08	2.64E+08	2.42E+08
7	3.97E+08	4.29E+08	3.23E+08	2.95E+08	3.87E+08	5.21E+08	3.00E+08	2.63E+08
8	3.78E+08	4.22E+08	3.23E+08	2.92E+08	3.70E+08	6.02E+08	2.90E+08	2.77E+08
g/l								
Day	1	2	3	4	5	6	7	8
1	0.55	0.55	0.65	0.4	0.05	0.4	0.65	0.4

2	0.3	0.7	0.15	0.7	0.45	0.55	0.1	0.25
3	0.45	0.4	0.7	0.35	1.9	1.15	0.6	0.45
6	2.9	1.15	0.95	0.55	2.5	2.7	0.85	0.65
7	1.9	0.65	1.25	1	2.1	5.7	0.95	0.3
8	5.75	1.4	1.15	1.15	2.3	6	0.55	1
px	0.74	0.12	0.07	0.11	0.32	0.80	0.07	0.09
Specific Growth Rate								
μ	0.59	0.61	0.57	0.55	0.59	0.64	0.55	0.55
td	1.16	1.13	1.21	1.24	1.17	1.08	1.24	1.26
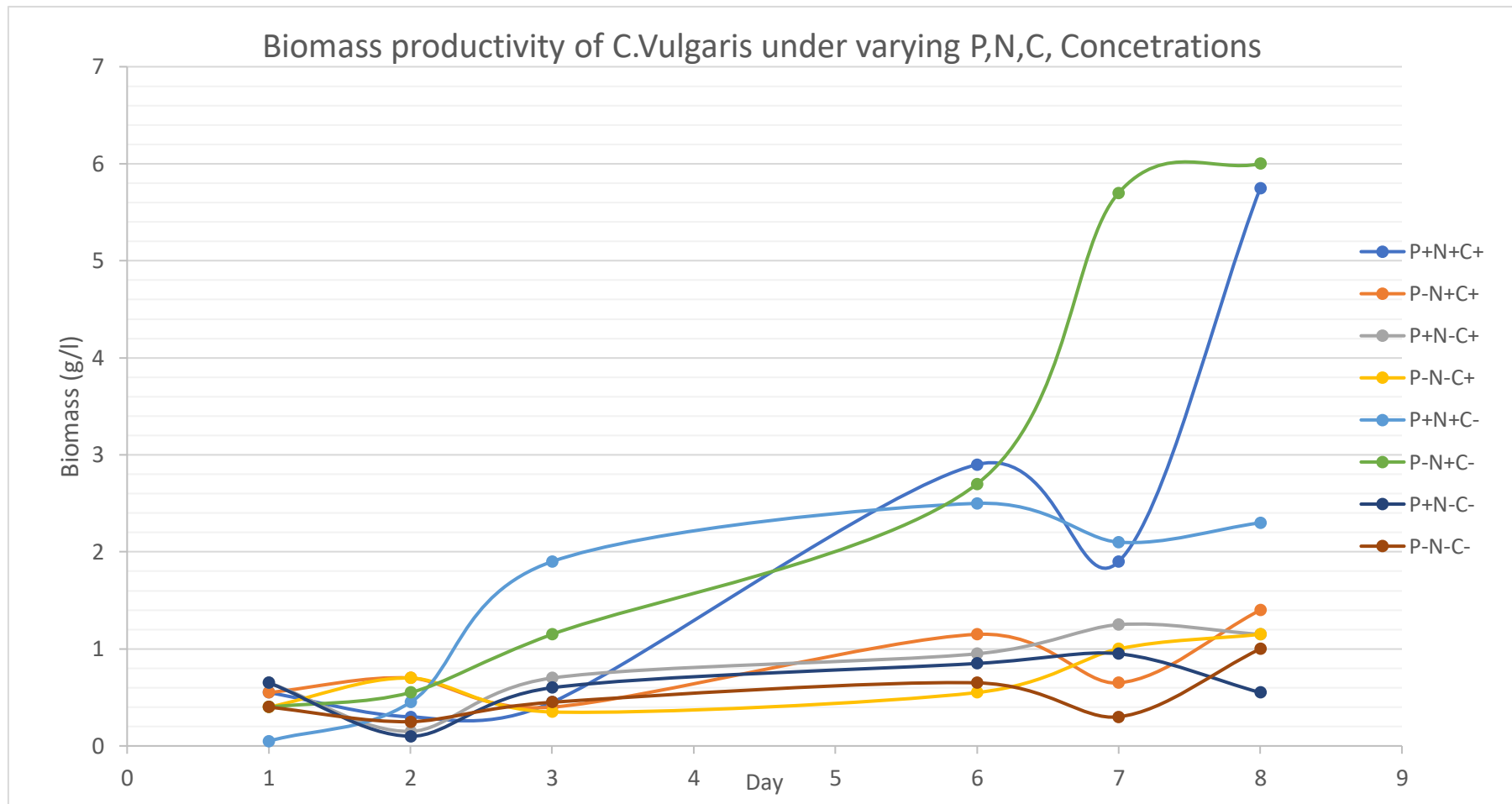
Figure B-1 : Biomass concentration trend of the eight experiments in the Series 2 DoE.
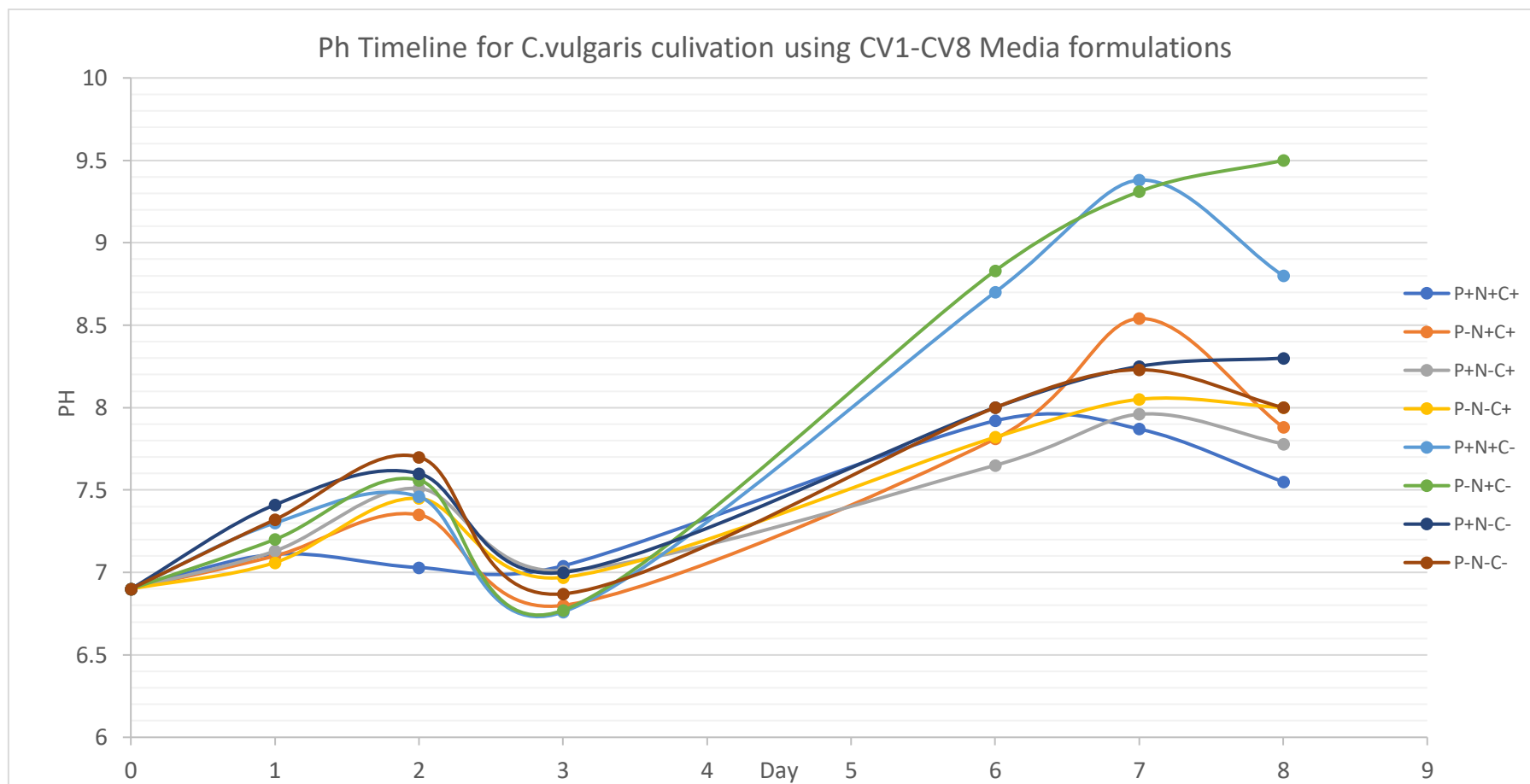
Figure B-2 Ph Trend of the eight experiments in the series 2 DoE

Table B-6 : Price per litre of media for original BBM, BBM-N and BBM revised.

	Supplier / Purchase Code	Price/Container Amount	BBM	BBM -0N	BBM R1
Macronutrients		*£/Mass*	*p/lit*	*p/lit*	*p/lit*
NaNO3	Sigma-Aldridge / S5022-1KG	69.5 £/kg	1.737	0.000	6.921
CaCl2·2H2O	Sigma-Aldridge / C3306-500G	49.5 £/500g	0.124	0.124	0.367
MgSO4·7H2O	Sigma-Aldridge / M2773-1KG	99.5 £ /kg	0.736	0.736	1.019
K2HPO4	Sigma-Aldridge / P8281-500g	60 £/500g	0.899	0.899	1.229
KH2PO4	Sigma-Aldridge / P9791-1KG	61.5 £/kg	1.080	1.080	0.081

NaCl	Sigma-Aldridge / S5886-1KG	33.75 £/kg	0.085	0.085	0.054
Trace Metals			0.000	0.000	0.000
Na2EDTA•2H2O	Sigma-Aldridge / E6635-1KG	161 £/kg	0.072	0.072	0.000
FeCl3 6H2O	Sigma Aldridge/ 44944-100G	25.2 £/100g	0.015	0.015	0.770
MnCl2•4H2O	Sigma-Aldridge / M5005-500G	88 £/500g	0.004	0.004	0.008
ZnCl2	Sigma-Aldridge / Z0152-1KG	85.5£ /kg	0.000	0.000	0.001
CoCl2•6H2O	Sigma-Aldridge / C2911-100g	63 £/100g	0.001	0.001	0.000
Na2MoO4•2H2O	Sigma-Aldridge /	49.5 £/100g	0.001	0.001	0.000

M1651-100G					
Total Price (p/lit)			4.753	3.016	10.450

Table B-7: Price per litre of media for the eight examined media formulations Assuming glycerol is free.

Macronutrient	Cost (p/Lit)							
	P+N+C+	**P-N+C+**	**P+N-C+**	**P-N-C+**	**P+N+C-**	**P-N+C-**	**P+N-C-**	**P-N-C-**
NaNO3	3.6811	3.6861	0.7258	0.7258	3.6861	3.6861	0.7258	0.7258
CaCl2.2H2O	0.1238	0.1238	0.1238	0.1238	0.1238	0.1238	0.1238	0.1238
MgSO4.7H2O	0.7463	0.7463	0.7463	0.7463	0.7463	0.7463	0.7463	0.7463
K2HPO4	0.9000	0.00001	0.9000	0.0000	0.9000	0.0000	0.9000	0.0000
KH2PO4	0.1513	0.1023	0.1513	0.1023	0.1513	0.1023	0.1513	0.1023
NaCl	0.0844	0.0844	0.0844	0.0844	0.0844	0.0844	0.0844	0.0844
Micronutrients								

EDTA	0.0725	0.0725	0.0725	0.0725	0.0725	0.0725	0.0725	0.0725
$FeCl_3.6H_2O$	0.0147	0.0147	0.0147	0.0147	0.0147	0.0147	0.0147	0.0147
$MnCl_2.4H_2O$	0.0043	0.0043	0.0043	0.0043	0.0043	0.0043	0.0043	0.0043
$ZnCl_2$	0.0003	0.0003	0.0003	0.0003	0.0003	0.0003	0.0003	0.0003
$CoCl_2.6H_2O$	0.0008	0.0008	0.0008	0.0008	0.0008	0.0008	0.0008	0.0008
$Na_2MoO_4.2H_2O$	0.0012	0.0012	0.0012	0.0012	0.0012	0.0012	0.0012	0.0012
$C_3H_8O_3$	-	-	-	-	-	-	-	-
Total (p/Lit)	5.78	4.8	2.8	1.87	5.78	4.83	2.82	1.87

Table B-8: Commercial fertiliser ingredients and their concentrations).

Commercial Name	Bone Meal	Epsom Salts (Chemical Formula)	Miracle Grow	Sulphate of Iron (Chemical Formula)
Element	Mass percentage (%)			
N	3		24	
O		53.16		63.28
Mg		20.19		

Element				
P	9		3.5	
S		26.64	0.2	11.53
K			16	
Mn			5	
Fe			0.19	19.5
Cu			0.03	
H				5.07
Zn			0.3	
Total	12.000	99.999	49.220	99.38

Table B-9 EDX results from the commercial fertiliser ingredients and their concentrations (Adapted from Cox, (2018)).

EDX	Commercial Product (Fertiliser, pH buffer, nutrient enrichment)					
Element	**Acid buffer**	**Alkaline buffer**	**Bone Meal**	**Epsom Salts**	**Miracle Grow**	**Sulphate of Iron**
C	28.80	20.13	57.17	10.94	38.67	17.07
N			4.57		13.31	
O	51.92	45.95	26.40	64.39	21.26	50.06
Na	19.20	13.19	0.25	0.19	0.69	
Mg			0.10	10.79	0.06	0.43
Al	0.14	0.06	0.97	0.16	0.18	0.09

Si			8.87			0.18
P			1.04		3.25	
S	0.06	20.71	0.33	13.37	1.16	11.42
Cl			0.32	0.26	10.71	
K			0.29	0.22	10.08	
Ca			2.07			
Ti						0.39
Mn					0.14	
Fe			0.28		0.67	20.43
Cu			0.18			
Total	**100.11**	**100.03**	**102.81**	**100.31**	**100.17**	**100.05**

Table B-10 Replicating the 4 best media recipe from series 2 experiments with commercial fertilisers, an biomass capacity of each element in he media mix. (Adapted from Cox, (2018))

Component	Amount used (mg)			
	CV1	CV2	CV5	CV6
Miracle grow	365.5	365.5	365.5	365.5
Bone meal	68.27	0	68.27	0
Sulphate of Iron	19	19	19	19
Epsom Salts	35.17	35.17	35.17	35.17

Acid Buffer	25	25	25	25	
Alkaline buffer	150	150	150	150	
Glycerol	1604	1639.38	0	38.923	
Element	Biomass capacity of each element for formula (g)				
	1	2	5	6	
C	5.00	5.00	0.99	1.00	
N	5.12	5.00	5.12	5.00	
P	5.00	3.38	5.00	3.38	
K	18.75	18.75	18.75	18.75	
Cl	∞	∞	∞	∞	
Mg	5.00	5.00	5.00	5.00	
S	31.26	14.55	31.26	14.55	
Na	∞	∞	∞	∞	
Fe	5.93	5.93	5.93	5.93	
Mn	1206.27	1206.27	1206.27	1206.27	
Co	∞	∞	∞	∞	
Ca	0.00	0.00	0.00	0.00	
Zn	155.09	155.09	155.09	155.09	
Mo	∞	∞	∞	∞	

Table B-11 Price per litre of media with low cost commercial fertilisers (Adapted from Cox, (2018))

	Price per weight (£/kg)	Price per weight (p/g)	Price per component in recipe (p)			
			CV1	CV2	CV5	CV6
Miracle grow	£16/4.5kg	0.356	0.130	0.130	0.130	0.130
Epsom salts	£3.99/1.5kg	0.266	0.009	0.009	0.009	0.009
sulphate of iron	£2.99/1.5kg	0.199	0.004	0.004	0.004	0.004
Bone meal	£12.37/10kg	0.124	0.008	0.000	0.008	0.000
Acid buffer	£12.99/300g	0.040	0.001	0.001	0.001	0.001
Alkaline buffer	£12.99/600g	2.165	0.325	0.325	0.325	0.325
Glycerol	£10/L	1.000	1.604	1.639	0.039	0.039
Total			2.081	2.108	0.477	0.508

Appendix C **Light**
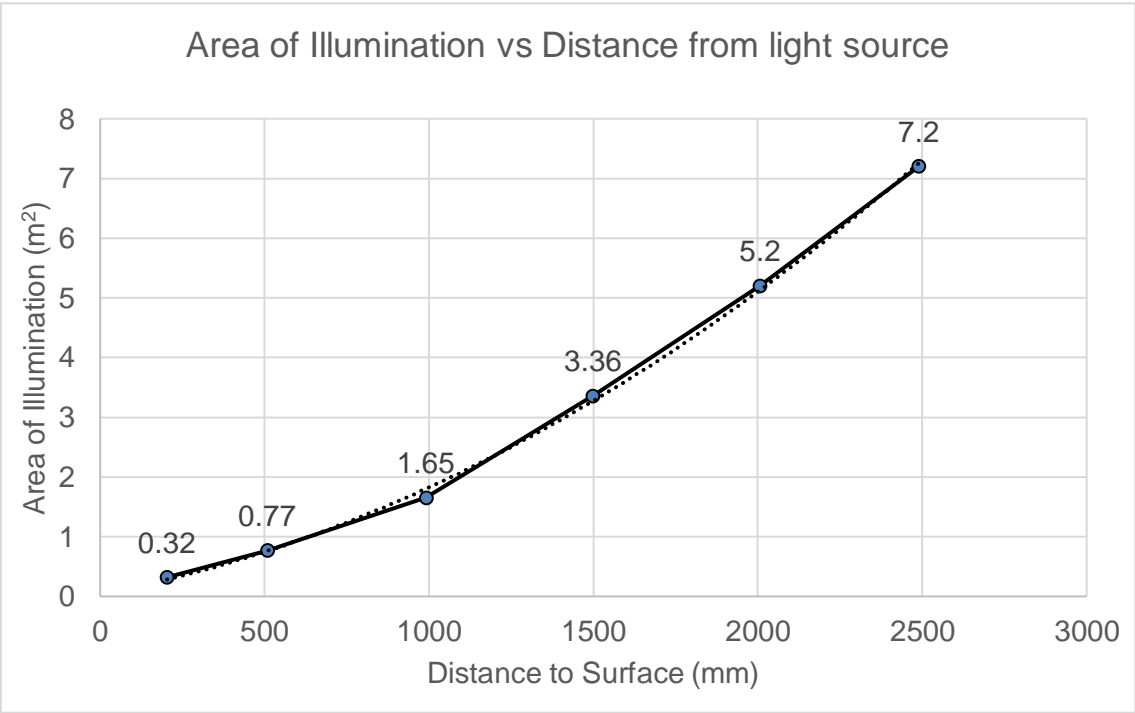
Figure C-1 Illuminated Area vs Distance data fitting curve
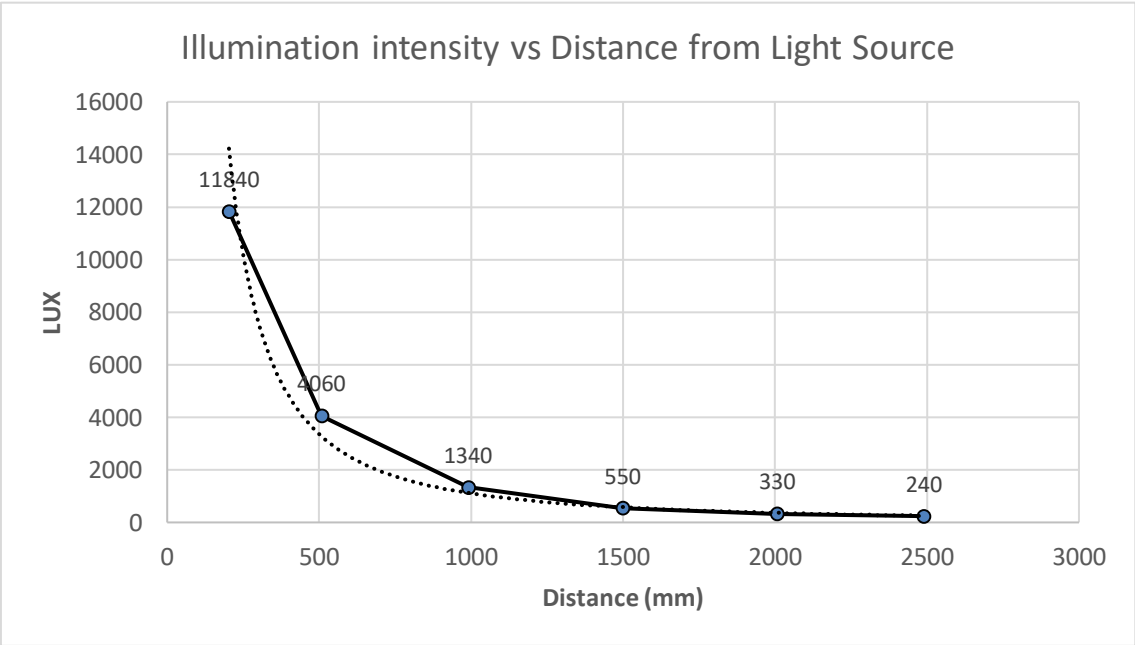
Figure C-2 Distance versus illumination intensity (Lx).
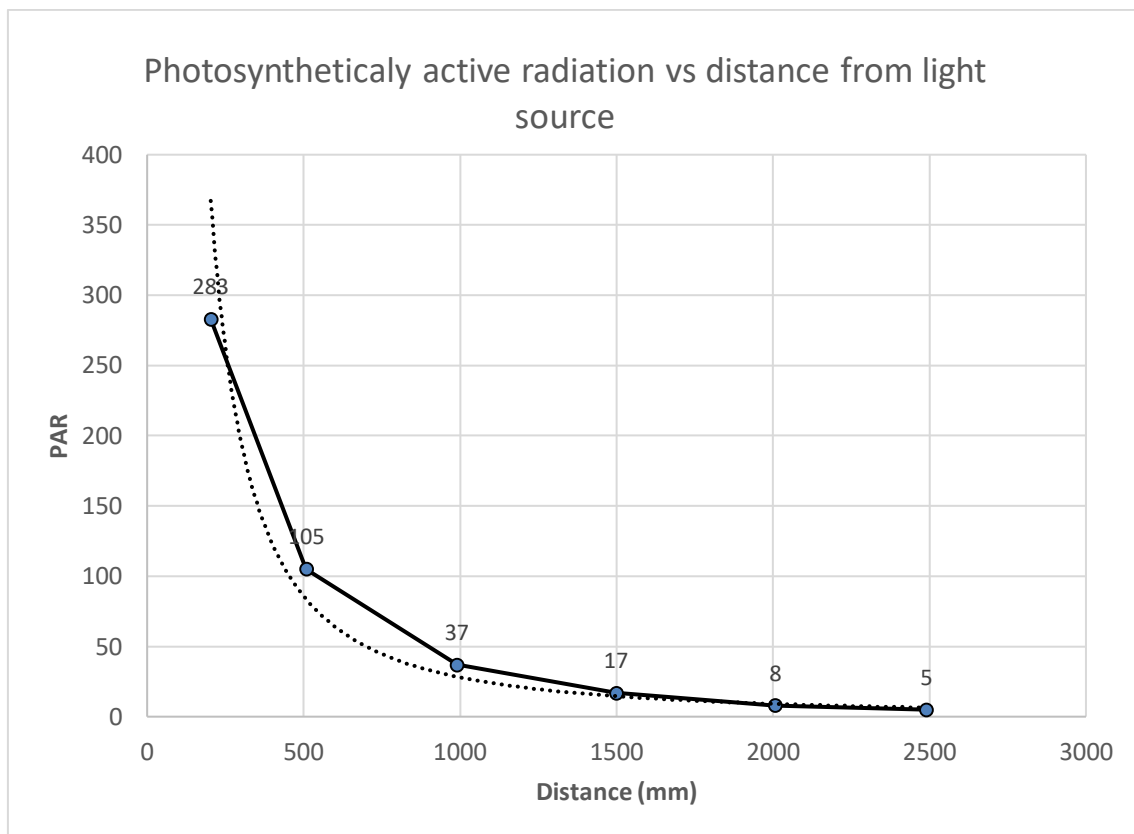
Figure C-3 Distance vs PAR data fitting curve
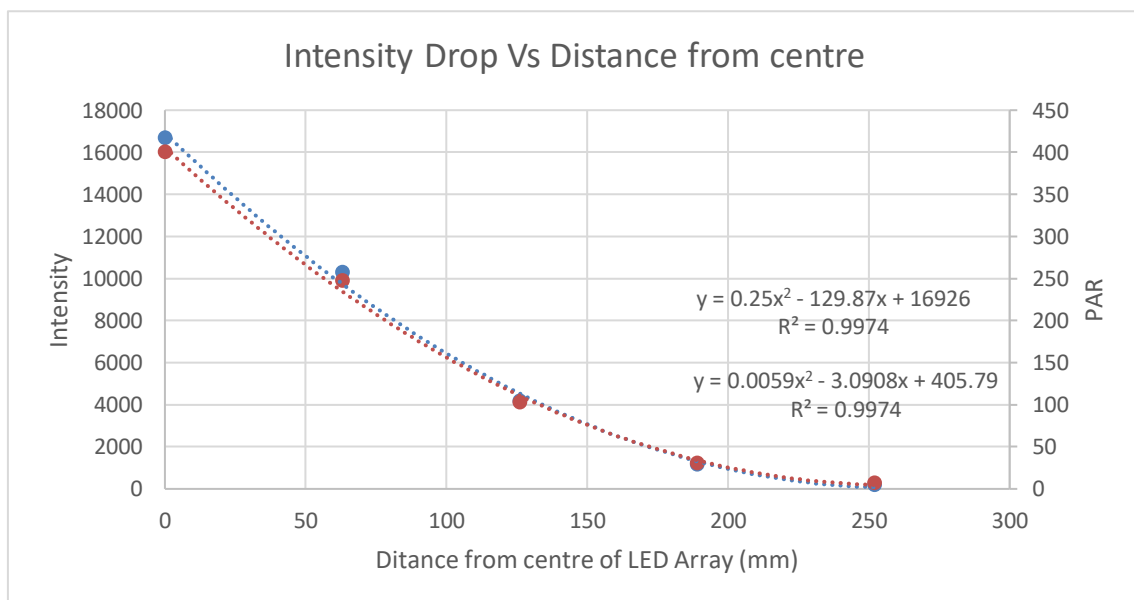
Figure C-4 Assuming a axis along the length of the light bar, the drop on intensity (Ix and PAR) of either side of the axis at set distances.

Appendix D **Characterisation of mixing in C-OBR.**

D.1 Cam Shaft Oscillatory Mechanism System Design.

The cam system induces oscillation to the plunger by rotating an inclined plate, on which a cam roller is pressed against by a spring. The cam rollers XY coordinate position is fixed and is only displaced along the Z axis as the plate rotates. Oscillatory frequency is controlled by the rotational velocity of the plate, whereas the amplitude is controlled by the plate's angle of inclination.

Much like the SYOM, the cam oscillatory mechanism (COM) is designed with cost and simplicity in mind, however the design specification for this system included the development of electronically adjusted amplitude, therefore the design was inevitably much more complex. The system design was split into three sections, the reactor contact section (3), the oscillatory parameter control section (2), and the motor and slip-ring housing section (1).
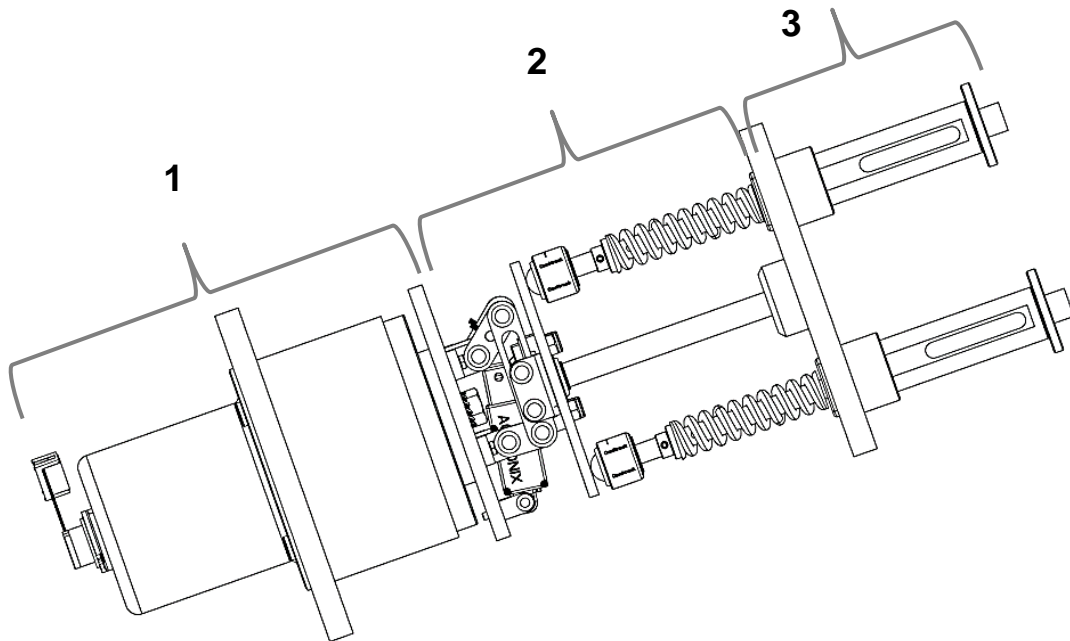
Figure D-1 Side view of the CO mechanism showing the three sections, indicating the tiered design process (1-3).

333

Starting off with section (2), the rotating plate (2a), serves as a mounting platform for a dual four bar actuated tilt control mechanism (2b). The actuation is provided by a 5V high load bearing actuator (2c), which as is portrayed by the adjacent figure when fully extended the contact platform (2d) is at a neutral angle, and when fully retracted, the angle of the plate is at 30° to the mounting platform (2a). The feature to retract the actuator in order to reach the maximum angle was purposefully made, so that the actuator the potential operating loads were always within the actuator duty. The contact platform (2d) is connected to (2b) via a roller sliding feature (2e) and is connected to the top half of section two, via a ball and socket mechanism (2f). Features 2e and 2f, were implemented in the design to overcome a conceptual difficulty in the operation of a 4-bar linkage, which is the off-axis tilt, or shift of axis of the supported member, in this case 2d.
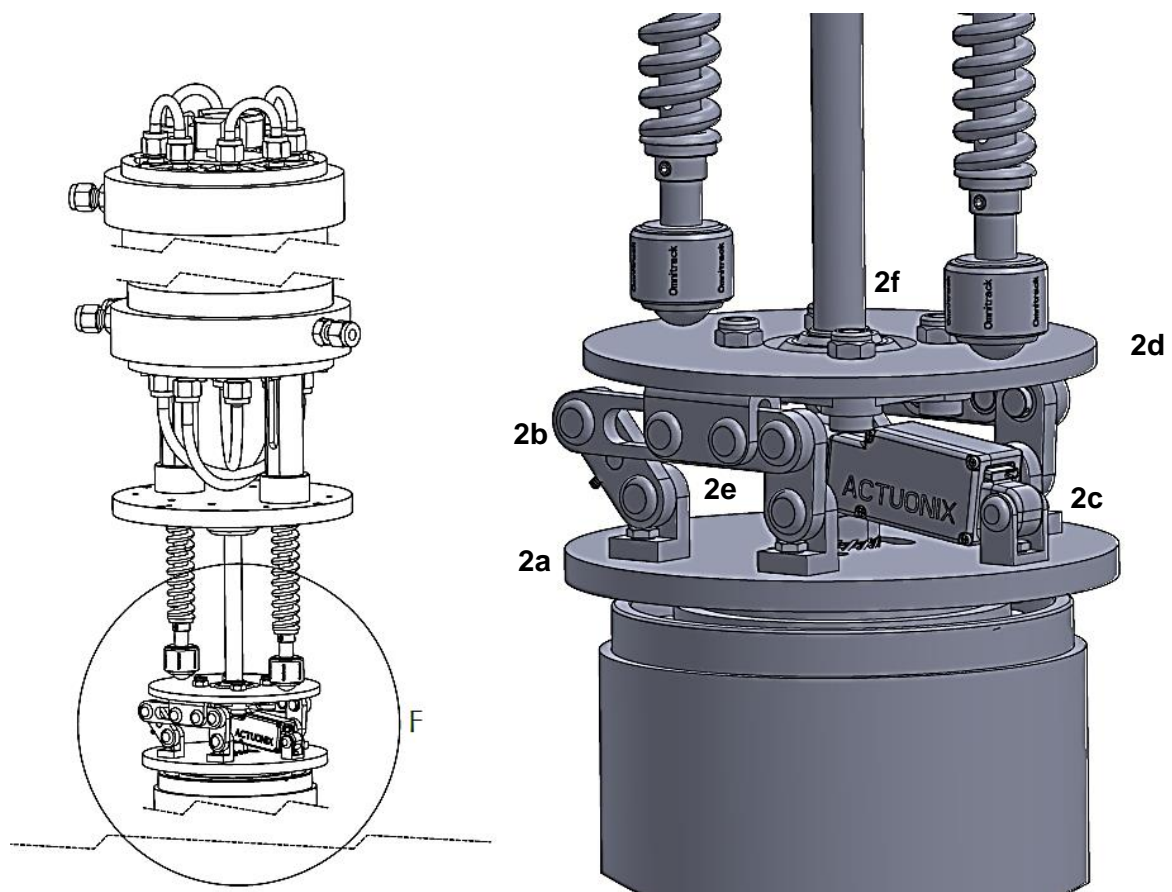
Figure D-2 LHS: Side view of the CO mechanism. RHS: Detail view of section 2 of the COM. With annotations indicating each component.

To overcome this, the feature 2e was designed to enable 2d to remain on the rotational axis of 2a. As demonstrated in the schematic below, the retraction of the actuator induces motion M1 to 2b, since 2d is attached to a support structure via 2e, it forced 2d in motion M2, therefore keeping 2d and 2a on the same axis of rotation.
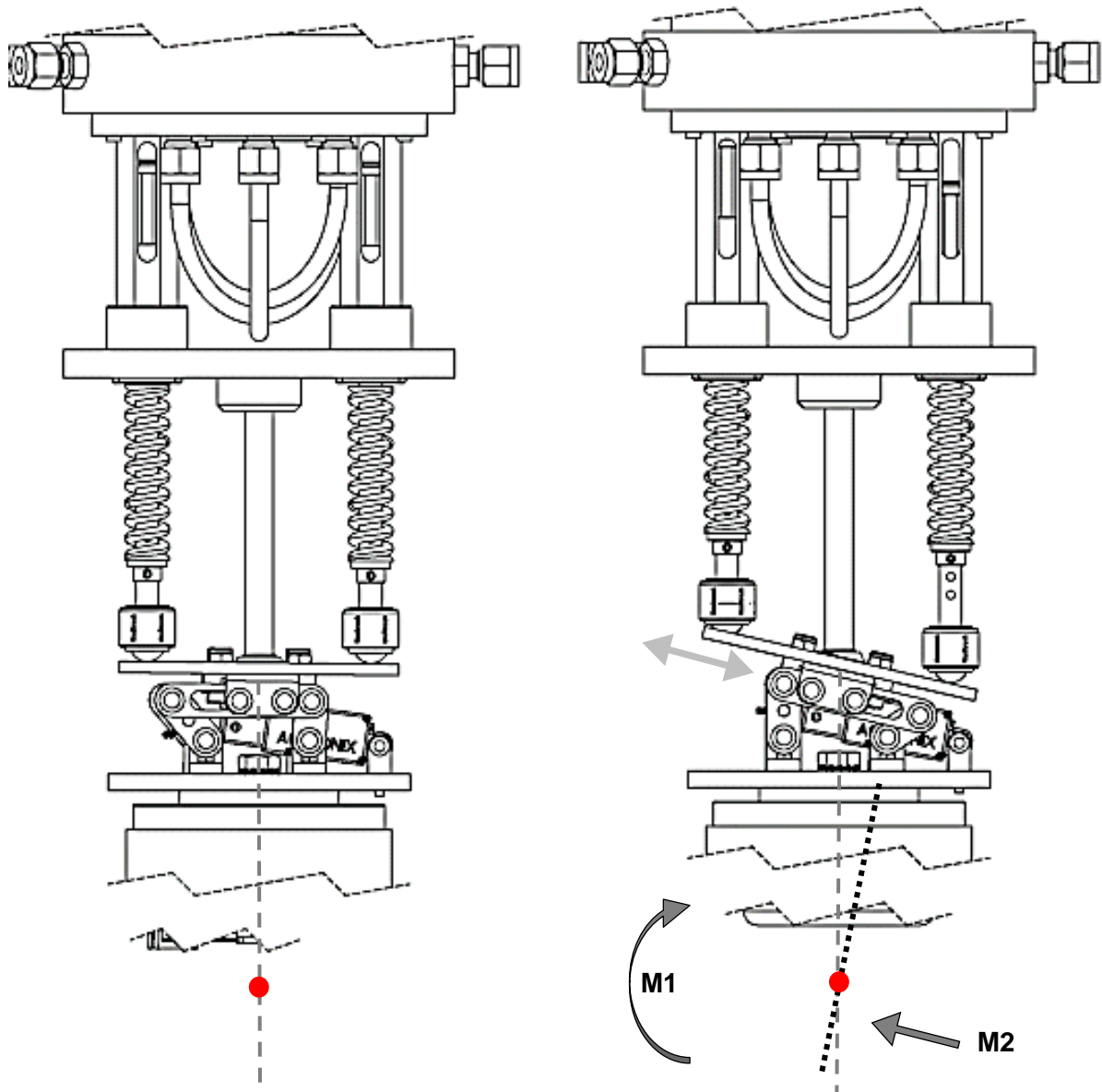
Figure D-3 Graphical representation of the mechanism, during operation. Depicted are the two extreme positions (LHS - neutral / RHS - maximum amplitude).

Section 3 contains the plunger (3b) and tube (3a) assembly, like the SYOM system, as seen in detail- D in the figure below. Whereas in section 1, both the motor (1b), motor pin and slip-ring (1a) are all housed below the roller bearing (1c). This arrangement enables the motor, slip-ring and wiring to be securely housed.
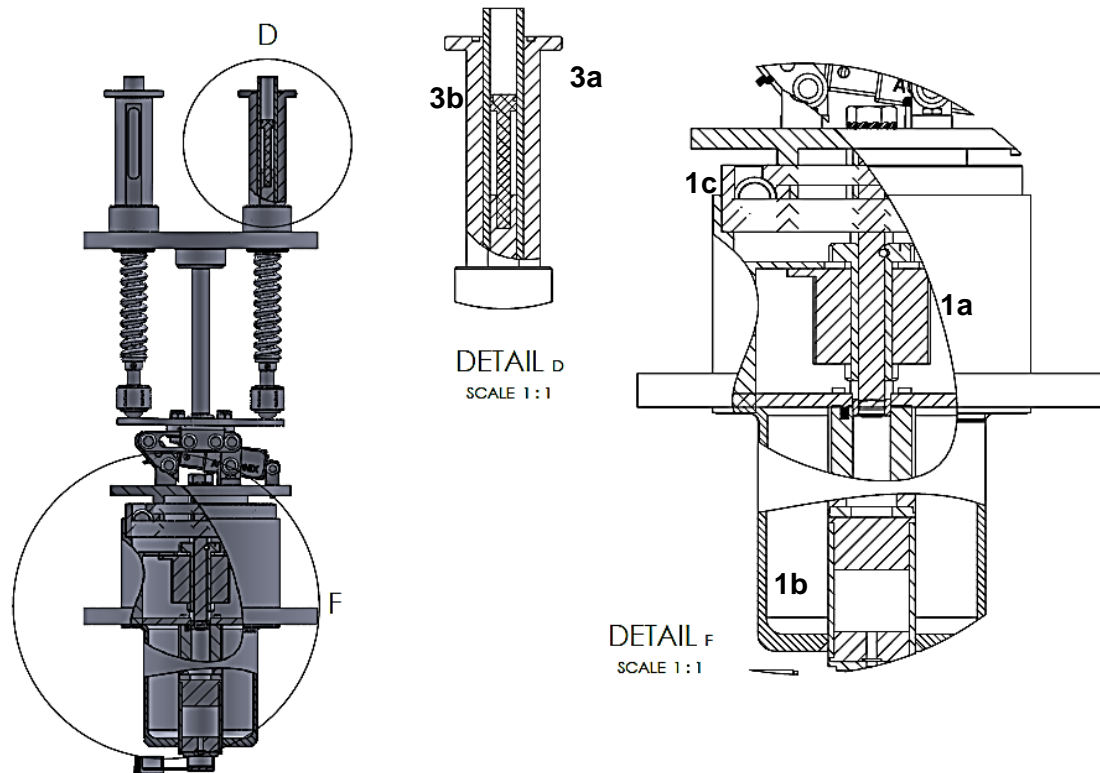
Figure D-4 Sectionally broken side view of the COM. Detailed view of the broken sections (MID and RHS).

D.2 Flow Regime Characterisation Experiments

Table D-1 Microscale Tracer Experiment results, showing the parameters sets (Amplitude, Frequency and net flow) versus the response (TiS number).

Amplitude (mm)	Frequency (Hz)	Net Flow (ml/min)	TiS Number (N)
0.5	3	1	33
0.5	2	1	80
0.5	5	1	68.7
0.5	1	1	32
0.5	4	1	56.8
1	3	1	24.5
1	1	1	38.9
1	2	1	24.7
1	5	1	16.5
1	4	1	26
1.5	1	1	19.2
1.5	2	1	9.4
1.5	5	1	18.2
1.5	4	1	14.5
1.5	3	1	13.3
2	4	1	13.8
2	5	1	15
2	2	1	9.4

2	3	1	12.7
2	1	1	9.4
2.5	2	1	8
2.5	4	1	9.6
2.5	3	1	10.7
2.5	5	1	7.8
2.5	1	1	7.5
0.5	4	2	46.8
1	3	2	27.2
2.5	4	2	11.5
1	5	2	23.8
1	2	2	28.6
2.5	2	2	12.9
1	4	2	36.4
1.5	1	2	23
0.5	1	2	24.8
2	4	2	15.2
2.5	3	2	8.7
2.5	5	2	14
0.5	2	2	21.3
2	5	2	12.8
2	2	2	10.3

1.5	4	2	27.7
1	1	2	43.2
1.5	5	2	27.7
1.5	3	2	26.5
2	3	2	21.6
1.5	2	2	26.6
2	1	2	15.5
2.5	1	2	9.9
0.5	5	2	38.9
0.5	3	2	30
1.5	4	3	28.6
1	3	3	14.6
1	5	3	21.3
0.5	4	3	30.3
2	3	3	14.6
1	2	3	26
2.5	1	3	10
2.5	2	3	12
2.5	3	3	13.3
1.5	5	3	22.5
1.5	2	3	23.5
2.5	5	3	15.6

0.5	2	3	15.9
0.5	1	3	18.7
1.5	3	3	23.3
0.5	5	3	30.6
2	5	3	17.4
1.5	1	3	26.4
2	1	3	16.2
10.5	3	3	27.3
1	1	3	14.7
2	4	3	18.6
1	4	3	39.2
2.5	4	3	17
2	2	3	17
1.5	5	4	16
2.5	2	4	12.7
1.5	4	4	15
0.5	2	4	20
2	1	4	14.7
1	4	4	13.6
1.5	1	4	13.9
2	2	4	13.9
2.5	3	4	7

1.5	2	4	12.5
1	3	4	27
2.5	4	4	12.4
0.5	5	4	38.1
2	5	4	13.7
0.5	1	4	13.5
1	5	4	24.6
0.5	3	4	27.6
2	3	4	15.1
2.5	5	4	17
2.5	1	4	13.6
1	1	4	22
1.5	3	4	26.3
1	2	4	35.1
2	4	4	18.4

Table D-2 Microscale Tracer Experiment results, showing the parameters sets (Amplitude, Frequency and net flow) versus the response (TiS number).

Amplitude (mm)	Frequency (Hz)	Net Flow (ml/min)	TiS Number (N)
3	0.25	2	-
1	0.75	2	-

3	1.25	2	-
	0.5	2	-
4	0.25	2	-
2	0.25	2	13.4
4	0.5	2	-
4	1	2	-
1	1.25	2	-
2	1	2	21.5
2	0.75	2	10.8
3	0.5	2	-
5	1.25	2	-
3	0.75	2	-
5	0.75	2	-
4	1.25	2	-
1	0.25	2	-
2	0.5	2	10.2
5	0.25	2	-
3	1	2	-
2	1.25	2	25.1
5	0.5	2	-
4	0.75	2	-
5	1	2	-

1	1	2	-
5	0.5	4	6
4	0.75	4	6.2
3	0.75	4	14
3	0.25	4	10.2
1	0.5	4	5.1
4	1.25	4	18.9
3	0.5	4	10.4
5	1	4	4.5
3	1	4	23.4
1	1.25	4	16.6
1	0.25	4	6.7
2	0.5	4	12.4
1	1	4	15.3
5	0.25	4	6.9
5	0.75	4	4.7
2	0.75	4	9.7
5	1.25	4	4.4
1	0.75	4	9.3
2	1.25	4	18.3
4	0.5	4	6.6
4	0.25	4	8.6

2	0.25	4	10.4
4	1	4	8.3
2	1	4	18.5
3	1.25	4	21.4
1	0.25	6	6.6
5	0.75	6	8.8
1	0.75	6	7.1
4	0.25	6	10.8
5	1.25	6	5.9
3	0.5	6	11.7
3	0.75	6	9.4
1	1.25	6	11.4
2	1.25	6	22.3
4	0.5	6	8.9
5	1	6	8.5
4	0.75	6	7.3
4	1	6	6.7
1	1	6	10
3	0.25	6	12.9
2	0.25	6	7.2
3	1.25	6	14.5
5	0.25	6	4.5

4	1.25	6	6.6
2	1	6	21.2
5	0.5	6	8.4
2	0.75	6	19.4
3	1	6	8.8
2	0.5	6	17.6
1	0.5	6	6.7
2	0.75	8	27.4
1	0.75	8	-
4	0.25	8	-
3	1	8	29.2
3	0.5	8	24.1
2	0.25	8	-
2	1.25	8	34.7
4	1	8	-
5	0.5	8	17.2
1	0.5	8	-
2	0.25	8	11.8
4	0.75	8	-
3	1.25	8	27.3
2	0.5	8	27.5
5	0.75	8	21.2

3	0.25	8	16.4
4	0.5	8	-
1	1.25	8	-
4	1.25	8	-
2	1	8	34.3
5	0.25	8	15.6
1	1	8	-
3	0.75	8	34.6
5	1.25	8	21.5
5	1	8	14.5

Table D-3 Combined data table between 4mm and 8mm scales. Showing the non-dimensional parameters for each experimental data point.

Exp No	f	$\dot{f}$	D	St	u	Re	Re_o	ψ	Experimental (TiS)	Predicted TiS Number	Error in Prediction
-	(Hz)	ml/min	mm	-	-	-	-	-			
1	2	1	4	0.060	0.00133	5.29	250.62	47.4	8	3.44	4.56
2	4	1	4	0.060	0.00133	5.29	501.25	94.7	9.6	4.53	5.07
3	3	1	4	0.060	0.00133	5.29	375.94	71	10.7	2.94	7.76
4	5	1	4	0.060	0.00133	5.29	626.56	118.4	7.8	10.14	2.34
5	1	1	4	0.060	0.00133	5.29	125.31	23.7	7.5	9.89	2.39

6	4	2	4	0.060	0.00265	10.59	501.25	47.4	11.5	11.29	0.21
7	2	2	4	0.060	0.00265	10.59	250.62	23.7	12.9	10.82	2.08
8	3	2	4	0.060	0.00265	10.59	375.94	35.5	8.7	11.93	3.23
9	5	2	4	0.060	0.00265	10.59	626.56	59.2	14	16.38	2.38
10	1	2	4	0.060	0.00265	10.59	125.31	11.8	9.9	15.49	5.59
11	1	3	4	0.060	0.00398	15.88	125.31	7.9	10	13.64	3.64
12	2	3	4	0.060	0.00398	15.88	250.62	15.8	12	12.10	0.10
13	3	3	4	0.060	0.00398	15.88	375.94	23.7	13.3	11.94	1.36

14	5	3	4	0.060	0.00398	15.88	626.56	39.5	15.6	15.56	0.04
15	4	3	4	0.060	0.00398	15.88	501.25	31.6	17	13.08	3.92
16	2	4	4	0.060	0.00531	21.17	250.62	11.8	12.7	15.14	2.44
17	3	4	4	0.060	0.00531	21.17	375.94	17.8	7	9.54	2.54
18	4	4	4	0.060	0.00531	21.17	501.25	23.7	12.4	12.32	0.08
19	5	4	4	0.060	0.00531	21.17	626.56	29.6	17	16.11	0.89
20	1	4	4	0.060	0.00531	21.17	125.31	5.9	13.6	14.37	0.77
21	1.25	2	8	0.064	0.0007	2.65	313.28	118.44		13.11	0.00

22	0.75	2	8	0.064	0.0007	2.65	187.97	71.06		0.95	0.00
23	0.25	2	8	0.064	0.0007	2.65	62.66	23.69		3.15	0.00
24	0.5	2	8	0.064	0.0007	2.65	125.31	47.37		2.10	0.00
25	1	2	8	0.064	0.0007	2.65	250.62	94.75		6.03	0.00
26	0.5	4	8	0.064	0.0013	5.29	125.31	23.69	6	2.77	3.23
27	1	4	8	0.064	0.0013	5.29	250.62	47.37	4.5	6.69	2.19
28	0.25	4	8	0.064	0.0013	5.29	62.66	11.84	6.9	2.31	4.59
29	0.75	4	8	0.064	0.0013	5.29	187.97	35.53	4.7	4.23	0.47

30	1.25	4	8	0.064	0.0013	5.29	313.28	59.22	4.4	10.16	5.76
31	0.75	6	8	0.064	0.002	7.94	187.97	23.69	8.8	8.51	0.29
32	1.25	6	8	0.064	0.002	7.94	313.28	39.48	5.9	12.25	6.35
33	1	6	8	0.064	0.002	7.94	250.62	31.58	8.5	10.05	1.55
34	0.25	6	8	0.064	0.002	7.94	62.66	7.90	4.5	7.45	2.95
35	0.5	6	8	0.064	0.002	7.94	125.31	15.79	8.4	7.64	0.76
36	0.5	8	8	0.064	0.0027	10.58	125.31	11.84	17.2	12.53	4.67
37	0.75	8	8	0.064	0.0027	10.58	187.97	17.77	21.2	13.06	8.14

38	0.25	8	8	0.064	0.0027	10.58	62.66	5.92	15.6	12.50	3.10
39	1.25	8	8	0.064	0.0027	10.58	313.28	29.61	21.5	15.62	5.88
40	1	8	8	0.064	0.0027	10.58	250.62	23.69	14.5	14.08	0.42
41	0.25	2	8	0.080	0.0007	2.65	50.12	18.95		0.92	0.00
42	0.5	2	8	0.080	0.0007	2.65	100.25	37.90		2.71	0.00
43	1	2	8	0.080	0.0007	2.65	200.50	75.80		10.14	0.00
44	1.25	2	8	0.080	0.0007	2.65	250.62	94.75		15.79	0.00
45	0.75	2	8	0.080	0.0007	2.65	150.37	56.85		5.78	0.00

46	0.75	4	8	0.080	0.0013	5.29	150.37	28.42	6.2	8.25	2.05
47	1.25	4	8	0.080	0.0013	5.29	250.62	47.37	18.9	12.70	6.20
48	0.5	4	8	0.080	0.0013	5.29	100.25	18.95	6.6	6.99	0.39
49	0.25	4	8	0.080	0.0013	5.29	50.12	9.47	8.6	6.37	2.23
50	1	4	8	0.080	0.0013	5.29	200.50	37.90	8.3	10.15	1.85
51	0.25	6	8	0.080	0.002	7.94	50.12	6.32	10.8	12.13	1.33
52	0.5	6	8	0.080	0.002	7.94	100.25	12.63	8.9	12.31	3.41
53	0.75	6	8	0.080	0.002	7.94	150.37	18.95	7.3	12.91	5.61

54	1	6	8	0.080	0.002	7.94	200.50	25.27	6.7	13.95	7.25
55	1.25	6	8	0.080	0.002	7.94	250.62	31.58	6.6	15.42	8.82
56	0.25	8	8	0.080	0.0027	10.58	50.12	4.74		17.96	0.00
57	1	8	8	0.080	0.0027	10.58	200.50	18.95		18.70	0.00
58	0.75	8	8	0.080	0.0027	10.58	150.37	14.21		18.13	0.00
59	0.5	8	8	0.080	0.0027	10.58	100.25	9.47		17.89	0.00
60	1.25	8	8	0.080	0.0027	10.58	250.62	23.69		19.59	0.00
61	4	1	4	0.080	0.00133	5.29	401.00	75.80	13.8	9.16	4.64

62	5	1	4	0.080	0.00133	5.29	501.25	94.70	15	13.58	1.42
63	2	1	4	0.080	0.00133	5.29	200.50	37.90	9.4	9.89	0.49
64	3	1	4	0.080	0.00133	5.29	300.75	56.80	12.7	9.17	3.53
65	1	1	4	0.080	0.00133	5.29	100.25	18.90	9.4	15.06	5.66
66	4	2	4	0.080	0.00265	10.59	401.00	37.90	15.2	15.22	0.02
67	5	2	4	0.080	0.00265	10.59	501.25	47.40	12.8	16.45	3.65
68	2	2	4	0.080	0.00265	10.59	200.50	18.90	10.3	16.63	6.33
69	3	2	4	0.080	0.00265	10.59	300.75	28.40	21.6	15.28	6.32

70	1	2	4	0.080	0.00265	10.59	100.25	9.50	15.5	15.54	0.04
71	3	3	4	0.080	0.00398	15.88	300.75	18.90	14.6	18.31	3.71
72	5	3	4	0.080	0.00398	15.88	501.25	31.60	17.4	17.24	0.16
73	1	3	4	0.080	0.00398	15.88	100.25	6.30	16.2	17.25	1.05
74	4	3	4	0.080	0.00398	15.88	401.00	25.30	18.6	14.57	4.03
75	2	3	4	0.080	0.00398	15.88	200.50	12.60	17	17.35	0.35
76	1	4	4	0.080	0.00531	21.17	100.25	4.70	14.7	18.16	3.46
77	2	4	4	0.080	0.00531	21.17	200.50	9.50	13.9	13.01	0.89

78	5	4	4	0.080	0.00531	21.17	501.25	23.70	13.7	16.23	2.53
79	3	4	4	0.080	0.00531	21.17	300.75	14.20	15.1	15.90	0.80
80	4	4	4	0.080	0.00531	21.17	401.00	18.90	18.4	19.44	1.04
81	0.25	2	8	0.106	0.0007	2.65	37.59	14.21		4.30	0.00
82	1.25	2	8	0.106	0.0007	2.65	187.97	71.06		19.49	0.00
83	0.5	2	8	0.106	0.0007	2.65	75.19	28.42		7.01	0.00
84	0.75	2	8	0.106	0.0007	2.65	112.78	42.64		10.45	0.00
85	1	2	8	0.106	0.0007	2.65	150.37	56.85		14.61	0.00

86	0.75	4	8	0.106	0.0013	5.29	112.78	21.32	14	12.15	1.85
87	0.25	4	8	0.106	0.0013	5.29	37.59	7.11	10.2	9.69	0.51
88	0.5	4	8	0.106	0.0013	5.29	75.19	14.21	10.4	10.74	0.34
89	1	4	8	0.106	0.0013	5.29	150.37	28.42	23.4	13.92	9.48
90	1.25	4	8	0.106	0.0013	5.29	187.97	35.53	21.4	16.06	5.34
91	0.5	6	8	0.106	0.002	7.94	75.19	9.47	11.7	16.37	4.67
92	0.75	6	8	0.106	0.002	7.94	112.78	14.21	9.4	17.07	7.67
93	0.25	6	8	0.106	0.002	7.94	37.59	4.74	12.9	15.92	3.02

358

94	1.25	6	8	0.106	0.002	7.94	187.97	23.69	14.5	19.19	4.69
95	1	6	8	0.106	0.002	7.94	150.37	18.95	8.8	18.01	9.21
96	1	8	8	0.106	0.0027	10.58	150.37	14.21	29.2	23.30	5.90
97	0.5	8	8	0.106	0.0027	10.58	75.19	7.11	24.1	22.49	1.61
98	1.25	8	8	0.106	0.0027	10.58	187.97	17.77	27.3	23.98	3.32
99	0.25	8	8	0.106	0.0027	10.58	37.59	3.55	16.4	22.35	5.95
100	0.75	8	8	0.106	0.0027	10.58	112.78	10.66	34.6	22.80	11.80
101	1	1	4	0.110	0.00133	5.29	75.19	14.20	19.2	19.69	0.49

102	2	1	4	0.110	0.00133	5.29	150.37	28.40	9.4	18.03	8.63
103	5	1	4	0.110	0.00133	5.29	375.94	71.00	18.2	21.81	3.61
104	4	1	4	0.110	0.00133	5.29	300.75	56.80	14.5	19.10	4.60
105	3	1	4	0.110	0.00133	5.29	225.56	42.60	13.3	17.84	4.54
106	1	2	4	0.110	0.00265	10.59	75.19	7.10	23	20.39	2.61
107	4	2	4	0.110	0.00265	10.59	300.75	28.40	27.7	21.68	6.02
108	5	2	4	0.110	0.00265	10.59	375.94	35.50	27.7	23.56	4.14
109	3	2	4	0.110	0.00265	10.59	225.56	21.30	26.5	20.51	5.99

110	2	2	4	0.110	0.00265	10.59	150.37	14.20	26.6	20.07	6.53
111	4	3	4	0.110	0.003988	15.88	300.75	18.90	28.6	23.58	5.02
112	5	3	4	0.110	0.003988	15.88	375.94	23.70	22.5	21.52	0.98
113	2	3	4	0.110	0.003988	15.88	150.37	9.50	23.5	18.04	5.46
114	3	3	4	0.110	0.003988	15.88	225.56	14.20	23.3	20.57	2.73
115	1	3	4	0.110	0.003988	15.88	75.19	4.70	26.4	21.58	4.82
116	5	4	4	0.110	0.00531	21.17	375.94	17.80	16	18.38	2.38
117	4	4	4	0.110	0.00531	21.17	300.75	14.20	15	20.65	5.65

118	1	4	4	0.110	0.00531	21.17	75.19	3.60	13.9	14.91	1.01
119	2	4	4	0.110	0.00531	21.17	150.37	7.10	12.5	18.91	6.41
120	3	4	4	0.110	0.00531	21.17	225.56	10.70	26.3	15.90	10.40
121	0.25	2	8	0.159	0.0007	2.65	25.06	9.47	13.4	5.84	7.56
122	1	2	8	0.159	0.0007	2.65	100.25	37.90	21.5	18.30	3.20
123	0.75	2	8	0.159	0.0007	2.65	75.19	28.42	10.8	13.83	3.03
124	0.5	2	8	0.159	0.0007	2.65	50.12	18.95	10.2	9.67	0.53
125	1.25	2	8	0.159	0.0007	2.65	125.31	47.37	25.1	23.10	2.00

126	0.5	4	8	0.159	0.0013	5.29	50.12	9.47	12.4	12.58	0.18
127	0.75	4	8	0.159	0.0013	5.29	75.19	14.21	9.7	14.49	4.79
128	1.25	4	8	0.159	0.0013	5.29	125.31	23.69	18.3	18.80	0.50
129	0.25	4	8	0.159	0.0013	5.29	25.06	4.74	10.4	10.82	0.42
130	1	4	8	0.159	0.0013	5.29	100.25	18.95	18.5	16.57	1.93
131	1.25	6	8	0.159	0.002	7.94	125.31	15.79	22.3	21.86	0.44
132	0.25	6	8	0.159	0.002	7.94	25.06	3.16	7.2	17.07	9.87
133	1	6	8	0.159	0.002	7.94	100.25	12.63	21.2	20.50	0.70

134	0.75	6	8	0.159	0.002	7.94	75.19	9.47	19.4	19.25	0.15
135	0.5	6	8	0.159	0.002	7.94	50.12	6.32	17.6	18.11	0.51
136	0.75	8	8	0.159	0.0027	10.58	75.19	7.11	27.4	25.03	2.37
137	1.25	8	8	0.159	0.0027	10.58	125.31	11.84	34.7	26.75	7.95
138	0.25	8	8	0.159	0.0027	10.58	25.06	2.37	11.8	23.63	11.83
139	0.5	8	8	0.159	0.0027	10.58	50.12	4.74	27.5	24.29	3.21
140	1	8	8	0.159	0.0027	10.58	100.25	9.47	34.3	25.85	8.45
141	3	1	4	0.160	0.00133	5.29	150.37	28.40	24.5	29.47	4.97

142	1	1	4	0.160	0.00133	5.29	50.12	9.50	38.9	26.67	12.23
143	2	1	4	0.160	0.00133	5.29	100.25	18.90	24.7	28.70	4.00
144	5	1	4	0.160	0.00133	5.29	250.62	47.40	16.5	32.99	16.49
145	4	1	4	0.160	0.00133	5.29	200.50	37.90	26	30.93	4.93
146	3	2	4	0.160	0.00265	10.59	150.37	14.20	27.2	28.02	0.82
147	5	2	4	0.160	0.00265	10.59	250.62	23.70	23.8	30.35	6.55
148	2	2	4	0.160	0.00265	10.59	100.25	9.50	28.6	25.51	3.09
149	4	2	4	0.160	0.00265	10.59	200.50	18.90	36.4	30.89	5.51

150	1	2	4	0.160	0.00265	10.59	50.12	4.70	43.2	26.99	16.21
151	3	3	4	0.160	0.00398	15.88	150.37	9.50	14.6	24.38	9.78
152	5	3	4	0.160	0.00398	15.88	250.62	15.80	21.3	28.19	6.89
153	2	3	4	0.160	0.00398	15.88	100.25	6.30	26	25.59	0.41
154	1	3	4	0.160	0.00398	15.88	50.12	3.20	14.7	21.43	6.73
155	4	3	4	0.160	0.00398	15.88	200.50	12.60	39.2	28.96	10.24
156	4	4	4	0.160	0.00531	21.17	200.50	9.50	13.6	23.01	9.41
157	3	4	4	0.160	0.00531	21.17	150.37	7.10	27	24.10	2.90

158	5	4	4	0.160	0.00531	21.17	250.62	11.80	24.6	29.42	4.82
159	1	4	4	0.160	0.00531	21.17	50.12	2.40	22	19.41	2.59
160	2	4	4	0.160	0.00531	21.17	100.25	4.70	35.1	25.38	9.72
161	4	4	4	0.300	0.00531	21.20	100.20	4.70	36.5	28.26	8.24
162	0.75	2	8	0.318	0.0007	2.65	37.59	14.21		10.46	0.00
163	0.5	2	8	0.318	0.0007	2.65	25.06	9.47		5.24	0.00
164	1.25	2	8	0.318	0.0007	2.65	62.66	23.69		21.14	0.00
165	0.25	2	8	0.318	0.0007	2.65	12.53	4.74		0.10	0.00

166	1	2	8	0.318	0.0007	2.65	50.12	18.95		15.76	0.00
167	0.5	4	8	0.318	0.0013	5.29	25.06	4.74	5.1	5.56	0.46
168	1.25	4	8	0.318	0.0013	5.29	62.66	11.84	16.6	13.98	2.62
169	0.25	4	8	0.318	0.0013	5.29	12.53	2.37	6.7	2.83	3.87
170	1	4	8	0.318	0.0013	5.29	50.12	9.47	15.3	11.13	4.17
171	0.75	4	8	0.318	0.0013	5.29	37.59	7.11	9.3	8.33	0.97
172	0.25	6	8	0.318	0.002	7.94	12.53	1.58	6.6	7.13	0.53
173	0.75	6	8	0.318	0.002	7.94	37.59	4.74	7.1	10.98	3.88

174	1.25	6	8	0.318	0.002	7.94	62.66	7.90	11.4	14.94	3.54
175	1	6	8	0.318	0.002	7.94	50.12	6.32	10	12.95	2.95
176	0.5	6	8	0.318	0.002	7.94	25.06	3.16	6.7	9.04	2.34
177	0.75	8	8	0.318	0.0027	10.58	37.59	3.55		14.84	0.00
178	0.25	8	8	0.318	0.0027	10.58	12.53	1.18		11.83	0.00
179	0.5	8	8	0.318	0.0027	10.58	25.06	2.37		13.33	0.00
180	1.25	8	8	0.318	0.0027	10.58	62.66	5.92		17.93	0.00
181	1	8	8	0.318	0.0027	10.58	50.12	4.74		16.38	0.00

182	3	1	4	0.320	0.00133	5.29	75.19	14.20	33	48.28	15.28
183	2	1	4	0.320	0.00133	5.29	50.12	9.5	80	43.43	36.57
184	5	1	4	0.320	0.00133	5.29	125.31	23.7	68.7	56.59	12.11
185	1	1	4	0.320	0.00133	5.29	25.06	4.7	32	40.58	8.58
186	4	1	4	0.320	0.00133	5.29	100.25	18.9	56.8	53.25	3.55
187	4	2	4	0.320	0.00265	10.59	100.25	9.5	46.8	39.69	7.11
188	1	2	4	0.320	0.00265	10.59	25.06	2.4	24.8	30.76	5.96
189	2	2	4	0.320	0.00265	10.59	50.12	4.7	21.3	36.07	14.77

190	5	2	4	0.320	0.00265	10.59	125.31	11.8	38.9	45.25	6.35
191	3	2	4	0.320	0.00265	10.59	75.19	7.1	30	37.86	7.86
192	4	3	4	0.320	0.00398	15.88	100.25	6.3	30.3	33.04	2.74
193	2	3	4	0.320	0.00398	15.88	50.12	3.2	15.9	24.78	8.88
194	1	3	4	0.320	0.00398	15.88	25.06	1.6	18.7	23.50	4.80
195	5	3	4	0.320	0.00398	15.88	125.31	7.9	30.6	34.48	3.88
196	3	3	4	0.320	0.00398	15.88	75.19	4.7	27.3	31.64	4.34
197	2	4	4	0.320	0.00531	21.17	50.12	2.4	20	17.44	2.56

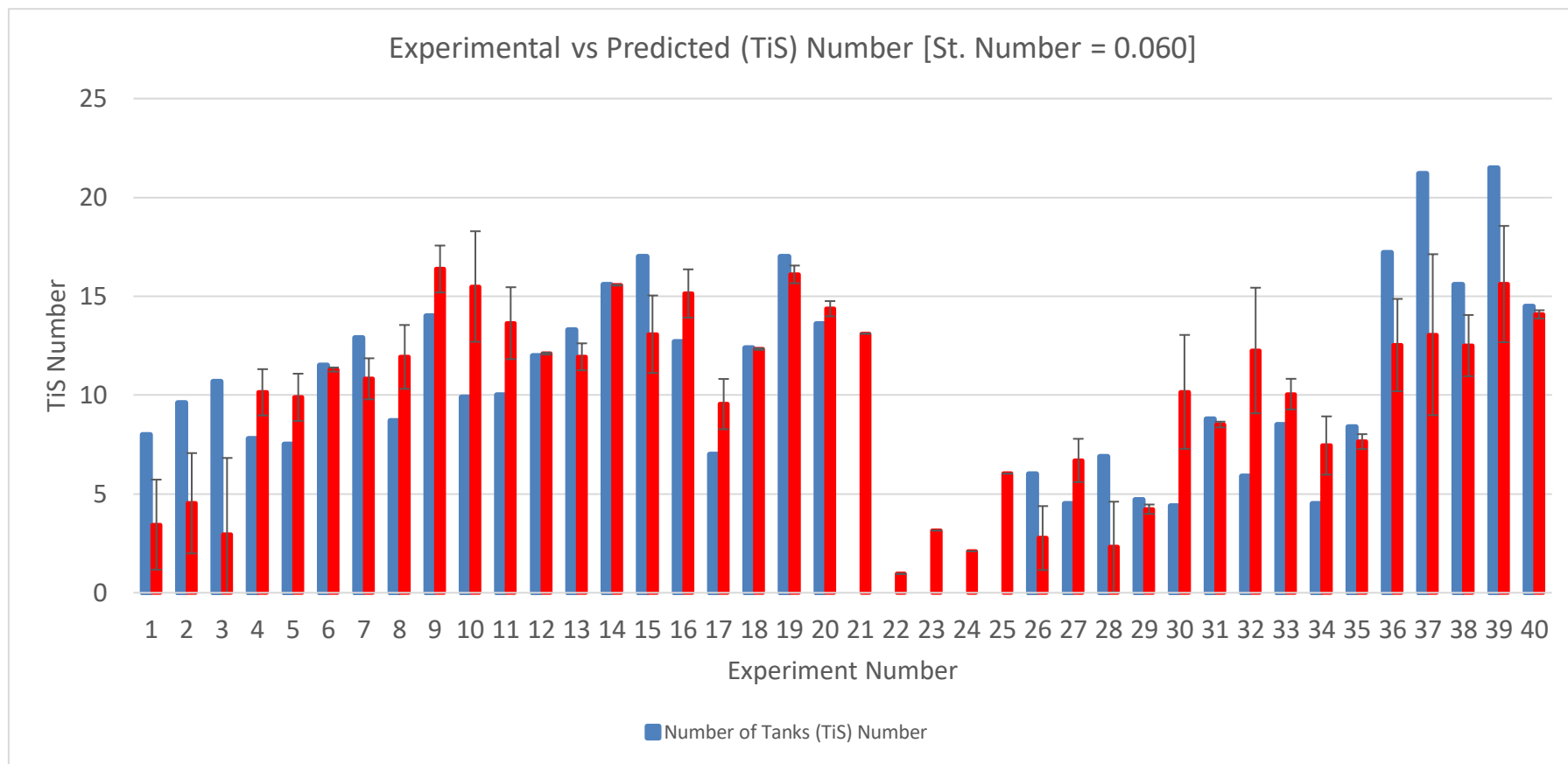| 198	5	4	4	0.320	0.00531	21.17	125.31	5.9	38.1	28.22	9.88
199	1	4	4	0.320	0.00531	21.17	25.06	1.2	13.5	16.38	2.88
200	3	4	4	0.320	0.00531	21.17	75.19	3.6	27.6	18.57	9.03

Figure D-5 Experimental versus predicted Tank in Series numbers for experiments across two micro and meso scale with Strouhal number approximately 0.06. Experiment numbers correspond to table D.3
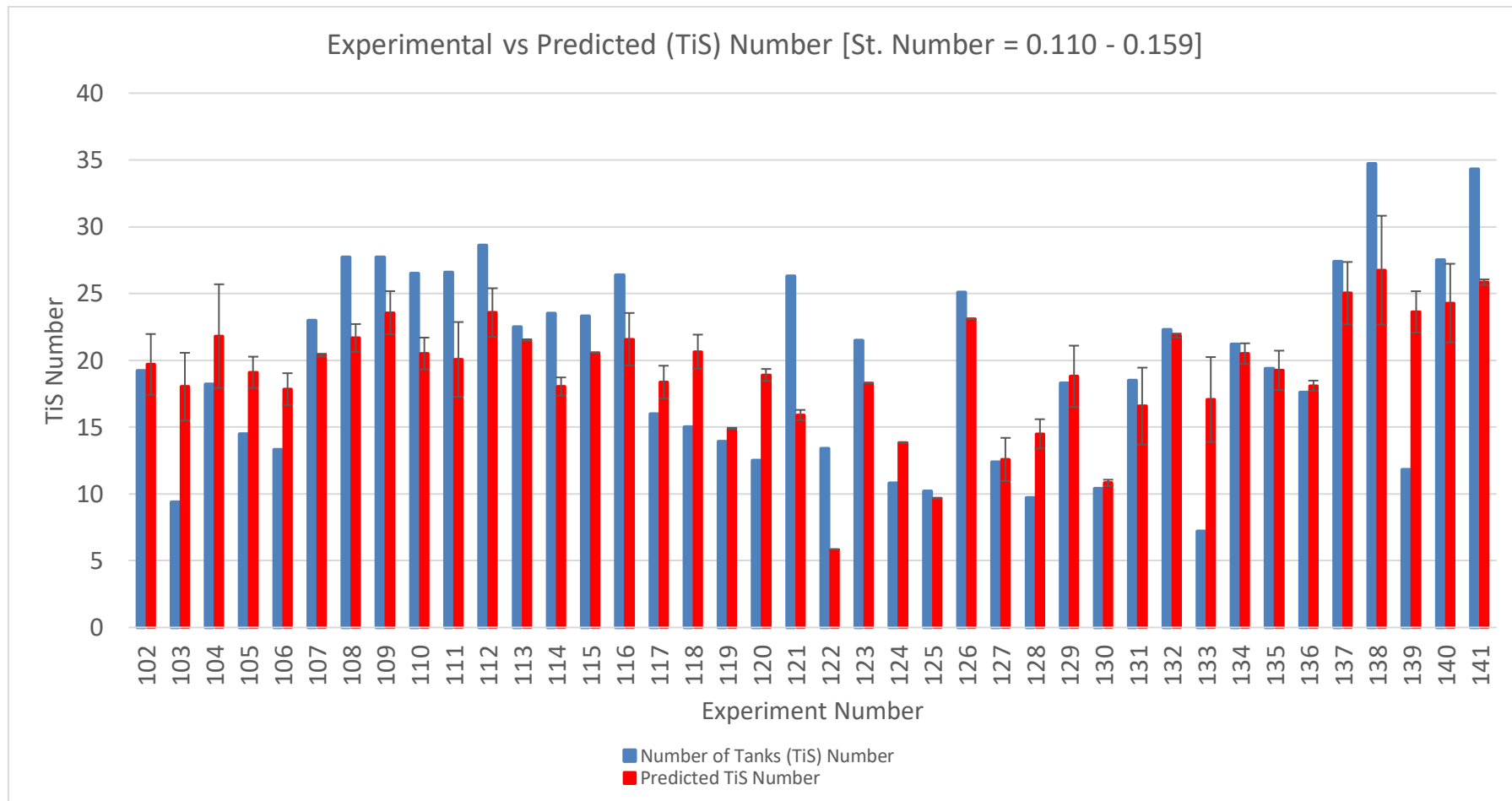
Figure D-6 Experimental versus predicted Tank in Series numbers for experiments across two micro and meso scale with Strouhal number approximately 0.110-0.159. Experiment numbers correspond to table D.3
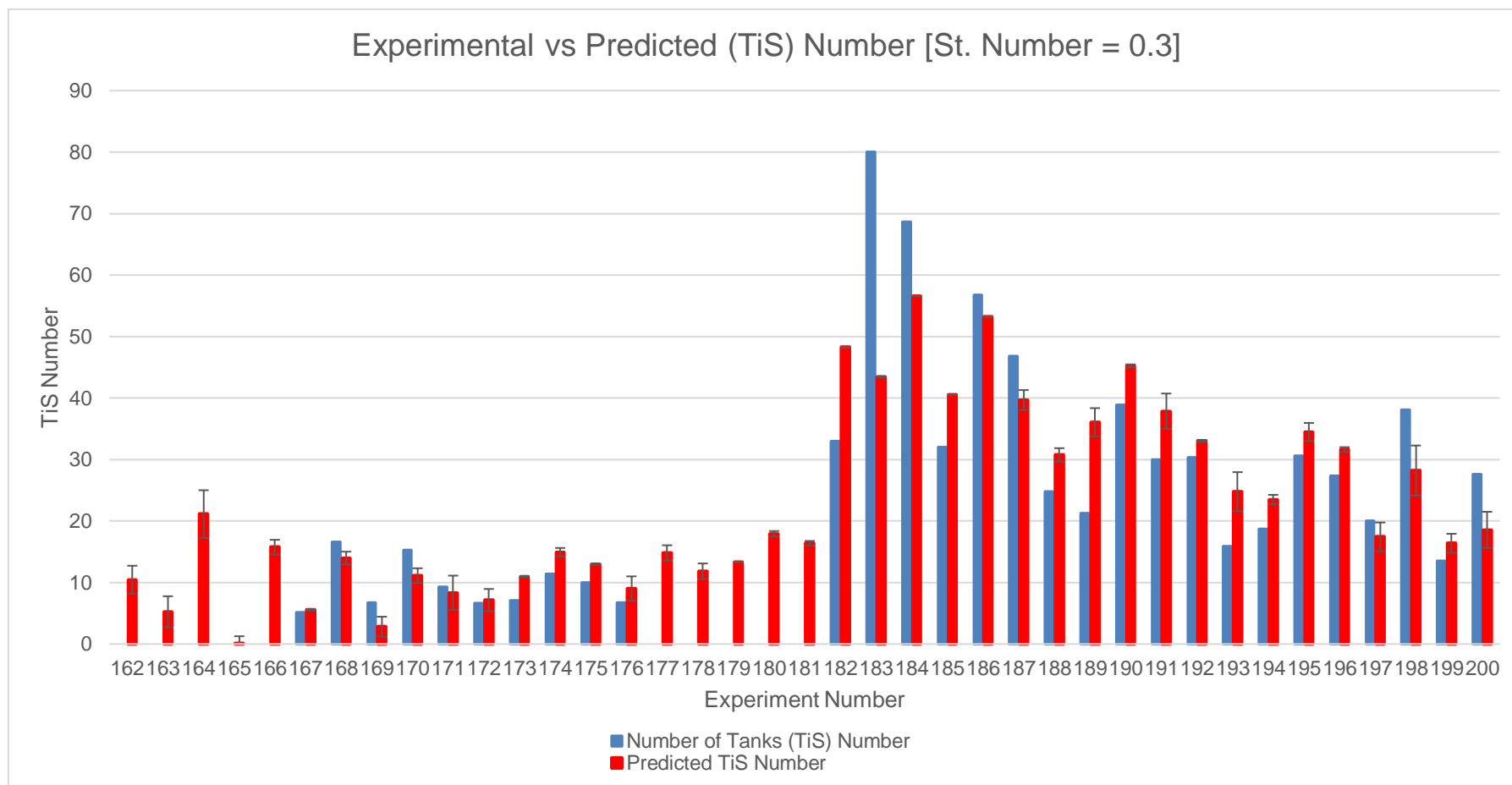
Figure D-7 Experimental versus predicted Tank in Series numbers for experiments across two micro and meso scale with Strouhal number approximately 0.3. Experiment numbers correspond to table D

Appendix E **Sensors**

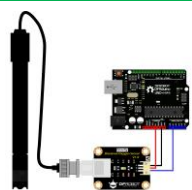**Table E-1 Comparison of the Dissolved O2 Sensors (Reproduced from Jegoux, (2018))**

Sensor	Analog Dissolved Oxygen Sensor / Meter Kit For Arduino SEN0237-A	Analog Dissolved Oxygen Sensor / Meter Kit For Arduino SEN0237-A
Supplier	DFRobot	Atlas Scientific
Measuring range	0-20 mg/L	0-100 mg/L
Temperature conditions	0-40 °C	1-50 °C
Accuracy	unknown	unknown
Response time	98% in 90 s	0.3 mg/L/s
Service life	1 year	> 5 years
Maintenance	Membrane cap: every 1-2 months Solution: every month	Every 18 months
Price	$ 169.00	$ 283.00

Table E-2 comparison of pH sensors (Reproduced from Jegoux, (2018))

Sensor	Analog pH Sensor / Meter Kit For Arduino SEN0161	Analog pH Sensor / Meter Pro Kit For Arduino FIT0348	Atlas Scientific pH Kit	Atlas Scientific Industrial pH Kit
Supplier	DFRobot	DFRobot	Atlas Scientific	Atlas Scientific

Measuring range	0-14 pH	0-14 pH	0.001-14.000 pH	0.001-14.000 pH
Temperature conditions	0-60°C	0-60°C	1-99°C	1-99°C
Accuracy (25°C)	± 0.1 pH	< 0.02 pH	± 0.0001	± 0.0001
Response time	< 1 min	10 s	95% in 1 s	95% in 1 s
Price	$ 29.50	$ 56.95	$ 164	$ 303

Table E-3 Comparison of Turbimetry sensors (Reproduced from Jegoux, (2018))

Sensor	Analog Turbidity sensor for Arduino SEN0189	OBS-3+
Supplier	DFRobot	Campbell Scientific
Measuring range	0-5 V (to be converted into NTU)	0-4000 NTU
Temperature conditions	5-90 °C	0-40 °C
Accuracy	unknown	2% of reading or 0.5 NTU
Warm-up time	unknown	2 s
Response time	< 500 ms	unknown
Price	$ 9.90	≈ $ 1600

E.1 Motor Control

Figure E-1 Sanyo Denki 103H7 Motor (RS-Components, 2019)
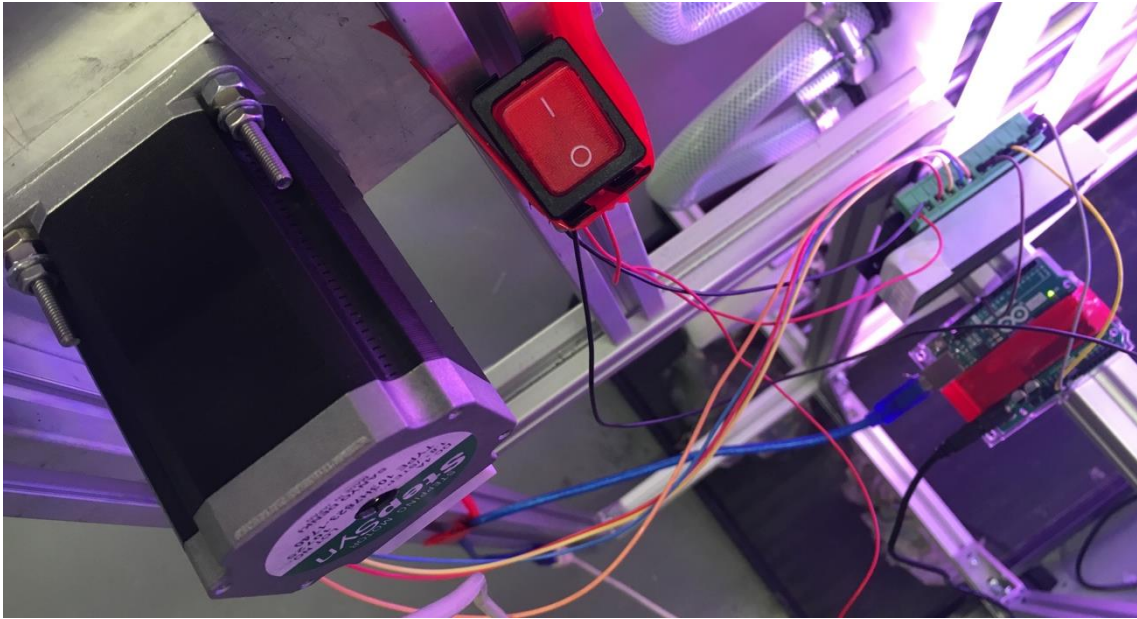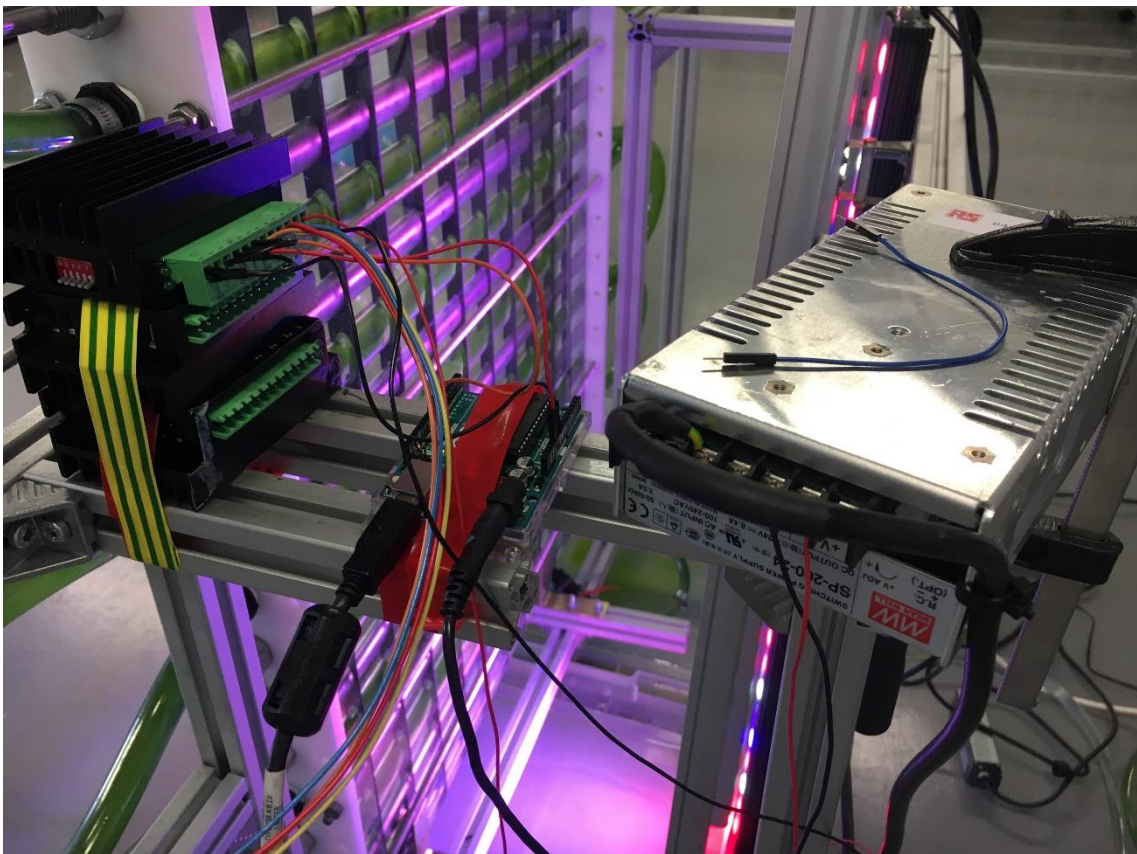
Figure E-2 Oscillatory motor setup with TB6600, on/off switch and Arduino.

Figure_Apx E-3 TB6600, Arduino and SP200-24 power supply (Jegoux, 2018).

■ Features :

* Universal AC input / full range
* Built-in active PFC function, PF>0.93
* Protections: Short circuit / Overload / Over voltage / Over temperature
* Built-in cooling fan speed control
* Built-in constant current limiting circuit
* Built-in fan speed control
* Remote ON-OFF control(Optional)
* LED indicator for power on
* 100% full load burn-in test
* Fixed switching frequency at PFC:67KHz PWM:134KHz
* 3 years warranty

SPECIFICATION

MODEL		SP-200-3.3	SP-200-5	SP-200-7.5	SP-200-12	SP-200-13.5	SP-200-15	SP-200-24	SP-200-27	SP-200-48
OUTPUT	DC VOLTAGE	3.3V	5V	7.5V	12V	13.5V	15V	24V	27V	48V
	RATED CURRENT	40A	40A	26.7A	16.7A	14.9A	13.4A	8.4A	7.5A	4.2A
	CURRENT RANGE	0 ~ 40A	0 ~ 40A	0 ~ 26.7A	0 ~ 16.7A	0 ~ 14.9A	0 ~ 13.4A	0 ~ 8.4A	0 ~ 7.5A	0 ~ 4.2A
	RATED POWER	132W	200W	200.2W	200.4W	201.1W	201W	201.6W	202.5W	201.6W
	RIPPLE & NOISE (max.) Note.2	100mVp-p	100mVp-p	100mVp-p	100mVp-p	100mVp-p	100mVp-p	150mVp-p	150mVp-p	250mVp-p
	VOLTAGE ADJ. RANGE	3.14 ~ 3.63V	4.75~ 5.5V	7.13 ~ 8.25V	11.4 ~ 13.2V	12.8 ~ 14.9V	14.3 ~ 16.5V	22.8 ~ 26.4V	25.7 ~ 29.7V	45.6 ~ 52.8V
	VOLTAGE TOLERANCE Note.3	±2.0%	±2.0%	±2.0%	±2.0%	±2.0%	±2.0%	±1.0%	±1.0%	±1.0%
	LINE REGULATION	±0.5%	±0.5%	±0.5%	±0.5%	±0.5%	±0.5%	±0.5%	±0.5%	±0.5%
	LOAD REGULATION	±1.0%	±1.0%	±1.0%	±0.5%	±0.5%	±0.5%	±0.5%	±0.5%	±0.5%
	SETUP, RISE TIME	600ms, 40ms at full load								
	HOLD UP TIME (Typ.)	20ms at full load								
INPUT	VOLTAGE RANGE	85 ~ 264VAC 120 ~ 370VDC								
	FREQUENCY RANGE	47 ~ 63Hz								
	POWER FACTOR (Typ.)	PF>0.93/230VAC PF>0.97/115VAC at full load								
	EFFICIENCY (Typ.)	69%	76%	78.5%	84%	84%	84%	85%	85%	85%
	AC CURRENT (Typ.)	3.5A/115VAC 1.7A/230VAC								
	INRUSH CURRENT (Typ.)	COLD START 50A/230VAC								
	LEAKAGE CURRENT	<2mA / 240VAC								
PROTECTION	OVERLOAD	105 ~ 150% rated output power								
		Protection type : Constant current limiting, recovers automatically after fault condition is removed								
	OVER VOLTAGE	3.63 ~ 4.46V	5.5 ~ 6.75V	8.25 ~ 10.13V	13.2 ~ 16.2V	14.85 ~ 18.2V	16.5 ~ 20.25V	26.4 ~ 32.4V	29.7 ~ 36.45V	52.8 ~ 64.8V
		Protection type : Shut down o/p voltage, re-power on to recover								
	OVER TEMPERATURE	Shut down o/p voltage, recovers automatically after temperature goes down								
FUNCTION	REMOTE CONTROL(OPTION)	CN1:4 ~ 10VDC POWER ON, <0 ~ 0.8VDC POWER OFF								
ENVIRONMENT	WORKING TEMP.	-10 ~ +60℃ (Refer to output load derating curve)								
	WORKING HUMIDITY	20 ~ 90% RH non-condensing								
	STORAGE TEMP., HUMIDITY	-20 ~ +85℃, 10 ~ 95% RH								
	TEMP. COEFFICIENT	±0.05%/℃ (0 ~ 50℃)								
	VIBRATION	10 ~ 500Hz, 2G 10min./1cycle, 60min. each along X, Y, Z axes								
SAFETY & EMC (Note 4)	SAFETY STANDARDS	UL60950-1, TUV EN60950-1, CCC GB4943 approved								
	WITHSTAND VOLTAGE	I/P-O/P:3KVAC I/P-FG:2KVAC O/P-FG:0.5KVAC								
	ISOLATION RESISTANCE	I/P-O/P, I/P-FG, O/P-FG:100M Ohms / 500VDC / 25℃/70% RH								
	EMC EMISSION	Compliance to EN55032 (CISPR32) Class B,EN61000-3-2,-3								
	EMC IMMUNITY	Compliance to EN61000-4-2,3,4,5,6,8,11; ENV50204, EN55024, light industry level, criteria A								
OTHERS	MTBF	183.8K hrs min. MIL-HDBK-217F (25℃)								
	DIMENSION	199*99*50mm (L*W*H)								
	PACKING	0.85Kg; 20pcs/17.9Kg/1.28CUFT								
NOTE		1. All parameters NOT specially mentioned are measured at 230VAC input, rated load and 25℃ of ambient temperature. 2. Ripple & noise are measured at 20MHz of bandwidth by using a 12" twisted pair-wire terminated with a 0.1uf & 47uf parallel capacitor. 3. Tolerance : includes set up tolerance, line regulation and load regulation. 4. The power supply is considered a component which will be installed into a final equipment. All the EMC tests are been executed by mounting the unit on a 360mm*360mm metal plate with 1mm of thickness. The final equipment must be re-confirmed that it still meets EMC directives. For guidance on how to perform these EMC tests, please refer to "EMI testing of component power supplies." (as available on http://www.meanwell.com)								

File Name:SP-200-SPEC 2017-07-14

Figure E-4 MEANWELL SP200W power Supply (Mouser, 2019)
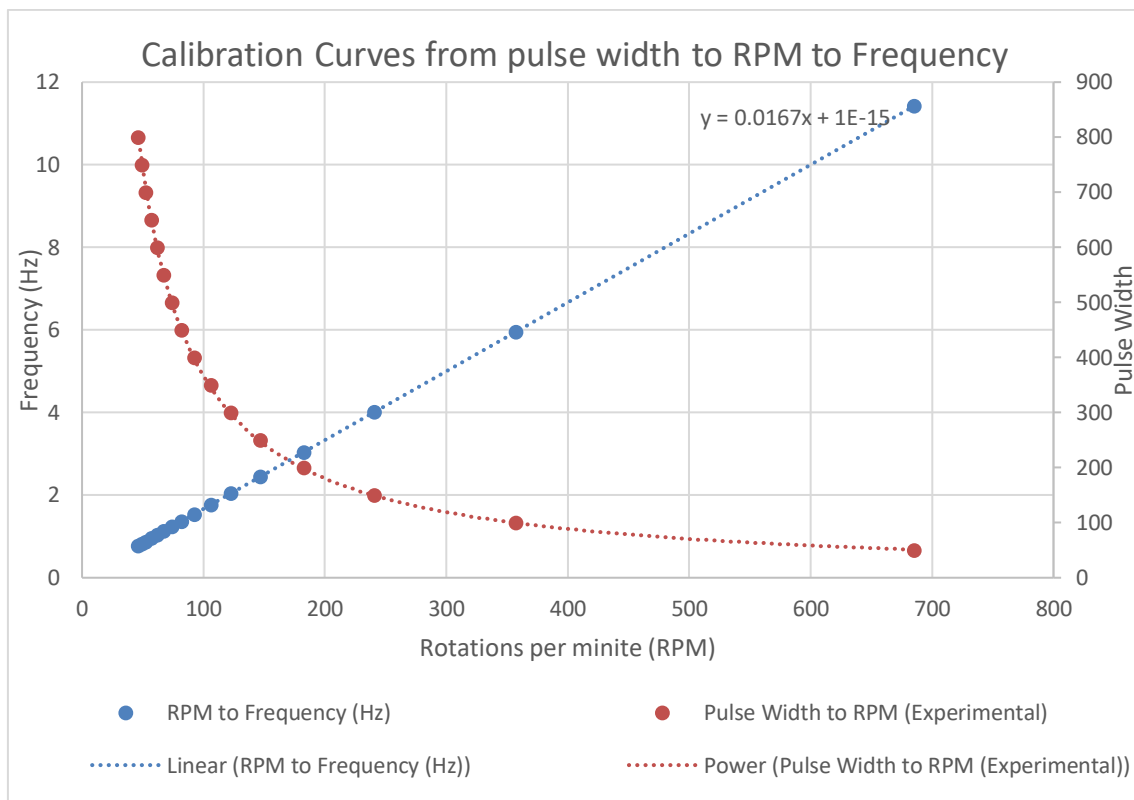
Figure E-5 experimentally derived calibration curve from pulse width to frequency in RPM and Hz
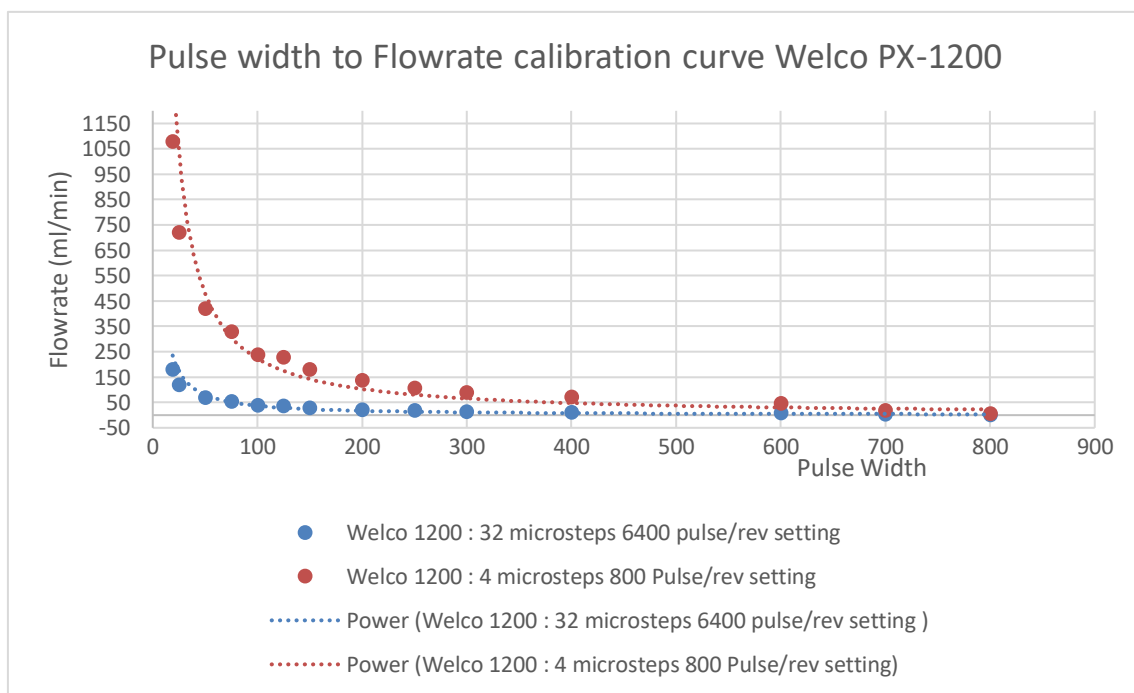

Figure E-6 Experimentally derived calibration curve for PX1200 peristaltic pump control between pulse width settings and flowrates in 4 and 32 microstep settings.
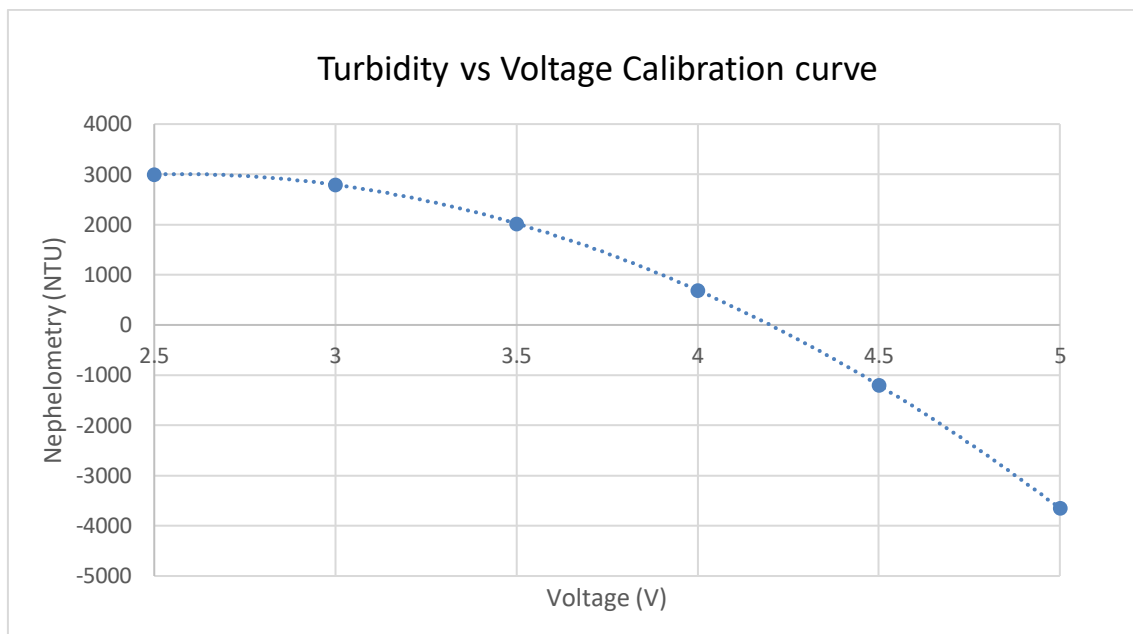
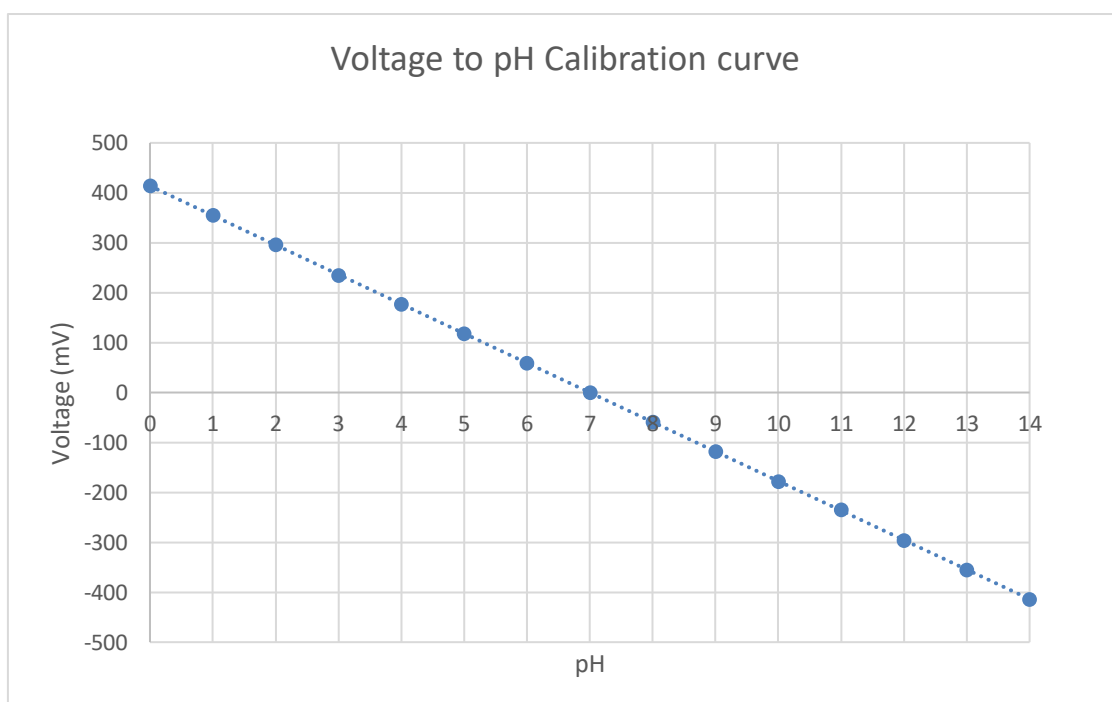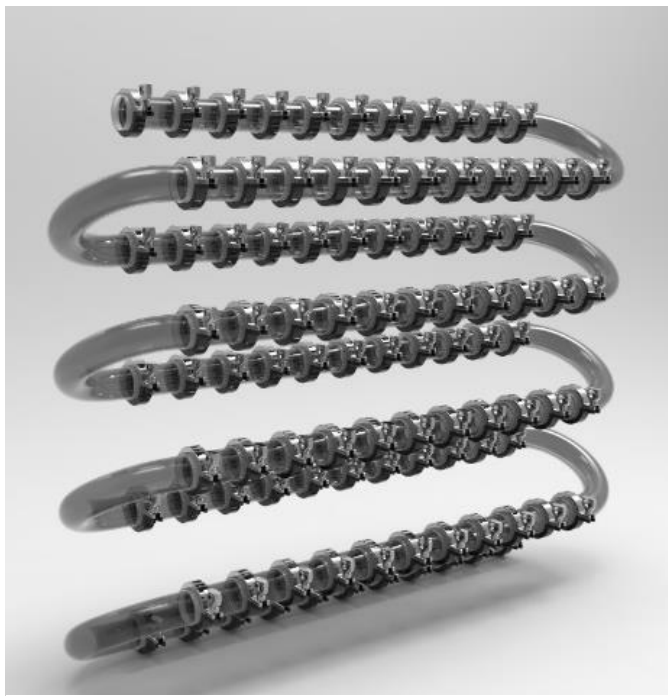**Figure E-7 Voltage to Turbimetry (NTU) calibration for the turbimetry sensor (DF-Robot 2019b).**

Figure E-8 Voltage to pH calibration curve (Mouser, 2019)

Appendix F **Scale up: Flow characterisation.**

F.1 Conceptual Design : 1m^3 Scenario

Figure_Apx F-2 Photorealistic rendering of a Helical oscillatory baffled flow photobioreactor (HOBFpbr) concept design

For large scale tubular PBRs the typical configuration is a helical arrangement of the tubes. In the case of generating a OBR design out of this concept one would arrive at a design much like the one in the adjacent figure. Where the modular baffled disks would be replaced by modular baffled tube sections, which assemble in series using a rubber O-ring housed internally and a rubber sleeve, which is compressed by a standard clamp with internal diameter equal to the tube's outer diameter. Light cycle modulation would still be feasible, by making each baffled section from an opaque
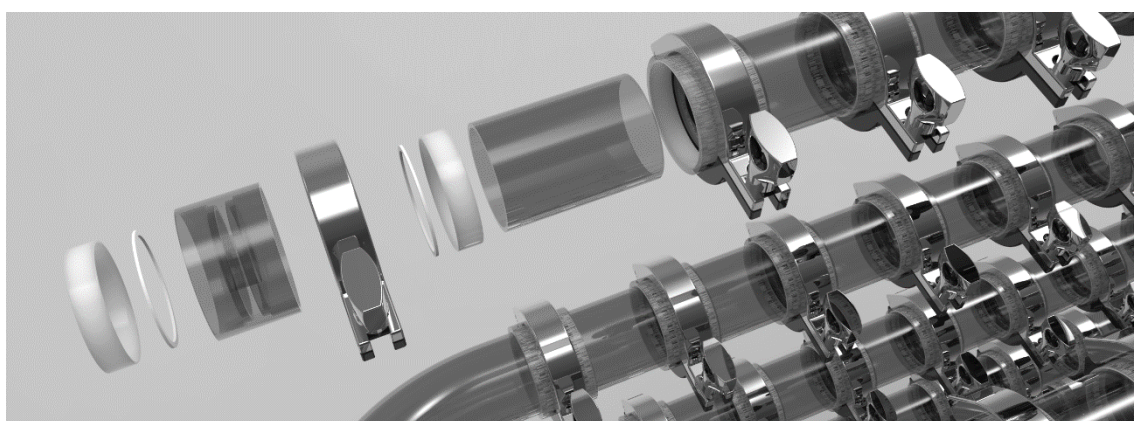

Figure F-1 Photorealistic rendering of the exploded view of the components of the HOBFpbr. (Transparent – Baffled and Conduit spacing. White – Gaskets and o-rings).
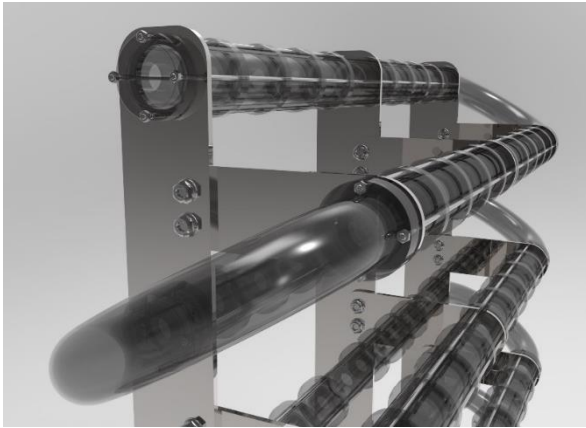
Figure F-3 HOBFpbr concept, using vertical rigid panels as support structures

Figure F-4 Photorealistic rendering of the HOBFpbr concept, showing external light arrangement.

and clear material, albeit this design loses its attractiveness in assembly and disassembly. The support structure of the reactor would need to be cheap, strong and flexible, since it will have to endure heavy dynamic loads, of the both the liquid flow and the rotating machinery.

Supports and mounting structures are a crucial issue, would influence the PBR's shape and size. The reactor members structural support, lighting and mounting system are combined.
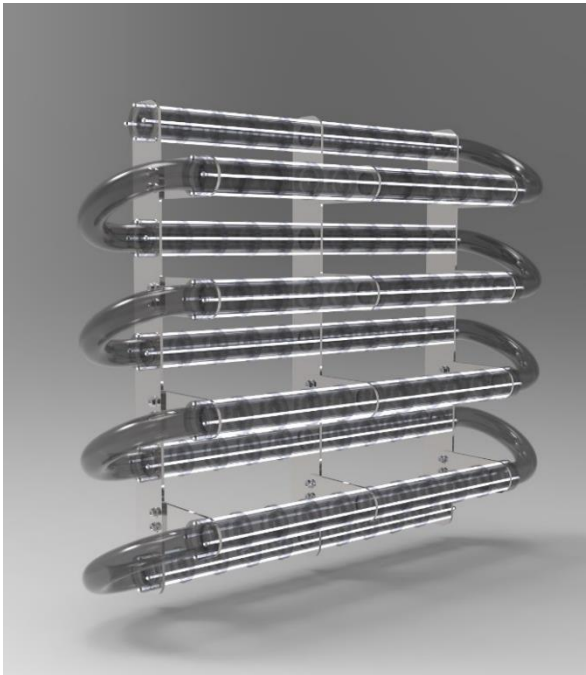
As with the mesoscale system, the reactors support system can be used to mount peripheral equipment such as pumps, holding tanks, sensors and other electrical equipment, given the appropriate care is given.

The holding tank is also a great consideration in a PBR system. Depending on the system itself it has multiple roles, as has been mentioned in tubular reactors gas exchange and nutrient supply is considerably the most important. Drawing inspiration from tubular PBR systems, if the holding tank is separate to the light harvesting unit (tubular section) their volumes must be operationally comparable. However more attention must be given to the material, agitation and sealing characteristics of the holding tank rather than the volumetric capacity.
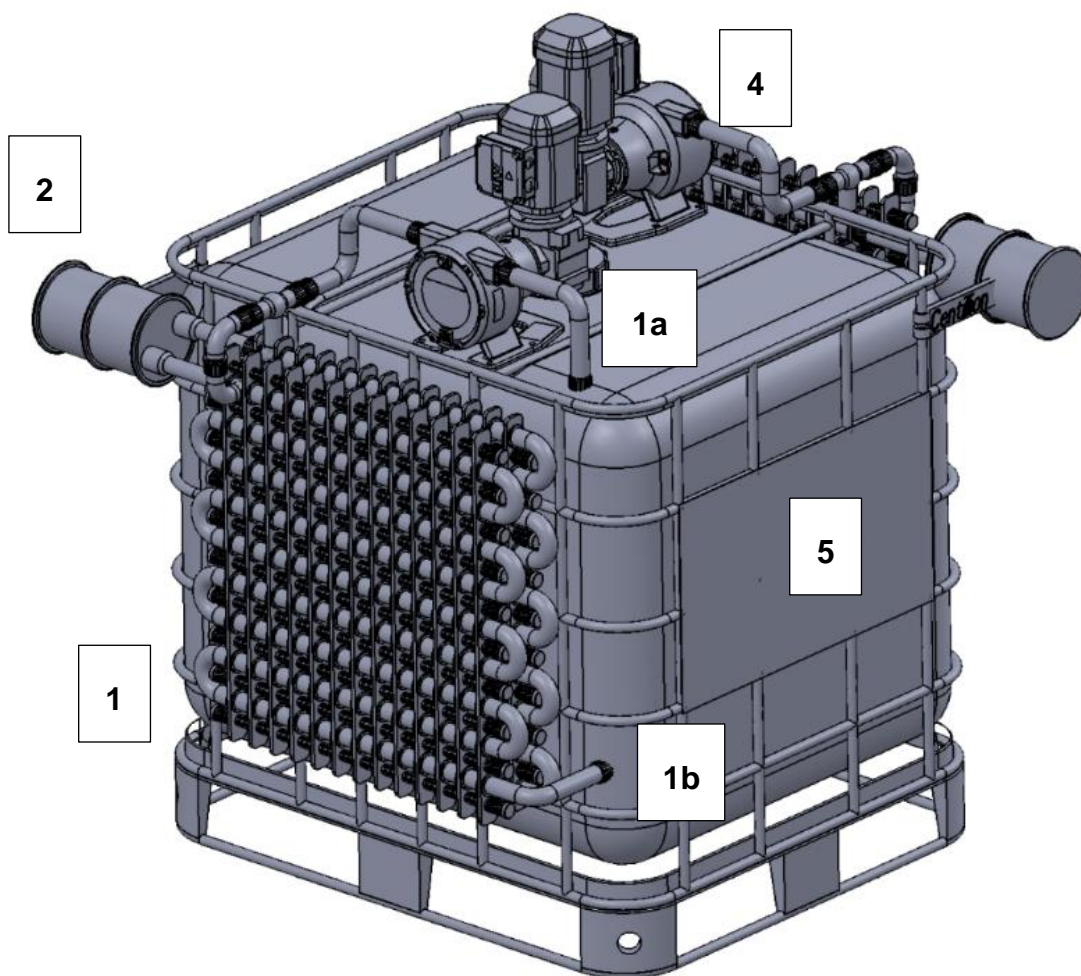
Figure F-5 Conceptual two tier OBFpbr system on IBC 1000L tank, with annotations

Incorporating all points into one conceptual design would lead to a system like that one shown above. A complete reactor (1) mounted on the steel frame of the IBC tank (5), with the reactor inlet (1a) feeding the reactor with the use of a peristaltic pump (4), closing the loop through reactor outlet (1b) back into the tank. Oscillatory flow is generated by the oscillatory mechanism (2). The overall size for this system is approximately $1m^3$. The volumetric capacities of the reactors and tank are 40L and 1000L respectively. Additional scale out of such a system can be achieved by adding more rails to each reactor, thus increasing the size of

the reactor in increments of 10L per rail, which translates to a maximum of 250L per m^2. Or adding two additional reactors on the unoccupied surfaces of the IBC

Figure F-6 Photorealistic rendering of the IBC two tier OBFpbr system
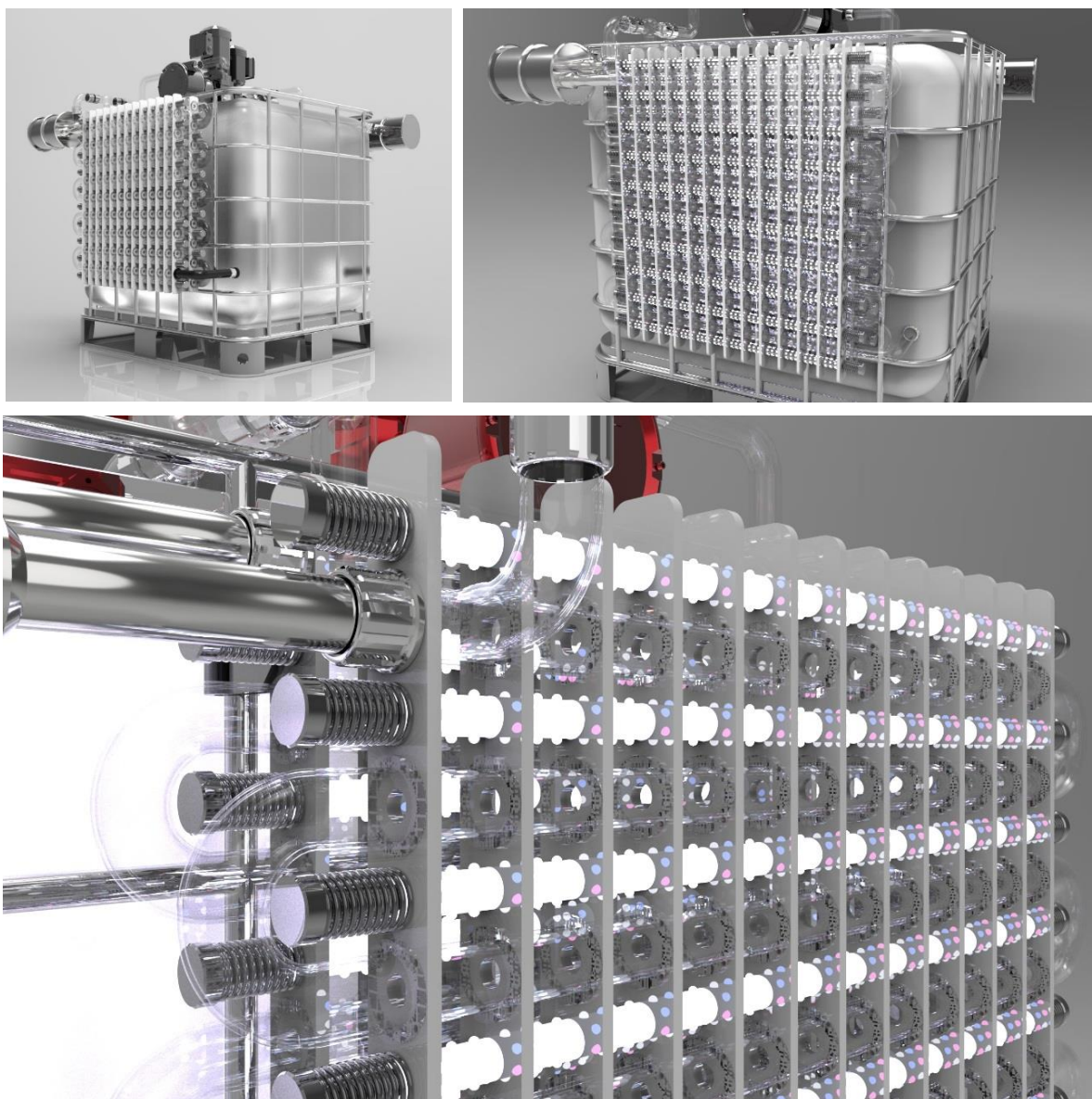
tank increasing the light harvesting unit volume.

At maximum capacity this system would potentially hold 2000L at 400L/m^3. Overall this design has the potential to be applied at an industrial scale, as it appeals as a modular scalable, flexible, and eventually autonomous system. A system which can be stacked or arranged into expandable bioprocessing cells

with a low spatial footprint. Such a system would be advantageous in any modern facility.

One major downfall with the design is the high number of components, complexity of design and maintenance. For example, for a 20L system approximately 96 baffled members are required to be clamped and attached between the baffled walls
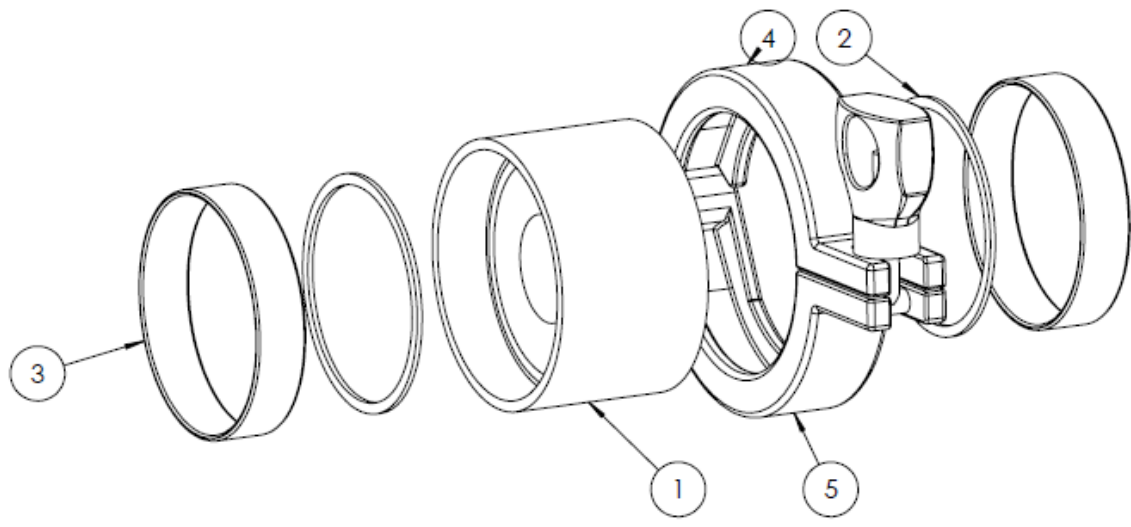
Figure F-7 Example of a single baffle intersection point. 1 Baffled passage, 2 Tube baffle nitrile O-ring, 3 Neoprene tube support sleeve, 4,5 Compression clamp.

This drives the capital as well as operational costs up. On the other hand, for this design to be cost effective it would have to be constructed cheap enough so that all wetted parts are disposed of with every cycle rather than maintained and reused. Which is possible with certain manufacturing routes but is currently beyond the scope of the project.

F.2 Flow Characterisation:

Table F-1 Pilot Scale RTD studies parameter sets and results.

Amplitude	Frequency	Net Flow	Diameter	Str Number	velocity	Reynolds N	Reo Number	Velocity Ratio	Number of Tanks
X_o	f	$\dot{f}$	D	St	u	Re	Re_o	ψ	TiS
mm	hZ	L/min	mm	-	m/s	-	-	-	-
28	0.83	16.6	36	0.11	0.27	9824.42	5256.76	0.54	21.26
28	1.42	4.1	36	0.11	0.07	2456.12	8993.50	3.66	37.04
18	0.83	4.1	36	0.16	0.07	2456.12	3379.35	1.38	32.38
18	1	4.1	36	0.16	0.07	2456.12	4071.50	1.66	35.22
18	1.42	4.1	36	0.16	0.07	2456.12	5781.54	2.35	46.81
8	1.67	4.1	36	0.36	0.07	2456.12	3021.96	1.23	10.05
8	0.83	25	36	0.36	0.41	14736.60	1501.93	0.10	31.88

8	0.83	33.3	36	0.36	0.55	19648.78	1501.93	0.08	44.8
8	1.67	33.3	36	0.36	0.55	19648.78	3021.96	0.15	17.73
8	1.67	25	36	0.36	0.41	14736.60	3021.96	0.21	49.32
8	1.67	4.1	36	0.36	0.07	2456.12	3021.96	1.23	85.75
8	2.5	16	36	0.36	0.27	9824.42	4523.89	0.46	33.66
8	2.5	25	36	0.36	0.41	14736.60	4523.89	0.31	15.52
8	1	4.1	36	0.36	0.07	2456.12	1809.56	0.74	76.79
8	1.42	4.1	36	0.36	0.07	2456.12	2569.57	1.05	36.58

Table F-2 Tracer Experiment validation section experiments.

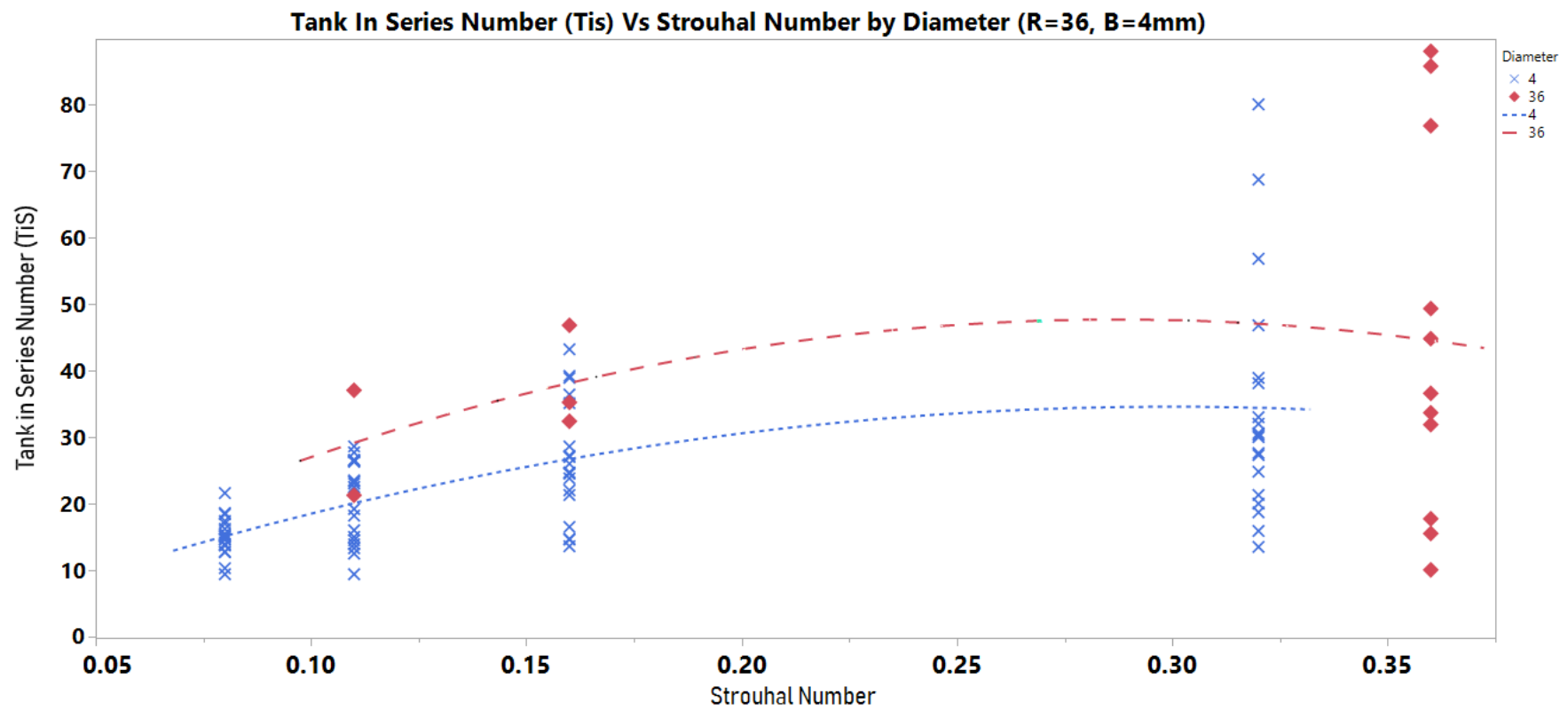| Validation									
Amplitude	Frequency	Net Flow	Diameter	Str Number	velocity	Reynolds N	Reo Number	Velocity Ratio	Number of Tanks
X_o	f	$\dot{f}$	D	St	u	Re	Re_o	ψ	TiS
mm	hZ	l/min	mm	-	m/s	-	-	-	-
8	1	4.1	36	0.36	0.07	2456	1809.6	0.74	87.98
8	1	3	36	0.36	0.03	1768	1809.6	1.02	75.6
8	1	3	36	0.36	0.03	1768	1809.6	1.02	78.8
8	1	3	36	0.36	0.03	1768	1809.6	1.02	70.2

Figure F-8 Scale up Similarity between micro and kilo scale (4mm and 36mm). TiS vs Strouhal Numbers

Appendix G **Scale up experimentation**

G.1 Operational Protocol for the operation of the Bioprocess line.

Decontamination / Sterilisation:

1. 250L of sterile tap-water is pumped into T-2 using a 55W UV flow sterilisation system and 5um flow filter (Filterman, UK), at a flowrate of 100L/h. The flowrate of the water input is set to operate 20 times below the maximum operational flowrate of the UV-flow sterilisation module, thus maximising the contaminant kills.

2. Whilst T-2 is being filled each of the reactor system tanks (T-1, T-7, T-8, T-9) are manually cleaned, by spraying 10 litres of 8-15% IPA and water solution, using a popular market manual pressure pump with a long nozzle, on the walls and surrounding surfaces (tank screw-cap, air vents, tank inputs) of the tank. Upon completion the tank cap and vents are covered with two layers or sterile gauge sprayed with 15% IPA solution and caped with an additional 500mm square sheet of aluminium foil.

3. T-3 is manually filled with 20 litres of IPA.

4. 50L of T-2 and 15L T-3 are diverted to T-1 by manually releasing CO/R V17 and CO/R V18. The contents are mixed at M/V-9 and are diverted to C.Pump 6 using the tank head pressure. When C.Pump 6 is primed the solution is diverted to M/V-11 via 3/W V13, from which it enters the system at CO/R V24 which is the secondary tank input.

5. The solution is fully dispensed into T-1 whilst the tank outlet CO/R V1 is shut. Once this operation is completed C.Pump 6 is temporarily ceased and all valves in the pipework between T-2, T-3 and T-1 are shut.

6. CO/R V1 is manually turned to the open position and the contents of T-1 are pushed to C.Pump 1. At which point are flowed through the reactor at a flowrate of 280 L/h. At the reactor outlet the flow is diverted to a waste

holding tank T-11 via 3W V2. This flushing operation lasts approximately 10 minites, at which when completed all valves are turned to the shut position and C.Pump 1 ceases operation.

7. 200L of T-2 and 5L T-3 are diverted to T-1 by manually releasing CO/R V17 and CO/R V18. The contents are mixed at M/V-9 and are diverted to C.Pump 6 using the tank head pressure. When C.Pump 6 is primed the solution is diverted to 3/W V9 via 3/W V13, from which it enters the system at 3/W V1. Once in the system, the flow is diverted towards the reactor input, and towards the 3/W V2 which diverts the flow back in the tank.

8. Once the operation is complete, the contents of T-1 and allowed to circulate for 5-10h through the tank to sterilise the system.

9. Once this operation is complete the contents of the system are transferred into T-7, via 3/W V1, 3/W V9, CO/R V20, 3/W V10 and 3/W V2, at which point it enters the second subsystem, at which point is flowed through the reactor and back into the tank and left circulating for 5-10h.

Reactor Priming & Inoculation

10. The system attached to T-1 is now ready for cultivation. A concentrated solution of media (10x concentration) is manually poured into T-6. The media's volume is dictated by the dilution ratio and the tank volume requirements for the experimental procedure.

11. Sterile water is pumped into T5 to a volume required so that when mixed with the volume of the concentrated media creates adequate media.

12. Depending on the desired concentration of media, a portion of the contents of T-6 are deposited into T-5 via CO/R V19 and M/V15. At T-5 The mixture is repeatedly flushed through a 55W-UV-C tank (T-14) via C-pump 7, for approximately 15 minutes cycles.

13. Once the cycles are complete, M/V16 diverts the media to CO/R V29, which when released allows the media to fill T1 via C-pump 5 and M/V14.

14. The media enters the FP-OpbR system via CO/R V2 and M/V1 which directs the flow towards the reactor.

15. At the exit of the reactor, valve 3/W V2 directs the initial 10L of liquid towards the waste collection. This initial volume of media is fouled from decontamination liquid being left in the reactor.

16. The valve immediately re-directs the flow towards T1 with CO/R V1 shut. Thus, allowing all media to settle in the tank.

17. Once the desired volume of media is transferred to the system, valve CO/R1 is opened and C-Pump1 circulates the media through the system until most of the trapped air bubbles are removed from the system. The oscillatory mechanism attached to system T1 is turned on, to completely prime the system. The system is left to operate for approximately 10-15 minites, whilst observing the transparent pipes for any foulants or debris being circulated.

18. The process parameters are then set to the oscillatory mechanism and pump.

19. A dense volume of algae cultivated under environmental conditions outlined in section 3.2.2.2.2. Is manually transferred into the reactor system, via a capped port 150mm diameter on system T1.

20. The reactor LED light strips are turned on and the system is left to circulate for 60-90 minites.

21. A 50ml sample is taken via port 3/W V2, and labelled with the strain type, date and tank number. This signifies the start of the experiment.

<u>Cultivation monitoring</u>

22. A sample of the culture is extracted periodically, and is analysed via light microscopy, and optical density. The methodology used is described in section **Error! Reference source not found.**.

G.2 Various Views of the Centillion bioprocessing line at the Cranfield Centillion Pilot Plant B301 MK43 0R.

Figure G-1 Bioprocessing Line: Interconnecting pipework (View 1), showing the 3 main pipelines going through the system, connecting each system with the others.

Figure G-2 Bioprocessing Line: Interconnecting pipework (View 2), showing the 3 main pipelines going through the system, connecting each system with the others

Figure G-3 Showing the clean in place tanks (RHS) and the T1 cultivation system (LHS)

Figure G-4 Showing underneath the clean in place tanks, the pipework connected the main water tank with the concentrated cleaning agent junction.

Figure G-5 View of the complete bioprocessing line, from right to left, the CIP and media tanks, the 4 system tanks and on the background the two 1600L harvesting tanks

Figure G-6 Complete bioprocessing line, additional view showing purple effect of RBWiR lights.